U.S. Department
of Commerce

Volume 117
Number 3
July 2019

Fishery Bulletin

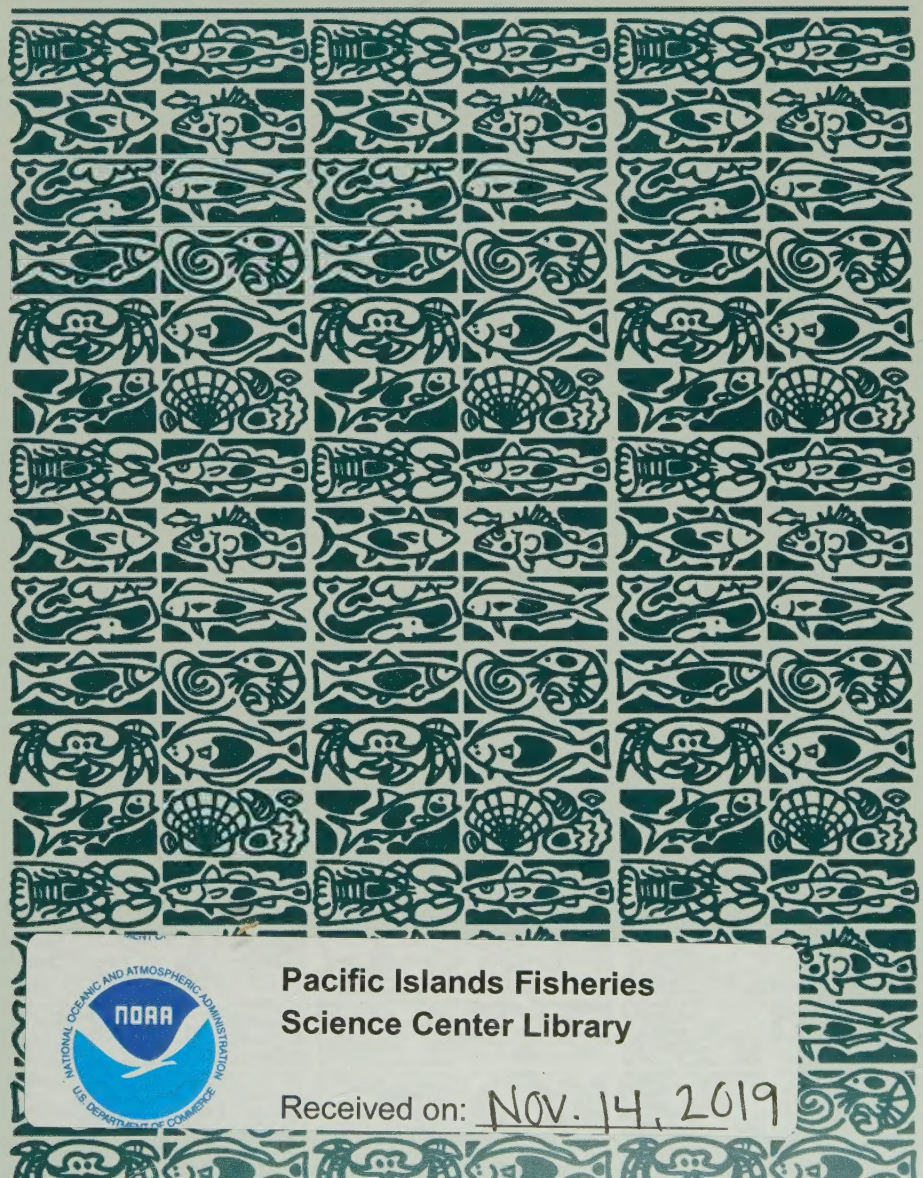

Pacific Islands Fisheries
Science Center Library

Received on: NOV. 14, 2019

U.S. Department of Commerce

Wilbur L. Ross Jr.
Secretary

National Oceanic and Atmospheric Administration

Neil A. Jacobs
Acting Administrator

National Marine Fisheries Service

Chris Oliver
Assistant Administrator
for Fisheries

Fishery Bulletin (ISSN 0090-0656) is published quarterly by the Scientific Publications Office, National Marine Fisheries Service, NOAA, 7600 Sand Point Way NE, Seattle, WA 98115-0070.

Although the contents of this publication have not been copyrighted and may be reprinted entirely, reference to source is appreciated.

The Secretary of Commerce has determined that the publication of this periodical is necessary according to law for the transaction of public business of this Department. Use of funds for printing of this periodical has been approved by the Director of the Office of Management and Budget.

For Sale by the Superintendent of Documents, U.S. Government Publishing Office, Washington, DC 20401. Subscription price per year: $32.00 domestic and $44.80 foreign. Cost per single issue: $19.00 domestic and $26.60 foreign. **See back for order form.**

Fishery Bulletin

Scientific Editor
José I. Castro
National Marine Fisheries Service, NOAA
263 13th Avenue South
Saint Petersburg, Florida 33701

Managing Editor
Kathryn Dennis
Scientific Publications Office
National Marine Fisheries Service, NOAA
1845 Wasp Boulevard, Building 176
Honolulu, Hawaii 96818

Associate Editor
Cara Mayo
Scientific Publications Office
National Marine Fisheries Service, NOAA
7600 Sand Point Way NE
Seattle, Washington 98115-0070

Editorial Board

Henry L. Bart Jr.	Tulane University, New Orleans, Louisiana
Matthew D. Campbell	National Marine Fisheries Service, Pascagoula, Mississippi
Shannon L. Cass-Calay	National Marine Fisheries Service, Miami, Florida
William B. Driggers III	National Marine Fisheries Service, Pascagoula, Mississippi
Gretchen L. Grammer	South Australian Research and Development Institute, Adelaide, Australia
Richard Langton	National Marine Fisheries Service, Walpole, Maine (retired)
Richard S. McBride	National Marine Fisheries Service, Woods Hole, Massachusetts
Richard L. Merrick	National Marine Fisheries Service, Falmouth, Massachusetts (retired)
Richard D. Methot	National Marine Fisheries Service, Seattle, Washington
Lisa J. Natanson	National Marine Fisheries Service, Narragansett, Rhode Island
Joseph M. Quattro	University of South Carolina, Columbia, South Carolina
Mark S. Peterson	University of Southern Mississippi, Ocean Springs, Mississippi
John F. Walter III	National Marine Fisheries Service, Miami, Florida
Bruce Wright	Aleutian Pribilof Island Association, Anchorage, Alaska

***Fishery Bulletin* website: https://spo.nmfs.noaa.gov/fb.htm**

Fishery Bulletin carries original research reports on investigations in fishery science, engineering, and economics. It began as the Bulletin of the United States Fish Commission in 1881; it became the Bulletin of the Bureau of Fisheries in 1904 and the *Fishery Bulletin* of the U.S. Fish and Wildlife Service in 1941. Separates were issued as documents through volume 46; the last document was no. 1103. Beginning with volume 47 in 1931 and continuing through volume 62 in 1963, each separate appeared as a numbered bulletin. A new system began in 1963, with volume 63, in which papers are bound together in a single issue. Beginning with volume 70, number 1, January 1972, *Fishery Bulletin* became a periodical, issued quarterly. In this form, it is available by subscription from the Superintendent of Documents, U.S. Government Publishing Office, Washington, DC 20401. It is also available free in limited numbers to libraries, research institutions, and state and federal agencies and in exchange for other scientific publications.

U.S. Department of Commerce
Seattle, Washington

Volume 117
Number 3
July 2019

Fishery Bulletin

Contents

Articles

125–139 **Alexander Q. Fogg, Joseph T. Evans, Mark S. Peterson, Nancy J. Brown-Peterson, Eric R. Hoffmayer, and G. Walter Ingram Jr.**

Comparison of age and growth parameters of invasive red lionfish (*Pterois volitans*) across the northern Gulf of Mexico

140–150 **Christina L. Conrath**

Reproductive potential of light dusky rockfish (*Sebastes variabilis*) and northern rockfish (*S. polyspinis*) in the Gulf of Alaska

151–168 **Bradford C. Chase, Scott Elzey, Sara M. Turner, and Matt H. Ayer**

Fecundity and reproductive life history of anadromous rainbow smelt (*Osmerus mordax*) in coastal waters of Massachusetts

169–179 **Katherine Torres-Palacios, Paola A. Mejía-Falla, Andrés F. Navia, Víctor H. Cruz-Escalona, Roberto Félix-Uraga, and Casimiro Quiñonez-Velázquez**

Age and growth parameters of the Panamic stingray (*Urotrygon aspidura*)

Short contributions

180–188 **Anna M. Holder and John C. Field**

An exploration of factors that relate to the occurrence of multiple brooding in rockfishes (*Sebastes* spp.)

189–195 **William B. Driggers III and Kristin M. Hannan**

Efficacy of 2 common bait types in reducing bycatch of coastal sharks on bottom longline gear in the absence of choice

The National Marine Fisheries Service (NMFS) does not approve, recommend, or endorse any proprietary product or proprietary material mentioned in this publication. No reference shall be made to NMFS, or to this publication furnished by NMFS, in any advertising or sales promotion that would indicate or imply that NMFS approves, recommends, or endorses any proprietary product or proprietary material mentioned herein or that has as its purpose an intent to cause directly or indirectly the advertised product to be used or purchased because of this NMFS publication.

The NMFS Scientific Publications Office is not responsible for the contents of the articles.

Articles

196–210 **Kym Jacobson, Rebecca Baldwin, Michael Banks, and Robert Emmett**

Use of parasites to clarify residency and migration patterns of Pacific sardine (*Sardinops sagax*) in the California Current

211–219 **Winsor H. Watson III, Elizabeth Morrissey, Stephanie Sykes, Abigail S. Clark, and Steven Jury**

Experimental analyses of the mechanisms leading to American lobster (*Homarus americanus*) ventless trap saturation

220–233 **Matt Perkinson, Tanya Darden, Maggie Jamison, Matt J. Walker, Michael R. Denson, James Franks, Read Hendon, Susanna Musick, and Eric S. Orbesen**

Evaluation of the stock structure of cobia (*Rachycentron canadum*) in the southeastern United States by using dart-tag and genetics data

234–244 **Jeremy P. Harris, Charles Hutchinson, and Sharon Wildes**

Using otolith morphometric analysis to improve species discrimination of blackspotted rockfish (*Sebastes melanostictus*) and rougheye rockfish (*S. aleutianus*)

245–257 **José S. Méndez-Macías, Vanessa M. Velázquez-Chiquito, Colombo Estupiñán-Montaño, and Felipe Galván-Magaña**

Trophic ecology and ontogenetic shift in the diet of the sicklefin smoothhound (*Mustelus lunulatus*) in the southeastern Pacific Ocean

258–271 **Frederick A. Goetz and Thomas P. Quinn**

Behavioral thermoregulation by adult Chinook salmon (*Oncorhynchus tshawytscha*) in estuary and freshwater habitats prior to spawning

273–276 **Guidelines for authors**

National Marine Fisheries Service
NOAA

Fishery Bulletin
established in 1881

Spencer F. Baird
First U.S. Commissioner of Fisheries and founder of *Fishery Bulletin*

Comparison of age and growth parameters of invasive red lionfish (*Pterois volitans*) across the northern Gulf of Mexico

Alexander Q. Fogg (contact author)[1,2]
Joseph T. Evans[3]
Mark S. Peterson[1]
Nancy J. Brown-Peterson[4]
Eric R. Hoffmayer[5]
G. Walter Ingram Jr.[5]

Email address for contact author: fogg.alex@gmail.com

[1] Division of Coastal Sciences
School of Ocean Science and Engineering
University of Southern Mississippi
703 East Beach Drive
Ocean Springs, Mississippi 39564

[2] Okaloosa County Board of County Commissioners
Emerald Coast Convention and Visitors Bureau
1540 Miracle Strip Parkway
Fort Walton Beach, Florida 32548

[3] Marine Resource Research Institute
South Carolina Department of Natural Resources
217 Fort Johnson Road
Charleston, South Carolina 29412

[4] Center for Fisheries Research and Development
School of Ocean Science and Engineering
University of Southern Mississippi
703 East Beach Drive
Ocean Springs, Mississippi 39564

[5] Mississippi Laboratories
Southeast Fisheries Science Center
National Marine Fisheries Service, NOAA
3209 Frederic Street
Pascagoula, Mississippi 39567

Abstract—Invasive red lionfish (*Pterois volitans*) have spread rapidly throughout the northern Gulf of Mexico (GOM) partly because of their high growth rate. Red lionfish were collected from the northern GOM across 3 ecological regions from 2012 through 2015. For male and female red lionfish, relationships between weight and total length (TL) were different by ecological region. Males achieved a greater mean weight adjusted for TL (333.6 g [standard error (SE) 3.6]) than females (195.1 g [SE 3.7]). A subsample of 1607 pairs of sagittal otoliths (from 744 males, 716 females, and 147 fish of unknown or undetermined sex) was used to assign ages. Ages ranged from 0.0 to 4.5 years (mean: 1.4 years), and these estimated ages and the dates of capture for specimens confirm the presence of red lionfish in the northern GOM in 2008, 2 years prior to the first detection of this species there. There were differences in age and growth between sexes within and among ecological regions, with males achieving higher growth rates and larger asymptotic lengths than females (all comparisons: $P<0.01$). These findings, coupled with other life history information, aid in discerning differences in distribution of red lionfish populations and are essential for creating management plans for mitigation of their effects on ecosystems.

Manuscript submitted 31 July 2018.
Manuscript accepted 7 June 2019.
Fish. Bull. 117:125–139 (2019).
Online publication date: 3 July 2019.
doi: 10.7755/FB.117.3.1

The views and opinions expressed or implied in this article are those of the author (or authors) and do not necessarily reflect the position of the National Marine Fisheries Service, NOAA.

The invasive red lionfish (*Pterois volitans*) and devil firefish (*P. miles*) have been reported as established in U.S. waters of the western North Atlantic Ocean and in the Caribbean Sea, and the red lionfish has been found in the Gulf of Mexico (GOM) (Morris and Akins, 2009; Schofield, 2010; Fogg et al., 2017); however, the devil firefish has not yet been detected in the GOM (Johnson et al., 2016). It is difficult to distinguish between these 2 species except through genetic analysis, and data from previous studies are not necessarily separated by species. Therefore, throughout this paper, we use the term *lionfish* to refer to specimens that are not identified to species but are a potential combination of red lionfish, devil firefish, and hybrids between the 2 species.

Lionfish were first documented in the United States off Dania Beach, on the eastern coast of Florida, in 1985 (U.S. Geological Survey, Nonindigenous Aquatic Species Database, website, accessed December 2015) and later documented in the GOM in 2009 (Aguilar-Perera and Tuz-Sulub, 2010; Nonindigenous Aquatic Species Database, accessed December 2015). By 2012, lionfish were commonly captured in the northern GOM (Fogg et al., 2013), and histological evidence of spawning-capable lionfish in the northern GOM was first observed from fish captured in May 2012 (Brown-Peterson and Hendon, 2013). Efforts to research lionfish species have increased as their invasion has expanded, but most work has focused on the effects of lionfish

species on native fish species and coral reef communities (Dahl and Patterson, 2014; Albins, 2015; Benkwitt, 2015; Ingeman and Webster, 2015; Rocha et al., 2015; Acero et al., 2019) and on aspects of landscape-level movements among reef systems and invasion control efforts (Frazer et al., 2012; Green et al., 2014; Tamburello and Côtè, 2015). Results from a recent study indicate that red lionfish have unique morphological functional traits that reduce the theoretical ecological space of 5 coral reef mesopredators of the Caribbean Sea (Rojas-Vélez et al., 2019). However, data are limited for age and growth of lionfish species throughout the geographic range that they have invaded.

Knowledge of weight–length relationships, size and age structure, and growth patterns are important for the successful assessment and management of species. This information can also be used to assess the effects of invasive species on native species and the ecosystems they inhabit. For example, although data such as weight–length relationships are generally useful for quantifying changes in size or age structure that relate to potential overexploitation of a species (Berkeley et al., 2004; Dulvy et al., 2004), such data also could be used as indicators of success in management of invasive species (Pasko and Goldberg, 2014). Additionally, weight–length relationships could be used to examine changes in population structure during post-culling activities or following large-scale disease or environmental perturbation (e.g., an algal bloom). Although a number of studies have reported basic weight and length data for invasive lionfish (Barbour et al., 2011; Fogg et al., 2013; Dahl and Patterson, 2014; Edwards et al., 2014; Sabido-Itzá et al., 2016), few make comparisons between regions or sexes.

Estimations of age and growth relationships for species within invaded geographic ranges are important for describing spatially explicit variation in life history. Larger and older fish tend to affect ecosystems differently than smaller and younger individuals because diet and habitat use can change with age and size (Curtis et al., 2017; Mizrahi et al., 2017; García-Rivas et al., 2018). Age and growth patterns of lionfish vary geographically. Johnson and Swenarton (2016) verified their length-based model outputs with ages determined from a subsample of 100 sectioned otoliths from fish (age 0–3; maximum size of 342 mm in total length [TL]) captured offshore of Jacksonville, Florida. Additional information from other studies conducted outside of the GOM illustrates this variation. Lionfish captured in Onslow Bay, North Carolina, had a maximum age of 8 years, with more than 90% of these fish (number of samples examined [n]=814) <3 years old (Potts et al., 2010; Barbour et al., 2011). Two red lionfish collected off the coast of South Carolina, at sizes of 352 and 389 mm TL, were determined to be 5 and 6 years old, respectively (Meister et al., 2005).

Limited data from regions in the GOM and the Caribbean Sea indicate similar variation. Red lionfish collected from the Dry Tortugas in the Florida Keys had a maximum age of 7 years (Dubel[1]). Rodríguez-Cortés et al. (2015) provided the first growth and mortality estimates for the southern region of the GOM (Mexico), although the modeled lengths of red lionfish (n=776; range: 90–389 mm TL) from that study were not verified by using otoliths. Edwards et al. (2014), using otoliths from 110 male and 128 female lionfish captured off Little Cayman, found a maximum age of only 5 years and confirmed annual annuli formation for fish from that region of the Caribbean Sea. However, no ages determined from analysis of wild-caught lionfish are as old as the ages of lionfish held in captivity (30–33 years; Potts et al., 2010).

Lionfish species have invaded different regions of the GOM and the Caribbean Sea at different times (Schofield, 2010) and can be found in vastly different ecosystems (Barbour et al., 2010; Jud et al., 2011; Claydon et al., 2012; Ruttenberg et al., 2012) and different densities (Green and Côté, 2009; Darling et al., 2011; Dahl and Patterson, 2014). Therefore, we expected that age and growth parameters would vary by location, a notion that Villaseñor-Derbez and Fitzgerald (2019) have since verified. Additionally, rapid growth rates generally lead to successful invasion of an area by a species; therefore, it is important to estimate growth rates (Copp and Fox, 2007). Although age and growth data have been reported for portions of the invaded geographic range, growth of red lionfish could differ between the southern and northern regions of their non-native range (Barbour et al., 2011). Therefore, we hypothesized that the age structure of red lionfish is much younger in the northern GOM than in other invaded regions where they have been established for a longer period. The goal of this study was to determine if differences in weight and length and in age and growth relationships exist by sex or across the northern GOM.

Materials and methods

Initially, we did not identify our specimens to species, instead putting them in a complex that comprises both *Pterois volitans* and *P. miles* because it was unknown at the beginning of our study if both species occurred in the GOM (Hamner et al., 2007; Brown-Peterson and Hendon, 2013; Fogg et al., 2013) or if there were hybrids in the GOM. Results from subsequent work, including a study that used specimens we provided for genetic analysis, indicate that the red lionfish is the only species detected to date in the northern GOM (Johnson et al., 2016). Therefore, we identify all specimens that we collected in the northern GOM throughout our study as *P. volitans*.

From 2012 through 2015, red lionfish were collected opportunistically every month (for details about specimen collection, see Fogg et al., 2017) across 3 ecological regions (or *ecoregions*) of the northern GOM: southeast (from the Florida Keys north to Anclote Keys, Florida), northeast (from the Anclote Keys north to Mobile Bay, Alabama), and central (west of Mobile Bay to Galveston Bay, Texas; 1 fish was collected west of Galveston Bay) (Fig. 1). Clearly identified, ecologically relevant ecoregions in the GOM and the Caribbean Sea vary and are debated because authors use somewhat different environmental data and quantitative approaches to delineate ecoregions

[1] Dubel, A. M. 2017. Age structure and growth of lionfish (*Pterois volitans*): the Dry Tortugas National Park. Internship Rep. 32, 40 p. Univ. Miami, Miami, FL. [Available from website.]

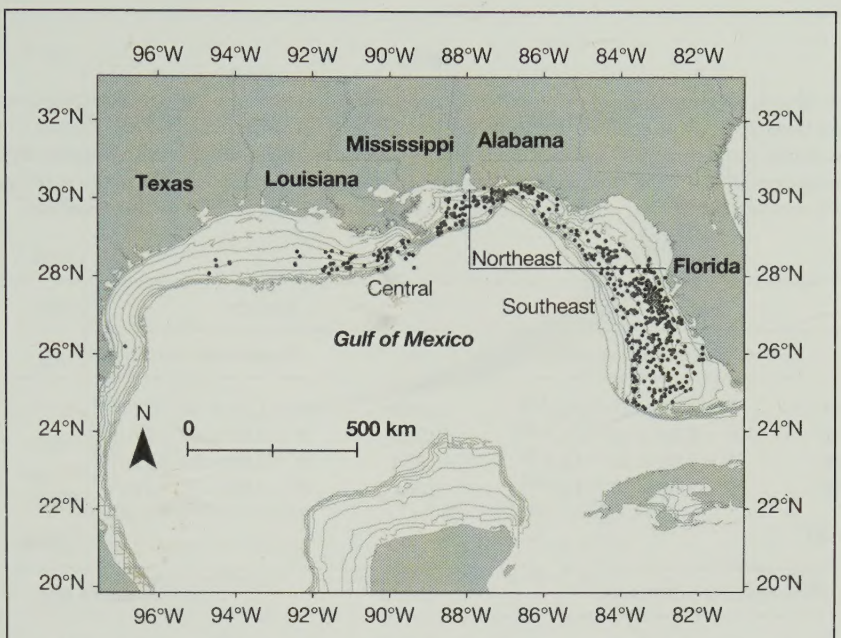

Figure 1

Map of the locations (black dots) and ecological regions (ecoregions) where red lionfish (*Pterois volitans*) were sampled from 2012 through 2015 in the northern Gulf of Mexico. Three ecoregions were sampled in this study: southeast (Florida Keys north to Anclote Keys, Florida), northeast (Anclote Keys north to Mobile Bay, Alabama), and central (west of Mobile Bay to Galveston Bay, Texas). The gray lines indicate depth contours from 10 to 200 m.

(e.g., Sullivan Sealey and Bustamante, 1999; Yáñez-Arancibia and Day, 2004; Spalding et al., 2007; Robertson and Cramer, 2014). Most ecoregions are identified on the basis of known biogeographic criteria, such as thermal regimes, habitat, floral and faunal assemblage composition, sediment structure, currents and bathymetry, and coastal structural complexity.

The northern tip of the Anclote Keys off the western coast of Florida, for example, has been identified as a point of a north–south ecoregion break (Beck and Odaya, 2001; Beck, 2003; Spalding et al., 2007) in the northern GOM. This boundary between the southeast and northeast ecoregions is used mostly because of the thermal differences between the 2 ecoregions; in the winter months, water temperatures are consistently lower in the northeast ecoregion than in the southeast ecoregion (temperature data were obtained from NOAA's National Data Buoy Center, website). The Mississippi River often is used to divide the northern GOM into east and west ecoregions; however, we follow the ecoregion delineation based on Beck (2003) and Yáñez-Arancibia and Day (2004), dividing our study area into central and northeast ecoregions. Our northeast ecoregion, which is considered the east ecoregion by Beck and Odaya (2001), Beck (2003), and Yáñez-Arancibia and Day (2004), is characterized by less freshwater input, sandier sediments, and enhanced water clarity compared with the central ecoregion where increased freshwater input, lower salinities, and muddy sediment input dominate. The northeast ecoregion is dominated by seagrass meadows, but the central ecoregion is mainly salt marsh (Beck, 2003; Yanez-Aráñcibia and Day, 2004).

Total length, measured in millimeters, and total weight, measured in grams, were recorded, and weight–length relationships were calculated by sex and ecoregion. These data were used to estimate the weight–length power functions. The weight–length data were log transformed (base 10) prior to an analysis of covariance (ANCOVA), with TL as the covariate. An ANCOVA was first completed for each sex separately, comparing the weight–length relationships found across each of the 3 ecoregions. If no significant differences were found across ecoregions, data were pooled and a second ANCOVA was completed to compare weight–length relationships for each ecoregion by sex. If the weight–length relationships for any ANCOVA violated the homogeneity of slopes assumption (parallelism), separate models were used. The estimated marginal means from these analyses were used to make comparisons between sexes of weight adjusted for mean TL. All ANCOVA were completed by using SPSS Statistics[2], vers. 20 (IBM Corp., Armonk, NY).

The sagittal otoliths were removed from red lionfish, and the left otolith was embedded and sectioned to a 300-µm thickness following Secor et al. (1991). Prepared otoliths

[2] Mention of trade names or commercial companies is for identification purposes only and does not imply endorsement by the National Marine Fisheries Service, NOAA.

Table 1

Comparisons of weight–length relationships of red lionfish (*Pterois volitans*) for each ecological region (ecoregion) sampled in the northern Gulf of Mexico from 2012 through 2015: southeast (Florida Keys north to Anclote Keys, Florida), northeast (Anclote Keys north to Mobile Bay, Alabama), and central (west of Mobile Bay to Galveston Bay, Texas). (**A**) Regression equations for comparisons by sex within each ecoregion. (**B**) Pairwise comparisons by sex between ecoregions. Between-sex and between-ecoregion comparisons of weight (W) were evaluated by using analysis of covariance with total length (TL) as the covariate.

A

	Male		Female		
Ecoregion	n	Regression equation	n	Regression equation	Comparison
Southeast	857	$W = 2.00 \times 10^{-6}(TL)^{3.34}$	671	$W = 1.00 \times 10^{-6}(TL)^{3.44}$	$F_{1,1528}$=12.68, P<0.001
Northeast	1181	$W = 3.00 \times 10^{-6}(TL)^{3.26}$	1239	$W = 3.00 \times 10^{-6}(TL)^{3.30}$	$F_{1,2420}$=2.32, P=0.128
Central	368	$W = 3.00 \times 10^{-6}(TL)^{3.30}$	354	$W = 2.00 \times 10^{-6}(TL)^{3.41}$	$F_{1,722}$=6.84, P=0.090
Pooled	2406	$W = 3.00 \times 10^{-6}(TL)^{3.29}$	2264	$W = 2.00 \times 10^{-6}(TL)^{3.37}$	$F_{1,4670}$=21.96, P<0.001

B

Ecoregion comparison	Males	Females
Southeast vs. northeast	$F_{1,2038}$=8.16, P=0.004	$F_{1,1910}$=27.72, P<0.001
Northeast vs. central	$F_{1,1549}$=1.42, P=0.223	$F_{1,1593}$=10.19, P=0.001
Southeast vs. central	$F_{1,1225}$=0.86, P=0.354	$F_{1,1025}$=0.61, P=0.436
Pooled ecoregions	$F_{2,2406}$=4.17, P=0.015	$F_{2,2264}$=15.88, P<0.001

were read by 2 independent readers to assign age information. The average percent error (APE) between readers was estimated following Vanderkooy and Guindon-Tisdel[3]. Otolith sections had 2 distinct band types, with the opaque bands formed during slow growth periods and the translucent bands formed during periods of faster growth (see fig. 7 in Fogg, 2017; Vanderkooy and Guindon-Tisdel[3]). Any otoliths with discrepancies in ages between the 2 readers were reexamined, and if a consistent age could not be determined for an otolith, it was removed from analysis. Following agreement on an age, marginal increment analysis was conducted by measuring marginal increments (to the nearest 0.001 mm) and comparing them to the width of the previous complete annuli by using the following equation (Tanaka et al., 1981): $C=W_n/W_{n-1}$, where C is the index of completion, W_n is the width of the marginal increment, and W_{n-1} is the width of the previous complete annulus. This method was used to confirm the periodicity of annuli formation. To determine ages when the most recent band was incomplete (indicating only a partial year of growth), we assigned one of 4 otolith margin codes to the incomplete outer ring, as viewed under transmitted light (Vanderkooy and Guindon-Tisdel[3]): 1 (opaque), 2 (1/3 translucent), 3 (1/2 translucent), and 4 (2/3 translucent). Each marginal code equals 0.25 years.

Because our sample collections lacked smaller fish (<100 mm TL), a truncated normal distribution was used to fit a 3-parameter von Bertalanffy growth curve to the age data, and separate model parameters were determined for each sex and ecoregion for comparison (Diaz et al.[4]). Because the von Bertalanffy growth curve is nonlinear, a sum of squares reduction test (Schabenberger and Pierce, 2002) was used with statistical software SAS (vers. 9.4; SAS Institute, Inc., Cary, NC), instead of a traditional analysis of variance to determine if there were differences in growth between ecoregions and sexes by comparing nonlinear trends between groups (α=0.05). The sum of squares reduction test was conducted by fitting a full and reduced model to the data. The test statistic (F) was calculated following this equation: $F=[(SSRR-SSRF)/(DFRR-DFRF)]/MSRF$, where $SSRR$ and $SSRF$ are the residual sums of squares from the reduced and full model, respectively, $DFRR$ and $DFRF$ are the residual degrees of freedom for the reduced and full model, respectively, and $MSRF$ is the mean sum of squares from the full model. This test evaluates the $SSRF$ when the $SSRR$ is removed from the model.

Results

The slopes of the weight–length relationships for male and female red lionfish were significantly different within the southeast ecoregion and did not differ in the 2 other ecoregions (ANCOVA: $F_{1,1528}$=12.68, P<0.001) (Table 1A, Fig. 2). The weight–length relationships from data pooled

[3] VanderKooy, S., and K. Guindon-Tisdel. 2003. A practical handbook for determining the age of Gulf of Mexico fishes. Gulf States Mar. Fish. Commission Publ. 111, 109 p. [Available from website.]

[4] Diaz, G. A., C. E. Porch, and M. Ortiz. 2004. Growth models for red snapper in U.S. Gulf of Mexico waters estimated from landings with minimum size limit restrictions. Southeast Data Assessment and Review SEDAR7-AW-01, 13 p. [Available from website.]

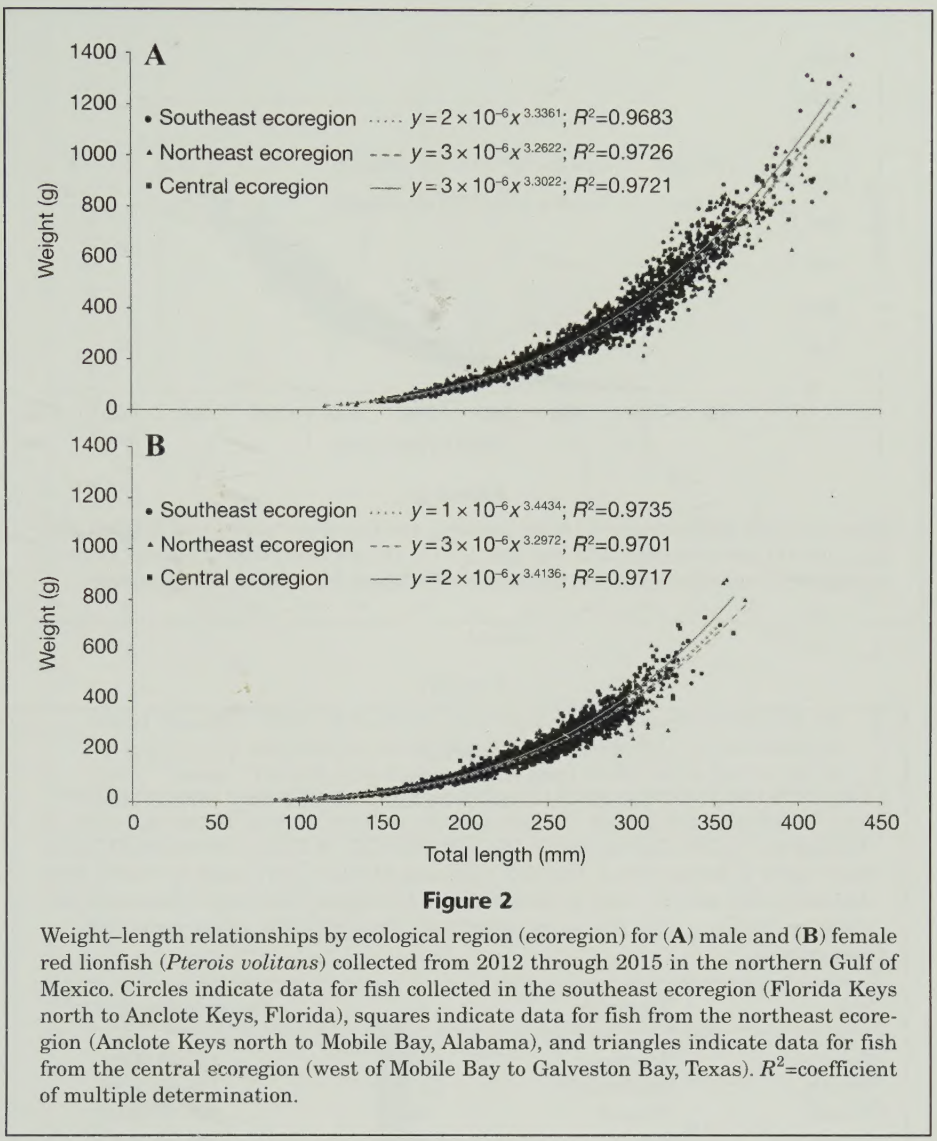

Figure 2

Weight–length relationships by ecological region (ecoregion) for (**A**) male and (**B**) female red lionfish (*Pterois volitans*) collected from 2012 through 2015 in the northern Gulf of Mexico. Circles indicate data for fish collected in the southeast ecoregion (Florida Keys north to Anclote Keys, Florida), squares indicate data for fish from the northeast ecoregion (Anclote Keys north to Mobile Bay, Alabama), and triangles indicate data for fish from the central ecoregion (west of Mobile Bay to Galveston Bay, Texas). R^2=coefficient of multiple determination.

across all 3 ecoregions for red lionfish had significantly different slopes by sex (ANCOVA: $F_{1,4670}$=21.96, P<0.001; Table 1A), indicating that females had a steeper weight–length relationship than males (Table 1A, Fig. 3) and, therefore, had a greater weight at a given TL. Pairwise comparisons of weight–length relationships by ecoregion (Table 1B) revealed a significant difference for male red lionfish only between the southeast and northeast ecoregions (ANCOVA: $F_{1,2038}$=8.16, P=0.004; Table 1B); whereas, significant differences were observed for female red lionfish in all comparisons between ecoregions except between the southeast and central ecoregions (ANCOVA: $F_{1,1025}$=0.61, P=0.436; Table 1B). However, in all ecoregions, males attained larger weights when adjusted for TL than females (Table 2). For a number of comparisons of ecoregions (Table 1B), weight–length relationships were significantly different, but the differences in weight were minimal on the basis of their estimated marginal means adjusted for TL (females: 18.21 g; males: 22.75 g; Table 2), and male red lionfish achieved a greater mean weight (333.62 g [standard error (SE) 3.58]) compared to females (195.13 [SE 3.69]) (Table 2).

From the 4250 pairs of otoliths that were extracted, a subsample of 1607 pairs of otoliths (744 males, 716 females, and 147 fish of unknown or undetermined sex) were randomly selected and processed from red lionfish ranging in size from 81 to 434 mm TL. Age agreement was reached for 1412 pairs of otoliths (87.9%) from that subsample. The APE for analysis of otoliths from the southeast ecoregion was 7.7, the APE for the northeast ecoregion was 14.2, and the APE for the central ecoregion was 11.7. With analysis results from all 3 ecoregions pooled, the APE between readers was 12.1. Annual increment formation was confirmed by using marginal increment analysis, with marginal increment widths most complete in May and gradually decreasing until a minimum index of completion

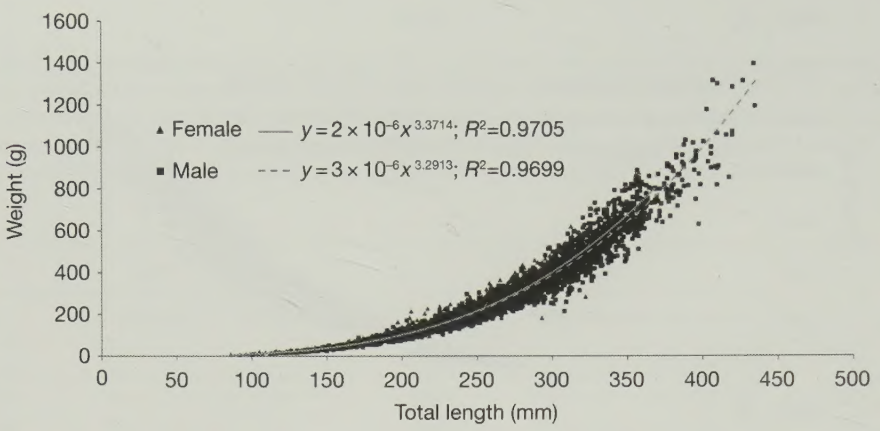

Figure 3

Weight–length relationships for male (squares) and female (triangles) red lionfish (*Pterois volitans*) collected from 2012 through 2015 in the northern Gulf of Mexico. Data are pooled for all sampled ecological regions. R^2=coefficient of multiple determination.

Table 2

Estimated marginal mean weight, in grams and adjusted for total length in millimeters, for invasive red lionfish (*Pterois volitans*) collected from 2012 through 2015 in 3 ecological regions (ecoregions) in the northern Gulf of Mexico: southeast (Florida Keys north to Anclote Keys, Florida), northeast (Anclote Keys north to Mobile Bay, Alabama), and central (west of Mobile Bay to Galveston Bay, Texas). Estimates are given for females, males, and sexes pooled with standard errors of the mean (SEs) in parentheses.

Sex	Ecoregion	*n*	Estimated weight (SE)
Female	Southeast	668	187.98 (1.69)
Female	Northeast	1227	193.88 (1.22)
Female	Central	348	206.19 (2.35)
Female	Pooled	2243	195.13 (3.69)
Male	Southeast	844	325.20 (2.36)
Male	Northeast	1101	334.50 (2.01)
Male	Central	346	347.95 (3.61)
Male	Pooled	2291	333.62 (3.58)
Pooled	Southeast	1512	258.75 (4.79)
Pooled	Northeast	2328	253.52 (3.86)
Pooled	Central	694	294.96 (7.07)

was reached in October and November, indicating the beginning of annuli formation (Fig. 4). Ages of red lionfish ranged from 0.5 to 4.5 years (Fig. 5), with 93% of aged red lionfish <2 years old. The smallest and youngest specimen collected in this study was a 81-mm-TL, 0.5-year-old fish of unknown sex, and the oldest specimen was a 380-mm-TL, 4.5-year-old male. The largest fish collected was a 434-mm-TL male, but its estimated age was 3.5 years. The state record for the longest lionfish caught in the northern GOM (459 mm TL) was for a fish collected off Pensacola, Florida (record available from website).

There were significant differences in age and growth parameters by sex and by ecoregion (all comparisons: P<0.001; for comparisons of modeled estimates with the sum of squares reduction test, see Table 3; for observed values, see Figure 6). Female red lionfish from the southeast ecoregion had the highest growth rate (K) and asymptotic length (L_∞) and achieved a greater length at age than

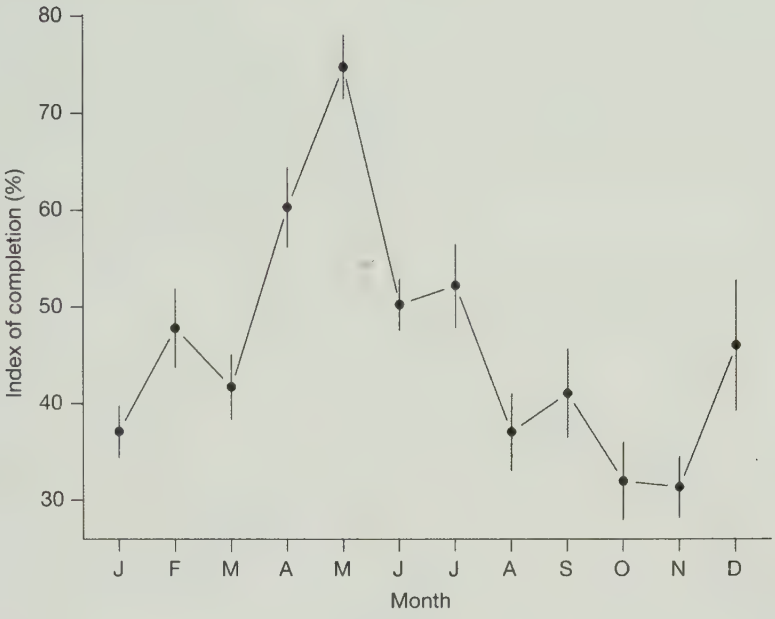

Figure 4

Plot of the mean index of marginal increment completion by month for red lionfish (*Pterois volitans*) collected from 2012 through 2015 in the northern Gulf of Mexico. Number of samples ranged from 30 in December to 192 in June. Vertical lines indicate standard errors of the mean.

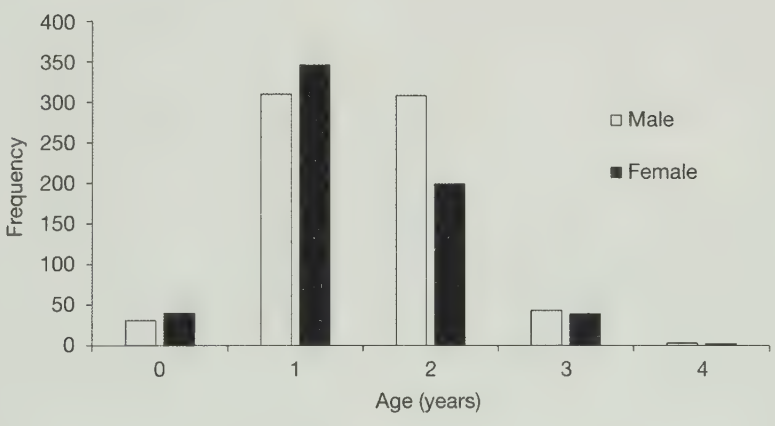

Figure 5

Age-frequency distribution of male and female red lionfish (*Pterois volitans*) collected from the northern Gulf of Mexico from 2012 through 2015.

females in the other 2 ecoregions (Table 3A, Fig. 6A). Similarly, male red lionfish from the southeast ecoregion also had the highest K and L_∞ values and achieved a greater length at age than males in the other 2 ecoregions (Table 3A, Fig. 6B). Data pooled by sex revealed a similar pattern, with the highest K and L_∞ values estimated for red lionfish from the southeast ecoregion and lowest values estimated for red lionfish from the central ecoregion (Table 3A, Fig. 6C). Separate comparisons were made by sex for each ecoregion, with male red lionfish achieving higher K and L_∞ values than females in all 3 ecoregions (all comparisons: $P<0.05$; Table 3B, Fig. 7, A–C). Model

Table 3

Estimates of von Bertalanffy growth curve parameters for invasive red lionfish (*Pterois volitans*) collected from 2012 through 2015 in 3 ecological regions (ecoregions) in the northern Gulf of Mexico: southeast (SE; Florida Keys north to Anclote Keys, Florida), northeast (NE; Anclote Keys north to Mobile Bay, Alabama), and central (C; west of Mobile Bay to Galveston Bay, Texas). The parameters are growth rate (K), asymptotic length (L_∞, given in millimeters in total length), and theoretical age when the length is zero (t_0). (**A**) Comparisons among ecoregions by sex. (**B**) Comparisons between sexes by ecoregion. A sum of square reduction test was used to determine differences in growth between ecoregions and sex by comparing nonlinear trends between groups (α=0.05).

A

	Pooled			Female			Male		
Parameter	SE	NE	C	SE	NE	C	SE	NE	C
K	0.569	0.544	0.539	0.574	0.549	0.542	0.576	0.547	0.543
L_∞	423.0	393.0	389.0	382.0	366.8	360.9	426.0	394.4	390.7
t_0	−0.155	−0.079	−0.341	−0.165	−0.089	−0.350	−0.170	−0.086	−0.354
	$F_{12,1412}$=27.143, P<0.001			$F_{12,626}$=7.303, P<0.001			$F_{12,695}$=12.606, P<0.001		

B

	Southeast		Northeast		Central		Pooled	
Parameter	Male	Female	Male	Female	Male	Female	Male	Female
K	0.576	0.574	0.547	0.549	0.543	0.542	0.550	0.508
L_∞	426.0	382.0	394.4	366.8	390.7	360.9	405.2	368.4
t_0	−0.170	−0.165	−0.086	−0.089	−0.354	−0.350	0.414	−0.482
	$F_{8,453}$=2.412, P=0.008		$F_{8,489}$=2.012, P=0.030		$F_{8,379}$=2.362, P=0.010		$F_{8,1321}$=16.226, P<0.001	

parameters determined from data pooled across all 3 ecoregions indicate that males also had higher K and L_∞ values than females (Table 3B, Fig. 7D).

Discussion

The results of this study reveal significant ecoregion- and sex-specific patterns in age, growth, and weight–length relationships of red lionfish. The K values of red lionfish collected from the southeast ecoregion were higher than those of red lionfish from the northeast and central ecoregions. Although it was expected that K values would be greater for the red lionfish collected in the southeast ecoregion, the L_∞ values of many fish species are usually lower in the more southern regions of their geographic range than in the more northern regions (Boehlert and Kappenman, 1980) because fish species from northern latitudes typically achieve larger sizes than fish species from southern latitudes (Lindsey, 1966). The observed anomaly in L_∞ values may also be a result of density-dependent growth, as has been documented in invasive red lionfish on small artificial reefs in the Bahamas (Benkwitt, 2013). Red lionfish collected from the northeast ecoregion in particular came from much smaller and isolated artificial and natural reefs and were found in much higher densities compared with densities observed on the reefs in the southeast ecoregion (senior author, unpubl. data).

The results of our marginal increment analysis indicate that annuli on otoliths from red lionfish were most complete in the spring (March–May) and least complete in the fall (September–October), a finding similar to that for another scorpaenid, the native blackbelly rosefish (*Helicolenus dactylopterus*), off the coasts of North and South Carolina (White et al., 1998). In contrast, black scorpionfish (*Scorpaena porcus*) from the Adriatic Sea had their most complete annuli in the late summer (July–September; La Mesa et al., 2010). Comparable thermal regimes between the northern GOM and North and South Carolina likely are the reason for the similar trends in annuli formation between invasive red lionfish and native blackbelly rosefish; similar trends have been documented in red snapper (*Lutjanus campechanus*) from similar thermal regimes (Nelson and Manooch, 1982). Black scorpionfish from the Adriatic Sea likely have delayed annuli completion compared with the annuli formation of the red lionfish in our study because of the relatively cooler sea-surface temperatures (~11°C) that that they experience in the spring. Sea-surface temperatures in the Adriatic Sea warm to above 20°C in July (La Mesa et al., 2010), similar to sea-surface temperatures observed in March in the northern GOM. Therefore, water temperature may drive annuli completion in these species, as has been reported for other species and regions (Pearson, 1996).

Age estimation was challenging for some red lionfish in our study, with an APE of 12.1 between readers for

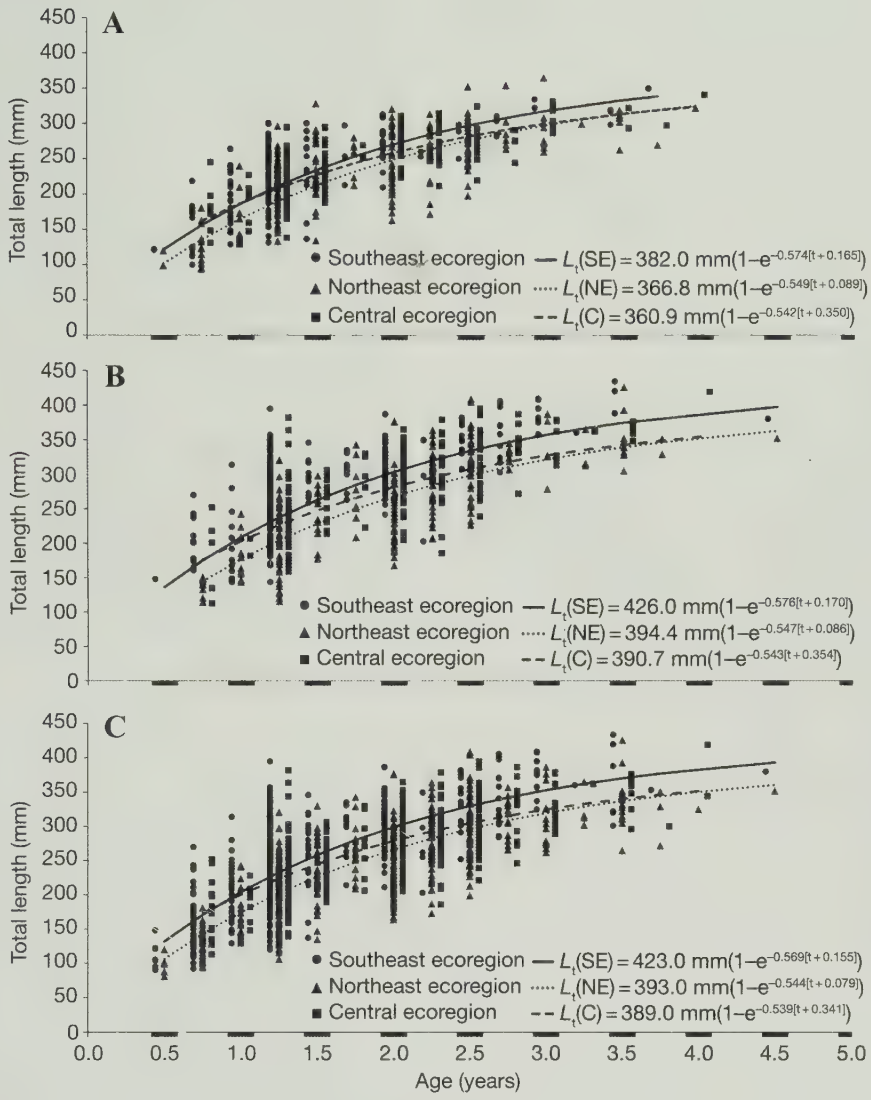
A
B
C
Total length (mm)
Age (years)
Southeast ecoregion — L_t(SE) = 382.0 mm(1–e$^{-0.574[t+0.165]}$)
Northeast ecoregion ····· L_t(NE) = 366.8 mm(1–e$^{-0.549[t+0.089]}$)
Central ecoregion -- L_t(C) = 360.9 mm(1–e$^{-0.542[t+0.350]}$)
Southeast ecoregion — L_t(SE) = 426.0 mm(1–e$^{-0.576[t+0.170]}$)
Northeast ecoregion ····· L_t(NE) = 394.4 mm(1–e$^{-0.547[t+0.086]}$)
Central ecoregion -- L_t(C) = 390.7 mm(1–e$^{-0.543[t+0.354]}$)
Southeast ecoregion — L_t(SE) = 423.0 mm(1–e$^{-0.569[t+0.155]}$)
Northeast ecoregion ····· L_t(NE) = 393.0 mm(1–e$^{-0.544[t+0.079]}$)
Central ecoregion -- L_t(C) = 389.0 mm(1–e$^{-0.539[t+0.341]}$)

Figure 6

The von Bertalanffy growth curves and associated equations for (**A**) female and (**B**) male red lionfish (*Pterois volitans*) as well as for (**C**) sexes pooled. Also plotted are observed lengths at age, by the 3 ecological regions (ecoregions) where red lionfish were collected from 2012 through 2015 in the northern Gulf of Mexico: southeast (Florida Keys north to Anclote Keys, Florida), northeast (Anclote Keys north to Mobile Bay, Alabama), and central (west of Mobile Bay to Galveston Bay, Texas).

otoliths from fish from all ecoregions pooled. This value is similar to the APE of 7 reported for analysis of otoliths from fish collected off northeast Florida (Johnson and Swenarton et al., 2016). However, all of our APE values are low compared with those of Edwards et al. (2014), who reported an APE of 58 between readers for lionfish collected in the Caribbean Sea. Differences in regional age determination may be expected because annuli in lionfish collected in tropical waters are likely to be more difficult to distinguish than annuli in lionfish living in more temperate regions. Lionfish in tropical waters likely have relatively consistent growth because of minimal variation in water temperatures, and fish in temperate waters experience periods of slow and fast growth (Pitcher and Hart, 1982).

The age of red lionfish from the northern GOM ranged from 0 to 4.5 years ($\bar{x}$=1.35), ages that are markedly lower than the maximum reported age of 30–33 years for a specimen held in an aquarium (Potts et al., 2010). Interestingly, the oldest age estimated in this study was 4.5 years

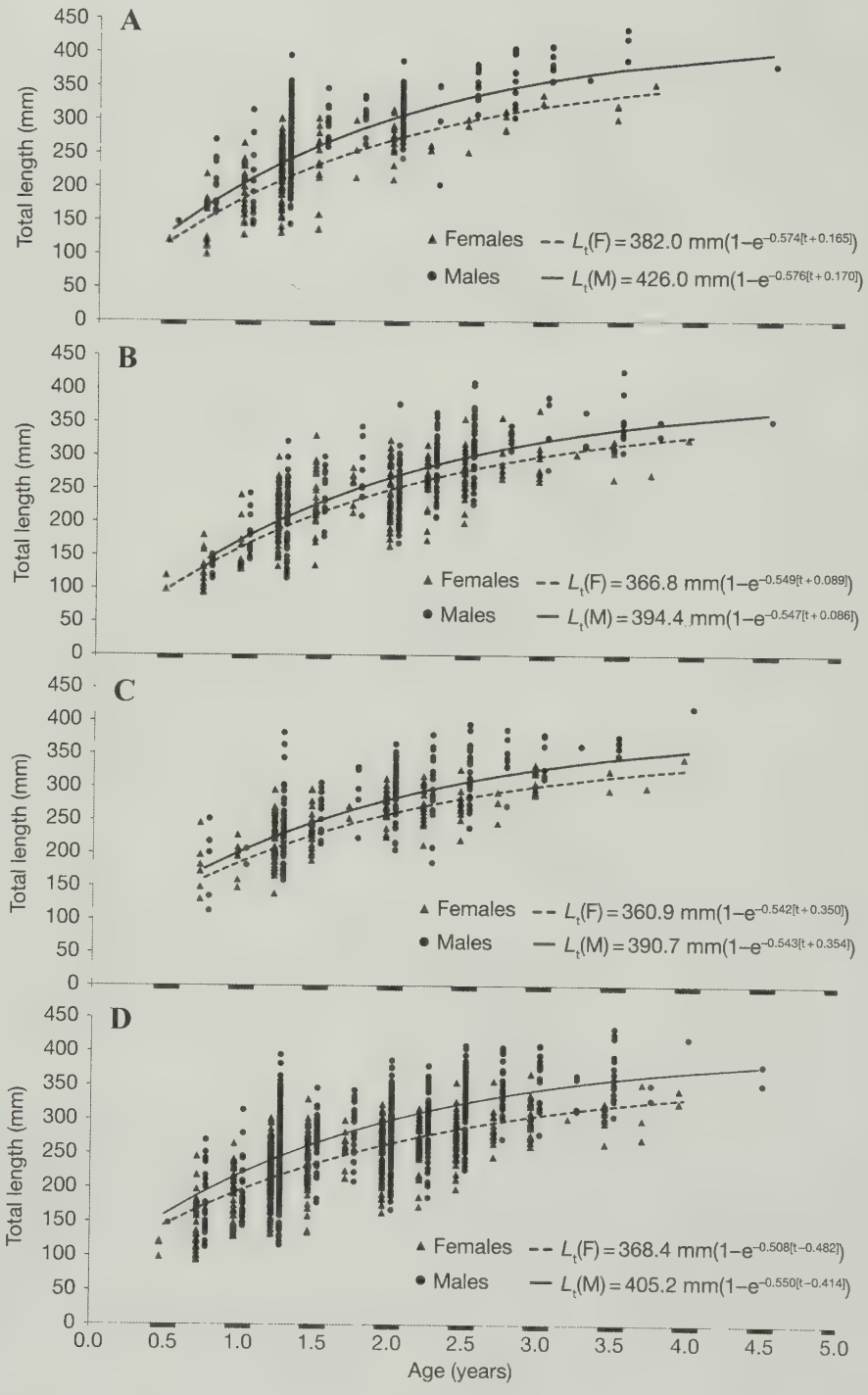
A
Total length (mm)
▲ Females -- $L_t(F) = 382.0\ mm(1-e^{-0.574[t+0.165]})$
● Males — $L_t(M) = 426.0\ mm(1-e^{-0.576[t+0.170]})$
B
Total length (mm)
▲ Females -- $L_t(F) = 366.8\ mm(1-e^{-0.549[t+0.089]})$
● Males — $L_t(M) = 394.4\ mm(1-e^{-0.547[t+0.086]})$
C
Total length (mm)
▲ Females -- $L_t(F) = 360.9\ mm(1-e^{-0.542[t+0.350]})$
● Males — $L_t(M) = 390.7\ mm(1-e^{-0.543[t+0.354]})$
D
Total length (mm)
▲ Females -- $L_t(F) = 368.4\ mm(1-e^{-0.508[t-0.482]})$
● Males — $L_t(M) = 405.2\ mm(1-e^{-0.550[t-0.414]})$
0.0 0.5 1.0 1.5 2.0 2.5 3.0 3.5 4.0 4.5 5.0
Age (years)

Figure 7

The von Bertalanffy growth curves and associated equations for red lionfish (*Pterois volitans*). Also plotted are observed lengths at age for female (triangles) and male (squares) red lionfish collected from 2012 through 2015 in the northern Gulf of Mexico, by ecological region (ecoregion), (**A**) southeast (Florida Keys north to Anclote Keys, Florida), (**B**) northeast (Anclote Keys north to Mobile Bay, Alabama), and (**C**) central (west of Mobile Bay to Galveston Bay, Texas), as well as for (**D**) all ecoregions pooled.

for a fish collected in November 2012, and the data from our study confirm the presence of red lionfish in the northern GOM as early as 2008, 2 years prior to the first detection in the region in 2010. Edwards et al. (2014) also found a single lionfish (*Pterois* sp.) with an estimated age that indicates it was present in the Caribbean Sea before the first detection off Little Cayman in 2010. Such delays in documented detections are expected because invasive species often are not detected immediately after introduction because of lag times associated with species expansion (Crooks and Soulé, 1999).

Age distribution of marine fish species is an important factor for assessing the health of a population (Berkeley et al., 2004). Typically, an established, healthy population will exhibit a "well-balanced" age structure (Brunel and Piet, 2013) with numerous larger, older individuals. In the northern GOM, 93% of red lionfish in our study were ≤2 years old in all 3 ecoregions. Similar results have been reported off Little Cayman (Edwards et al., 2014) and in the Atlantic Ocean off northeast Florida (Johnson and Swenarton, 2016) and North Carolina (Barbour et al., 2011), where the majority (>90%) of lionfish were ≤3 years old. The higher proportion of fish between the ages of 2 and 3 years found in Little Cayman and off northeast Florida and North Carolina is likely the result of lionfish having invaded those locations earlier than the northern GOM (Schofield, 2010).

Although red lionfish can live much longer than what has been described in this study and in studies in other invaded geographic areas, the truncated age-class distribution observed in this study is a further indication that the population of red lionfish in the northern GOM may still be stabilizing in the region because older individuals are not present or not captured. Red lionfish from the southern GOM that were aged in 2012 appeared to be much younger, with age and growth parameters that were much lower than those reported for this study and previous studies (Rodríguez-Cortés et al., 2015). This difference in age structure is likely a result of red lionfish being collected within the first 2 years of their invasion in the southern GOM. The difference also could be due to aging techniques: we determined age on the basis of otolith analysis, but Rodríguez-Cortés et al. (2015) estimated ages on the basis of size-frequency analysis that was not verified by using otoliths. It is important to now establish up-to-date region- and sex-specific age and growth parameters so that, in the future when the invasion of red lionfish theoretically has stabilized across the region (Benkwitt et al., 2017; Côté and Smith, 2018), the same parameters can be estimated to evaluate the success of the invasion.

There was an inconsistent pattern of differences in weight–length relationships among ecoregions with only males in the southeast ecoregion being heavier per length than males in the northeast ecoregion. In contrast, differences were found in females in all pairwise comparisons between ecoregions, except for the comparison of the southeast and central ecoregions. Overall, weight–length relationships based on data pooled for males and females and on estimated marginal means adjusted for TL indicate minor differences in weight among ecoregions: 18.21 g for females and 22.75 g for males.

Differences in weight–length relationships of lionfish have been reported throughout the range of the invasion among regions that are larger than the ecoregions used in our study (Suppl. Table) (online only). Some published comparisons of weight–length relationships have been based on data pooled across a range of locations within the sampled region (Barbour et al., 2011; Edwards et al., 2014; Sabido-Itzá et al., 2016), and the relationships derived from those pooled data differ from those presented here for the northern GOM. Another study compared weight–length data pooled by year, reporting a significant difference between the first and last year (2011–2013) (Dahl and Patterson, 2014). In contrast, Benkwitt et al. (2017) documented no changes in size structure in lionfish from the Bahamas over a 10-year period. Recently, Pusack et al. (2016) reported that red lionfish in their native range grow at a slower rate and achieve smaller maximum sizes than those in the range of their invasion. Finally, lionfish in the range they have invaded may be less susceptible to predation because of their larger size and would also be able to consume larger prey items (see review in Côté and Smith, 2018).

In this study, male red lionfish found in the northern GOM achieved greater weight and length than females. In contrast, results from early work in the northern GOM (Fogg et al., 2013) indicate no significant differences in weight–length relationships by sex for red lionfish. One explanation for these differences between studies may be that the data from Fogg et al. (2013) came from early in the invasion and, therefore, likely had not yet reached an asymptotic value. Although von Bertalanffy growth parameters were not reported by sex in other age and growth studies on invasive lionfish species (e.g., Potts et al. 2010; Barbour et al. 2011; Rodríguez-Cortés et al. 2015; Johnson and Swenarton 2016), age and growth and weight–length data quantified in our study confirm that sexual dimorphism exists with males growing larger and faster than females. Sexual dimorphic growth was documented also for invasive lionfish in Little Cayman by using otolith analysis, but weight–length relationships were not evaluated (Edwards et al., 2014). Males in our study achieved a greater length-at-age than females and, similar to males examined by Edwards et al. (2014), had significantly larger K and L_∞ values than females. Males of the related scorpeanid species, blackbelly rosefish, also appear to grow faster and slightly larger than females (White et al., 1998). In contrast, female black scorpionfish, native to the eastern Atlantic Ocean, Mediterranean Sea, and Black Sea, attain larger sizes than males (Bilgin and Çelik, 2009).

The differences observed between male and female red lionfish in age and growth and in weight–length relationships are likely a result of the greater resources that females allocate to reproductive output (Gadgil and Bossert, 1970). Female red lionfish mature in their first year of life and are capable of reproducing every few days during 11 months of the year (Fogg et al., 2017). These elevated and constant reproductive rates likely result in more

Table 4

Estimates of von Bertalanffy growth curve parameters, with sexes pooled, for invasive red lionfish (*Pterois volitans*) collected from 2012 through 2015 in 3 ecological regions (ecoregions) in the northern Gulf of Mexico: southeast (Florida Keys north to Anclote Keys, Florida), northeast (Anclote Keys north to Mobile Bay, Alabama), and central (west of Mobile Bay to Galveston Bay, Texas). The parameters are growth rate (K), asymptotic length (L_∞, given in millimeters in total length [TL]), and theoretical age when the length is zero (t_0). Because of truncated data sets (i.e., a lack of red lionfish <100 mm TL), a sum of squares reduction test was used to compare model parameters between all ecoregions and sexes. All comparisons were significantly different (P<0.01). For comparison, parameters pooled by sex are included for specimens from North Carolina (Barbour et al., 2011), Little Cayman (Edwards et al., 2014), Florida Keys (Swenarton et al., 2016), northeast (NE) Florida (Johnson and Swenarton et al., 2016), and Yucatan, Mexico (Rodríguez-Cortés et al., 2015).

	Northern Gulf of Mexico								
Parameter	Southeast	Northeast	Central	Pooled	North Carolina	Little Cayman	Florida Keys	NE Florida	Yucatan, Mexico
L_∞	423.0	393.0	389.0	400.2	425.2	349.0	411.0	448.0	420.0
K	0.569	0.544	0.539	0.560	0.470	0.420	0.700	0.470	0.880
t_0	−0.155	−0.079	−0.341	−0.210	−0.500	−1.010	0.000	0.000	−0.107

energy shunted to reproduction than to growth; therefore, growth in female red lionfish is reduced upon maturation. This trade-off of reduced growth in females as the energy is redirected to reproduction has been described in numerous fish species (Reznick, 1983; Roff, 1983; Parker, 1992).

Another potential reason that males grow larger than females is that males need to increase their chances of success in male rivalries and physical combat and, therefore, their opportunities for mating (Shine, 1989). Evidence of combat between large red lionfish (>350 mm TL, presumably males) has been observed in the northern GOM in the form of abrasions across the body. Recently, agonistic behavior between 2 large lionfish (*Pterois* spp.) has been observed and documented in Honduras (Fogg and Faletti, 2018).

Growth rates and other life history traits vary by region in other marine fish species (Choat and Axe, 1996; Ruttenberg et al., 2005). The K value for red lionfish in the northern GOM is greater than that reported for fish from Little Cayman (Edwards et al., 2014), North Carolina (Barbour et al., 2011), and northeast Florida (Johnson and Swenarton, 2016), although K values reported for fish from the Florida Keys (Swenarton et al., 2015) and Yucatan, Mexico (Rodríguez-Cortés et al., 2015), were much greater than those in all other studies (Table 4). The higher K value observed in the northern GOM could explain why densities of red lionfish are higher there than anywhere else in the geographic range that they have invaded (Dahl and Patterson, 2014). The pattern for age and growth of red lionfish in the northern GOM appears to be most similar to that of lionfish from the Atlantic Ocean off northeast Florida and North Carolina (Table 4). Similarities and differences in age and growth among studies could, in part, be driven by environmental thermal regimes (Lyons et al., 2017; Barker et al., 2018) in addition to other biological and ecological factors (South et al., 2017). However, age and growth will need to be reevaluated in the future because our study examined samples collected early in the invasion of the northern GOM region.

Age and growth data are important to assess potential changes to the population structure of red lionfish that result from implementation of management plans, disease events, and environmental incidents such as an algal bloom. For example, Chagaris et al. (2017) modeled how potential strategies for management of lionfish may affect several recreationally and commercially important native fish species on the West Florida Shelf. The age and growth relationships of lionfish used in their model were based on fish from outside of the region of the West Florida Shelf and, therefore, may not have correctly reflected population dynamics. Moreover, other management plans from agencies around the invaded region specifically mention the need for regional age and growth data (Morris[5]; ANSTF[6]; Johnston et al., 2015), and these plans noted the need for ongoing research. Accurate and region-specific weight–length, age, and growth data are vital for developing age-structured population models that can be used to evaluate potential effects of targeted removals on the red lionfish population (Barbour et al., 2011) and the potential population-level effects of large-scale disease for red lionfish and devil firefish (Harris et al.[7]). These data can also be applied to behavioral studies for which only size information is available (e.g., Garcia-Rivas et al., 2018).

Graham and Fanning (2017) reviewed management plans for invasive lionfish species in the Caribbean Sea, but research updates are needed so that future management

[5] Morris, J. A., Jr. (ed.). 2012. Invasive lionfish: a guide to control and management. Gulf Caribb. Fish. Inst., Spec. Publ. Ser. 1, 113 p. [Available from website.]

[6] ANSTF (Aquatic Nuisance Species Task Force). 2014. National invasive lionfish prevention and management plan, 48 p. Prepared by the Invasive Lionfish Control Ad-hoc Committee of the ANSTF. [Available from website.]

[7] Harris, H. E., A. Q. Fogg, R. P. E. Yanong, S. Frasca Jr., T. Cody, T. B. Waltzek, and W. F. Patterson III. 2018. First report of an emerging ulcerative skin disease in invasive lionfish. Univ. Fla., Inst. Food Agric. Sci., Ext. Data Inf. Source (EDIS) FA209, 7 p. [Available from website.]

activities, including local "culling" programs (Green et al., 2017; Mizrahi et al., 2017), lead to more accurate forecasting (Johnston et al., 2017) and effective regional management. Information from regional demographic data sets, coupled with identification of spatial and temporal patterns in the harvest vulnerability of older and larger lionfish, can be used to identify regions or seasons that need better protection or regulation (Zhou et al., 2010; Tobin et al., 2013). Data from this study can inform development of region-specific management strategies for controlling the invasion of lionfish in the GOM. This study provides the first regional estimates of life history parameters for red lionfish in the northern GOM, where populations of this invasive species appear to be not only established but also expanding their range (Dahl and Patterson, 2014; Dahl et al., 2016; Fogg et al., 2017). Life history information provided here can be incorporated into studies of competition between lionfish and reef fish species (see Rojas-Vélez et al., 2019) that will enhance management decision-making and stock assessments.

Acknowledgments

We thank Coast Watch Alliance and the volunteer divers and fishermen for their financial and logistical support. We also thank the undergraduate interns sponsored by the Marine Education Center at the Gulf Coast Research Laboratory, University of Southern Mississippi, for assistance in processing red lionfish. Additional travel and research support was provided by the Gulf and Caribbean Fisheries Institute, the Mississippi Chapter of the American Fisheries Society, and the Lytle Scholarship and Tom McIllwain Scholarship of the University of Southern Mississippi.

Literature cited

Acero P., A., D. Bustos-Montes, P. Pabón Quintero, C. J. Polo-Silva, and A. Sanjuan Muñoz.
2019. Feeding habits of *Pterois volitans*: a real threat to Caribbean coral reef biodiversity. *In* Impacts of invasive species on coastal environments: coasts in crisis (C. Makowski and C. W. Finkl, eds.), p. 269–314. Springer Intl. Publ., Cham, Switzerland.

Aguilar-Perera, A., and A. Tuz-Sulub.
2010. Non-native, invasive red lionfish (*Pterois volitans* [Linnaeus, 1758]: Scorpaenidae), is first recorded in the southern Gulf of Mexico, off the northern Yucatan Peninsula, Mexico. Aquat. Invasions 5:S9–S12.

Albins, M. A.
2015. Invasive Pacific lionfish *Pterois volitans* reduce abundance and species richness of native Bahamian coral-reef fishes. Mar. Ecol. Prog. Ser. 522:231–243.

Barbour, A. B., M. L. Montgomery, A. A. Adamson, E. Díaz-Ferguson, and B. R. Silliman.
2010. Mangrove use by the invasive lionfish *Pterois volitans*. Mar. Ecol. Prog. Ser. 401:291–294.

Barbour, A. B., M. S. Allen, T. K. Frazer, and K. D. Sherman.
2011. Evaluating the potential efficacy of invasive lionfish (*Pterois volitans*) removals. PLoS ONE 6(5):e19666.

Barker, B. D., A. Z. Horodysky, and D. W. Kerstetter.
2018. Hot or not? Comparative behavioral thermoregulation, critical temperature regimes, and thermal tolerances of the invasive lionfish *Pterois* sp. versus native western North Atlantic reef fishes. Biol. Invasions 20:45–58.

Beck, M. W.
2003. The sea around: conservation planning in marine regions. *In* Drafting a conservation blueprint: a practitioner's guide to planning for biodiversity (G. R. Groves, ed.), p. 319–344. Island Press, Washington, D.C.

Beck, M. W., and M. Odaya.
2001. Ecoregional planning in marine environments: identifying priority sites for conservation in the northern Gulf of Mexico. Aquat. Conserv. 11:235–242.

Benkwitt, C. E.
2013. Density-dependent growth in invasive lionfish (*Pterois volitans*). PLoS ONE 8(6):e66995.
2015. Non-linear effects of invasive lionfish density on native coral-reef fish communities. Biol. Invasions 17:1383–1395.

Benkwitt, C. E., M. A. Albins, K. L. Buch, K. E. Ingeman, T. L. Kindinger, T. J. Pusack, C. D. Stallings, and M. A. Hixon.
2017. Is the lionfish invasion waning? Evidence from the Bahamas. Coral Reefs 36:1255–1261.

Berkeley, S. A., M. A. Hixon, R. J. Larson, and M. S. Love.
2004. Fisheries sustainability via protection of age structure and spatial distribution of fish populations. Fisheries 29(8):23–32.

Bilgin, S., and E. Ş. Çelik.
2009. Age, growth and reproduction of the black scorpionfish, *Scorpaena porcus* (Pisces, Scorpaenidae), on the Black Sea coast of Turkey. J. Appl. Ichthyol. 25:55–60.

Boehlert, G. W., and R. F. Kappenman.
1980. Variation of growth with latitude in two species of rockfish (*Sebastes pinniger* and *S. diploproa*) from the northeast Pacific Ocean. Mar. Ecol. Prog. Ser. 3:1–10.

Brown-Peterson, N. J., and J. R. Hendon.
2013. Notes on the biology of invasive lionfish (*Pterois* spp.) from the northcentral Gulf of Mexico. Gulf Caribb. Res. 25:117–120.

Brunel, T., and G. J. Piet.
2013. Is age structure a relevant criterion for the health of fish stocks? ICES. J. Mar. Sci. 70:270–283.

Chagaris, D., S. Binion-Rock, A. Bogdanoff, K. Dahl, J. Granneman, H. Harris, J. Mohan, M. B. Rudd, M. K. Swenarton, R. Ahrens, et al.
2017. An ecosystem-based approach to evaluating impacts and management of invasive lionfish. Fisheries 42(8): 421–431.

Choat, J. H., and L. M. Axe.
1996. Growth and longevity in acanthurid fishes; an analysis of otolith increments. Mar. Ecol. Prog. Ser. 134:15–26.

Claydon, J. A. B., M. C. Calosso, and S. B. Traiger.
2012. Progression of invasive lionfish in seagrass, mangrove and reef habitats. Mar. Ecol. Prog. Ser. 448:119–129.

Copp, G. H., and M. G. Fox.
2007. Growth and life history traits of introduced pumpkinseed (*Lepomis gibbosus*) in Europe, and the relevance to its potential invasiveness. *In* Biological invaders in inland waters: profiles, distribution, and threats (F. Gherardi, ed.), p. 289–306. Springer, Dordrecht, Netherlands.

Côté, I. M., and N. S. Smith.
2018. The lionfish *Pterois* sp. invasion: has the worst-case scenario come to pass? J. Fish Biol. 92:660–689.

Crooks, J. A., and M. E. Soulé.
1999. Lag times in population explosions of invasive species: causes and implications. *In* Invasive species and biodiversity management (O. T. Sandland, P. J. Schei, and Å. Viken, eds.), p.103–125. Kluwer Acad. Publ., Dordrecht, Netherlands.

Curtis, J. S., K. R. Wall, M. A. Albins, and C. D. Stallings.
2017. Diet shifts in a native mesopredator across a range of invasive lionfish biomass. Mar. Ecol. Prog. Ser. 573: 215–228.

Dahl, K. A., and W. F. Patterson III.
2014. Habitat-specific density and diet of rapidly expanding invasive red lionfish, *Pterois volitans*, populations in the northern Gulf of Mexico. PLoS ONE 9(8):e105852.

Dahl, K. A., W. F. Patterson III, and R. A. Snyder.
2016. Experimental assessment of lionfish removals to mitigate reef fish community shifts on northern Gulf of Mexico artificial reefs. Mar. Ecol. Prog. Ser. 558:207–221.

Darling, E. S., S. J. Green, J. K. O'Leary, and I. M. Côté.
2011. Indo-Pacific lionfish are larger and more abundant on invaded reefs: a comparison of Kenyan and Bahamian lionfish populations. Biol. Invasions 13:2045–2051.

Dulvy, N. K., N. V. C. Polunin, A. C. Mill, and N. A. Graham.
2004. Size structural change in lightly exploited coral reef fish communities: evidence for weak indirect effects. Can. J. Fish. Aquat. Sci. 61:466–475.

Edwards, M. A., T. K. Frazer, and C. A. Jacoby.
2014. Age and growth of invasive lionfish (*Pterois* spp.) in the Caribbean Sea, with implications for management. Bull. Mar. Sci. 90:953–966.

Fogg, A. Q.
2017. Life history of the non-native invasive red lionfish (*Pterois volitans*) in the northern Gulf of Mexico. M.S. thesis, 160 p. Univ. South. Miss., Ocean Springs, MS.

Fogg, A. Q., and M. E. Faletti.
2018. Invasive lionfish (*Pterois* sp.) agonistic behavior observations. Bull. Mar. Sci. 94:1–2.

Fogg, A. Q., E. R. Hoffmayer, W. B. Driggers III, M. D. Campbell, G. J. Pellegrin, and W. Stein.
2013. Distribution and length frequency of invasive lionfish (*Pterois* sp.) in the northern Gulf of Mexico. Gulf Caribb. Res. 25:111–115.

Fogg, A. Q., N. J. Brown-Peterson, and M. S. Peterson.
2017. Reproductive life history characteristics of invasive red lionfish (*Pterois volitans*) in the northern Gulf of Mexico. Bull. Mar. Sci. 93(3):791-813.

Frazer, T. K., C. A. Jacoby, M. A. Edwards, S. C. Barry, and C. M. Manfrino.
2012. Coping with the lionfish invasion: can targeted removals yield beneficial effects? Rev. Fish. Sci. 20:185–191.

Gadgil, M., and W. H. Bossert.
1970. Life historical consequences of natural selection. Am. Nat. 104:1–24.

García-Rivas, M. D. C., S. Machkour-M'Rabet, G. Pérez-Lachaud, J. J. Schmitter-Soto, R. Céréghino, C. Doneys, N. St-Jean, and Y. Hénaut.
2018. Age-dependent strategies related to lionfish activities in the Mexican Caribbean. Environ. Biol. Fish. 101:563–578.

Graham, R. E., and L. M. Fanning.
2017. A comparison of eight country plans for the invasive Indo-Pacific lionfish in the wider Caribbean. Global Ecol. Conserv. 12:253–262.

Green, S. J., and I. M. Côté.
2009. Record densities of Indo-Pacific lionfish on Bahamian coral reefs. Coral Reefs 28:107.

Green, S. J., N. K. Dulvy, A. M. L. Brooks, J. L. Akins, A. B. Cooper, S. Miller, and I. M. Côté.
2014. Linking removal targets to the ecological effects of invaders: a predictive model and field test. Ecol. Appl. 24:1311–1322.

Green, S. J., E. B. Underwood, and J. L. Atkins.
2017. Mobilizing volunteers to sustain local suppression of a global marine invasion. Conserv. Lett. 10:726–735.

Hamner, R. M., D. W. Freshwater, and P. E. Whitfield.
2007. Mitochondrial cytochrome *b* analysis reveals two invasive lionfish species with strong founder effects in the western Atlantic. J. Fish Biol. 71(sb):214–222.

Ingeman, K. E., and M. S. Webster.
2015. Native prey mortality increases but remains density-dependent following lionfish invasion. Mar. Ecol. Prog. Ser. 531:241–252.

Johnson, E. G., and M. K. Swenarton.
2016. Age, growth and population structure of invasive lionfish (*Pterois volitans/miles*) in northeast Florida using a length-based, age-structured population model. PeerJ 4:e2730.

Johnson, J., C. E. Bird, M. A. Johnston, A. Q. Fogg, and J. D. Hogan.
2016. Regional genetic structure and genetic founder effects in the invasive lionfish: comparing the Gulf of Mexico, Caribbean and North Atlantic. Mar. Biol. 163:216

Johnston, M. A., S. R. Gittings, and J. A. Morris Jr.
2015. NOAA National Marine Sanctuaries lionfish response plan (2015–2018): responding, controlling, and adapting to an active marine invasion. NOAA Off. Mar. Sanctuaries, Mar. Sanctuaries Conserv. Ser. ONMS-15-01, 55 p. [Available from website.]

Johnston, M. W., A. M. Bernard, and M. S. Shivji.
2017. Forecasting lionfish sources and sinks in the Atlantic: are Gulf of Mexico reef fisheries at risk? Coral Reefs 36:169–181.

Jud, Z. R., C. A. Layman, J. A. Lee, and D. A. Arrington.
2011. Recent invasion of a Florida (USA) estuarine system by lionfish *Pterois volitans/P. miles*. Aquat. Biol. 13:21–26.

La Mesa, M., G. Scarcella, F. Grati, and G. Fabi.
2010. Age and growth of the black scorpionfish, *Scorpaena porcus* (Pisces: Scorpaenidae) from artificial structures and natural reefs in the Adriatic Sea. Sci. Mar. 74:677–685.

Lindsey, C. C.
1966. Body sizes of poikilotherm vertebrates at different latitudes. Evolution 20:456–465.

Lyons, T. J., Q. M. Tuckett, and J. E. Hill.
2017. Lower lethal temperatures for two commonly traded species of lionfishes: implications for establishment beyond *Pterois volitans* and *P. miles*. Copeia 105:630–633.

Meister, H. S., D. M. Wyanski, J. K. Loefer, S. W. Ross, A. M. Quattrini, and K. J. Sulak.
2005. Further evidence for the invasion and establishment of *Pterois volitans* (Teleostei: Scorpaenidae) along the Atlantic coast of the United States. Southeastern Nat. 4:193–206.

Mizrahi, M., J. K. Chapman, C. L. A. Gough, F. Humber, and L. G. Anderson.
2017. Management implications of the influence of biological variability of invasive lionfish diet in Belize. Manage. Biol. Invasions 8:61–70.

Morris, J. A., Jr., and J. L. Akins.
2009. Feeding ecology of invasive lionfish (*Pterois volitans*) in the Bahamian archipelago. Environ. Biol. Fish. 86:389–398.

Nelson, R. S., and C. S. Manooch III.
1982. Growth and mortality of red snappers in the west-central Atlantic Ocean and northern Gulf of Mexico. Trans. Am. Fish. Soc. 111:465-475.

Parker, G. A.
1992. The evolution of sexual size dimorphism in fish. J. Fish. Biol. 41(sB):1–20.

Pasko, S., and J. Goldberg.
2014. Review of harvest incentives to control invasive species. Manage. Biol. Invasions 5:263–277.

Pearson, D. E.
1996. Timing of hyaline-zone formation as related to sex, location, and year of capture in otoliths of the widow rockfish, *Sebastes entomelas*. Fish. Bull. 94:190–197.
Pitcher, T. J., and P. J. B. Hart.
1982. Fisheries ecology, 414 p. Croon Helm Ltd., London.
Potts, J. C., D. Berrane, and J. A. Morris Jr.
2010. Age and growth of lionfish from the western North Atlantic. Proc. Gulf Caribb. Fish. Inst. 63:314. [Available from website.]
Pusack, T. J., C. E. Benkwitt, K. Cure, and T. L. Kindinger.
2016. Invasive red lionfish (*Pterois volitans*) grow faster in the Atlantic Ocean than in their native Pacific range. Environ. Biol. Fish. 99571–579.
Reznick, D.
1983. The structure of guppy life histories: the tradeoff between growth and reproduction. Ecology 64:862–873.
Robertson, D. R., and K. L. Cramer.
2014. Defining and dividing the Greater Caribbean: insights from the biogeography of shorefishes. PLoS ONE 9(7): e102918.
Rocha, L. A., C. R. Rocha, C. C. Baldwin, L. A. Weigt, and M. McField.
2015. Invasive lionfish preying on critically endangered reef fish. Coral Reefs 34:803–806.
Rodríguez-Cortés, K. D., A. Aguilar-Perera, and J. L. Bonilla-Gómez.
2015. Growth and mortality of red lionfish, *Pterois volitans* (Actinopterygii: Scorpaeniformes: Scorpaenidae), in the Parque Nacional Arrecife Alacranes, southern Gulf of Mexico, as determined by size-frequency analysis. Acta Ichthyol. Piscat. 45:175–179.
Roff, D. A.
1983. An allocation model of growth and reproduction in fish. Can. J. Fish. Aquat. Sci. 40:1395–1404.
Rojas-Vélez, S., J. Tavera, and A. Acero.
2019. Unraveling lionfish invasion: Is *Pterois volitans* truly a morphologically novel predator in the Caribbean? Biol. Invasions 21:1921–1931.
Ruttenberg, B. I., A. J. Haupt, A. I. Chiriboga, and R. R. Warner.
2005. Patterns, causes and consequences of regional variation in the ecology and life history of a reef fish. Oecologia 145:394–403.
Ruttenberg, B. I., P. J. Schofield, J. L. Akins, A. Acosta, M. W. Feeley, J. Blondeau, S. G. Smith, and J. S. Ault.
2012. Rapid invasion of Indo-Pacific lionfishes (*Pterois volitans* and *Pterois miles*) in the Florida Keys, USA: evidence from multiple pre- and post-invasion data sets. Bull. Mar. Sci. 88:1051–1059.
Sabido-Itzá, M. M., A. Medina-Quej, A. Jesús-Navarrete, J. M. Gómez-Poot, and M. C. García-Rivas.
2016. Size structure as evidence of population establishment of *Pterois volitans* (Scorpaeniformes: Scorpaenidae) in the South Mexican Caribbean. Rev. Biol. Trop. 64:353–362.
Schabenberger, O., and F. J. Pierce.
2002. Nonlinear Models. *In* Contemporary statistical models for the plant and soil sciences, p. 183–293. CRC Press, Boca Raton, FL.
Schofield, P. J.
2010. Update on geographic spread of invasive lionfishes (*Pterois volitans* [Linnaeus, 1758] and *P. miles* [Bennett, 1828]) in the Western North Atlantic Ocean, Caribbean Sea and Gulf of Mexico. Aquat. Invasions 5:S117–S122.
Secor, D. H., Dean J. M., and E. H. Laban.
1991. Manual for otolith removal and preparation for microstructural examination. Belle W. Baruch Inst. Mar. Biol. Coast. Res. Tech. Publ. 1991-01, 85 p.
Shine, R.
1989. Ecological causes for the evolution of sexual dimorphism: a review of the evidence. Q. Rev. Biol. 64:419–461.
South, J., J. T. A. Dick, M. McCard, D. Barrios-O'Neill, and A. Anton.
2017. Predicting predatory impact of juvenile invasive lionfish (*Pterois volitans*) on a crustacean prey using functional response analysis: effects of temperature, habitat complexity and light regimes. Environ. Biol. Fish. 100:1155–1165.
Spalding, M. D., H. E. Fox, G. R. Allen, N. Davidson, Z. A. Ferdaña, M. Finlayson, B. S. Halpern, M. A. Jorge, A. Lombana, S. A. Lourie, et al.
2007. Marine ecoregions of the world: a bioregionalization of coastal and shelf areas. BioScience 57:573–583.
Sullivan Sealey, K., and G. Bustamante.
1999. Setting geographic priorities for marine conservation in Latin America and the Caribbean, 125 p. Nat. Conserv., Arlington, VA. [Available from website.]
Swenarton, M., E. G. Johnson, and L. Akins.
2015. Regional comparisons of lionfish (*Pterois* spp.) population demographics from the east coast of Florida. Proc. Gulf Caribb. Fish. Inst. 67:215–216. [Available from website.]
Tamburello, N., and I. M. Côté.
2015. Movement ecology of Indo-Pacific lionfish on Caribbean coral reefs and its implications for invasion dynamics. Biol. Invasions 17:1639–1653.
Tanaka, K., Y. Mugiya, and J. Yamada.
1981. Effects of photoperiod and feeding on daily growth patterns in otoliths of juvenile *Tilapia nilotica*. Fish. Bull. 79:459–466.
Tobin, A., L. Currey, and C. Simpfendorfer.
2013. Informing the vulnerability of species to spawning aggregation fishing using commercial catch data. Fish. Res. 143:47–56.
Villaseñor-Derbez, J. C., and S. Fitzgerald.
2019. Spatial variation in allometric growth of invasive lionfish has management implications. PeerJ 7:e6667.
White, D. B., D. M. Wyanski, and G. R. Sedberry.
1998. Age, growth, and reproductive biology of the blackbelly rosefish from the Carolinas, U.S.A. J. Fish Biol. 53: 1274–1291.
Yáñez-Arancibia, A., and J. W. Day.
2004. Environmental sub-regions in the Gulf of Mexico coastal zone: the ecosystem approach as an integrated management tool. Ocean Coast. Manage. 47:727–757.
Zhou, S., A. D. M. Smith, A. E. Punt, A. J. Richardson, M. Gibbs, E. A. Fulton, S. Pascoe, C. Bulman, P. Bayliss, and K. Sainsbury.
2010. Ecosystem-based fisheries management requires a change to the selective fishing philosophy. Proc. Natl. Acad. Sci. U.S.A. 107:9485–9489.

National Marine
Fisheries Service
NOAA

Fishery Bulletin
established in 1881

Spencer F. Baird
First U.S. Commissioner
of Fisheries and founder
of *Fishery Bulletin*

Reproductive potential of light dusky rockfish (*Sebastes variabilis*) and northern rockfish (*S. polyspinis*) in the Gulf of Alaska

Christina L. Conrath

Email address for contact author: christina.conrath@noaa.gov

Kodiak Laboratory
Resource Assessment and Conservation Engineering Division
Alaska Fisheries Science Center
National Marine Fisheries Service, NOAA
301 Research Court
Kodiak, Alaska 99615

Abstract—The reproductive potential of northern rockfish (*Sebastes polyspinis*) and light dusky rockfish (*S. variabilis*) in the Gulf of Alaska was examined by measuring the success of oocyte and embryo development. The potential annual fecundity, reproductive failure rates, and relationships of these parameters to maternal size were examined. Both species have a seasonally synchronous reproductive cycle with parturition occurring in the late spring to early summer. Northern rockfish had a mean relative fecundity of 165.1 oocytes/g for specimens captured in December and 109.6 embryos/g for specimens captured in May. Light dusky rockfish had a mean relative fecundity of 152.1 oocytes/g for specimens collected in December and 108.1 embryos/g for specimens captured in May. Reproductive failure was easiest to discern for the samples from fish collected in May, with partial and total failure primarily occurring because of lack of oocyte development or fertilization failure. Northern rockfish had a rate of total reproductive failure or skipped spawning of 16.3%, and light dusky rockfish had a total reproductive failure rate of 15.6%. As light dusky and northern rockfish grow larger throughout their lives, their relative fecundities increase and the likelihood of reproductive failure decreases. Fecundity values, failure rates, and maternal effects on the reproductive potential of these species can be used to inform future stock assessments.

Manuscript submitted 5 July 2018.
Manuscript accepted 27 June 2019.
Fish. Bull. 117:140–150 (2019).
Online publication date: 12 July 2019.
doi: 10.7755/FB.117.3.2

The views and opinions expressed or implied in this article are those of the author (or authors) and do not necessarily reflect the position of the National Marine Fisheries Service, NOAA.

The northern rockfish (*Sebastes polyspinis*) and light dusky rockfish (*S. variabilis*) are the second- and third-most commercially important rockfish species in Alaska waters, behind the Pacific ocean perch (*S. alutus*) (Hulson et al., 2015; Lunsford et al., 2016). Both species are captured predominately by bottom-trawl, catcher-processor fishing vessels or smaller shore-based trawlers operating out of Kodiak, Alaska (Clausen and Heifetz, 2002; Hulson et al., 2015). The stock assessments of these species in the Gulf of Alaska use a separable, age-structured model as the primary assessment tool. Input parameters to the model include fishery-dependent data, such as catch, age, size, composition, and maturity data, and fishery-independent data, including estimates of biomass and age and size composition based on biennial trawl surveys (Hulson et al., 2015; Lunsford et al., 2016).

Northern rockfish range from waters of northern British Columbia and Alaska, across the North Pacific Ocean, to the eastern part of Kamchatka Peninsula and the northern Kuril Islands in Russia (Allen and Smith, 1988). They are most abundant in Alaska waters from the central Gulf of Alaska to the western Aleutian Islands. Adult northern rockfish in the Gulf of Alaska are found in relatively shallow offshore banks of the outer continental shelf at depths of 75–150 m. They are the second-most abundant and commercially important rockfish in the Gulf of Alaska and the Aleutian Islands fisheries management areas (Clausen and Heifetz, 2002). Northern rockfish have supported a valuable domestic commercial fishery since 1990 in the Gulf of Alaska and were captured in foreign and joint venture fisheries prior to this period (Hulson et al., 2015).

Light dusky rockfish range from Hokkaido, Japan, through the Bering Sea and the Aleutian Islands, to Johnstone Strait, British Columbia (Love et al., 2002). Light dusky rockfish are commonly found at depths of 100–200 m in the Gulf of Alaska, and the highest catch per unit of effort generally occurs at depths of 100–149 m. Light dusky rockfish are most commonly associated with northern rockfish, Pacific ocean perch, and harlequin rockfish (*S. variegatus*), and bycatch of light dusky rockfish is highest in hauls of vessels targeting northern rockfish and vice versa (Reuter, 1999).

All species within the genus *Sebastes* mate using internal fertilization and give birth to planktonic larvae (Kendall and Lenarz, 1987). These species appear to be truly viviparous, meaning that the embryos receive sustenance from the mother in addition to yolk reserves during gestation (Boehlert et al., 1987).

Maturity ogives have been published for both of these species (Chilton, 2007, 2010), but little information is available about other reproductive parameters. Maternal effects, abortive maturity, spawning omission or skipped spawning, and spatial disparities in the quantity of broods have all been documented for members of this genus (Hannah and Parker, 2007; Beyer et al., 2015; Conrath, 2017). Reproductive potential or the number of viable larvae released by a population at parturition is influenced by both the number of developing oocytes (potential fecundity) and the proportion of adults that have incomplete spawning (partial reproductive failure) or fail to spawn (total reproductive failure or skipped spawning). The objective of this project was to assess the reproductive potential of light dusky and northern rockfish at 2 different sites within the Gulf of Alaska by examining a variety of reproductive parameters, including development of oocytes and embryos within the ovary, gonadosomatic indices, potential annual fecundity, annual rates of reproductive failure, and maternal effects. Values for these parameters will be provided to stock assessment scientists for the management of these and other rockfish species in this region.

Materials and methods

Two research cruises were conducted in May (spring) and December (winter) 2014. During each cruise, 2 sites in the central Gulf of Alaska were sampled: one at 49 Fathom Pinnacle and one on Snakehead Bank (Fig. 1). Both sites are located offshore of Kodiak Island near Middle and Southern Albatross Bank. We collected samples from female northern and light dusky rockfish at the site at 49 Fathom Pinnacle. Adult light dusky rockfish also were captured at the site at Snakehead Bank (Table 1). Each fish was measured for fork length (FL) and total weight, and the ovary was removed and preserved in a solution of 10% neutral buffered formalin.

A sample removed from the center of one lobe of the ovary from each specimen was embedded in paraffin and thin sectioned to 6 µm. Standard histological techniques were used to stain these tissue samples with hematoxylin and eosin (Sheehan and Hrapchak, 1980). These samples were used to examine the development of oocytes and embryos within the ovary, with stages defined on the basis of the terminology of Bowers (1992) (Table 2). Each sample was examined to determine which oocyte or embryo stages were present by using a compound microscope. The most advanced oocyte or embryo stage within the section was identified. In addition, the section was examined for the presence of atretic oocytes. Alpha atresia was characterized by the disintegration of the nucleus, irregularly shaped oocytes, disintegration of yolk, and the dissolution of the zona radiata. Beta atresia was characterized by oocytes having a compact structure composed of disorganized granulosa cells. Delta atresia was characterized by a dark yellow or brown pigment within the granulosa cells (Hunter and Macewicz, 1985a).

Figure 1

Map of the 2 sites where northern rockfish (*Sebastes polyspinis*) and light dusky rockfish (*S. variabilis*) were sampled off Kodiak Island near Middle and Southern Albatross Bank in the central Gulf of Alaska in May and December 2014. Female northern and light dusky rockfish were collected at the site on 49 Fathom Pinnacle (1). Adult light dusky rockfish were also captured at the site on Snakehead Bank (2).

Table 1

Fork length (FL), total weight (TW), gonadosomatic index (GSI), potential annual fecundity (PAF), measured as the number of developing oocytes or embryos present within the female, and relative fecundity (RF), measured as PAF/TW, of female light dusky rockfish (*Sebastes variabilis*) and northern rockfish (*S. polyspinis*) collected during cruises conducted in the spring (May) and winter (December) of 2014 at 2 sites in the Gulf of Alaska: 49 Fathom Pinnacle (49 FP) and Snakehead Bank (SHB). The range, mean, standard error of the mean (SE), and sample size (n) for each parameter are given.

Species	Season	Site	FL (cm)	TW (g)	GSI	PAF (no. of oocytes or embryos)	RF (oocytes/g or embryos/g)
Light dusky rockfish	Spring	49 FP	360–517 mean: 456 (n=100)	720–2342 mean: 1702 (n=100)	0.002–0.166 mean: 0.088 (SE 0.007, n=60)	31,510–330,700 mean: 190,300 (SE 11,450, n=40)	24.7–164 mean: 106 (SE 5.46, n=40)
		SHB	273–544 mean: 465 (n=105)	260–3474 mean: 1,963 (n=105)	0.001–0.197 mean: 0.088 (SE 0.008, n=68)	21,870–665,800 mean: 256,200 (SE 23,690, n=36)	18.3–216 mean: 111 (SE 6.97, n=36)
	Winter	49 FP	403–497 mean: 457 (n=138)	1,066–2212 mean: 1619 (n=138)	0.010–0.125 mean: 0.041 (SE 0.001, n=89)	49,290–455,100 mean: 258,237 (SE 7635, n=103)	46.2–273 mean: 158 (SE 4.08, n=103)
		SHB	332–525 mean: 445 (n=42)	636–2418 mean: 1494 (n=42)	0.004–0.043 mean: 0.028 (SE 0.001, n=28)	107,000–388,800 mean: 227,600 (SE 14,4000, n=32)	79.1–197 mean: 140 (SE 5.14, n=32)
Northern rockfish	Spring	49 FP	345–453 mean: 412 (n=127)	620–1466 mean: 1162 (n=127)	0.070–0.222 mean: 0.140 (SE 0.006, n=38)	62,650–212,000 mean: 130,700 (SE 6118, n=36)	53.2–176 mean: 110 (SE 4.81, n=36)
	Winter	49 FP	270–463 mean: 416 (n=157)	266–1738 mean: 1183 (n=157)	0.013–0.091 mean: 0.059 (SE 0.002, n=128)	33,690–346,600 mean: 197,100 (SE 5347, n=121)	43.9–251 mean: 165 (SE 4.02, n=121)

Table 2

Stages of oocyte and embryo development in ovaries of northern (*Sebastes polyspinis*) and light dusky (*S. variabilis*) rockfish. These stages, based on terminology of Bowers (1992), were used to identify the most advanced development stage present in samples from fish collected during May and December 2014 in the Gulf of Alaska.

Stage	Physical description
1. Primary growth	Oogonia, early perinuclear and late perinuclear ooyctes
2. Early yolk	Oocytes contain the earliest signs of yolk accumulation, small spherical globules of yolk in the periphery of the oocyte
3. Advanced yolk	Oocyte content is at least 50% yolk droplets, nucleus still well defined
4. Migratory nucleus	Nucleus migrates to the periphery of the oocyte, nuclear membrane becomes irregular, nucleoli disappear
5. Ovulation	Yolk material begins to merge and form a single united mass
6. Early embryo	Blastoderm cap present with a large yolk mass
7. Embryo body	Embryo body appears, blastoderm cap of cells develops into recognizable tissue
8. Eyed embryo	Retinal pigmentation becomes apparent and is well defined
9. Embryo-reduced yolk	Yolk attached to the embryo is reduced in size and may only be present as droplets
10. Postovulatory follicles	The follicles that remain after parturition

Postovulatory follicles are the follicular structure that remains after the oocyte or larvae has been extruded (Hunter and Macewicz, 1985b).

Fish maturity status or class was determined by examining the most advanced oocyte stage present and the amount and types of atresia present. Fish were considered mature if there was evidence that they would spawn within the current reproductive year or evidence that they had spawned in a prior year. Immature fish included both those fish that had no oocyte development beyond stage 2 and those fish in which development had been resorbed (abortive mature). Mature fish included fish with incomplete or complete advanced oocyte development of stage 3 or higher and fish with no advanced development that were skipped spawners (Table 3).

Table 3

Classifications used to determine maturity of northern rockfish (*Sebastes polyspinis*) and light dusky rockfish (*S. variabilis*) collected in May and December 2014 in the Gulf of Alaska. POF=postovulatory follicles. For stages of oocyte and embryo development, see Table 2.

Class	Oocyte or embryo development	Description
Immature	Primary growth	No oocyte development beyond stage 2.
	Abortive maturity	Oocyte development is initiated, then oocytes are resorbed. No evidence of prior spawning. Identified histologically by presence of widespread alpha atresia, but no POFs or beta or delta atresia.
Mature	Development	Oocyte or embryo development at stage 3 or at a more advanced stage of development.
	Partial development (incomplete fertilization)	Some oocytes within the ovary are at stage 3 or at a more advanced stage of development. Some oocytes are not developing, because of incomplete fertilization. Identified histologically by the presence of oocytes at the one-cell blastodisc stage.
	No development (skipped spawning)	
	Resting	No initiation of oocyte development. Identified histologically by development in stage 1 or 2 with evidence of a prior spawning (beta or delta atresia or POFs).
	Resorbing	Oocyte development is initiated, but oocytes are later resorbed. Identified histologically by widespread alpha atresia and evidence of a prior spawning (beta or delta atresia or POFs).
	Fertilization failure	Oocytes develop but are not fertilized; therefore, no embryogenesis occurs. Identified histologically by the presence of oocytes at the one-cell blastodisc stage. In skipped spawners, all developing oocytes are at this oocyte stage of development.

The ovary was patted dry at the laboratory, and a wet weight was recorded. A gonadosomatic index (GSI) was calculated for all mature fish by using the following equation: *GSI*=gonad weight/total body weight. The mean and standard error of these values for each species during each season were determined. Ovary weights were unavailable for some fish whose ovary contained advanced embryos because the ovary structure was difficult to maintain. This delicate ovary structure was particularly prevalent in samples collected in May that contained eyed embryos with a thin and fragile ovarian wall that made it difficult to weigh the ovary without losing some of the embryos.

Fecundity was estimated at each site by using all individuals caught in December that had both lobes of their ovary and all specimens caught in May that had at least one complete lobe of their ovary. The difference between months sampled in which individuals were included was necessary because of the small number of individuals with a complete ovary that were collected in May. If only one lobe of the ovary was available, the total ovary weight was estimated by multiplying the weight of the complete lobe by 2. Individual potential annual fecundity was estimated by using a gravimetric approach in which the weight of a subsample of oocytes or embryos present was extrapolated to estimate the total ovary weight. Fecundity was estimated by using only fish that had an ovary that was composed predominately of oocytes or embryos at a development stage of 3 or higher and that had no evidence of partial or total reproductive failure. In December, all ovaries examined contained oocytes that were in either the migratory nucleus or ovulation stages, whereas in May all ovaries contained eyed embryos. Therefore, values of fecundity for specimens captured in December are given in number of oocytes or number of oocytes per gram, and values of fecundity for specimens captured in May are given in either number of embryos or number of embryos per gram. Two subsamples were collected from randomly chosen quadrants of one lobe of the ovary. If the coefficient of variation from the 2 initial samples was greater than 5%, 2 additional subsamples were collected. The individual potential annual fecundity was determined by averaging the fecundity estimates taken for each sample and multiplying by the total ovary weight. In addition, relative fecundity was determined by dividing potential annual fecundity by the total weight of the fish.

Reproductive failure in adult light dusky and northern rockfish was defined as partial or total lack of oocyte or embryo development in mature fish. Partial reproductive failure was identified by the presence of developing oocytes and non-developing oocytes within the ovary of a fish and was caused by incomplete fertilization (Fig. 2). Mature fish with no oocyte development were considered to be experiencing total reproductive failure and were classified as skipped spawners. Three types of skipped spawning similar to those defined by Rideout et al. (2005) were identified: resting skipped spawning (no initiation of oocyte development), resorbing skipped spawning

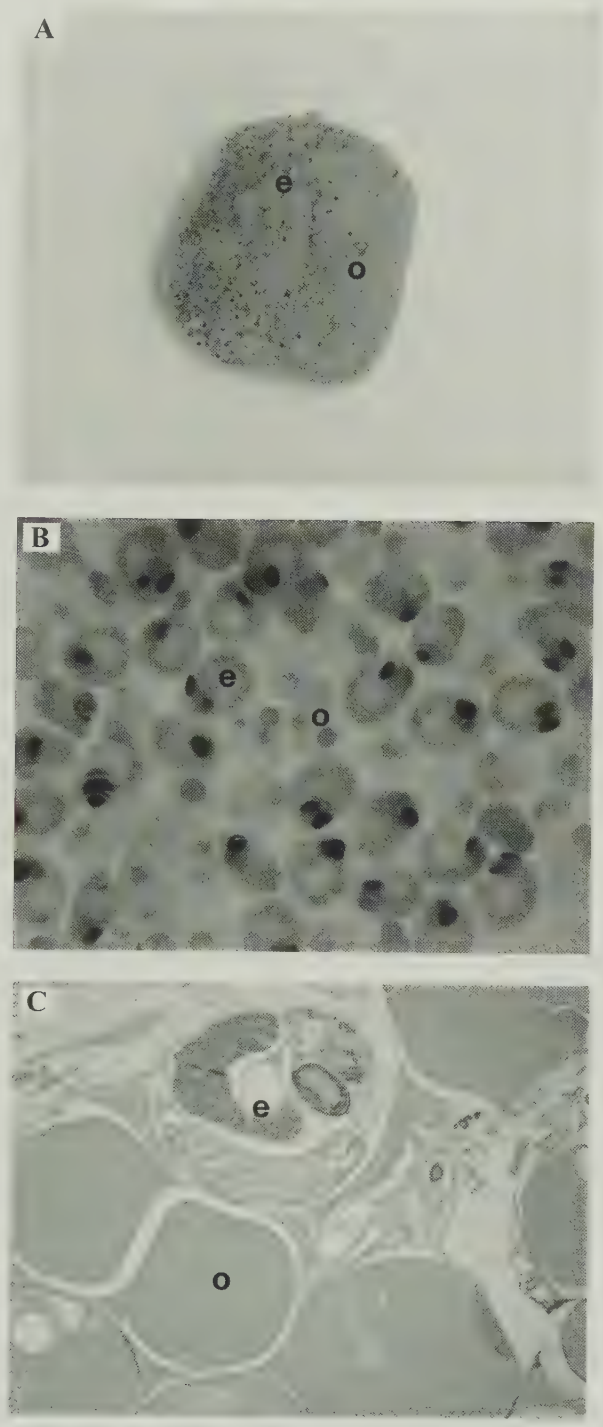

Figure 2

Images of ovary samples from northern rockfish (*Sebastes polyspinis*) collected in May 2014 in the Gulf of Alaska, showing partial reproductive failure due to incomplete fertilization. (**A**) A whole section of one lobe of an ovary. The left side of the lobe has fertilized embryos in the eyed stage (e), and the majority of the ovary is filled with unfertilized oocytes (o). (**B**) Several eyed embryos (e) and unfertilized oocytes (o) under a dissecting microscope. (**C**) A histological section with eyed embryos (e) and unfertilized oocytes (o).

(oocytes that had initiated development were degenerating), and skipped spawning caused by fertilization failure (oocytes developed to the one-cell blastodisc stage but were not fertilized, and embryogenesis was not initiated) (Fig. 3). The proportion of adult northern and light dusky rockfish that had ovaries with partial or total reproductive failure were examined during the May and December sampling periods (Table 3).

Generalized linear models, with Gaussian distribution for response variables, were used to examine effects of maternal size, site, and season on relative fecundity.

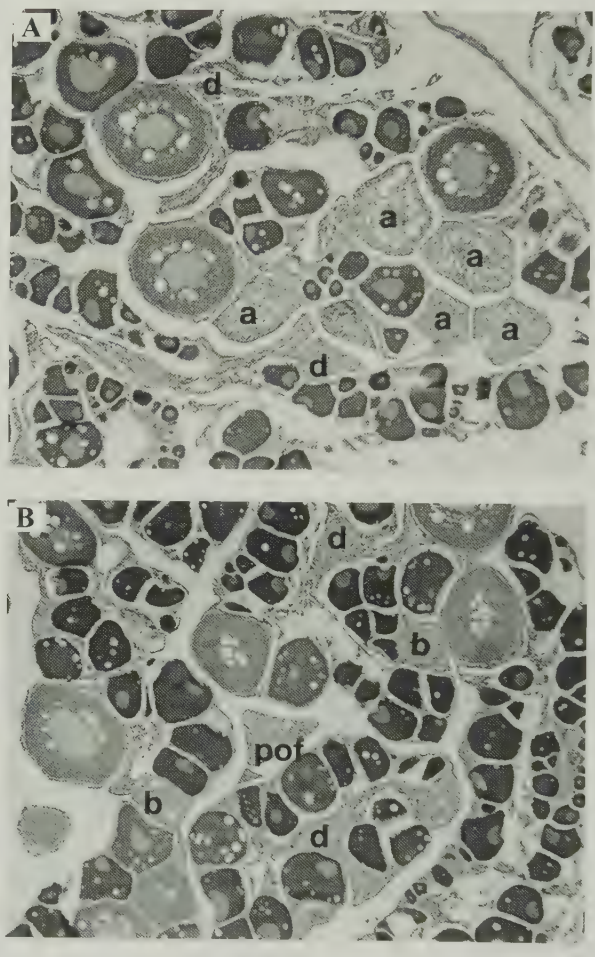

Figure 3

Images of sections of oocytes from northern rockfish (*Sebastes polyspinis*) captured in December 2014 in the Gulf of Alaska, showing 2 types of total reproductive failure or skipped spawning, with beta atresia (b), delta atresia (d), and potential postovulatory follicles (POF) that indicate a prior spawning. (**A**) Resorbing type of skipped spawning: section with alpha atresia (a) that indicates resorption of recently developing oocytes. (**B**) Resting type of skipped spawning: section with no alpha atresia or recent development present, a prior spawning is evident on the basis of late stage beta and delta atresia or the presence of post ovulatory follicles.

Diagnostic plots of residual trends verses fitted values and standardized residuals versus theoretical quantiles (Q-Q plots) were examined visually for trends for each model. Generalized linear models with a binomial distribution were used to examine the effect of maternal size on reproductive failure. To test for overdispersion, each binomial model was repeated by using quasi-binomial distribution, and the dispersion parameter was examined. A backward stepwise approach was used to populate the models with explanatory parameters that were statistically significant (α=0.05). The GSI values were compared by site in each season. Effects of season, fish length, and site were considered in models fitted to relative fecundity data. Effects of fish length and site were considered in models fitted to values of fertilization failure and incomplete fertilization for fish captured in the month of May and to values of total reproductive failure for fish captured in May and December. Reproductive parameter values from the 2 sites sampled were combined if the site was not significantly related to the parameter being examined (α=0.05). The Akaike information criterion was used to determine which model best fit the data. The generalized linear models were completed by using the packages stats4 (vers. 3.2.0) and multcomp (vers. 3.2.5; Hothorn et al., 2008) in statistical software R, vers. 3.2.0 (R Core Team, 2015).

Results

Catches of northern and light dusky rockfish within both study sites were dominated by adult individuals with very few immature individuals and no individuals exhibiting abortive maturation. No adult northern rockfish were captured at the site on Snakehead Bank; therefore, comparisons between sites were limited to data for light dusky rockfish captured in both seasons. During May, all mature light dusky rockfish collected throughout both of the sampled sites that lacked evidence of reproductive failure had ovaries that were dominated by eyed embryos. This finding was also true for nearly all northern rockfish; one female contained embryos at the embryo body stage. During December, all mature individuals of both species had ovaries that were dominated by oocytes that were either in the late migratory nucleus or early ovulation stage unless there was evidence of reproductive failure. Both species were found to have highly synchronous oocyte and embryo development, and the timing of this development was very similar between the 2 species.

The GSI values for northern rockfish were generally higher than those for light dusky rockfish, and these values for both species were higher in May prior to parturition than in December (Table 1). The mean GSI for light dusky rockfish in May was not significantly related to site (P=0.71). The mean GSI for light dusky rockfish captured in the month of December was considerably higher at 49 Fathom Pinnacle than at Snakehead Bank. There were no obvious trends in residuals in the model diagnostic plots for the GSI.

Estimates of fecundity were generally lower for northern rockfish than light dusky rockfish during both seasons, with higher values found during the winter (Table 1). Relative fecundity was calculated to compensate for the relationship between fecundity and size and was also greater for both species in December. Light dusky and northern rockfish had similar values of mean relative fecundity during each season. The mean relative fecundity of northern rockfish was 109.6 embryos/g for specimens captured in May and 165.1 oocytes/g for specimens captured in December. The mean relative fecundity of dusky rockfish was 108.1 embryos/g for fish captured in May and 152.1 oocytes/g for fish collected in December. Parameters tested in the model to explain variation in relative fecundity included site (for light dusky rockfish only), season, and FL (Table 4). Relative fecundity estimates were significantly higher (P<0.001) in December than in May for both species and increased with size for both species (Fig. 4).

Total and partial reproductive failure occurred in both light dusky and northern rockfish and were found in both seasons. Reproductive failure was more prevalent and easier to discern in the specimens caught in May because of the advanced state of embryo development; therefore, only the data from the cruise conducted in May were used for this analysis. The proportion of adult individuals in which total reproductive failure had occurred was very similar for both species (16.3% for northern rockfish and 15.6% for light dusky rockfish), but the proportion of fish undergoing partial reproductive failure was higher in northern rockfish (14.9%) than in light dusky rockfish (3.7%). The most common type of total reproductive failure in northern rockfish, with 68.4% of cases, was the fertilization failure type of skipped spawning, and 31.6% of cases of total reproductive failure were due to the resting type of skipped spawning. For light dusky rockfish, more than half of total reproductive failure was due to the resting type of skipped spawning (55.2%), a smaller proportion was due to the fertilization failure type of skipped spawning (41.4%), and just one fish (3.4%) was experiencing the resorbing type of skipped spawning. Rates of reproductive failure of light dusky rockfish were not significantly different between sites; therefore, failure rates for light dusky rockfish from both sites were combined in this analysis (total reproductive failure: P=0.63; fertilization failure and incomplete fertilization: P=0.38).

Larger fish of both species (>42 cm FL) were significantly less likely to experience total reproductive failure, particularly failure due to resting skipped spawning (Fig. 5). The relationship of total reproductive failure caused by resting skipped spawning and FL was significant for both species (light dusky rockfish: P=0.011; northern rockfish: P=0.044), but the relationship between total reproductive failure caused by fertilization failure was significant only for northern rockfish (light dusky rockfish: P=0.238; northern rockfish: P=0.002). Partial or total reproduction failure due to incomplete fertilization or fertilization failure, however, was not significantly related to FL for either species (light dusky rockfish:

Table 4

Results from use of generalized linear models to explain variation in relative fecundity of adult northern rockfish (*Sebastes polyspinis*) and light dusky rockfish (*S. variabilis*) captured in May and December 2014 in the Gulf of Alaska. Parameters include season, site (light dusky rockfish only), and fork length. Entries for the model that was determined to have the best fit to data for each species are italicized. Differences in Akaike information criterion (ΔAIC) between the best fit model and the other models for each species are given.

Species	Model	Parameters	*P*	ΔAIC
Northern rockfish	*1*	*Season*	*<0.001*	
		Fork length	*0.031*	
	2	Season	<0.001	2.8
	3	Fork length	0.043	48.7
Light dusky rockfish	1	Season	<0.001	0.3
		Site	0.206	
		Fork length	<0.001	
	2	*Fork length*	*<0.001*	
		Season	*<0.001*	
	3	Season	<0.001	29.5

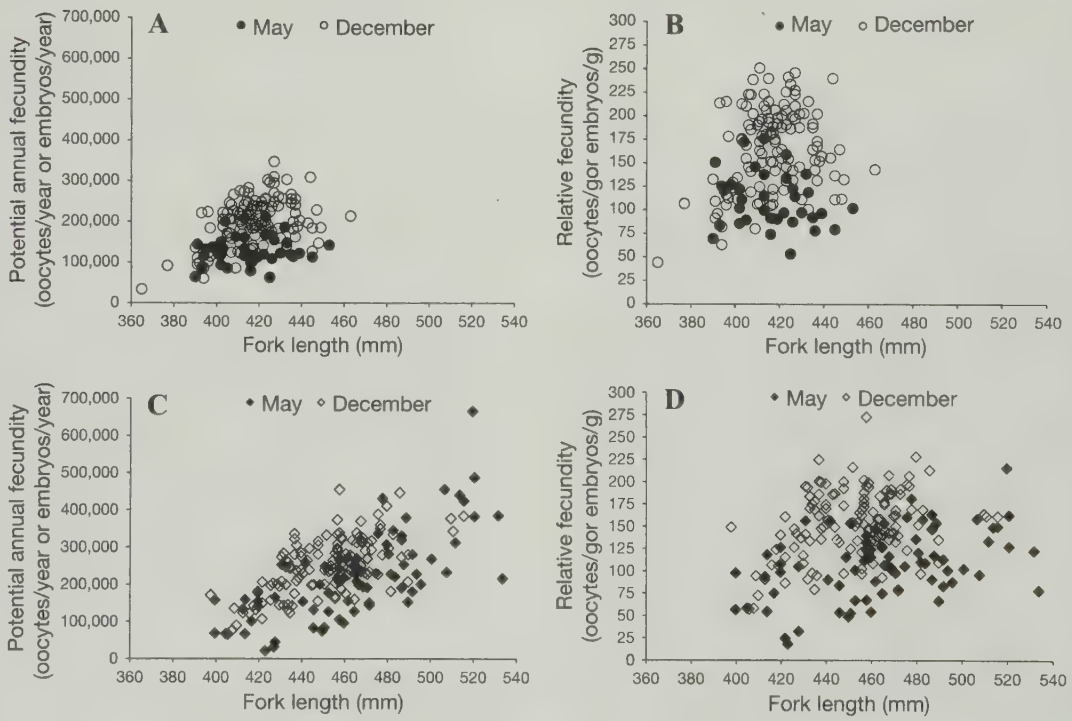

Figure 4

Relationships of potential annual fecundity, measured as number of developing oocytes or embryos, and of relative fecundity, calculated as potential annual fecundity divided by total weight, to fork length for (**A** and **B**) northern rockfish (*Sebastes polyspinis*) and (**C** and **D**) light dusky rockfish (*S. variabilis*) collected during May and December 2014. Black circles and diamonds represent data for fish collected in May. Open circles and diamonds represent data for fish collected in December.

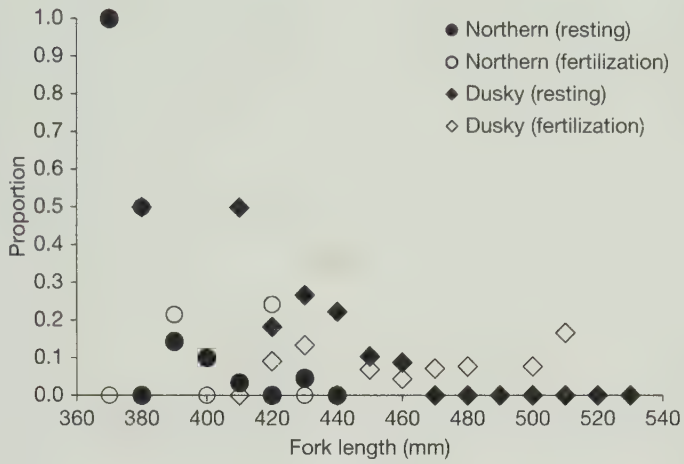

Figure 5

Proportion of northern rockfish (*Sebastes polyspinis*) and light dusky rockfish (*S. variabilis*), captured in May 2014 in the Gulf of Alaska, that experienced skipped spawning caused by fertilization failure (open circles or diamonds) or the resting type of skipped spawning (black circles or diamonds), by fork length.

P=0.278; northern rockfish: P=0.096). The quasi-binomial models all had dispersion values that were close to 1 (<1.1), indicating that there was little overdispersion in all of these models.

Discussion

Light dusky and northern rockfish within the Gulf of Alaska have a highly synchronous reproductive cycle with nearly all individuals having ovaries dominated by oocytes or embryos in the same state of development in any period of the year. I calculated similar GSI values for both species during each of the 2 seasons. Although I sampled only during 2 periods of the year, results from this study are consistent with a synchronous annual cycle with parturition occurring in the early summer months. Fish of both species captured in December were in mid-vitellogenesis, and those captured in May were in late embryogenesis, indicating that they were nearing parturition. This timing is similar to that reported for northern rockfish in the Gulf of Alaska by Chilton (2007), who observed parturition occurring from April through June. Similarly, May has previously been reported as the peak month of parturition for light dusky rockfish in the Gulf of Alaska (Chilton, 2010). Northern rockfish in the Aleutian Islands appear to have a similar reproductive cycle, but the peak month of parturition is April (TenBrink and Spencer, 2013), indicating that reproductive events may occur earlier in the year in the region of the Aleutian Islands.

Fecundity estimates for both species were lower during the spring. Some loss of embryos occurred during capture in May because embryos are expelled as a result of the expansion of the swim bladder, potentially contributing to lower fecundity estimates during this period. However, it is also possible that some decrease in fecundity occurs during oocyte development. It is important to note that collections for this study occurred during 2 different reproductive cycles with the collections in May occurring in the reproductive year of 2014 and the collections in December occurring in the following reproductive year of 2015, and there may be interannual differences in fecundity due to environmental factors. It is assumed that the fecundity estimates for specimens collected in December may be more accurate because of the difficulty of collecting whole ovaries in May during the period of time close to parturition.

There are no published estimates of fecundity for either of these species in the Gulf of Alaska, but fecundity of northern rockfish has been examined in the Aleutian Islands. TenBrink and Spencer (2013) found that average fecundity of this species was 89,320 oocytes for northern rockfish ranging in size from 28 to 43 cm FL. They found that individuals of this species produce more oocytes than is explained by a proportional relationship between fecundity and maternal weight. The large disparity between the mean fecundity reported by TenBrink and Spencer (2013) and the mean fecundity calculated in this study is likely due to the larger sizes of fish examined in our study (37–46 cm FL). For most *Sebastes* species, there is a relationship between fecundity and size of fish, and for many of these species relative fecundity increases with the size of fish (Boehlert at al., 1982; Bobko and Berkeley, 2004; Dick, 2009).

It is important to distinguish reproductive failure from abortive maturation. Abortive maturation occurs when

immature fish that have not previously reproduced initiate oocyte development through vitellogenesis but have this process interrupted and their developing oocytes reabsorbed (Hannah and Parker, 2007; Conrath and Knoth, 2013). This phenomenon is commonly found in species that are members of the genus *Sebastes* (Nichol and Pikitch, 1994). It can be distinguished histologically because immature individuals will have no evidence of a prior spawning (beta and delta atresia or postovulatory follicles). In contrast to work that has examined abortive maturity that occurs in immature individuals, analysis of reproductive failure in this study included only those individuals that had reproduced in a prior year and were classified as mature adults. Almost all the individuals captured for this study were adults, and the average size of fish captured for this study (light dusky rockfish: 458 mm FL; northern rockfish: 414 mm FL) was quite a bit larger than the previously reported size at 50% maturity of either species, 310 mm FL for northern rockfish and 365 mm FL for light dusky rockfish (Chilton, 2007, 2010). This difference in size and maturity is likely the reason that no individuals undergoing abortive maturation were collected during this study.

Skipped spawning may ensure that fish of these species spawn only in years when adequate energy is available to produce viable embryos or to optimize their lifetime reproductive output. This pattern may be particularly important for rockfish species in Alaska that are long lived and have a periodic life history strategy (Winemiller and Rose, 1992). Skipped spawning may occur when fish experience decreased food availability (Rideout and Rose, 2006; McBride et al., 2015) and may be related to condition and energy reserves (Skjæraasen et al., 2012; Skjæraasen et al., 2015). If skipped spawning is related to energy reserves, it will likely vary temporally and the proportion of skipped spawners will fluctuate with changing environmental conditions. Interannual variability in the amount of skipped spawning has been documented for several teleost species, including haddock (*Melanogrammus aeglefinus*) in the northeast Arctic Ocean (Skjæraasen et al., 2015), Atlantic cod (*Gadus morhua*) off Newfoundland and Labrador, Canada (Rideout et al., 2006), and spring-spawning Atlantic herring (*Clupea harengus*) off Norway (Engelhard and Heino, 2006). It is important to consider not only annual changes in the amount of skipped spawning but spatial differences in rates of skipped spawning across the geographic range of a species.

The lack of fertilization type of skipped spawning has not been documented in rockfish species in this region prior to this study. This type of skipped spawning is similar to the retained type of skipped spawning described in Rideout et al. (2005) but differs for the live bearing species of the genus *Sebastes* because it is caused by lack of fertilization. In northern rockfish, there is some evidence from this study that the fertilization failure type of skipped spawning occurred more frequently in smaller fish (<42 cm FL); this relationship was not apparent in light dusky rockfish. Additional studies examining how incomplete fertilization or fertilization failure may relate to sex ratios, mate availability, mating behavior and competition, and female size and experience are needed.

However, it is suspected that the lack of fertilization success observed in this study may be due to a large copepod parasite (*Sarcotaces* sp.) that can be found within the body cavity of rockfish species. This parasite is found encysted in the skin and muscle tissue of marine fish, particularly in members of the genus *Sebastes* in the North Pacific Ocean (Meyers et al.[1]). In some species, this parasite may form a physical blockage in the body cavity or the reproductive tract and create problems with fertilization and spawning events. This parasite appears to occur frequently in dusky rockfish (*Sebastes ciliatus*) (Worton[2]), and this parasite is frequently seen in both light dusky and northern rockfish. The presence and number of this parasite were not consistently recorded in this study; therefore, calculating a correlation value between this parasitism and lack of fertilization was not possible. Further study is needed to examine the correlation between reproductive failure and the presence of this parasite.

Reproductive failure of northern and light dusky rockfish has not been documented in prior studies that examined the reproductive parameters of these species in the Gulf of Alaska (Chilton, 2007, 2010). TenBrink and Spencer (2013) in a study of the reproductive biology of Pacific ocean perch and northern rockfish mentioned that a small number of specimens may have been skipped spawners on the basis of the presence of postovulatory follicles and atretic oocytes, but skipped spawning apparently was not common. Specimens for this project were collected in 2014, when there was a warmwater anomaly in the Gulf of Alaska. This mass of warm water developed in the northeast Pacific Ocean during the winter of 2013–2014, and anomalies of warm sea-surface temperatures reached coastal waters of Alaska in May 2014 (Bond et al., 2015). This area of warm water was present through the end of 2015 and had widespread impacts on the oceanic and coastal ecosystems of the northeast Pacific Ocean (Cavole et al., 2016). It is possible that the 2 reproductive years covered by my study were impacted by this warmwater mass or other environmental conditions specific to this time period, and additional study of these processes during a more comprehensive time span is needed.

The greater contribution larger females make to several aspects of reproductive potential has been documented for members of the genus *Sebastes*; these aspects include increased fecundity (Beyer et al., 2015), increased larval quality (Berkeley et al., 2004), and earlier spawning, more protracted spawning, or both (Sogard et al., 2008). The results of this study indicate that larger females have higher relative fecundity and are less likely to experience total reproductive failure. The pattern of decreasing reproductive failure appears to be driven by a decrease in

[1] Meyers, T., T. Burton, C. Bentz, J. Ferguson, D. Stewart, and N. Starkey. 2019. Diseases of wild and cultured fishes in Alaska, 128 p. Alaska Dep. Fish Game, Anchorage, AK. [Available from website.]

[2] Worton, C. 2018. Personal commun. Alaska Department of Fish and Game, 351 Research Ct., Kodiak, AK 99615.

skipped spawning with size or age. This pattern has also been documented for deepwater rockfish species in the Gulf of Alaska (Conrath, 2017). A relationship between incomplete fertilization or fertilization failure and size was not observed in this study.

Reproductive failure has the potential to affect recruitment to the fishery of these 2 species in the Gulf of Alaska; therefore, it is critical to understand how this aspect of the life history of northern and light dusky rockfish should inform the management of these species. Research results indicate that spawning stock biomass or estimates of oocyte production per recruit can be inflated when adult fish that are not spawning are included as a part of the spawning stock (Rideout et al., 2005; Rideout and Rose, 2006; Sitar et al., 2014). Skipped spawning likely varies with metabolic condition, reflecting environmental parameters. Therefore, the proportion of a population of northern rockfish or light dusky rockfish that is not spawning likely varies annually, and there may be other temporal patterns in reproductive success related to changes in abundance of parasites, prey, and predators and in environmental parameters. Time-series data on reproductive parameters and specifically on rates of skipped spawning are needed to understand the implications for fish populations and their management (Rideout and Tomkeiwicz, 2011).

Acknowledgments

I thank B. Knoth, C. Rooper, D. Benjamin, M. Yang, and A. Vijgen for invaluable field and laboratory assistance. I am grateful to the captains and crew of the commercial fishing vessels chartered to participate in this research, the F/V *Gold Rush* and the F/V *Pacific Storm*, including B. Ashley, D. Ashely, and S. Hockema. I thank my funding sources: the North Pacific Research Board, the Alaska Coral and Sponge Initiative of the National Marine Fisheries Service, and the Habitat and Ecological Processes Research Program of the NOAA Alaska Fisheries Science Center.

Literature cited

Allen, M. J., and G. B. Smith.
1988. Atlas and zoogeography of common fishes in the Bering Sea and northeastern Pacific. NOAA Tech. Rep. NMFS 66, 151 p.

Berkeley, S. A., C. Chapman, and S. M. Sogard.
2004. Maternal age as a determinant of larval growth and survival in a marine fish, *Sebastes melanops*. Ecology 85:1258–1264.

Beyer, S. G., S. M. Sogard, C. J. Harvey, and J. C. Field.
2015. Variability in rockfish (*Sebastes* spp.) fecundity: species contrasts, maternal size effects, and spatial differences. Environ. Biol. Fish. 98:81–100.

Bobko, S. J., and S. A. Berkeley.
2004. Maturity, ovarian cycle, fecundity, and age-specific parturition of black rockfish (*Sebastes melanops*). Fish. Bull. 102:418–429.

Boehlert, G. W., W. H. Barss, and P. B. Lamberson.
1982. Fecundity of the widow rockfish, *Sebastes entomelas*, off the coast of Oregon. Fish. Bull. 80:881–884.

Boehlert, G. W., M. Kusakari, and J. Yamada.
1987. Reproductive mode and energy costs of reproduction in the genus *Sebastes*. *In* Proceedings of the international rockfish symposium; Anchorage, AK, 20–22 October 1986, p. 143–152. Alaska Sea Grant Rep. 87-02. Alaska Sea Grant Coll. Program, Univ. Alaska Fairbanks, Fairbanks, AK.

Bond, N. A., M. F. Cronin, H. Freeland, and N. Mantua.
2015. Causes and impacts of the 2014 warm anomaly in the NE Pacific. Geophys. Res. Lett. 42:3414–3420.

Bowers, M. J.
1992. Annual reproductive cycle of oocytes and embryos of yellowtail rockfish *Sebastes flavidus* (Family Scorpaenidae). Fish. Bull. 90:231–242.

Cavole, L. M., A. M. Demko, R. E. Diner, A. Giddings, I. Koester, C. M. L. S. Pagniello, M.-L. Paulsen, A. Ramirez-Valdez, S. M. Schwenck, N. K. Yen, et al.
2016. Biological impacts of the 2013–2015 warm-water anomaly in the Northeast Pacific: winners, losers, and the future. Oceanography 29:273–285.

Chilton, E. A.
2007. Maturity of female northern rockfish *Sebastes polyspinis* in the central Gulf of Alaska. Alaska Fish. Res. Bull. 12:264–269.
2010. Maturity and growth of female dusky rockfish (*Sebastes variabilis*) in the central Gulf of Alaska. Fish. Bull. 108:70–78.

Clausen, D. M., and J. Heifetz.
2002. The northern rockfish, *Sebastes polyspinis*, in Alaska: commercial fishery, distribution, and biology. Mar. Fish. Rev. 64(4):1–28.

Conrath, C. L.
2017. Maturity, spawning omission, and reproductive complexity of deepwater rockfish. Trans. Am. Fish. Soc. 146:495–507.

Conrath, C. L., and B. Knoth.
2013. Reproductive biology of Pacific ocean perch in the Gulf of Alaska. Mar. Coast. Fish. 5:21–27.

Dick, E. J.
2009. Modeling the reproductive potential of rockfishes (*Sebastes* spp.). Ph.D. diss., 229 p. Univ. Calif. Santa Cruz, CA.

Engelhard, G. H., and M. Heino.
2006. Climate change and condition of herring (*Clupea harengus*) explain long-term trends in extent of skipped reproduction. Oecologia 149:593–603.

Hannah, R. W., and S. J. Parker.
2007. Age-modulated variation in reproductive development of female Pacific ocean perch (*Sebastes alutus*) in waters off Oregon. *In* Biology, assessment, and management of North Pacific rockfishes. Alaska Sea Grant Rep. 07-01 (J. Heifetz, J. DiCosimo, A. J. Gharrett, M. S. Love, V. M. O'Connell, and R. D. Stanley, eds.), p. 161–180. Alaska Sea Grant Coll. Program, Univ. Alaska Fairbanks, Fairbanks, AK.

Hothorn, T., F. Bretz, and P. Westfall.
2008. Simultaneous inference in general parametric models. Biom. J. 50:346–363.

Hulson, P.-J. F., J. Heifetz, D. H. Hanselman, S. K. Shotwell, and J. N. Ianelli.
2015. Assessment of the northern rockfish stock in the Gulf of Alaska. *In* Stock assessment and fishery evaluation report for the groundfish resources of the Gulf of Alaska, p. 889–974. North Pacific Fish. Manage. Counc., Anchorage, AK. [Available from website.]

Hunter, J. R., and B. J. Macewicz.
1985a. Rates of atresia in the ovary of captive and wild northern anchovy, *Engraulis mordax*. Fish. Bull. 83:119–136.
1985b. Measurement of spawning frequency in multiple spawning fishes. *In* An egg production method for estimating spawning biomass of pelagic fish: application to the northern anchovy, *Engraulis mordax* (R. Lasker, ed.), p. 79–94. NOAA Tech. Rep. NMFS 36.

Kendall, A. W., Jr., and W. H. Lenarz.
1987. Status of early life history studies of northeast Pacific rockfishes. *In* Proceedings of the international rockfish symposium; Anchorage, 20–22 October 1986, p. 99–128. Alaska Sea Grant Rep. 87-02. Alaska Sea Grant Coll. Program, Univ. Alaska Fairbanks, Fairbanks, AK.

Love, M. S., M. Yoklavich, and L. Thorsteinson.
2002. The rockfishes of the northeast Pacific, 405 p. Univ. Calif. Press, Berkeley, CA.

Lunsford, C. R., S. K. Shotwell, P.-J. F. Hulson, and D. H. Hanselman.
2016. Assessment of the dusky rockfish stock in the Gulf of Alaska. *In* Stock assessment and fishery evaluation report for the groundfish resources of the Gulf of Alaska. North Pacific Fish. Manage. Counc., Anchorage, AK. [Available from website.]

McBride, R. S., S. Somarakis, G. R. Fitzhugh, A. Albert, N. A. Yaragina, M. J. Wuenschel, A. Alonso-Fernández, and G. Basilone.
2015. Energy acquisition and allocation to egg production in relation to fish reproductive strategies. Fish Fish. 16:23–57.

Nichol, D. G., and E. K. Pikitch.
1994. Reproduction of darkblotched rockfish off the Oregon coast. Trans. Am. Fish. Soc. 123:469–481.

R Core Team.
2015. R: a language and environment for statistical computing. R Foundation for Statistical Computing, Vienna, Austria. [Available from website, accessed April 2015.]

Reuter, R. F.
1999. Describing dusky rockfish (*Sebastes ciliatus*) habitat in the Gulf of Alaska using historical data. M.S. thesis, 83 p. Calif. State Univ., Hayward, CA.

Rideout, R. M., and G. A. Rose.
2006. Suppression of reproduction in Atlantic cod *Gadus morhua*. Mar. Ecol. Prog. Ser. 320:267–277.

Rideout, R. M., and J. Tomkiewicz.
2011. Skipped spawning in fishes: more common than you might think. Mar. Coast. Fish. 3:176–189.

Rideout, R. M., G. A. Rose, and M. P. M. Burton.
2005. Skipped spawning in female iteroparous fishes. Fish Fish. 6:50–72.

Rideout, R. M., M. J. Morgan, and G. R. Lilly.
2006. Variation in the frequency of skipped spawning in Atlantic cod (*Gadus morhua*) off Newfoundland and Labrador. ICES J. Mar. Sci. 63:1101–1110.

Sheehan, D. C., and B. B. Hrapchak.
1980. Theory and practice of histotechnology, 2nd ed., 481 p. Battelle Press, Columbus, OH.

Sitar, S. P., A. J. Jasonowicz, C. A. Murphy, and F. W. Goetz.
2014. Estimates of skipped spawning in lean and siscowet lake trout in southern Lake Superior: implications for stock assessment. Trans. Am. Fish. Soc. 143:660–672.

Skjæraasen, J. E., R. D. M. Nash, K. Korsbrekke, M. Fonn, T. Nilsen, J. Kennedy, K. H. Nedreaas, A. Thorsen, P. R. Witthames, A. J. Geffen, et al.
2012. Frequent skipped spawning in the world's largest cod population. Proc. Natl. Acad. Sci. U.S.A. 109:8995–8999.

Skjæraasen, J. E., K. Korsbrekke, T. Nilsen, M. Fonn, O. S. Kjesbu, G. E. Dingsør, and R. D. M. Nash.
2015. Skipped spawning in Northeast Arctic haddock *Melanogrammus aeglefinus*. Mar. Ecol. Prog. Ser. 526:143–155.

Sogard, S. M., S. A. Berkeley, and R. Fisher.
2008. Maternal effects in rockfishes *Sebastes* spp.: a comparison among species. Mar. Ecol. Prog. Ser. 360:227–236.

TenBrink, T. T., and P. D. Spencer.
2013. Reproductive biology of Pacific ocean perch and northern rockfish in the Aleutian Islands. North Am. J. Fish. Manage. 33:373–383.

Winemiller, K. O., and K. A. Rose.
1992. Patterns of life-history diversification in North American fishes: implications for population regulation. Can. J. Fish. Aquat. Sci. 49:2196–2218.

National Marine
Fisheries Service
NOAA

Fishery Bulletin
established in 1881

Spencer F. Baird
First U.S. Commissioner
of Fisheries and founder
of *Fishery Bulletin*

Fecundity and reproductive life history of anadromous rainbow smelt (*Osmerus mordax*) in coastal waters of Massachusetts

Bradford C. Chase (contact author)[1]
Scott Elzey[2]
Sara M. Turner[1]
Matt H. Ayer[2]

Email address for contact author: brad.chase@mass.gov

[1] Massachusetts Division of Marine Fisheries
836 South Rodney French Boulevard
New Bedford, Massachusetts 02744

[2] Massachusetts Division of Marine Fisheries
30 Emerson Avenue
Gloucester, Massachusetts 01930

Abstract—Abundance and harvest of rainbow smelt (*Osmerus mordax*) in the northwest Atlantic Ocean have declined sharply in recent decades, with a concurrent reduction in the historic geographic range of this species. These declines have occurred while management responses have been limited by information gaps on the life history of this species. We assessed reproductive attributes of rainbow smelt caught in marine waters during winter and compared their size and age characteristics to those of fish sampled from spring spawning runs in 4 coastal rivers in Massachusetts. Total fecundity of rainbow smelt was 4880–51,651 oocytes. Fecundity was positively related with total length (TL), total weight, ovarian weight, and age. Immature rainbow smelt were rarely caught during spawning runs but composed 10% of the marine samples. This observation, a maturity ogive for rainbow smelt from marine waters, and differences in TL of age-1 fish between marine and river samples confirm that age-1 rainbow smelt are not fully recruited to spawning runs. Samples from spawning runs had a higher proportion of age-1 rainbow smelt, a lower proportion of those age 3 or older, a higher instantaneous rate of total mortality, and a lower number of eggs produced per recruit than have been previously documented for rainbow smelt—all indications of declining population health.

Manuscript submitted 1 August 2018.
Manuscript accepted 5 July 2019.
Fish. Bull. 117:151–168 (2019).
Online publication date: 17 July 2019.
doi: 10.7755/FB.117.3.3

The views and opinions expressed or implied in this article are those of the author (or authors) and do not necessarily reflect the position of the National Marine Fisheries Service, NOAA.

The northwest Atlantic Ocean, including the Gulf of Maine, is among the fastest-warming marine areas in the world (Hare et al., 2016). The rainbow smelt (*Osmerus mordax*) is an anadromous species that has adapted to thrive in cold-water environments (Driedzic and Ewart, 2004; Driedzic and Short, 2007) and is restricted to the northwest Atlantic Ocean. Improvements are needed in our understanding of the life history and population dynamics of rainbow smelt to determine conservation strategies. The rainbow smelt is a small, short-lived fish that matures in coastal waters and migrates in spring to spawn in coastal rivers. This species formerly supported important commercial and recreational fisheries in the Canadian Maritime provinces and the U.S. waters of the Gulf of Maine (Goode, 1884; Kendall, 1926; Enterline et al., 2012). Rainbow smelt fisheries in Massachusetts were regulated for rod-and-reel harvest only for most of the 20th century. For estuary ice-shack fisheries and fall shoreline fisheries, popular more than 30 years ago, participation and harvest have declined to low levels (Chase[1]). Rainbow smelt can be essential to inland aquatic food webs (Kircheis and Stanley, 1981; O'Gorman et al., 1987; Sayers et al., 1989) and are considered important prey for a variety of fish and wildlife species in coastal rivers and marine habitats (Scott and Scott, 1988).

Overall, diadromous fish species have experienced severe population declines since the 18th century with most species at historically low levels of abundance in the northwest Atlantic Ocean (Limburg and Waldman, 2009). Anadromous rainbow smelt have experienced a substantial contraction of the southern part of their historical geographic range (Enterline et al., 2012), but details on their population dynamics and life history remain poorly known. In response to concerns over populations of rainbow smelt in New England, NOAA listed anadromous rainbow smelt as a species of concern in 2004 (Federal Register, 2004).

[1] Chase, B. C. 2006. Rainbow smelt (*Osmerus mordax*) spawning habitat on the Gulf of Maine coast of Massachusetts. Mass. Div. Mar. Fish. Tech. Rep. TR-30, 173 p. [Available from website.]

Table 1

Summary of key information from previous studies of the fecundity of rainbow smelt (*Osmerus mordax*) in coastal waters of Massachusetts and Canada and in the Great Lakes. Data provided are location, type of population, total number of samples (n), and ranges for size, measured as millimeters in total length (TL), and fecundity, measured as the number of mature oocytes prior to spawning.

Citation	Location	Type	n	Size (mm TL)	Fecundity (no. of oocytes)
McKenzie, 1964	New Brunswick	Anadromous	9	127–209	8500–69,600
Clayton, 1976	Massachusetts	Anadromous	11	127–204	7038–44,241
Chen, 1970	Grande Riviere, Quebec	Anadromous	48	160–225	21,390–75,570
Bailey, 1964	Lake Superior	Landlocked	10	185–224	21,534–40,894
Chen, 1970	Matamek Lake, Quebec	Landlocked	64	202–280	14,269–75,944
Chen, 1970	Lake Erie, Ontario	Landlocked	93	115–194	2700–37,520
Chen, 1970	Lake Ontario, Ontario	Landlocked	172	109–256	4766–100,780
Luey and Adelman, 1984	Lake Superior	Landlocked	208	145–225	4323–50,418

In response, a regional conservation plan for rainbow smelt in the Gulf of Maine was developed and documented range-wide declines in harvest records for rainbow smelt (Enterline et al., 2012). Similar concerns have been expressed for fisheries and populations of rainbow smelt in Canada (Trencia et al., 2005; Verreault et al., 2012).

Anadromous rainbow smelt reproduce during spring spawning runs in freshwater riffles a short distance above tidal influence (Kendall, 1926; McKenzie, 1964; Murawski et al., 1980; Chase[1]). Female rainbow smelt deposit demersal, adhesive eggs that incubate for 1–4 weeks, depending on water temperature (McKenzie, 1964; Chase et al.[2]), and hatched larvae are transported to estuarine waters. Female rainbow smelt complete spawning in 1–4 nights, whereas males remain longer on spawning grounds (Marcotte and Tremblay, 1948; Murawski et al., 1980). This brief female spawning period is consistent with reports that female rainbow smelt possess a single set of mature oocytes, with no differences in oocyte size and maturity among ovary locations (Chen, 1970; Clayton, 1976).

Rainbow smelt occur in anadromous and landlocked populations in northeastern North America, with differences in life history. Landlocked rainbow smelt are present naturally in some coastal lakes; however, most populations were introduced to the Great Lakes and many smaller watersheds early in the 20th century (Van Oosten, 1937; Evans and Loftus, 1987; and Mercado-Silva et al., 2006). Landlocked rainbow smelt grow slower and are smaller than anadromous rainbow smelt, and they mature at an older age (Bailey, 1964; Luey and Adelman, 1984; O'Malley et al., 2017). The maturity schedule and fecundity of landlocked rainbow smelt have been related to high recruitment variability (O'Gorman et al., 1987; Gorman, 2007; Stritzel Thomson et al., 2011), and comparable information on reproduction of anadromous rainbow smelt is not available. Fecundity has been reported for anadromous populations of rainbow smelt, but with small sample sizes (combined number of samples [n]=68, among 3 studies: McKenzie, 1964; Chen, 1970; and Clayton, 1976). Fecundity of landlocked rainbow smelt has been studied in the Great Lakes (Bailey, 1964; Chen, 1970; Luey and Adelman, 1984), with fecundities ranging from 2700 to 100,780 eggs (Table 1).

With a paucity of population data and gaps in basic life history information for anadromous rainbow smelt, limited support is available for management decisions on population status and vulnerability. Here, we aim to advance the understanding of the reproductive life history of rainbow smelt with improved estimates of fecundity, of size and age at maturity, and of length and age composition during spawning runs. We also estimated mortality and eggs per recruit and compared the results to historical data for rainbow smelt. A key assumption was that the apparent changes in abundance of rainbow smelt would be reflected in truncated age structure and increasing mortality. To achieve these objectives, rainbow smelt were sampled as part of an inshore winter trawl survey prior to spawning and later in 4 coastal rivers in Massachusetts during their spawning migrations.

Materials and methods

Historically, the range of rainbow smelt once extended as far south as Delaware Bay (Scott and Crossman, 1973), but more recent information indicates that populations south of Massachusetts are extinct or undetectable (Fried and Schultz[3]; Enterline et al., 2012). For this study, anadromous rainbow smelt were sampled near the present southern extent of their range in marine waters and

[2] Chase, B. C., J. H. Plouff, and M. Gabriel. 2008. An evaluation of the use of egg transfers and habitat restoration to establish an anadromous rainbow smelt spawning population. Mass. Div. Mar. Fish. Tech. Rep. TR-33, 16 p. [Available from website.]

[3] Fried, H. A., and E. T. Schultz. 2006. Anadromous rainbow smelt and tomcod in Connecticut: assessment of populations, conservation status, and need for restoration plan. Univ. Conn., Dep. Ecol. Evol. Biol., EEB Article 18, 262 p. [Available from website.]

Figure 1

Map of the study area in Massachusetts where rainbow smelt (*Osmerus mordax*) were sampled in 2004–2007 for analyses of their fecundity and reproductive life history. The black stars denote locations where fyke net sampling was conducted in 4 coastal rivers in the spring during spawning runs, and the black triangles denote the locations of tows completed in the winter during a trawl survey in marine waters. Sources for base map data: Esri, HERE, DeLorme, Mapmyindia. Base map data copyrighted OpenStreetMap contributors and the GIS user community.

coastal rivers from Cape Cod Bay to Plum Island Sound, Massachusetts, in the western Gulf of Maine (Fig. 1).

Reproductive analyses

Fecundity Rainbow smelt were collected and frozen whole during a trawl survey for Atlantic cod (*Gadus morhua*) conducted by staff of the Massachusetts Division of Marine Fisheries aboard a commercial vessel in winter from 2004 through 2007, by using a standardized 2-seam, high-rise bottom-trawl net with a 26.5-m sweep, 25.6-m headrope, 11.43-cm wing mesh, 7.62-cm codend mesh, and 5.08-cm mesh liner (Hoffman et al.[4,5]). The meshes were diamond-shaped, and their measurements were taken when they were stretched. The target time for tows was 30 min, and the functional headrope height was

[4] Hoffman, W. S., S. J. Correia, and D. E. Pierce. 2012. Results of an industry-based survey for Gulf of Maine cod, November 2003–May 2005. Mass. Div. Mar. Fish. Tech. Rep. TR-49, 37 p. [Available from website.]

[5] Hoffman, W. S., S. J. Correia, and D. E. Pierce. 2012. Results of an industry-based survey for Gulf of Maine cod, May 2006–December 2007. Mass. Div. Mar. Fish. Tech. Rep. TR-50, 45 p. [Available from website.]

approximately 4.5 m. This winter trawl survey provided an opportunity to sample maturing rainbow smelt prior to their spawning migration into coastal rivers and, therefore, to avoid bias associated with analyzing fecundity of fish intercepted during spawning runs when partially spawned fish are present and oocytes can be extruded during handling.

In the laboratory, frozen rainbow smelt were thawed, excess water was removed with absorbent paper, and total weight (TW, to the nearest 0.01 g), total length (TL, to the nearest 1 mm), and sex were recorded. Subsamples of female rainbow smelt for fecundity analysis were selected with a target sample size of 10 fish for each length bin of 10 mm. Scales were removed from the female subsamples between the lateral line and dorsal fin for age determination (Elzey et al.[6]). Female rainbow smelt have an asymmetrical ovarian pair with a left ovary larger than the right one. Ovaries were excised from females, excess tissue and water were removed, and ovarian weight (OW, to the nearest 0.01 g) and maturation stage (Crim and Glebe, 1990) were recorded. Any remaining ovarian tissue and membrane that could not be removed was assumed to represent a negligible weight relative to the total ovary weight. Body weight (BW) was recorded as TW–OW.

Two subsamples of oocytes were removed for fecundity analysis from each paired ovary: one subsample anterior and one subsample posterior of the midpoint of each ovary. The sampling protocol targeted 500 oocytes/subsample to estimate egg density. Subsamples were placed on absorbent paper, weighed (to the nearest 0.01 g), and fixed in 3% formalin in small jars; once in the jars, samples were shaken immediately to prevent oocytes from clumping together. Additionally, to confirm previous findings of synchrony in oocyte development (Chen, 1970; Clayton, 1976), 4 oocyte subsamples were collected from 4 rainbow smelt before samples were fixed to measure oocyte diameters. A finding that all oocytes developed at the same rate would support the use of determinate methods of fecundity estimation. Again, one subsample was collected anterior and one subsample posterior of the midpoint of each ovary. The diameter and maturity stage of 20 oocytes were recorded from each of these subsamples with an ocular micrometer (to the nearest 0.01 mm). The Kruskal–Wallis rank sum test was used to determine if there were differences in oocyte diameter among the locations in the ovary where oocyte samples were removed.

Fixed subsamples of oocytes were processed for fecundity analysis by counting all oocytes with a compound microscope at 10× magnification. We calculated total fecundity, the number of mature oocytes prior to spawning, for an individual rainbow smelt as the product of the mean number of oocytes per gram for the 4 oocyte subsamples and the TW of the paired ovaries (Nielsen and Johnson, 1983). Oocyte density (total estimated number of oocytes divided by OW) and relative fecundity (total fecundity divided by BW in grams) also were calculated as reproductive indices to compare among age classes.

Total fecundity estimates for each individual were regressed against TL, TW, OW, and age to determine the relationships of fecundity to size and age of rainbow smelt. Regressions and the Shapiro–Wilk normality test were run on nominal data by using the MASS package, vers. 7.3-45 (Venables and Ripley, 2002), in the statistical software R, vers. 3.3.0 (R Core Team, 2016). The response variable and some predictor variables were not normally distributed, and all nominal regressions had patterns of variance inconsistency. As a result, both dependent variables and independent variables were log transformed to improve normality and the constancy of variance (Sokal and Rohlf, 1995). All analyses were performed in R, vers. 3.3.0. The level of statistical significance for all analyses was 0.05.

Maturity Maturity and sex of marine samples of rainbow smelt were determined by macroscopic gonad examination. Immature rainbow smelt were readily identified because no development of gonadal tissue was visible; in contrast, the well-developed testis and ovaries of mature samples occupied a majority of the abdominal cavity space. Maturity ogives are important biological references used in stock assessments (ICES[7]) and are critical for description of the reproductive potential of a short-lived, anadromous fish, such as the rainbow smelt. Logistic models are commonly used to determine the relation between body size and sexual maturity (Roa et al., 1999). In our study, we applied a generalized linear model (GLM) with binomial error structure and logit link function by using the MASS package in R to model maturity of rainbow smelt (ICES[7]). All marine samples of rainbow smelt were assigned a maturity status (mature or immature) that was used as the response variable in the model, and TL was used as the explanatory variable. The GLM assumes that all samples are independent and generates a multiyear estimate of the maturity ogive for sexes combined. The GLM estimates maturity at length when 50% of the population is mature (L_{50}). A maturity ogive was not prepared for the samples collected with a fyke net during spawning runs because immature rainbow smelt were rare or absent at the 4 stations at coastal rivers where this fyke net sampling occurred.

Maturity and condition indices (Crim and Glebe, 1990) were generated to determine if maturation patterns were evident among age, size, and area subsets and to compare with earlier data sets (Chen, 1970; Clayton, 1976). Values of Fulton's condition factor, calculated as K=(TW/TL^3)×100,000, increase with increasing weight at a given length, an indication of better physical "condition" for a

[6] Elzey, S. P., K. J. Trull, and K. A. Rogers. 2015. Massachusetts Division of Marine Fisheries Age and Growth Laboratory: fish aging protocols. Mass. Div. Mar. Fish. Tech. Rep. TR-58, 43 p. [Available from website.]

[7] ICES (International Council for the Exploration of the Sea). 2008. Report of the workshop on maturity ogive estimation for stock assessment (WKMOG); Lisbon, Portugal, 3–6 June. ICES CM Documents 2008/ACOM:33, 72 p. [Available from website.]

fish (Ricker, 1975). Differences in condition factor among sample locations and sex were tested with the Kruskal–Wallis rank sum test and the Kruskal–Wallis multiple comparison test. The gonadosomatic index (GSI), calculated as (OW/BW)×100, and the fecundity index, calculated as total fecundity/TL^3, were determined for marine samples and the Fulton's condition factor was calculated for both the river and marine samples. Sex ratios of rainbow smelt sampled at all locations were tested for significant differences by using the chi-square test (α=0.05).

Size and age analyses

The Massachusetts Division of Marine Fisheries conducts annual fyke net sampling of rainbow smelt at spawning runs in coastal rivers to monitor abundance and size and age composition. Fyke nets were set in the Jones, Fore, Saugus, and Parker Rivers (Fig. 1) at mid-channel, intertidal locations downstream of spawning riffles to intercept spawning rainbow smelt 3 days a week over an 11-week spawning run (Chase et al., 2009; Enterline et al., 2012). Fyke nets were set in 2004–2007; however, the catch data for 2004 were not used because of changes in methods following that pilot season. The fyke nets have square wings that are 1.2 × 1.2 m and lead to a square entrance, also 1.2 × 1.2 m, that connects to 7 hoops with a terminal codend after 2 throats (all mesh sizes were 7 mm). At all locations, rainbow smelt were counted and measured for TL, and their sex was determined. Total length was measured for 100 male and female rainbow smelt from each haul, with all remaining rainbow smelt enumerated by sex. Spawning male rainbow smelt are readily identified by the presence of nuptial tubercles. At the Fore and Saugus Rivers, samples were collected randomly from each haul to additionally measure TW and to collect scales for aging. The subsamples for aging were collected with a weekly tally of 5 samples per 10-mm bin per sex.

Length and weight correction Measurements of the samples collected with a fyke net were made when fish were fresh, but the marine samples were frozen prior to processing. To allow direct comparison of length and weight data for the 2 sets of collections, a sample of rainbow smelt caught with a fyke net in the Fore River were measured for length and weight before and after they were frozen, and changes in length and weight were compared with regression analysis.

Length analysis The TL of rainbow smelt collected at the 4 stations where fyke net sampling occurred and caught during the trawl survey were evaluated for differences among locations and sexes by using the Kruskal–Wallis rank sum test and the Kruskal–Wallis multiple comparison test. Given limitations of sample sizes, all samples from the trawl survey were pooled for the study period. Length and length-at-age analyses (only for samples from the Fore River) were conducted on pooled samples for the study period when sample sizes allowed meaningful comparisons. The interpretation of length data among sample locations must be made cautiously because of the within-season repeat-spawning behavior of males (Murawski and Cole, 1978) and changes in size and age of rainbow smelt that occur temporally during a spawning run (Marcotte and Trembley, 1948; McKenzie, 1964).

Age analysis Age keys were prepared for Fore River samples and for the data pooled for samples from the Fore and Saugus Rivers. Age keys combined sexes and annual data for the study period. The pooled age key was applied to length frequencies of samples from the Saugus, Jones, and Parker Rivers to estimate age composition for those rivers. The age compositions were applied to the Chapman–Robson age-based survival estimator, by using the Fishmethods package, vers. 1.10-4 (Nelson, 2017) in R to estimate annual survival (S) and instantaneous total mortality (Z) rates. Annual age data for each sampling location were combined for the study periods to smooth the effect of year-class variation and as a practical approach to allow a comparison of sparsely reported population demographics for anadromous rainbow smelt. The annual age proportions estimated for rainbow smelt from fyke net sampling were compared with historical data (Murawski and Cole, 1978; Lawton et al.[8]) by using the chi-square test (α=0.05).

Length–weight analysis Length–weight data from the trawl survey samples were compared with length–weight data from the fyke net samples to examine seasonal differences in condition of rainbow smelt, and as an alternative means to consider if the pooled samples of rainbow smelt from the trawl survey composed a representative sample for fecundity analysis. We used linear regression on natural log-transformed TL and TW data for rainbow smelt collected for fecundity analysis and fyke net monitoring. The homogeneity of slopes was tested by analysis of covariance to determine if length or weight differed significantly by location, sex, or age class (P<0.05). Length was the independent variable, weight was the dependent variable, and location, sex, and age class were the group variables.

Results

Reproductive analyses

During the trawl survey in 2004–2007, 634 rainbow smelt were collected from 13 tows of the trawl between 11 January and 5 March (Fig. 1). Rainbow smelt were captured in nearshore, marine waters off Massachusetts at an average depth of 38 m (range: 19–89 m) with an

[8] Lawton, R., P. Brady, C. Sheehan, S. Correia, and M. Borgatti. 1990. Final report on spawning sea-run rainbow smelt (*Osmerus mordax*) in the Jones River and impact assessment of Pilgrim Station on the population, 1979–1981. Pilgrim Nuclear Power Station Mar. Environ. Monit. Program Rep. Ser. 4, 72 p. [Available from Mass. Div. Mar. Fish., 251 Causeway St., Ste. 400, Boston, MA 02114.]

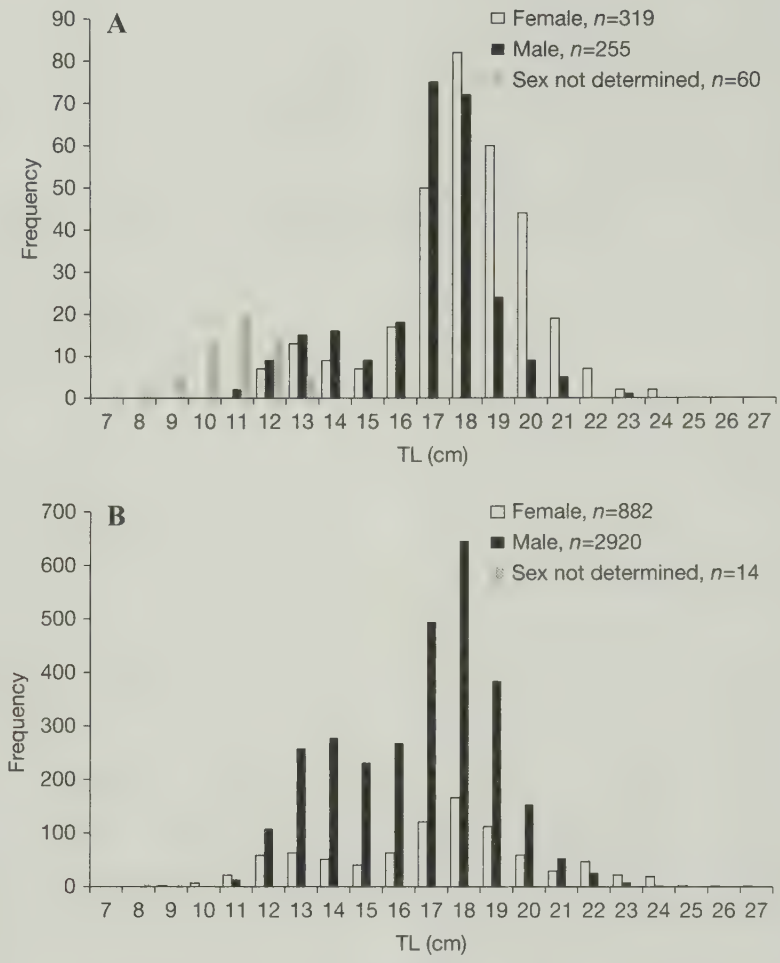

Figure 2

Length-frequency distribution of rainbow smelt (*Osmerus mordax*) caught (**A**) during a trawl survey off the coast of Massachusetts in 2004–2007 and (**B**) at a fyke net station in the Fore River in 2005–2007. Samples with sex not determined were immature rainbow smelt that had gonadal development that was insufficient for identifying sex. TL=total length.

average water temperature of 3.6°C at the surface (range: 0.7–8.9°C) and 3.5°C (range: 0.7–7.2°C) on the bottom. The highest catch rates for rainbow smelt occurred in Cape Cod Bay and Massachusetts Bay at an average depth of 26 m (range: 19–30 m). Of the total sample, 255 rainbow smelt were male (3 immature), 319 rainbow smelt were female (1 immature), and the sex could not be determined for 60 fish (all immature) (Fig. 2A). All samples used in fecundity analysis (n=110) were aged (except 3 fish for which the scale samples had degraded). Sex, TL, and TW were recorded for all captured rainbow smelt, except for fish caught during 3 tows of the trawl in 2007, when females in unfilled TL bins for fecundity analysis were collected and all other rainbow smelt had their TL measured and sex determined.

Fecundity Mean total fecundity in rainbow smelt increased 270% from age 1 to age 2 and 170% from age 2 to age 3 (Table 2). The highest variability in fecundity was observed for age-2 rainbow smelt (Fig. 3A) as a consequence of the wide range of size represented for this age (Fig. 2A). Mean and maximum total fecundity of age-3 and age-4 fish were nearly the same, and rainbow smelt of both ages had much higher minimum fecundity than fish in the younger age classes (Fig. 3A). In regression analysis, total fecundity of rainbow smelt increased significantly with each measure of size and age (Table 3). The best-fitting relationship was that of fecundity and TW, closely followed by that of fecundity and TL (Table 3, Fig. 4). Although the regression of fecundity versus age was significant, the occurrence of

Table 2

Summary statistics for rainbow smelt (*Osmerus mordax*) sampled during a trawl survey in marine waters off Massachusetts in 2004–2007 and for analysis of their fecundity. Data provided are sample size (n), mean length, measured in millimeters in total length (TL), mean total weight (TW), mean gonadosomatic index (GSI), mean ovarian weight (OW), mean egg density, relative fecundity, measured as the number of oocytes divided by body weight (BW), and fecundity, measured as the number of mature oocytes prior to spawning.

Age	n	Mean length (mm TL)	Mean TW (g)	Mean GSI	Mean OW (g)	Mean egg density (no. oocytes/OW)	Mean relative fecundity (no. oocytes/BW)	Fecundity (no. of oocytes)	Mean fecundity (no. of oocytes)
1	19	137	12.93	6.53	0.80	13,234	767	4880–14,102	9026
2	76	184	36.79	11.23	3.96	8529	747	7885–50,001	24,624
3	8	215	65.45	15.10	8.65	6118	789	25,559–51,651	42,957
4	4	231	88.34	25.39	17.42	2652	633	36,721–47,328	43,927

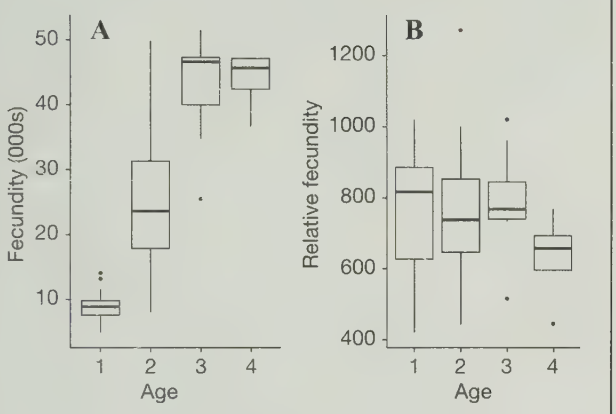

Figure 3

Boxplots (**A**) of total fecundity, measured as the number of mature oocytes prior to spawning, and (**B**) of relative fecundity, measured as the number of oocytes divided by body weight, by age class, for rainbow smelt (*Osmerus mordax*) sampled during a trawl survey in marine waters off Massachusetts in 2004–2007. The lower and upper hinges of the box plots correspond to the 25th and 75th percentiles. The whiskers extend from the hinge to the farthest value no more than 1.5 times the interquartile range (distance between the 25th and 75th percentiles). Data beyond the end of the whiskers, called *outlying points*, are plotted individually.

only 4 age classes and low sample sizes for age-3 and age-4 rainbow smelt resulted in the lowest coefficient of multiple determination (R^2) among predictor variables (Table 3). Mean oocyte density (number of eggs per gram) declined sharply with age (Table 2). Mean oocyte density was 5 times higher in age-1 rainbow smelt than in age-4 rainbow smelt. Overall, relative fecundity was similar among age classes (Fig. 3B) with declines in oocyte density with age compensated by increases in body and ovary size.

Maturity ogive A multiyear maturity ogive for both sexes combined was estimated from the sample of 634 rainbow smelt collected with a trawl in marine waters, with 64 immature fish included (Fig. 5). The GLM was significant for the intercept and TL ($P<0.001$) and estimated L_{50} at 126.2 mm TL. Maturity ogive estimates were not possible for the samples collected in coastal rivers with a fyke net during spawning runs because of the near absence of immature rainbow smelt. However, mean length of age-1 rainbow smelt (range: 140–147 mm TL) was greater at the locations of fyke net sampling than the L_{50}, indicating that not all age-1 rainbow smelt are recruited to spawning runs (Table 4). Our data are not sufficient to produce annual ogives or separate ogives for each sex. A slight difference in maturity ogive between sexes may occur given the differences in mean length.

Oocyte diameter The diameters of oocytes from the ovaries of a subsample of 4 rainbow smelt were measured before samples were fixed in formalin to determine if oocyte diameter and maturity differed among locations in the ovary where oocytes were removed. There was no variation in oocyte appearance or stage among samples: all had dense, dark yellow yolk, consistent with maturing oocytes of later vitellogenic stages (Crim and Glebe, 1990). No significant differences were found among the 4 subsamples of rainbow smelt by using the Kruskal–Wallis rank sum test (χ^2=3.91, 5.78, 11.07, and 6.72; degrees of freedom (df)=6; $P>0.05$). No further oocyte diameter measurements were made given the confirmation of the reports by Chen (1970) and Clayton (1976) that oocyte maturity of rainbow smelt was evenly distributed along ovaries and the subsequent finding that fixing the remaining samples in 3% formalin reduced oocyte size and distorted shape.

Size and age analyses

Fyke net samples During spawning runs in the spring of 2005–2007, 13,428 rainbow smelt were caught with fyke nets at locations in 4 coastal rivers (Table 5). Rainbow smelt were caught routinely with relatively high frequency of occurrence in hauls at each location. The fyke

Table 3

Regression coefficients from analysis of the relationships of fecundity and independent variables of size and age for rainbow smelt (*Osmerus mordax*) collected in marine waters off Massachusetts during 2004–2007. Variables were log-transformed for all regressions. Standard errors of the mean (SEs) are given for intercept and slope values. All values for the *F*-statistic are significant ($P<0.001$). R^2=coefficient of multiple determination; $S^2_{y\cdot x}$=residual mean square.

Variable	*n*	R^2	$S^2_{y\cdot x}$	*F*	Intercept (SE)	Slope (SE)
Length	110	0.891	0.040	884.9	−6.404 (0.549)	3.166 (0.106)
Total weight	110	0.899	0.037	961.1	6.765 (0.104)	0.927 (0.030)
Ovarian weight	110	0.739	0.096	305.7	9.411 (0.042)	0.518 (0.030)
Age	107	0.524	0.174	115.4	7.721 (0.209)	2.062 (0.192)

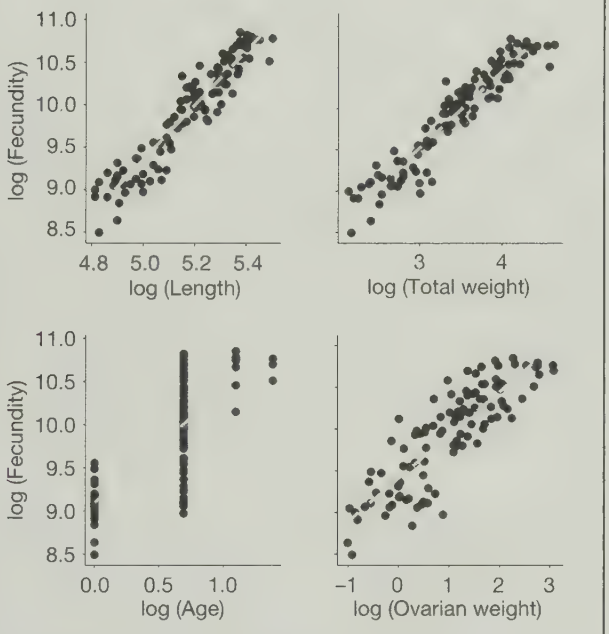

Figure 4

Regressions of the relationships between fecundity and the size and age of rainbow smelt (*Osmerus mordax*) sampled in marine waters off Massachusetts during a trawl survey in 2004–2007. See Table 2 for summary statistics from fecundity analysis and Table 3 for regression coefficients. The vertical clusters of points in the log (Age) graph represent ages 1–4 from left to right, respectively. The dashed lines indicate the fitted regression model values. Lengths are given as total lengths in millimeters, and weights are total weights given in grams.

net sampling at the location in the Fore River had the highest total catch, frequency of occurrence, and catch per unit of effort (number of rainbow smelt per overnight haul) among the 4 rivers. The results that follow include comparisons of size and age data for rainbow smelt caught during the trawl survey and fyke net sampling.

Length and weight correction A random sample of rainbow smelt was collected with the fyke net in the Fore River to measure length and weight when fish were fresh (<12 h after collection) and again after they had been frozen for 3 months. Regressions were generated for both TL and TW. No differences were found in the regression slopes between sexes through analysis of covariance. Therefore, the relationship between data for fresh and frozen samples that was used to correct the TL of trawl samples was determined with this equation: $TL_{Fresh}=-1.88893+0.99075TL_{Frozen}$ ($n=59$, $R^2=0.985$, $P<0.001$). The following equation was used to determine the relationship between data for fresh and frozen samples that was used to correct the TW of trawl samples: $TW_{Fresh}=-0.07561+0.98369TW_{Frozen}$ ($n=59$, $R^2=0.996$, $P<0.001$). When applied to data for trawl-caught rainbow smelt, these corrections increased post-frozen length and weight measurements by approximately 2–4% and decreased Fulton's condition factor by approximately 4%.

Length analysis Differences in TL among rainbow smelt from the 4 fyke net stations and from the trawl samples were evaluated for the study period by using the Kruskal–Wallis rank sum test and the Kruskal–Wallis multiple comparison test. Several trends were revealed from the analysis of pooled length data (Fig. 6). At all locations, males were shorter than females. Also, males and females from the southernmost station in the Jones River were shorter than those from all other locations, and males from the northernmost station in the Parker River were significantly longer than those from all other locations. Among samples from the trawl survey, the Fore River, and the Saugus River, there were no differences in TL except for females from the Fore River and Saugus River. This finding supports the premise that it was suitable to pool data from the trawl samples for the study area and compare length and age distributions to data from samples collected in coastal rivers. This analysis and these length-frequency data raise no concerns over possible size selection that could have resulted from the use of trawl sampling gear (Fig. 2A).

Analysis of differences in TL among aged rainbow smelt found significant differences beyond those revealed from the previously mentioned analysis of pooled length data.

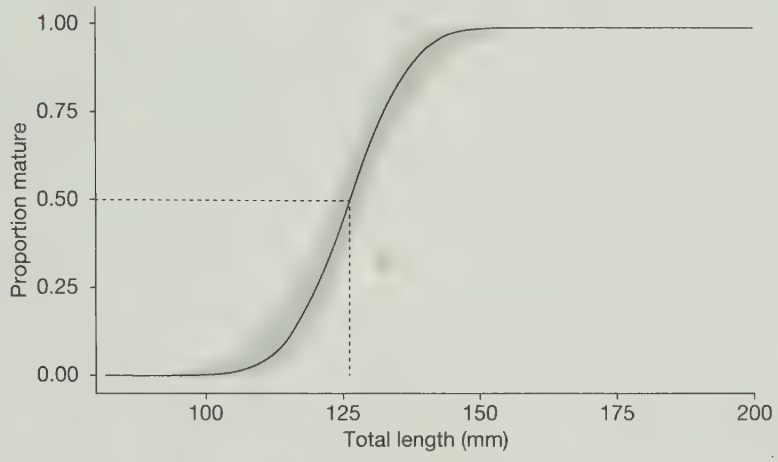

Figure 5

Maturity ogive for rainbow smelt (*Osmerus mordax*) sampled in marine waters off Massachusetts in 2004–2007 (n=634), derived for sexes combined from a generalized linear model with binomial error and logit link functions. The dashed line indicates the length at which 50% of the population was mature, 126 mm in total length. The gray area indicates the 95% confidence interval of the maturity ogive. The ogive coefficients are significant (P<0.001) for the intercept (standard error [SE] 4.226) and total length (SE 0.033).

Table 4

Summary of total lengths (TLs) of rainbow smelt (*Osmerus mordax*) for which age was determined in this study. Fish were sampled in Massachusetts in marine waters during a trawl survey in 2004–2007 and in the Fore and Saugus Rivers with fyke nets in 2005–2007. Significant differences in TL among age and location groups were tested with the Kruskal–Wallis rank sum and multiple comparison tests (α=0.05). Asterisks (*) indicate groups with significantly different TLs within each age and sex category.

Age	Sex	Sampling location or type	(n)	Mean (mm)	SE
1	Male	Trawl survey	0		
		Fore River	174	140*	0.88
		Saugus River	149	147*	0.98
2	Male	Trawl survey	0		
		Fore River	382	180*	0.61
		Saugus River	144	189*	1.12
1	Female	Trawl survey	19	137*	2.46
		Fore River	77	142	1.45
		Saugus River	51	145*	1.46
2	Female	Trawl survey	75	184	2.61
		Fore River	159	191	1.16
		Saugus River	39	205*	2.16

All fish from the Saugus River were larger at age 1 and age 2 than fish from the Fore River and the trawl survey, except for age-1 female rainbow smelt from the Fore River (Table 4). Total lengths of age-1 and age-2 females from the Fore River were not different from those of females from the trawl survey. Year-to-year TL comparisons were limited to the Fore River because of sample sizes. Differences were found among 3 comparisons of annual data for samples from the Fore River: males caught in 2005 and 2007 and females sampled in 2007 with females captured in both 2005 and 2006. These comparisons of length statistics may reflect changes in annual growth rates and cohort strength; however, these results can be confounded by pooling samples by year.

Table 5

Summary of fyke net sampling of rainbow smelt (*Osmerus mordax*) in 4 coastal rivers of Massachusetts during 2005–2007. Data provided are drainage area of each river; mean monthly discharge of each river, given as cubic meters per second averaged for the month of April over the period 2005–2007; sample size (n); mean catch per unit of effort (overnight haul) (CPUE); and frequency of occurrence (FOC) in hauls of fyke nets.

River	Drainage area (km^2)	Discharge (m^3/s)	Year	n	CPUE	FOC
Parker	156.4	2.8	2005	924	35.5	0.53
			2006	123	4.2	0.66
			2007	563	24.5	0.61
Saugus	124.8	1.9	2005	141	4.4	0.56
			2006	1458	48.6	0.87
			2007	2433	76.0	0.61
Fore	93.5	2.4	2005	2131	71.0	0.90
			2006	1014	35.0	0.90
			2007	3435	107.3	0.81
Jones	76.7	2.1	2005	489	15.3	0.72
			2006	614	21.3	0.93
			2007	103	3.2	0.50

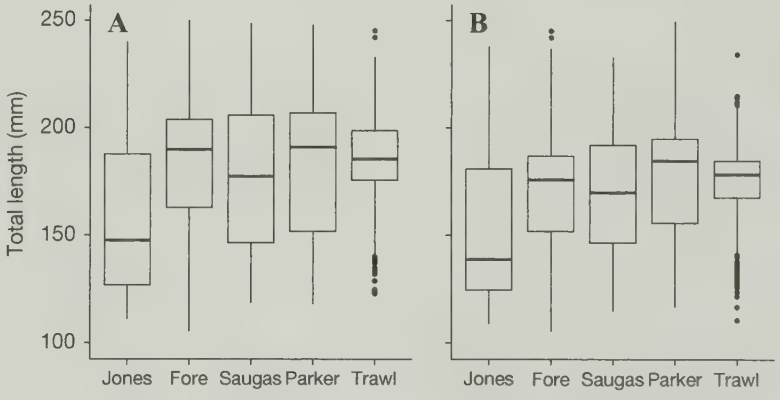

Figure 6

Boxplots of total length of (**A**) female and (**B**) male rainbow smelt (*Osmerus mordax*) sampled in Massachusetts in 4 coastal rivers with fyke nets in 2005–2007 and in marine waters during a trawl survey in 2004–2007. Lengths of female rainbow smelt caught in the Jones River are significantly different (Kruskal–Wallis rank sum test: α=0.05) from the lengths of females sampled at all other sampling locations, and the lengths of females from the Fore River are significantly different from those of females from the Saugus River. Lengths of male rainbow smelt caught in the Jones and Parker Rivers are significantly different from lengths of males from all other locations.

Age analysis For samples caught both with a trawl net in marine waters and with a fyke net in coastal rivers, age 2 was the most abundant age class of rainbow smelt, and few rainbow smelt older than age 2 were present (Table 2, Fig. 7). Age-1 rainbow smelt composed the next most common age class with evidence of fluctuations in annual recruitment. Despite our collection of a relatively large sample of rainbow smelt from the trawl survey (n=634), this sample produced only 12 age-3 and 4 age-4 female rainbow smelt for fecundity analysis.

The age data for rainbow smelt from fyke net sampling were compared with data from 2 previous studies that aged rainbow smelt during spawning runs in the Parker and Jones Rivers (Murawski and Cole, 1978; Lawton et al.[8]). A lower proportion of age-1 rainbow smelt were caught from the Jones and Parker Rivers in 4 of the

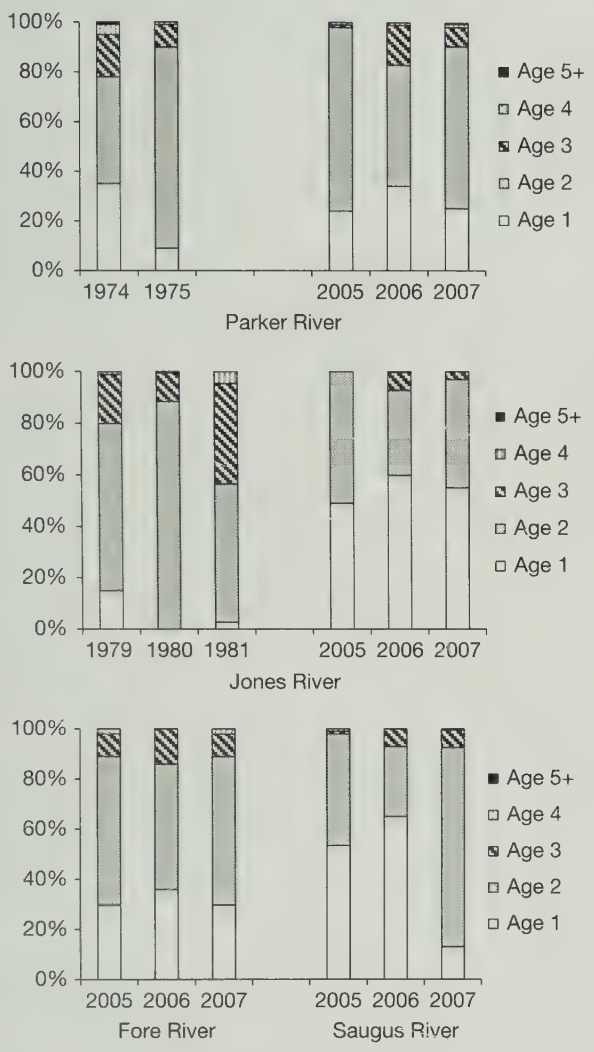

Figure 7

Age-frequency distribution for rainbow smelt (*Osmerus mordax*) sampled in 4 coastal rivers in Massachusetts during spawning runs in the spring of 2005–2007 as part of this study and for rainbow smelt caught during previous sampling in the Parker River (Murawski and Cole, 1978) and the Jones River (Lawton et al., 1990). Age-frequency distribution for fish from the Parker and Jones Rivers were significantly different between years (chi-square test: df=3, $P<0.01$), except for rainbow smelt caught at the Parker River in 1974 and 2006 ($P=0.444$) and at the Jones River in 2006 and 2007 ($P=0.220$).

5 annual samples in those studies than in each of the annual samples of our study (Fig. 7). The change is most pronounced in the Jones River, with an average annual frequency of 6% for age-1 rainbow smelt from 1979 through 1981 and 55% from 2005 through 2007. Additional evidence of changes in age structure was found in the Jones River: the average annual frequency of age-3 fish decreased from 23% during 1979–1981 to 3% during 2005–2007. These comparisons indicate a shift in age composition with a larger role for age-1 rainbow smelt in spawning runs.

The Chapman–Robson age-based survival estimator used in this study produced lower estimates of S and higher values of Z for rainbow smelt caught in the Jones and Parker Rivers than the estimates reported for the previous studies (Table 6). For all data sets of ages of rainbow smelt, Z estimates were calculated by using the Chapman–Robson estimator with years and sexes combined. Samples from the Fore River, with the highest representation of rainbow smelt older than age 2, had S and Z estimates closest to those of samples from the Parker and Jones Rivers in the earlier studies. Rainbow smelt from the Jones and Saugus Rivers had lower S and higher Z than samples from the Fore River and those examined in Murawski and Cole (1978) and Lawton et al.[8], as well as in another earlier study for which age data were reported for rainbow smelt in the Miramichi River in New Brunswick, Canada (McKenzie, 1964).

Length–weight analysis Length and weight data for the rainbow smelt from fyke net sampling and the trawl survey were evaluated as a measure of fish condition and to determine if differences occurred among sampling locations (Table 7). All regressions of the relationship of length and weight exhibited allometric growth with minor apparent differences between the trawl samples collected in winter and fyke net samples collected in spring. For all comparisons, the regression slopes were larger for females than males. There were no differences in the same-sex regression slopes for rainbow smelt collected at the Fore and Saugus Rivers. However, for both sexes, the regression slopes for the fyke net samples collected in coastal rivers did differ from those for the trawl samples collected in marine waters. Female rainbow smelt were significantly heavier at length than males for all locations, and the marine samples were heavier at length than the river samples.

Sex ratio The trawl samples collected in winter included significantly more females than males (1.3:1.0 female-to-male ratio; chi-square test: $\chi^2=7.13$, df=1, $P=0.008$), and the fyke net samples collected in spring included significantly more males than females (male-to-female ratios: Jones River, 1.8:1.0; Fore River, 3.3:1.0; Saugus River, 10.6:1.0; and Parker River, 5.7:1.0; chi-square test: $\chi^2=88$, 1092, 1653, and 533, respectively, df=1, $P<0.001$). The higher number of males captured with the fyke net is a sampling bias that resulted from males spawning more frequently than females (Marcotte and Tremblay, 1964; McKenzie, 1964; Murawski et al., 1980). It is possible that the unbalanced sex ratio found in trawl samples is biased by a higher proportion of males than females for the 60 immature rainbow smelt that were excluded from the sex ratio estimate.

Condition indices Fulton's condition factor for the trawl samples from marine waters and for the fyke net samples from the Fore and Saugus Rivers ranged between

Table 6

Estimates of survival (S) and total instantaneous mortality (Z) of rainbow smelt (*Osmerus mordax*) sampled in 4 coastal rivers of Massachusetts in 2005–2007 for this study and of rainbow smelt in previous studies. For all data sets, annual age keys were applied to length-frequency data, and age data from sample years and sexes were combined and applied to the Chapman–Robson age-based survival estimator with age-1 fish excluded.

Sampling location or type	Years	Source	n	S (SE)	Z (SE)
Fore River	2005–2007	This study	2762	0.12 (0.004)	2.11 (0.03)
Saugus River	2005–2007	This study	1427	0.11 (0.008)	2.23 (0.07)
Jones River	2005–2007	This study	526	0.08 (0.011)	2.52 (0.14)
Parker River	2005–2007	This study	803	0.10 (0.010)	2.27 (0.10)
Trawl survey	2004–2007	This study	517	0.10 (0.013)	2.28 (0.12)
Miramichi River	1949–1953	McKenzie, 1964	18,072	0.28 (0.003)	1.27 (0.01)
Parker River	1974–1975	Murawski and Cole, 1978	1595	0.16 (0.008)	1.82 (0.05)
Jones River	1979–1981	Lawton et al., 1990	34,268	0.18 (0.002)	1.71 (0.01)

Table 7

Regression coefficients from length–weight analysis (log-transformed total length and total weight data) for rainbow smelt (*Osmerus mordax*) sampled in Massachusetts in 2004–2007 in marine waters during a trawl survey and at the Fore River and Saugus River with fyke nets. SE=standard error; R^2=coefficient of multiple determination; I=immature rainbow smelt with undetermined sex.

Sampling location or type	Sex	Age	n	Intercept (a)	Slope (b)	Slope SE	R^2
Fore and Saugus Rivers combined	F	All	353	−13.11	3.20	0.03	0.96
	M	All	899	−12.88	3.14	0.02	0.97
Fore River	F	All	285	−13.12	3.21	0.04	0.96
	M	All	597	−12.81	3.13	0.02	0.97
	F	1	76	−11.28	2.83	0.13	0.87
	F	2	159	−12.55	3.10	0.12	0.81
	F	3	43	−13.97	3.37	0.18	0.89
Saugus River	F	All	68	−13.08	3.19	0.08	0.96
	M	All	302	−12.96	3.15	0.03	0.97
	F	1	28	−15.30	3.63	0.25	0.89
	F	2	39	−10.16	2.64	0.25	0.75
Trawl survey	F	All	277	−14.23	3.41	0.04	0.96
	M	All	215	−14.59	3.47	0.05	0.96
	I	All	59	−12.76	3.09	0.14	0.89
	F	2	76	−13.48	3.26	0.10	0.94

0.5 and 0.6, and values were similar to those estimated by Chen (1970), except immature rainbow smelt from the trawl survey had an average factor <0.5. Females had higher values than males for each sampling location in Kruskal–Wallis rank sum tests: χ^2=170.41 (Fore River), χ^2=38.57 (Saugus River), χ^2=34.40 (marine waters), df=1, P<0.001. Kruskal–Wallis multiple comparison tests found the condition factor for males from the Saugus River to be lower than that for males from both the Fore River and marine waters, but among females, only rainbow smelt from the Fore River and trawl survey had different values (the factor for samples from the Fore River was higher). Fulton's condition factor for age-2 females differed for all locations (Kruskal–Wallis rank sum test: χ^2=17.71, df=2,

$P<0.001$). The GSI values ranged from 3.5% to 38.1% and increased with length and age (Table 2).

Discussion

The comparison of rainbow smelt caught during winter in coastal waters off Massachusetts to rainbow smelt caught during spring spawning runs in coastal rivers contributes information about sparsely described aspects of the reproductive life history of anadromous rainbow smelt. Data from this comparison provide quantitative relationships of fecundity with size and age, a maturity ogive, the first ogive available for anadromous rainbow smelt, and biological references necessary to investigate influences on recruitment of rainbow smelt. Age and length data indicate that the role of age-1 rainbow smelt in spawning populations may be increasing. During the study period, the proportion of age-1 rainbow smelt in spawning runs was higher than proportions previously found in Massachusetts (Murawski and Cole, 1978; Lawton et al.[8]), and differences in the size of age-1 rainbow smelt and their proportion of the run age composition were observed between proximate spawning runs. The point of increasing participation of age-1 rainbow smelt in spawning runs is supported by our data; however, future investigations should consider that the collection methods were not identical between studies, raw length and age data were not available for samples in the other studies, and age composition data in all studies were derived from pooled age keys.

The cause of differences in life history characteristics among populations of rainbow smelt is not well described. Our findings of differences in length and age imply that maturation and growth rates vary over a modest geographical range. Kovach et al. (2013) conducted an analysis of genetic population structure for anadromous rainbow smelt from the Gulf of Maine, including samples from the 4 fyke net stations in Massachusetts, and found differences within this small geographic range but no river-level genetic variation. The populations of the Fore River and Saugus River were most similar genetically (and were also examined as a single Boston Harbor group). The populations of the Parker River and Jones River were related to the Boston Harbor group, but a majority of their genetic distinctiveness was associated with other populations north of the Parker River and south of the Jones River.

Fecundity and maturation

The small sample sizes of previous studies of fecundity in rainbow smelt limited the quantitative analyses of fecundity data and the interpretation of life history relevance. The number of samples collected from the trawl survey and used in fecundity analysis in our study (n=110) more than doubled that of the largest previous study of anadromous rainbow smelt (n=48; Chen, 1970), and analyses with those samples included fecundity regression relationships with 4 size and age predictor variables. Our collection of late-winter, marine rainbow smelt avoided biases associated with sampling during active spawning runs. The sample size of 110 was reached by pooling trawl tows and years, and pooling data does not allow inferences on annual or geographic differences. The general similarities in length distributions, length–weight relationships, and age structure among the sample locations indicate that pooling samples from the trawl survey over the study range (approximately 120 km) was suitable for regression analysis. A similar conclusion can be made on the pooling of age samples by year and sex and the application of age keys to sample rivers where rainbow smelt were not aged. Our analysis would be improved with the ability to consider annual differences in age composition by river and sex. However, the suspected influences of differences in annual growth rates and cohort strength on changes in mean length do not appear to translate to large changes in length-at-age data and age modes for this fast growing, short-lived species.

Our finding of increasing total fecundity and generally stable relative fecundity with age is interesting because of the implication of the higher reproductive potential of the uncommon older rainbow smelt due to higher fecundity and large oocyte size (Hixon et al., 2014). However, neither our study nor past reproductive studies of rainbow smelt have quantitatively addressed this point. Further investigation is needed on the role of oocyte size and fecundity in anadromous smelt reproductive potential.

The 2 previous studies with higher numbers of samples for fecundity analysis were focused on landlocked populations of rainbow smelt (n=172, Chen, 1970; n=208, Luey and Adelman, 1984). Chen (1970) found that fecundity for 3 landlocked populations and 1 anadromous population of rainbow smelt was significantly related to fork length, BW, OW, and age. His estimates of relative fecundity for the 4 stocks indicate that the anadromous stock was the most productive and had the highest mean Fulton's condition factor for both sexes. Luey and Adelman (1984) found significant differences in growth, fecundity–length relationship, and length distribution among 3 regions in western Lake Superior over a range of 220 km; yet the differences were slight. They suspected that these population differences were related to selective pressures (environmental and predatory) from the relatively recent introduction of rainbow smelt to the Great Lakes (Luey and Adelman, 1984). They also found few significant differences in length frequency among gear types, years, and sampling locations but consistent differences in length distribution between males and females (Luey and Adelman, 1984).

A comparison of the maturity ogive derived from marine samples to the length-at-age data from river samples indicates that not all age-1 rainbow smelt are recruited to annual spawning runs. Our study also provides evidence of a higher proportion of age-1 rainbow smelt in the spawning runs than has been found in previous studies. The actual extent of changes in the maturity

schedule of anadromous rainbow smelt cannot be determined because of the lack of previous ogive estimates, sampling differences, and limited historical information on cohort dynamics and raw length data. Our work highlights important data gaps, especially the lack of understanding of the environmental and phenotypic triggers on maturity of rainbow smelt and of the underlying influences that caused the increase of age-1 rainbow smelt in spawning runs.

Eggs per recruit

The estimates of Z and fecundity at age generated in this study were applied to an eggs-per-recruit (EPR) analysis that used the Fishmethods package in R and compared inputs from previous studies of rainbow smelt in the Parker River (Murawski and Cole, 1978), Jones River (Lawton et al.[8]), and Miramichi River (McKenzie, 1964). The purpose of the EPR analysis was to determine how lifetime fecundity responds to changes in fishing mortality (F). We introduce the EPR analysis here, in the "Discussion" section, because of its dependency on historical references for model input parameters and exploratory approach. The model assumes that fecundity has not changed over time and requires assigned values for F and natural mortality (M); however, no empirical measurements exist for rainbow smelt in our study area. Murawski and Cole (1978) used McKenzie's (1964) age data for rainbow smelt from the Miramichi River to derive Z (1.043) and tagging data to derive F (0.062) and used the equation $Z=M+F$ to estimate M as 0.981; then they applied M to derive an F of 0.268 for the population of rainbow smelt in the Parker River during 1974–1975. These values were used in our study as starting points for a sensitivity analysis on assumed levels of M and F given the estimates of Z.

The most influential inputs for the EPR model are M and the proportion of fish mature at each age (PMAT). The only value available for the proportion of mature age-1 anadromous rainbow smelt is the 0.6 derived from the trawl survey data used in this study. The first run of the EPR model was made with PMAT fixed at 0.6 for all data sets except the data set from the study of rainbow smelt from the Miramichi River where slower growth resulted in no age-1 rainbow smelt participating in the spawning run. The results shown in Figure 8A indicate that samples from the Parker and Jones Rivers in the 1970s and 1980s had the highest EPR despite having higher Z than those from the Miramichi River. The Miramichi River sample had the strongest presence of older rainbow smelt; however, with no age-1 rainbow smelt in the spawning run at that location, lifetime EPR was lower. Results of the EPR analysis indicate that the rainbow smelt populations in rivers in our study had relatively low and stable EPR and that reducing F caused little improvement to EPR because Z was dominated by M. The model estimated that EPR for rainbow smelt in the Jones River declined 38% from that reported in Lawton et al.[8] and that EPR for those in the Parker River declined 24% from that reported in Murawski and Cole (1978) (at F=0.200 on the x-axis, Fig. 8A).

In the interest of investigating the role of age-1 maturity, PMAT was reduced to 0.3 for the data sets based on samples from the Parker and Jones Rivers for a second run of the model. The decline in EPR from the model run with a PMAT of 0.6 to the model run with a PMAT of 0.3 for hypothetical spawning runs reflects the importance of age-1 participation in the spawning runs sampled for this study: with PMAT reduction, the EPR for samples from the Jones River declined 32% and the EPR for samples from the Parker River declined 29% (at F=0.200 on the x-axis, Fig. 8B). The third run of the EPR model was used to analyze the potential for reduced F in samples collected during spawning runs for this study (Fig. 8C). For the first run of the EPR model, F was set at 0.268, the Murawski and Cole (1978) estimate for rainbow smelt from the Parker River, for all samples of spawning runs except those from the Miramichi River for which an F estimate of 0.062 was available. However, the fishery for rainbow smelt in the 1970s occurred during winter from ice shacks set in the intertidal Parker River. That ice-shack fishery is essentially gone because it is uncommon in recent winters for estuary ice to be thick enough to safely support shack fishing. Therefore, the third EPR analysis set F at 0.000, with Z equal to M (Fig. 8C). Under this scenario of high M, the decline in EPR estimated in our study from the EPR reported for earlier studies was 44% for samples from the Jones River and 33% for samples from the Parker River (at F=0.200 on the x-axis, Fig. 8C). Changes in growth and maturity are possible influences that caused the proportion of age-1 rainbow smelt found in spawning runs sampled in our study to increase. However, this influence cannot be separated from cohort dynamics without further studies.

Evidence from our study and previous studies (Murawski and Cole, 1978; O'Malley et al., 2017) supports the premise that age-1 anadromous rainbow smelt are partially recruited to spring spawning runs. Further, our data indicate that the proportion of age-1 rainbow smelt in spawning runs in the study area has increased from the level observed several decades ago and that the presence of rainbow smelt older than age 2 has declined. The decline in the proportion of older rainbow smelt in the spawning run is the primary influence that results in higher Z estimates in this study. The higher proportion of age-1 rainbow smelt does not directly affect Z estimates because this cohort is not fully recruited and excluded from survival estimates. It has been noted that more males than females are precocious at age 1 in spawning runs of anadromous rainbow smelt (Murawski and Cole, 1978; Sutter, 1980). In this study, a higher proportion of males than females was found for mature age-1 rainbow smelt at each river sampled with a fyke net, at ratios similar to the sex ratios for all ages combined from fyke net sampling; however, the bias created by a higher rate of repeat spawning in males limits the quantification of the true sex ratio.

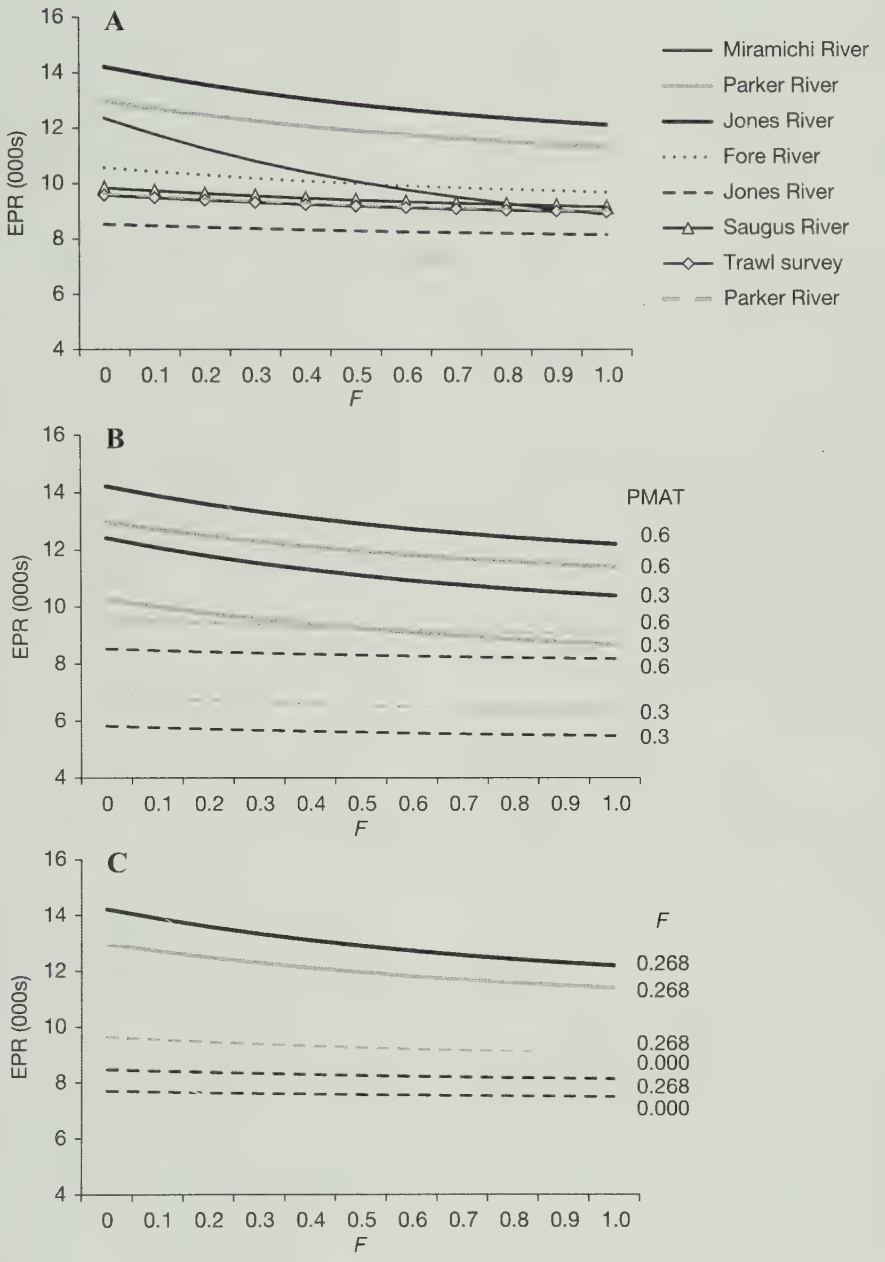

Figure 8

Eggs-per-recruit curves, which examine variation in lifetime fecundity in response to changes in fishing mortality (F), for anadromous rainbow smelt sampled in Massachusetts in 4 coastal rivers with fyke nets in 2005–2007 (this study) and in marine waters during a trawl survey in 2004–2007 (this study) and sampled in the Miramichi River, Canada, in 1949–1953 (McKenzie, 1964), the Parker River in 1974–1975 (Murawski and Cole, 1978), and the Jones River in 1979–1981 (Lawton et al., 1990). (**A**) Curves for fish collected from several sampling locations in this study and in previous studies, with the proportion of fish mature at age (PMAT) assigned as 0.6 for all but one of the locations and as 0.0 for the Miramichi River. (**B**) Curves with the PMAT set as 0.6 and 0.3 for samples from the Parker River (gray lines) and Jones River (black lines) for previous studies (solid lines) and this study (dashed lines). (**C**) Curves with the F component of Z set as 0.268 or 0.000 for samples from the Parker River and Jones River for previous studies and this study.

Implications for populations of rainbow smelt

A synopsis of information on stocks of rainbow smelt in the Gulf of Maine led to the conclusion that sharp declines have occurred in fisheries for and abundance of rainbow smelt in recent decades (Enterline et al., 2012). In Massachusetts, participation in rainbow smelt fisheries has declined to very low levels, and fisheries have ceased in most estuarine rivers where winter ice is no longer sufficient to support fishing. However, empirical measures of changes in population data related to this declining trend are absent. The fecundity data presented here indicate that reproductive potential has been lost with the decline in the proportion of rainbow smelt in spawning runs that are age 3 or older. This change is most pronounced in the spawning runs in the Jones River, where our data indicate that large increases in age-1 rainbow smelt and decreases in rainbow smelt age 3 or older have occurred. The results of analysis indicate declines of 20–40% in EPR from previous studies to this study for populations sampled in the Jones and Parker Rivers, and these estimates are most influenced by changes in Z, which does not include partially recruited age-1 rainbow smelt. Given these age structure changes and that rainbow smelt age 3 or older are nearly 5 times as fecund as age-1 rainbow smelt, spawning runs today may be recruitment limited. Despite this implication, the high proportion of age-1 rainbow smelt in spawning runs observed in this study may be important for population survival: current spawning runs would experience even lower EPR with lower levels of maturation among age-1 fish. Further investigations on recruitment relationships and fecundity of rainbow smelt with sampling from a wider geographic range and longer temporal scale are needed to assist management and restoration efforts for rainbow smelt.

Size at age has been reported to decline with increasing latitude for spawning populations of anadromous rainbow smelt (McKenzie, 1964; Pouliot, 2002; Enterline et al., 2012; O'Malley et al., 2017). A large majority of landlocked and anadromous rainbow smelt in populations from eastern Maine northward historically matured at age 2 (Rupp, 1959; McKenzie, 1964; Chen, 1970). Age-1 rainbow smelt are known to spawn at variable rates in U.S. waters of the Gulf of Maine, with higher percentages found in Massachusetts, lower percentages in rivers of western Maine, and near absence in Canadian Maritime provinces (Warfel et al., 1943; McKenzie, 1964; Murawski and Cole, 1978; Pouliot, 2002; Enterline et al., 2012). In Massachusetts, age-2 rainbow smelt have been found to form the predominant cohort in spawning runs, with low, fluctuating percentages observed for age-1 and age-3 cohorts, age-4 fish being uncommon, and fish of ages 5–6 rarely observed (Murawski and Cole, 1978; Lawton et al.[8]).

Temperature-related differences in growth rates may be a cause of the decline in proportion of age-1 rainbow smelt in spawning runs with increasing latitude. Murawski and Cole (1978) back-calculated length at age from scales of rainbow smelt from the Parker River and found close agreement with the actual mean length at age, except for age-1 fish. The lower back-calculated size at age-1 indicates that only larger age-1 rainbow smelt were recruited to the spawning run. The proportion of age-1 females was also lower than that of age-1 males in the spawning run, and Z was lower in females than in males (Murawski and Cole, 1978). These findings suggest a trade-off for maturation of rainbow smelt in which fast-growing rainbow smelt that mature in their first year may realize greater lifetime reproductive potential but are exposed to higher mortality than fish that mature later. Both our study and the previous studies of rainbow smelt in Massachusetts found a higher proportion of males than females among age-1 fish in spawning runs (Murawski and Cole, 1978; Sutter, 1980; Lawton et al.[8]). The difference between sexes may be related to the longer schedule and larger energy allocation required for oogenesis than for spermatogenesis that has been found in landlocked rainbow smelt (Chen, 1970; Foltz and Norden, 1977).

The maturation schedules of species of Pacific salmon (*Oncorhynchus* spp.) are likely the best studied of all diadromous species. Natural selection influences maturation strategies in Pacific salmon species as reflected by oocyte size and fecundity (Campbell et al., 2006). Phenotypic differences in egg size and maturation in species of Pacific salmon have been related to water temperature and growth rates, with fast growth, early maturation, high fecundity, and small egg size thought to be a response to lower survival rates (Murray and McPhail, 1988; Kinnison et al., 1998). Further work is needed to determine if the selective pressures on Pacific salmon species are similar to those on anadromous rainbow smelt, given their phylogenetic proximity.

Luey and Adelman (1984) suggested that landlocked populations of rainbow smelt are prone to selective pressures on their reproductive life history because they are small, fast growing, and short-lived. The variability of size and age in spawning populations of anadromous rainbow smelt in the broader geographic region of New England (Chase et al., 2009; Enterline et al., 2012; O'Malley et al., 2017) supports the expectation of a link between growth rates and maturation schedule. Results from genetic analyses of rainbow smelt in our study area by Kovach et al. (2013) provide evidence of gene flow among the 4 locations where fyke nets were deployed and indicate that larval dispersal is most influenced by circulation patterns in the Gulf of Maine and that the circulation patterns were more influential to population genetic structure than natal homing. More information is needed to determine environmental influences, maturation thresholds, and population recruitment consequences across a wider geographic range for the species.

Our data provide evidence of differences in length and suggest that there are differences in growth among populations of rainbow smelt over a small spatial scale. However, the spatial and temporal scales of our data do not allow inferences on interpopulation differences in reproductive life history traits. Further work is needed to determine the nature of phenotypic divergence in reproductive life history of anadromous rainbow smelt across the geographic range of this species and on the population-level consequences of phenotypic plasticity in age and size at maturity.

Acknowledgments

We appreciate B. Hoffman for coordinating collection of marine samples and the field and laboratory assistance of intern N. Delphin from Manchester High School, fyke net technicians K. Taylor, C. Woodhead, and K. Magowan, and K. Broomstein, an American Fisheries Society Hutton Scholar. We thank G. Nelson, E. Schultz, G. Skomal, and anonymous reviewers for comments on previous versions. We received financial support through the Sportfish Restoration Act and from the NOAA Protected Species Program.

Literature cited

Bailey, M. M.
1964. Age, growth, maturity, and sex composition of the American smelt, *Osmerus mordax* (Mitchill), of western Lake Superior. Trans. Am. Fish. Soc. 93:382–395.

Campbell, B., B. R. Beckman, W. T. Fairgrieve, J. T. Dickey, and P. Swanson.
2006. Reproductive investment and growth history in female coho salmon. Trans. Am. Fish. Soc. 135:164–173.

Chase, B. C., M. H. Ayer, and S. P. Elzey.
2009. Rainbow smelt population monitoring and restoration on the Gulf of Maine coast of Massachusetts. Am. Fish. Soc. Symp. 69:899–901.

Chen, M. Y.
1970. Reproduction of American smelt, *Osmerus mordax* (Mitchill). Ph.D. diss., 254 p. Univ. Waterloo, Ottawa, Canada.

Clayton, G. R.
1976. Reproduction, first year growth, and distribution of anadromous rainbow smelt, *Osmerus mordax*, in the Parker River and Plum Island Sound estuary, Massachusetts. M.S. thesis, 105 p. Univ. Mass., Amherst, MA.

Crim, L. W., and B. D. Glebe.
1990. Reproduction. *In* Methods for fish biology (C. B. Schreck and P. B. Moyle, eds.), p. 529–553. Am. Fish. Soc., Bethesda, MD.

Driedzic, W. R., and K. V. Ewart.
2004. Control of glycerol production by rainbow smelt (*Osmerus mordax*) to provide freeze resistance and allow foraging at low winter temperatures. Comp. Biochem. Physiol. B 139:347–357.

Driedzic, W. R., and C. E. Short.
2007. Relationship between food availability, glycerol and glycogen levels in low-temperature challenged rainbow smelt (*Osmerus mordax*). J. Exp. Biol. 210:2866–2872.

Enterline, C. L., B. C. Chase, J. M. Carloni, and K. E. Mills.
2012. A regional conservation plan for anadromous rainbow smelt in the U.S. Gulf of Maine, 100 p. Maine Dep. Mar. Res., Augusta, ME. [Available from website.]

Evans, D. O., and D. H. Loftus.
1987. Colonization of inland lakes in the Great Lakes region by rainbow smelt, *Osmerus mordax*: their freshwater niche and effects on indigenous fishes. Can. J. Fish. Aquat. Sci. 44(S2):249–266.

Federal Register.
2004. Endangered and threatened species; establishment of species of concern list, addition of species to species of concern list, description of factors for identifying species of concern, and revision of candidate species list under the Endangered Species Act. Fed. Regist. 69:19975–19979. [Available from website.]

Foltz, J. W., and C. R. Norden.
1977. Seasonal changes in food consumption and energy content of smelt (*Osmerus mordax*) in Lake Michigan. Trans. Am. Fish. Soc. 106:230–234.

Goode, G. B.
1884. The fisheries and fishery industries of the United States, 881 p. Government Printing Office, Washington, DC.

Gorman, O. T.
2007. Changes in a population of exotic rainbow smelt in Lake Superior: boom to bust, 1974–2005. J. Great Lakes Res. 33:75–90.

Hare, J. A., D. L. Borggaard, K. D. Friedland, J. Anderson, P. Burns, K. Chu, P. M. Clay, M. J. Collins, P. Cooper, P. S. Fratantoni et al.
2016. Northeast Regional Action Plan—NOAA Fisheries Climate Science Strategy. NOAA Tech. Memo. NMFS-NE-239, 72 p. [Available from website.]

Hixon, M. A., D. W. Johnson, and S. M. Sogard.
2014. BOFFFFs: on the importance of conserving old-growth age structure in fishery populations. ICES J. Mar. Sci. 71: 2171–2185.

Kendall, W. C.
1926. The smelts. Bull. Bur. Fish. 42:217–375.

Kinnison, M. T., M. J. Unwin, W. K. Hershberger, and T. P. Quinn.
1998. Egg size, fecundity, and development rate of two introduced New Zealand chinook salmon (*Oncorhynchus tshawytscha*) populations. Can. J. Fish. Aquat. Sci. 55: 1946–1953.

Kircheis, F. W., and J. G. Stanley.
1981. Theory and practice of forage-fish management in New England. Trans. Am. Fish. Soc. 110:729–737.

Kovach, A. I., T. S. Breton, C. Enterline, and D. L. Berlinsky.
2013. Identifying the spatial scale of population structure in anadromous rainbow smelt (*Osmerus mordax*). Fish. Res. 141: 95–106.

Limburg, K. E., and J. R. Waldman.
2009. Dramatic declines in North Atlantic diadromous fishes. BioScience 59:955–965.

Luey, J. E., and I. R. Adelman.
1984. Stock structure of rainbow smelt in western Lake Superior: population characteristics. Trans. Am. Fish. Soc. 113:709–715.

Marcotte, A., and J. L. Tremblay.
1948. Notes sur la biologie de l'éperlan (*Osmerus mordax* Mitchell) de la Province de Québec. Stn. Biol. Saint-Laurent Contrib. 18, 107 p. [Available from Direction de la protection de la faune du Bas-Saint-Laurent et de la Gaspésie–Îles-de-la-Madeleine, 92, 2e Rue Ouest, bureau 207, Rimouski, Quebec, Canada G5L 8B3.]

McKenzie, R. A.
1964. Smelt life history and fishery of the Miramichi River, New Brunswick. Fish. Res. Board Can., Bull. 144, 77 p.

Mercado-Silva, N., J. D. Olden, J. T. Maxted, T. R. Hrabik, and M. J. V. Zanden.
2006. Forecasting the spread of invasive rainbow smelt in the Laurentian Great Lakes region of North America. Conserv. Biol. 20:1740–1749.

Murawski, S. A., and C. F. Cole.
1978. Population dynamics of anadromous rainbow smelt *Osmerus mordax*, in a Massachusetts river system. Trans. Am. Fish. Soc. 107:535–542.

Murawski, S. A., G. R. Clayton, R. J. Reed, and C. F. Cole.
1980. Movements of spawning rainbow smelt, *Osmerus mordax*, in a Massachusetts estuary. Estuaries 3:308–314.

Murray, C. B., and J. D. McPhail.
1988. Effect of incubation temperature on the development of five species of Pacific salmon (*Oncorhynchus*) embryos and alevins. Can. J. Zool. 66:266–273.

Nelson, G.
2017. Fishmethods: fishery science methods and models. Vers. 1.10-4. [Available from website, accessed March, 2018.]

Nielsen, L. A., and D. L. Johnson (eds).
1983. Fisheries techniques, 732 p. Am. Fish. Soc., Bethesda, MD.

O'Gorman, R., R. A. Bergstedt, and T. H. Eckert.
1987. Prey fish dynamics and salmonine predator growth in Lake Ontario 1974–84. Can. J. Fish. Aquat. Sci. 44(S2): 390–403.

O'Malley, A. J., C. Enterline, and J. Zydlewski.
2017. Size and age structure of anadromous and landlocked populations of rainbow smelt. North Am. J. Fish. Manage. 37:326–336.

Pouliot, G.
2002. Dynamique de la population d'éperlans arc-en-ciel (*Osmerus mordax*) du sud de l'estuaire du Saint-Laurent par l'analyse de cohortes de reproducteurs fréquentant la rivière Fouquette entre 1994 à 2001, 47 p. Société de la faune et des parcs du Québec, Direction de l'aménagement de la faune de la r égion du Bas-Saint-Laurent, Québec, Canada.

R Core Team.
2016. R: a language and environment for statistical computing. R Foundation for Statistical Computing, Vienna, Austria. [Available from website, accessed May 2016.]

Ricker, W. E.
1975. Computation and interpretation of biological statistics of fish populations. Fish. Res. Board Can., Bull. 191, 382 p.

Roa, R., B. Ernst, and F. Tapia.
1999. Estimation of size at sexual maturity: and evaluation of analytical and resampling procedures. Fish. Bull. 97:570–580.

Rupp, R. S.
1959. Variation in the life history of American smelt in inland waters of Maine. Trans. Am. Fish. Soc. 88:241–252.

Sayers, R. E., Jr., J. R. Moring, P. R. Johnson, and S. A. Roy.
1989. Importance of rainbow smelt in the winter diet of landlocked Atlantic salmon in four Maine lakes. North Am. J. Fish. Manage. 9:298–302.

Scott, W. B., and E. J. Crossman.
1973. Freshwater fishes of Canada. Fish. Res. Board Can., Bull. 184, 966 p.

Scott, W. B., and M. G. Scott.
1988. Atlantic fishes of Canada. Can. Bull. Fish. Aquat. Sci. 219, 731 p.

Sokal, R. R., and F. J. Rohlf.
1995. Biometry: the principles and practice of statistics in biological research, 3rd ed., 887 p. W. H. Freeman and Co., New York.

Stritzel Thomson, J. L., D. L. Parrish, S. L. Parker-Stetter, L. G. Rudstam, and P. J. Sullivan.
2011. Growth rates of rainbow smelt in Lake Champlain: effects of density and diet. Ecol. Freshw. Fish 20:503–512.

Sutter, F. C., III.
1980. Reproductive biology of anadromous rainbow smelt (*Osmerus mordax*) in the Ipswich Bay area, Massachusetts. M.S. thesis, 49 p. Univ. Mass., Amherst, MA.

Trencia, G., G. Verreault, M. Legault, and V. Tremblay.
2005. L' éperlan arc-en-ciel (*Osmerus mordax*) anadrome du sud de l'estuaire du Saint-Laurent: une population en voie de désignation comme espèce vulnérable. Nat. Can. 129(1):86–95.

Van Oosten, J.
1937. The dispersal of smelt, *Osmerus mordax* (Mitchill), in the Great Lakes region. Trans. Am. Fish. Soc. 66:160–171.

Venables, W. N., and B. D. Ripley.
2002. Modern applied statistics with S, 4th ed., 498 p. Springer, New York.

Verreault, G., G. Trencia, and M. Legault.
2012. The rainbow smelt restoration plan for the St. Lawrence estuary: where are we eight years later? *In* Fourth North American workshop on rainbow smelt: extended abstract proceedings; Portland, ME, 24–25 January 2011 (C. H. Wood, C. Enterline, K. Mills, B. C. Chase, G. Verreault, J. Fischer, and M. H. Ayer, eds.), 62–64 p. Mass. Div. Mar. Fish. Tech. Rep. TR-51. [Available from website.]

Warfel, H. E., T. P. Frost, and W. H. Jones.
1943. The smelt, *Osmerus mordax*, in Great Bay, New Hampshire. Trans. Am. Fish. Soc. 72:257–262.

National Marine
Fisheries Service
NOAA

Fishery Bulletin
established in 1881

Spencer F. Baird
First U.S. Commissioner
of Fisheries and founder
of *Fishery Bulletin*

Age and growth parameters of the Panamic stingray (*Urotrygon aspidura*)

Katherine Torres-Palacios (contact author)[1,3]
Paola A. Mejía-Falla[1,2]
Andrés F. Navia[1]
Víctor H. Cruz-Escalona[3]
Roberto Félix-Uraga[3]
Casimiro Quiñonez-Velázquez[3]

Email address for contact author: ktorres@squalus.org

[1] Fundación Colombiana para la Investigación y Conservación de Tiburones y Rayas
SQUALUS
Calle 10A #72-35
Apartamento 310E
760033 Cali, Valle del Cauca, Colombia

[2] Wildlife Conservation Society Colombia
Avenida 5N #22N-11
760046 Cali, Valle del Cauca, Colombia

[3] Centro Interdisciplinario de Ciencias Marinas
Instituto Politécnico Nacional
Avenida Instituto Politécnico Nacional s/n
Colonia Playa Palo de Santa Rita
Apartado Postal 592
23096 La Paz, Baja California Sur, Mexico

Abstract—The aim of this study was to estimate the age and growth parameters of the Panamic stingray (*Urotrygon aspidura*) of the Pacific coast of Colombia. Vertebral centra were removed from 309 individuals and used for estimation of age. The results of edge type and marginal increment analysis indicate an annual formation of band pairs. The maximum ages estimated were 7.5 and 5.5 years for female and male Panamic stingrays, respectively. Individual growth was described through a multi-model approach and inference, by using von Bertalanffy, Gompertz, and logistic models with 2 and 3 parameters each and a two-phase growth model with 4 and 5 parameters. A two-phase growth function of 5 parameters with adjusted age provided the best description of growth for females (asymptotic disc width [DW_∞]=24.71 cm, growth coefficient [k]=0.47 cm/year, disc width at birth [DW_0]=8.18 cm, age at transition between 2 phases [t_h or inflection point of the curve]=2.32 years, and maximum difference in disc width at age between von Bertalanffy and two-phase models [h]=0.36) and males (DW_∞=15.96 cm, k=1.63 cm/year, DW_0=8.07 cm, t_h= 2.22 years, h=0.54). The growth curves were dissimilar between sexes mainly after the inflection point, and differences were found for all parameters, except for t_h. The Panamic stingray is a fast-growing and short-lived elasmobranch, similar to other species of the Urotrygonidae.

Manuscript submitted 24 October 2018.
Manuscript accepted 16 July 2019.
Fish. Bull. 117:169–179 (2019).
Online publication date: 30 July 2019.
doi: 10.7755/FB.117.3.4

The views and opinions expressed or implied in this article are those of the author (or authors) and do not necessarily reflect the position of the National Marine Fisheries Service, NOAA.

Understanding the growth, age, maturation processes, and longevity of elasmobranch species is necessary to evaluate population status and to predict variations over time (Cailliet and Goldman, 2004), as well as to develop management and conservation initiatives (Harry et al., 2010; Smart et al., 2013). Rajiformes are the batoid group for which the greatest number of studies on age and growth have been carried out (Shark-References, vers. 2015, bibliography database available from website), mainly because of their size and commercial importance. Conversely, small species of no commercial importance, such as those belonging to the Urolophidae and Urotrygonidae (Order Myliobatiformes), have received less attention, despite being abundant bycatch in shrimp trawl fisheries (Rico-Mejía and Rueda, 2007; Santander-Neto, 2015; Clarke et al., 2016).

Age and growth studies for the Urotrygonidae, both in the American Pacific and Atlantic Oceans, have identified that species of the genus *Urobatis* (Babel, 1967; Hale and Lowe, 2008; Morales-Azpeitia et al., 2013; Smith et al., 2013; Spieler et al., 2013) as well as those of the genus *Urotrygon* (Mejía-Falla et al., 2014; Guzmán-Castellanos, 2015; Santander-Neto, 2015) have high growth rates, low maximum ages, and early maturation, compared with other batoid species (Frisk, 2010) and with elasmobranchs in general (Cortés, 2000).

The Panamic stingray inhabits the Eastern Tropical Pacific (Robertson and Allen, 2015) and is abundant as bycatch in the shrimp trawl fishery of that region (Amezcua et al., 2006; Navia et al., 2009; Navarro-González et al., 2012). Despite its high incidence in this fishery, this species has been little studied with work done on only

its diet (Navarro-González et al., 2012) and morphology (González-Isáis and Montes-Domínguez, 2016; Montes-Domínguez and González-Isáis, 2017; Navarro-González et al., 2018). Consequently, it is categorized as a data deficient species in the International Union for Conservation of Nature IUCN Red List (Valenti and Robertson, 2009).

The high catch volumes of Panamic stingrays in the shrimp trawl fishery in the central zone of the Pacific coast of Colombia, the significant increase in the dominance of this species in the elasmobranch assemblage of the study area, the decrease in the catch rate (Navia and Mejía-Falla, 2016), and the lack of information on its life history traits highlight the importance of contributing relevant information for future population assessments. The aim of this study was to estimate and compare the age and growth parameters of male and female Panamic stingrays, by using a multi-model approach and inference.

Material and methods

Specimen collection

Individuals of the Panamic stingray were collected from an area of small-scale, shallow-water shrimp fishing operations in the central zone of the Pacific coast of Colombia (from 4°34′N, 77°21′W to 2°31′N, 78°34′W), during 2006–2009 and 2015. The number of animals collected was lower during the first quarter of the year, given the closure of the shrimp trawl fishery in these months along the Pacific coast of Colombia. This area has sandy–muddy substrate and shallow (<8.3-m depth), warm (between 25°C and 29°C), and brackish (salinity between 21.8 and 25.6) waters (Mejía-Falla, 2012).

Rays were measured (disc width [DW], in centimeters), their sex was determined, they were eviscerated, and part of the vertebral column from the abdominal region was extracted, tagged, and frozen until analysis was done later in the laboratory. Differences in DW between sexes were evaluated by using a Mann–Whitney test.

Vertebrae processing and band-pair counts

Vertebrae were cleaned manually by using a scalpel to eliminate the excess of muscle and connective tissue and to obtain the vertebral centra. The diameter of vertebrae was measured sagittally, and then the vertebrae were grouped in 3 size categories: large (2.50–3.30 mm), medium (1.60–2.49 mm), and small (0.70–1.59 mm). Tests were carried out by using different thicknesses of cut, stains, and times of staining for each vertebra size. Vertebral sections were rinsed with distilled water and polished before being observed. The best combination for the visualization of bands was 0.4-mm sagittal sections, stained with light green (0.05%) for 5 min for small vertebrae and with methylene blue (0.001%) for 10 min for medium vertebrae and for 20 min for large vertebrae. Sections were observed by using an optical microscope under transmitted light. Photographs were taken along with the respective scale by using the Zen lite[1] (blue ed., vers. 1.0) microscope software for light microscopy systems (Carl Zeiss Microscopy, LLC, Jena, Germany), and the growth bands were measured along the border of the corpus calcareum of each vertebra, by using the Zen lite microscope software.

Two readers (reader 1 had the most experience) performed a training exercise of counting the bands of a subsample (sample size [n]=100) to refine the methods, identification criteria, and counts of translucent bands. The following criteria were established: 1) identification of the presence of a pair of growth bands (one translucent and one opaque), defined as a band pair; 2) identification of a birth band through a change in the angle of the corpus calcareum in the closest place to the focus of the vertebra; and 3) enumeration of translucent bands. The 2 readers then did an independent band count of the whole sample, without knowing the sex or size of the specimens. The translucent-band counts were compared, and if the band counts did not coincide between readings (with differences in band counts of 3 or more), a third reading was made to reach a consensus; if no consensus was reached, the sample was discarded.

Bias and precision between readers

Different methods were employed to evaluate bias and precision of readings, on the basis of independent readings (Cailliet and Goldman, 2004). The bias between readers was evaluated through an age-bias plot (Campana et al., 1995) and Bowker's test for symmetry (Hoenig et al., 1995). The age-bias plot relates the band-pair count of reader 1 (x-axis) versus the mean band-pair count of reader 2 (y-axis). The second test was used to evaluate whether differences between readings by reader 1 and 2 were due to random events (P>0.05) or systematic errors (P<0.05), by using a chi-square test.

The percentage of vertebrae that could be read was calculated as (number of read vertebrae/total number of samples)×100. The percentage of agreement between readers was calculated as (number of agreements/total number of readings)×100, taking into account differences of 0, 1, and 2 band pairs.

The average percent error (APE) and the coefficient of variation (CV) between readers were also evaluated, taking into account variations of each reading with respect to the mean value of readings, as follows (Beamish and Fournier, 1981; Campana et al., 1995; Campana, 2001):

$$APE = \left[\frac{1}{n}\left(\frac{1}{R}\sum_{i=1}^{R}\frac{\left|x_{ij}-\bar{x}_j\right|}{\bar{x}_j}\right)\right]\times 100 \text{ and} \qquad (1)$$

[1] Mention of trade names or commercial companies is for identification purposes only and does not imply endorsement by the National Marine Fisheries Service, NOAA.

$$CV = \left[\frac{1}{n} \left(\frac{\sqrt{\sum_{i=1}^{R} \frac{\left(x_{ij} - \bar{x}_j\right)^2}{R}}}{\bar{x}_j} \right) \right] \times 100, \quad (2)$$

where x_{ij} = the i_{th} reading for individual j;
$\bar{x}_j$ = the average band-pair count for individual j;
R = the number of readings (one for each reader); and
n = the number of readings for the entire sample.

Low values of these indices indicate greater precision between readers (Campana, 2001).

Periodicity in band-pair formation

The periodicity in the formation of vertebral band pairs in Panamic stingrays was evaluated through the analysis of edge type (qualitative approach) and of the marginal increment (MI) index (quantitative approach). For the edge type, the band at the edge of each vertebra (opaque or translucent and growing or ending band) was identified, and the monthly frequency of each combination was calculated. The MI was estimated on the basis of the following measures taken of each vertebral sagittal section with the Zen lite microscope software: radius (R, or distance from the focus to the vertebral edge), and distance from the focus to the last (R_n) and next-to-last (R_{n-1}) completely formed band. The MI was estimated by using this equation: $MI=(R-R_n)/(R_n-R_{n-1})$ (Hayashi, 1976), and the average value was calculated and plotted per month. Differences in MIs among months were evaluated by using a Kruskal–Wallis test.

Growth models and parameters

Two data sets of age were built; the first considers the months with peaks of reproduction, and the second does not include this reproductive information (Harry et al., 2010; Mejía-Falla et al., 2014). In the first case (adjusted analysis), the time between birth and the first band formation was considered, on the basis of the reproductive cycle of the species obtaining a mean value for all data. Along the Pacific coast of Colombia, Panamic stingray present 2 birth peaks per year (in January and August; P. Mejía-Falla, unpubl. data), and the month of growth band formation occurs in October–November (see the "Results" section). Therefore, the times between birth and formation of the first growth band (9–10 or 2–3 months) have a mean of 6 months (0.5 years), a value that was subtracted from the total number of translucent bands counted. For the second data set, it was assumed that the first band pair is formed 1 year after birth, irrespective of reproductive seasonality; therefore, a value of 1 was subtracted from the total number of translucent bands counted. For example, an individual with 3 translucent bands counted had an age of 2.5 years for the first data set and an age of 2.0 years for the second data set.

A multi-model approach was used to describe growth. Eight models were fitted by using age and DW data of individuals: the von Bertalanffy growth model (VBGM; von Bertalanffy, 1938), Gompertz growth model (Ricker, 1979), and logistic growth model (Ricker, 1979) were fitted with 2 and 3 parameters, and the two-phase growth model (TPGM; Soriano et al., 1992) was fitted with 4 and 5 parameters (Suppl. Table 1) (online only). Models with 2 and 4 parameters include a DW_0 parameter, for which the birth DW at 7.5 cm was used (P. Mejía-Falla, unpubl. data). The parameter DW_∞ is the theoretical asymptotic width, representing the average disc width at age that individuals in a stock would attain if they grew indefinitely. The annual k is the relative growth rate at which a stingray reaches DW_∞ at age. The parameter t_0 is the theoretical age at zero, a point on the time axis when mean DW at age is zero. Models with 4 and 5 parameters included t_h, which is the age at which the transition between the 2 phases occurs (inflection point), and h is the maximum difference in DW at age between the VBGM and the TPGM at the t_h.

Parameters of the models were estimated by maximum likelihood method. The most adequate model was chosen on the basis of biological and statistical fit. Biological fit was based on known maximum DW, DW at birth, and DW at maturity (26.5, 7.5, and 15 cm DW, respectively; P. Mejía-Falla, unpubl. data). Statistical relevance was evaluated by calculating Akaike information criterion (AIC_i, Akaike, 1973), as well as the difference in AIC_i between models (Δ_i) and Akaike weight (w_i), for each i_{th} model, as follows:

$$AIC_i = 2\ln(L) + 2p, \quad (3)$$

$$\Delta_i = AIC_i - AIC_{min}, \text{ and} \quad (4)$$

$$w_i = \frac{e^{\left(-0.5\Delta_i\right)}}{\sum e^{\left(-0.5\Delta_i\right)}}, \quad (5)$$

where p = the number of parameters;
L = maximum likelihood;
Δ_i = the difference between each model's AIC_i; and
AIC_{min} = the lowest AIC_i of all models.

Models with Δ_i values between 0 and 2 have substantial statistical support, those with values between 4 and 7 have moderate support, and those with values >10 have no support (Burnham and Anderson, 2002). With multimodel inference, if one model does not obtain an Akaike weight value over 0.9 or if several models have substantial statistical support, it is advisable to estimate a weighted average of parameters on the basis of the models with support, along with the associated unconditional standard error (SE) (Burnham and Anderson, 2002), as follows:

$$\bar{\theta}_i = \sum_{i=1}^{n} w_i \times \hat{\theta} \quad \text{and} \quad (6)$$

$$SE(\bar{\theta}) = \sum_{i=1}^{n} w_i \times \left[\text{var}\left(\hat{\theta}_i\right) + \left(\hat{\theta}_i - \bar{\theta}\right)^2 \right]^{1/2}, \quad (7)$$

where $SE(\bar{\theta})$ = the standard error of the mean $\bar{\theta}$;
$\bar{\theta}$ = the parameter to be averaged;

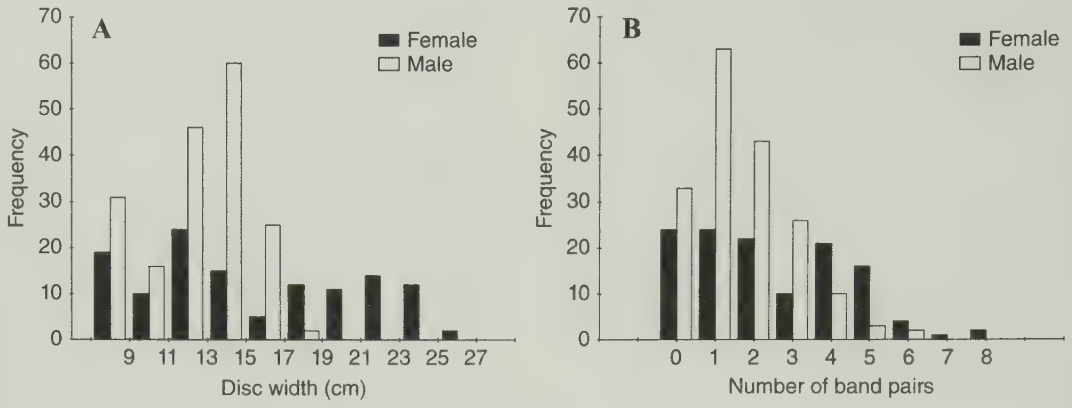

Figure 1

Frequency distribution of (**A**) sizes (disc width) and (**B**) ages (number of band pairs) for female and male Panamic stingrays (*Urotrygon aspidura*) collected in the central zone of the Pacific coast of Colombia in 2006–2009 and 2015 by small-scale, shallow-water shrimp fishing operations.

i = the model;
w_i = the Akaike weight of model i;
$\text{var}\left(\hat{\theta}_{i/i}\right)$ = the variance of the estimated parameter for model i; and
$\hat{\theta}$ = the estimated parameter for model i.

Finally, differences in growth curves between sexes for the selected models were tested by using a likelihood ratio test (Kimura, 1980; Haddon, 2001).

Results

A total of 309 specimens of the Panamic stingray (184 males and 125 females) were analyzed, and only 5 specimens were discarded for poor definition of band pairs and problems with reaching a consensus in reading. Female DW ranged from 7.1 to 26.5 cm, and male DW ranged from 7.0 to 18.5 cm, with most males measuring 11–15 cm DW (Fig. 1A). Females were significantly larger (15.6 cm DW [standard deviation [SD] 5.5, n=124) than males (12.6 cm DW [SD 2.6], n=180, Z=3.92, P<0.0001).

Readings of vertebral sections had high reproducibility, with no systematic bias between readers (P=0.25; Fig. 2), high percentage of agreement between readers (87.4% with no differences in readings and 99.0% with differences of only 1 band pair), and relatively low error (APE=4.06%, CV=6.25%, n=309). Females had a maximum of 8 band pairs, but most of them (56.5%) had between 0 and 2 band pairs. Males had a maximum of 6 band pairs, and 91.7% of them had between 0 and 3 band pairs (Fig. 1B). From seasonally adjusted data, the maximum ages were 7.5 and 5.5 years for females and males, respectively.

The analysis of edge type did not show a completely clear pattern with respect to the monthly deposition of band pairs. This result could have been influenced by the low number of specimens collected during the first quarter of the year (Suppl. Table 2) (online only). However, it was possible to observe a trend that indicates annual accumulation, with the opaque band forming from the first months of the year until July and the translucent band forming approximately from August until February (Fig. 3A).

There were significant differences in MI among months (Kruskal–Wallis test: H=24.06, P=0.008, n=141). Monthly variations of the MI indicate that band pairs start to form the opaque band during the first months of the year, with higher mean values in October and November when the translucent band is formed (Fig. 3B). Despite the small sample size during February–May, these results indicate an annual periodicity in the formation of band pairs.

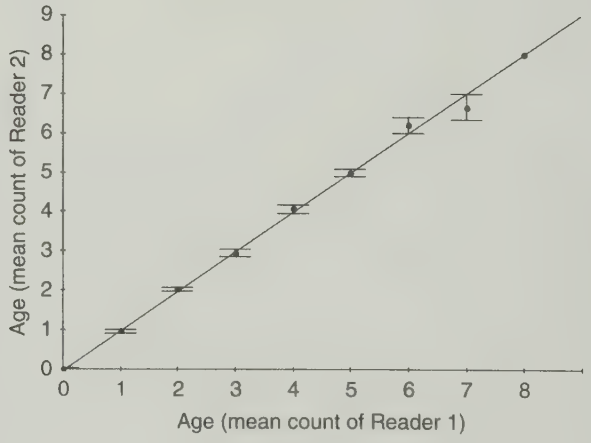

Figure 2

Age-bias plot of band-pair counts for Panamic stingrays (*Urotrygon aspidura*) collected in the central zone of the Pacific coast of Colombia in 2006–2009 and 2015. The black dots correspond to the mean counts of Reader 2 relative to those of Reader 1, and the bars indicate standard errors of the mean. The diagonal line indicates a one-to-one relationship.

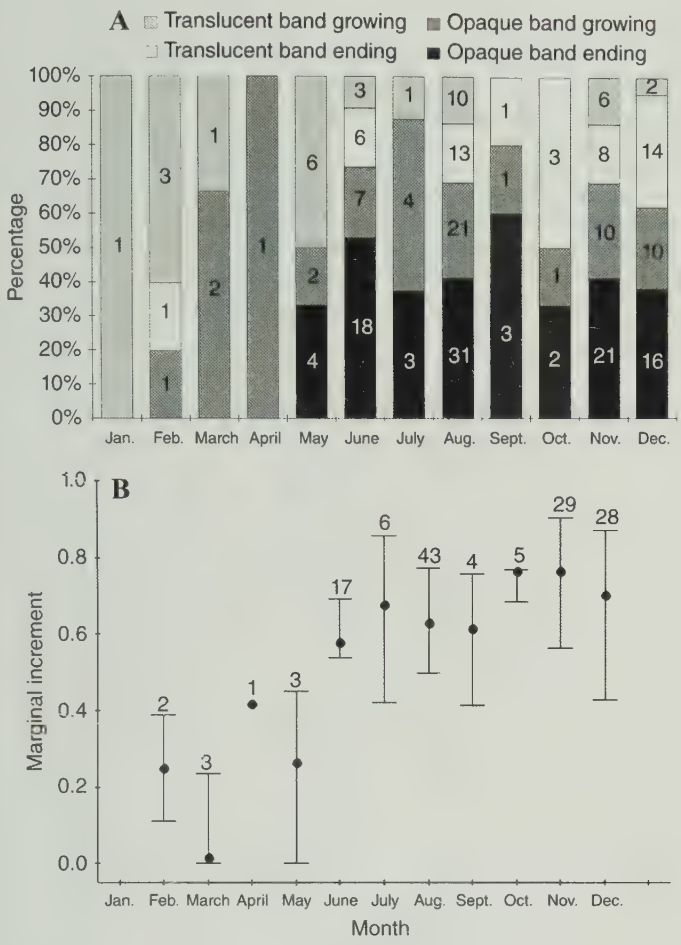

Figure 3

Monthly variation in the formation of vertebral band pairs of Panamic stingrays (*Urotrygon aspidura*) collected in the central zone of the Pacific coast of Colombia in 2006–2009 and 2015. (**A**) Percentage of Panamic stingrays (sample size [*n*]=237) that had 1 of 4 edge types: opaque band growing or ending and translucent band growing or ending. Numerals inside column sections indicate the number of vertebrae with that edge type. (**B**) Marginal increment index (n=141), with black dots corresponding to the median and the error bars indicating the 25th and 75th percentiles. Numerals above the top error bars indicate the sample size for each month.

Growth estimation analyses were more conclusive when seasonally adjusted age data were used, with both the 4- and 5-parameter models (TPGM-4 and TPGM-5) for both sexes having the higher Akaike weight values (Tables 1 and 2). Parameters estimated from multi-model inference based on those TPGMs for both sexes are provided at the end of Tables 1 and 2.

The TPGM-5 was chosen for both sexes on the basis of statistical (AIC_i) and biological (known maximum DW, DW at birth, and DW at maturity) fit (Tables 1 and 2, Fig. 4). The growth curves from the TPGM-5 were significantly different between sexes (likelihood ratio test: χ^2=115.6, df=5, P<0.0001), although the inflection point was similar between sexes (likelihood ratio test: χ^2=1.024, df=1, P=0.312; Tables 1 and 2; Fig. 4). Female Panamic stingrays had a larger asymptotic DW (likelihood ratio test: χ^2=748.1, df=1, P<0.0001) and a lower growth coefficient (likelihood ratio test: χ^2=65.2, df=1, P<0.0001) than male Panamic stingrays.

Discussion

Despite the significant increase in the number of age and growth studies in batoids, only 3 of the 16 American round ray species of the Urotrygonidae have been aged (Mejía-Falla et al., 2014; Guzmán-Castellanos, 2015; Santander-Neto, 2015). Our results agree with those of previous studies and demonstrate that the Panamic stingray is a fast-growing and short-lived species. This finding has considerable implications for the population assessment and management of this species.

The results from our study indicate that the vertebrae of Panamic stingrays, despite their small size, were adequate structures for evaluation and estimation of age for this species, with lower APE and CV values for readings than the averages of the age studies reported by Campana (2001) (APE<5.5% and CV<7.6%) and those observed in readings for species of the Urotrygonidae (average APE=4.24%; Mejía-Falla et al., 2014; Guzmán-Castellanos, 2015; Santander-Neto, 2015).

The region of the vertebral column chosen for extraction of the centra sample and the centra size have effects on the counting of shark growth band pairs, with the largest ones showing more pairs of bands (Natanson et al., 2018). In this study, we used the largest centra of each specimen from the abdominal region, to maintain homogeneity in samples and reduce those effects. This issue can be addressed by alternative techniques, such as bomb radiocarbon dating or chemical fluorochrome marking, but these techniques are costly and are not easily accessible.

Despite the limited sample size in the first months of the year, the results of MI analysis indicate that band-pair formation tends to be annual in Panamic stingrays, with constant MI growth from the beginning of the year until October and November. Although MI analysis has been considered a validation method (Campana, 2001), in this study, we used it as a method for verification of the periodicity in band deposition (Cailliet and Goldman, 2004). This annual band-pair deposition based on MI has been described for numerous species from the Urolophidae and Urotrygonidae (White et al., 2001; White et al., 2002; White and Potter, 2005; Mejía-Falla et al., 2014; Guzmán-Castellanos, 2015; Santander-Neto, 2015). Yearly periodicity of band-pair formation has been

Table 1

Parameters and statistical criteria for the von Bertalanffy growth model (VBGM), two-phase growth model (TPGM), Gompertz growth model (GGM), and logistic growth model (LGM) used to describe the growth of female Panamic stingrays (*Urotrygon aspidura*) (sample size [*n*]=124) collected in the central zone of the Pacific coast of Colombia in 2006–2009 and 2015. Two data sets are presented; the adjusted data set considers the months with peaks of reproduction and the unadjusted data set does not consider them. The parameters and criteria are asymptotic disc width (DW_∞, in centimeters), birth size (DW_0, fixed to 7.5 cm for models with 2 and 4 parameters), annual growth rate (k), theoretical age at zero (t_0), age at transition between 2 phases or inflection point (t_h), maximum difference in DW at age between the VBGM and TPGM at the t_h (h), Akaike information criterion (AIC_i), difference in AIC_i between models (Δ_i), and Akaike weight (w_i). Weighted averages from the TPGM are given with standard errors of the mean (SEs). Numerals after the model abbreviation indicate the number of parameters used in that model. Dashes indicate that data were not available because variables were not included in a model.

Model	DW_∞	k	t_0	t_h	h	DW_0	AIC_i	Δ_i	w_i
Unadjusted data									
VBGM-3	29.32	0.24	−1.80	–	–	10.28	556.61	1.65	0.17
VBGM-2	25.46	0.42	–	–	–	7.50	615.64	60.68	0.00
GGM-3	26.82	0.40	−0.12	–	–	10.33	556.02	1.06	0.22
GGM-2	23.91	0.69	–	–	–	7.50	618.25	63.29	0.00
LGM-3	25.60	0.57	0.67	–	–	10.38	555.95	0.99	0.23
LGM-2	20.40	0.79	–	–	–	12.50	628.75	73.79	0.00
TPGM-5	24.93	0.47	−1.21	1.93	0.31	10.31	554.96	0.00	0.38
TPGM-4	24.03	0.68	–	2.14	0.46	7.50	614.67	59.71	0.00
Adjusted data									
VBGM-3	29.60	0.22	−1.53	–	–	8.63	536.69	6.84	0.02
VBGM-2	26.64	0.31	–	–	–	7.50	542.49	12.65	0.00
GGM-3	26.89	0.38	0.26	–	–	8.91	537.30	7.45	0.01
GGM-2	24.51	0.54	–	–	–	7.50	549.79	19.94	0.00
LGM-3	25.62	0.55	1.08	–	–	9.13	538.23	8.38	0.01
LGM-2	20.07	0.60	–	–	–	12.34	652.41	122.56	0.00
TPGM-5	24.71	0.47	−0.91	2.32	0.36	8.18	530.01	0.16	0.46
TPGM-4	24.02	0.57	–	2.24	0.53	7.50	529.85	0.00	0.50
Weighted average from TPGM (SE)	24.35 (0.59)	0.52 (0.09)	–	2.28 (0.07)	0.45 (0.15)	–	–	–	–

validated through the use of tetracycline for the round stingray (*Urobatis halleri*), white-blotched river stingray (*Potamotrygon leopoldi*), and little skate (*Leucoraja erinacea*) (Hale and Lowe, 2008; Cicia et al., 2009; Charvet et al., 2018). This validation does not imply a generalized pattern for batoids, but it does allow inference that yearly periodicity occurs regularly in this group, regardless of the taxonomic classification, habitats, or latitudinal distributions of the species.

Although band pairs may begin to form during the first trimester of the year, starting with the opaque band, the reduced sample size during those months limited our capacity to determine with precision in which month this process starts. Several studies have also reported on the difficulty in validating band formation in sharks and rays (O'Shea et al., 2013; Cailliet, 2015); therefore, it has been assumed that 1 pair is formed each year. Carlson et al. (1999) and Lessa et al. (2006) attribute this difficulty to a bias of MI values and inconclusive analyses due to long sampling periods (several years) during which births occur over a long time span and organisms from the same cohort are born at different times of the year. Such multiple births could be the case for the Panamic stingray, as the reproductive information available for this species (P. Mejía-Falla et al., unpubl. data) and for a sympatric species, the thorny stingray (*Urotrygon rogersi*) (Mejía-Falla et al., 2014), indicates that there is continuous reproduction throughout the year with 2–3 reproductive events per year.

In female and male Panamic stingrays, differences in age and growth parameters were observed. The maximum estimated female age was 7.5 years, whereas the maximum estimated male age was 5.5 years. Similar values have also been recorded for other species of this family, such as the smalleyed round stingray (*U. microphthalmum*) with 8.5 years for females of and 5.5 years for males (Santander-Neto, 2015) and the thorny stingray with 8 years for females and 6 years for males (Mejía-Falla et al., 2014). In contrast, the blotched stingray (*U. chilensis*) has

Table 2

Parameters and statistical criteria for the von Bertalanffy growth model (VBGM), two-phase growth model (TPGM), Gompertz growth model (GGM), and logistic growth model (LGM) used to describe the growth of male Panamic stingrays (*Urotrygon aspidura*) (sample size [*n*]=180) collected in the central zone of the Pacific coast of Colombia in 2006–2009 and 2015. Two data sets are presented; the adjusted data set considers the months with peaks of reproduction. The parameters and criteria are the asymptotic disc width (DW_∞, in centimeters), birth size (DW_0, fixed to 7.5 cm for models with 2 and 4 parameters), annual growth rate (k), age at transition between 2 phases or inflection point (t_h), maximum difference in DW at age between the VBGM and TPGM at the t_h (h), Akaike information criterion (AIC_i), difference in AIC_i between models (Δ_i), and Akaike weight (w_i). Weighted averages from the TPGM are given with standard errors of the mean (SEs). Numerals after the model abbreviation indicate the number of parameters used in that model. Dashes indicate that data were not available because variables were not included in a model.

Model	DW_∞	k	t_0	t_h	h	DW_0	AIC_i	Δ_i	w_i
Unadjusted data									
VBGM-3	15.99	0.79	−1.47	–	–	10.97	736.08	0.00	0.27
VBGM-2	15.31	1.65	–	–	–	7.50	924.74	188.65	0.00
GGM-3	15.84	0.93	−1.08	–	–	10.97	736.42	0.34	0.22
GGM-2	15.22	2.00	–	–	–	7.50	924.88	188.79	0.00
LGM-3	15.72	1.08	−0.77	–	–	10.97	736.75	0.67	0.19
LGM-2	17.05	0.72	–	–	–	10.93	737.38	1.30	0.14
TPGM-5	17.11	0.81	−1.33	2.60	0.40	10.95	736.83	0.75	0.18
TPGM-4	16.81	1.45	–	2.56	0.68	7.50	927.01	190.92	0.00
Adjusted data									
VBGM-3	15.08	1.34	−0.63	–	–	8.59	640.61	4.10	0.08
VBGM-2	14.85	1.76	–	–	–	7.50	646.70	10.19	0.00
GGM-3	14.82	1.90	−0.28	–	–	8.20	644.78	8.27	0.01
GGM-2	14.71	2.26	–	–	–	7.50	647.85	11.35	0.00
LGM-3	14.70	2.38	−0.10	–	–	8.17	646.05	9.55	0.01
LGM-2	14.65	1.52	–	–	–	9.84	674.94	38.43	0.00
TPGM-5	15.96	1.63	−0.48	2.22	0.54	8.07	636.51	0.00	0.64
TPGM-4	15.94	1.81	–	2.16	0.67	7.50	638.30	1.80	0.26
Weighted average from TPGM (SE)	15.95 (0.01)	1.68 (0.15)	–	2.20 (0.05)	0.58 (0.11)	–	–	–	–

older ages of 14 years for females and 12 years for males (Guzmán-Castellanos, 2015). The Panamic stingray can be considered a short-lived species (<8 years), similar to other species belonging to Urotrygonidae (Hale and Lowe, 2008; Mejía-Falla et al., 2014; Santander-Neto, 2015), whereas in other ray families, such as Dasyatidae and Rajidae, maximum ages can exceed 17 years (Francis et al., 2001; Licandeo et al., 2006; Smith et al., 2007; Aversa et al., 2011; Başusta and Sulikowski, 2012; O'Shea et al., 2013).

Traditionally, the most used model to describe elasmobranch growth (Cailliet et al., 2006) has been the VBGM; however, numerous studies indicate that other models can be better adjusted (Araya and Cubillos, 2006; Smart et al., 2016). The Gompertz growth model has been used with batoid species (Neer and Cailliet, 2001; Neer and Thompson, 2005; Matta and Gunderson, 2007; Ainsley et al., 2011), and the TPGM, which incorporates changes in growth rates during the lives of organisms, usually has been related with changes in energy investment in reproductive processes (Araya and Cubillos, 2006; Aversa et al., 2011).

Differences in the age parameters obtained between the adjusted and the unadjusted age data, the former being more similar to the biological data, demonstrate the importance of considering the reproductive and size characteristics of each species, as well as the multi-model approach, to obtain more reliable growth parameters (Harry et al., 2010; Mejía-Falla et al., 2014). However, most age studies do not include adjustment based on the reproductive cycle, ignoring the potential effects that lack of adjustment could have on the demographic analyses and, therefore, on the fishery management of these cartilaginous fish species (Cailliet, 2015).

It has been suggested that the use of different models (or a multi-model approach) in growth studies allows researchers to select the model that is best adjusted to the data (Katsanevakis, 2006; Smart et al., 2016). For demographic modeling purposes, of the 8 models applied to describe the DW–age relationship in the Panamic stingray,

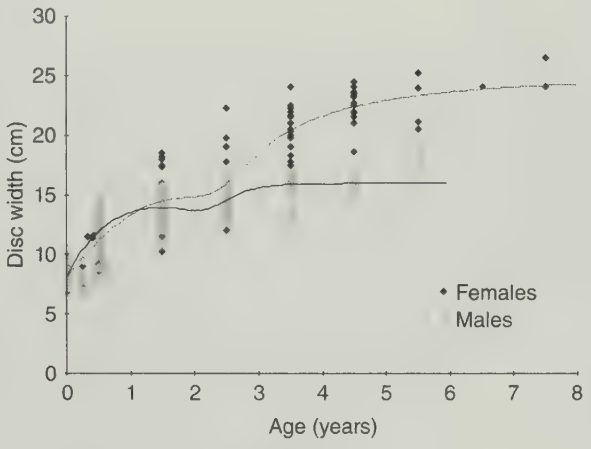

Figure 4

Two-phase growth model with 5 parameters that describes the growth of female (black diamonds, dotted line) and male (gray dots, solid line) Panamic stingrays (*Urotrygon aspidura*) collected in the central zone of the Pacific coast of Colombia in 2006–2009 and 2015. Adjusted data for age and disc width were used, meaning that data take into account the months with peaks of reproduction.

the growth parameters obtained from the TPGM-5 were considered best for describing the growth of this species. Similarly, TPGM was the best fitted to data for female blotched stingrays (Guzmán-Castellanos, 2015) and to data for female thorny stingrays (Mejía-Falla et al., 2014), making it the most appropriate model in the 3 age studies carried out to date for the genus *Urotrygon*.

The TPGM divides growth in 2 phases that could be related to changes in habitat, feeding habits, or the energetic investment of species (Aversa et al., 2011). The inflection point of females in this model occurred at 2.3 years and coincided with the size at first maturity estimated for the Panamic stingray. This size at maturity occurred at 25 cm TL and corresponds to a DW between 13.8 and 15.0 cm in our study (P. Mejía-Falla, unpubl. data). This change in growth rates (and their relationship with size at first maturity) has been associated with a higher energy investment in the development of reproductive organs, coinciding in some species with the change from juvenile to adult (Carlson and Baremore, 2005; Braccini et al., 2007; Aversa et al., 2011). As a consequence, the trajectory in the growth rate allows us to distinguish between before and after maturity (Araya and Cubillos, 2006), with maturation starting before reproduction (Aversa et al., 2011) and possibly reflected in a lower investment of energy in growth (Mejía-Falla et al., 2014).

Missing the smallest and largest individuals in a sample can affect growth models and produce biased growth parameters (Haddon, 2001; Pilling et al., 2002; Smart et al., 2015; D'Alberto et al., 2017). The variables were sensitive to the low number of older age classes for both sexes and, for males, to the influence that the predominance of DW of 12–15 cm can have on data. This data sensitivity ensured that growth curves did not reach an asymptote resulting in underestimation of DW_∞ (Fisher et al., 2013) and led to DW_∞ estimates of 24.71 cm for females and 15.96 cm for males. The wide range in DW_0 could have been affected by a prolonged birthing period (Lessa et al., 2006) in the TPGMs for both sexes. Additionally, the low number of samples for certain size and age classes in our study may have contributed to the variability in k.

Among elasmobranchs, females reach greater asymptotic sizes and have lower growth rates than males (e.g., Ismen, 2003; Skomal and Natanson, 2003; Başusta et al., 2008; Kume et al., 2008). These differences in growth between sexes was observed for the Panamic stingray, with females reaching a DW_∞ of 24.71 cm and a k of 0.47 cm/year and males reaching a DW_∞ of 15.96 cm and a k of 1.63 cm/year. Such differences between sexes have usually been attributed to males reaching maturity earlier than females. Females would have the evolutionary advantage of increasing their size to increase fecundity or to have the capacity of sheltering more embryos and reaching maximum capacity (Aversa et al., 2011; Klimley, 2013).

Differences in growth between sexes have been found in other species of the Urotrygonidae and Urolophidae, such as the thorny stingray, smalleyed round stingray, round stingray, lobed stingaree (*Urolophus lobatus*), sparsely-spotted stingaree (*U. paucimaculatus*), masked stingaree (*Trygonoptera personata*), and western shovelnose stingaree (*T. mucosa*) (White et al., 2001; White et al., 2002; White and Potter, 2005; Hale and Lowe, 2008; Mejía-Falla et al., 2014; Guzmán-Castellanos, 2015; Santander-Neto 2015). Compared with those species, the Panamic stingray has a higher growth rate, the highest reported for an elasmobranch so far. This species provides more evidence for the fact that smaller organisms grow faster and have a shorter lifespan than larger organisms (White and Sommerville, 2010; Aversa et al., 2011).

Although traditionally elasmobranchs have been described as K strategists, and they are therefore very vulnerable to fisheries, the results of recent studies give evidence that this pattern is not a general one in this group and that some species have life history traits that make them more productive and resistant to fisheries (Simpfendorfer, 1993; Cailliet et al., 2005; Mejía-Falla et al., 2014; White et al., 2014). This pattern was found for the Panamic stingray, a small-sized species with a short life and fast growth, characteristics that are similar to those found in its sympatric species, the thorny stingray (Mejía-Falla et al., 2014).

These life history characteristics have been advantageous for these species, allowing them to endure years of continuous fishing pressure (Rueda et al., 2006). Therefore, these characteristics make them 2 of the most abundant elasmobranch species in our study area, unlike other elasmobranchs, such as the Pacific smalltail shark (*Carcharhinus cerdale*), scalloped hammerhead (*Sphyrna lewini*), scoophead (*S. media*), sicklefin smoothhound (*Mustelus lunulatus*), and longtail stingray (*Hypanus longus*), among others (Navia and Mejía-Falla, 2016). Despite

its abundance, analyses of the reproductive biology and demography of the Panamic stingray are necessary to define its real vulnerability to fisheries activities.

Acknowledgments

Funding for this study was provided by Colciencias-Colombia (RC 156-2010), Padi Foundation, and Iniciativa de Especies Amenazadas. We thank H. Paredes, F. Cuero, and SQUALUS staff for support with field work. The senior author was funded by scholarships from the Consejo Nacional de Ciencia y Tecnología (Mexico) and Instituto Politécnico Nacional (IPN) for studies toward her master's degree. C. Quiñonez and V. Cruz were supported by IPN programs, Estímulos al Desempeño de los Investigadores and Comisión de Operación y Fomento de Actividades Académicas.

Literature cited

Ainsley, S. M., D. A. Ebert, and G. M. Cailliet.
2011. Age, growth, and maturity of the whitebrow skate, *Bathyraja minispinosa*, from the eastern Bering Sea. ICES J. Mar. Sci. 68:1426–1434.

Akaike, H.
1973. Information theory as an extension of the maximum likelihood principle. *In* Second international symposium on information theory; Tsahkadsor, Armenia, 2–8 September 1971 (B. N. Petrov and F. Csáki, eds.), p. 267–281. Akadémiai Kiadó, Budapest, Hungary.

Amezcua, F., J. Madrid-Vera, and H. Aguirre-Villaseñor.
2006. Efecto de la pesca artesanal de camarón sobre la ictiofauna en el sistema lagunar de Santa María la Reforma, suroeste del Golfo de California. Cienc. Mar. 32:97–109.

Araya, M., and L. A. Cubillos.
2006. Evidence of two-phase growth in elasmobranchs. Environ. Biol. Fish. 77:293–300.

Aversa, M. I., S. L. Dans, N. A. García, and E. A. Crespo.
2011. Growth models fitted to *Dipturus chilensis* length-at-age data support a two phase growth. Rev. Chil. Hist. Nat. 84:33–49.

Babel, J. S.
1967. Reproduction, life history, and ecology of the round stingray, *Urolophus halleri* Cooper. Calif. Dep. Fish Game, Fish Bull. 137, 104 p.

Başusta, N., and J. A. Sulikowski.
2012. The oldest estimated age for roughtail stingray [*Dasyatis centroura* (Mitchill, 1815)] from the Mediterranean Sea. J. Appl. Ichthyol. 28:641–642.

Başusta, N., S. A. Demirhan, E. Çiçek, A. Başusta, and T. Kuleli.
2008. Age and growth of the common guitarfish, *Rhinobatos rhinobatos*, in Iskenderun Bay (north-eastern Mediterranean, Turkey). J. Mar. Biol. Assoc. U.K. 88:837–842.

Beamish, R. J., and D. A. Fournier.
1981. A method for comparing the precision of a set of age determinations. Can. J. Fish. Aquat. Sci. 38:982–983.

Braccini, J. M., B. M. Gillanders, T. I. Walker, and J. Tovar-Avila.
2007. Comparison of deterministic growth models fitted to length-at-age data of the piked spurdog (*Squalus megalops*) in south-eastern Australia. Mar. Freshw. Res. 58: 24–33.

Burnham, K. P., and D. R. Anderson.
2002. Model selection and multimodel inference: a practical information-theoretic approach, 2nd ed., 488 p. Springer Science, New York.

Cailliet, G. M.
2015. Perspectives on elasmobranch life-history studies: a focus on age validation and relevance to fishery management. J. Fish. Biol. 87:1271–1292.

Cailliet, G. M., and K. J. Goldman.
2004. Age determination and validation in chondrichthyan fishes. *In* Biology of sharks and their relatives (J. C. Carrier, J. A. Musick, M. R. Heithaus, eds.), p. 399–447. CRC Press, Boca Raton, FL.

Cailliet, G. M., J. A. Musick, C. A. Simpfendorfer, and J. D. Stevens.
2005. Ecology and life history characteristics of chondrichthyan fish. *In* Sharks, rays and chimaeras: the status of the chondrichthyan fishes. Status survey (S. L. Fowler, R. D. Cavanagh, M. Camhi, G. H. Burgess, G. M. Cailliet, S. V. Fordham, C. A. Simpfendorfer, and J. A. Musick, eds.), p. 12–18. IUCN, Gland, Switzerland.

Cailliet, G. M., W. D. Smith, H. F. Mollet, and K. J. Goldman.
2006. Age and growth studies of chondrichthyan fishes: the need for consistency in terminology, verification, validation, and growth function fitting. Environ. Biol. Fish. 77:211–228.

Campana, S. E.
2001. Accuracy, precision and quality control in age determination, including a review of the use and abuse of age validation methods. J. Fish Biol. 59:197–242.

Campana, S. E., M. C. Annand, and J. I. McMillan.
1995. Graphical and statistical methods for determining the consistency of age determinations. Trans. Am. Fish. Soc. 124:131–138.

Carlson, J. K., and I. E. Baremore.
2005. Growth dynamics of the spinner shark (*Carcharhinus brevipinna*) off the United States southeast and Gulf of Mexico coasts: a comparison of methods. Fish. Bull. 103:280–291.

Carlson, J. K., E. Cortés, and A. G. Johnson.
1999. Age and growth of the blacknose shark, *Carcharhinus acronotus*, in the eastern Gulf of Mexico. Copeia 1999:684–691.

Charvet, P., F. M. Santana, K. L. De Lima, and R. Lessa.
2018. Age and growth of the endemic Xingu River stingray *Potamotrygon leopoldi* validated using fluorescent dyes. J. Fish. Biol. 92:1985–1999.

Cicia, A. M., W. B. Driggers III, G. W. Ingram Jr., J. Kneebone, P. C. W. Tsang, D. M. Koester, and J. A. Sulikowski.
2009. Size and age estimates at sexual maturity for the little skate *Leucoraja erinacea* from the western Gulf of Maine, USA. J. Fish. Biol. 75:1648–1666.

Clarke, T. M., M. Espinoza, R. Ahrens, and I. S. Wehrtmann.
2016. Elasmobranch bycatch associated with the shrimp trawl fishery off the Pacific coast of Costa Rica, Central America. Fish. Bull. 114:1–17.

Cortés, E.
2000. Life history patterns and correlations in sharks. Rev. Fish. Sci. 8:299–344.

D'Alberto, B. M., A. Chin, J. J. Smart, L. Baje, W. T. White, and C. A. Simpfendorfer.
2017. Age, growth and maturity of oceanic whitetip shark (*Carcharhinus longimanus*) from Papua New Guinea. Mar. Freshw. Res. 68:1118–1129.

Fisher, R. A., G. C. Call, and R. D. Grubbs.
2013. Age, growth, and reproductive biology of cownose rays in Chesapeake Bay. Mar. Coast. Fish. 5:224–235.

Francis, M. P., C. Ó. Maolagáin, and D. Stevens.
2001. Age, growth, and sexual maturity of two New Zealand endemic skates, *Dipturus nasutus* and *D. innominatus*. N. Z. J. Mar. Freshw. Res. 35:831–842.

Frisk, M. G.
2010. Life history strategies of batoids. *In* Sharks and their relatives II: biodiversity, adaptive physiology, and conservation (J. C. Carrier, J. A. Musick, and M. R. Heithaus, eds.), p. 283–316. CRC Press, Boca Raton, FL.

González-Isáis, M., and H. M. Montes-Domínguez.
2016. Compared morphology of the cephalic musculature in five species of genus *Urotrygon* (Chondrichthyes: Urolophidae). Int. J. Morphol. 34:7–12.

Guzmán-Castellanos, A. B.
2015. Historia de vida de la raya chilena *Urotrygon chilensis* (Günther, 1872) en el sureste del Pacífico mexicano. Ph.D. diss., 133 p. Cent. Invest. Biol. Noroeste, La Paz, Mexico. [Available from website.]

Haddon, M.
2001. Modelling and quantitative methods in fisheries, 2nd ed., 465 p. CRC Press, Boca Raton, FL.

Hale, L. F., and C. G. Lowe.
2008. Age and growth of the round stingray *Urobatis halleri* at Seal Beach, California. J. Fish Biol. 73:510–523.

Harry, A. V., C. A. Simpfendorfer, and A. J. Tobin.
2010. Improving age, growth, and maturity estimates for aseasonally reproducing chondrichthyans. Fish. Res. 106: 393–403.

Hayashi, Y.
1976. Studies on the growth of the red tilefish in the East China Sea–II: estimation of age and growth from otolith-reading. Bull. Jpn. Soc. Sci. Fish. 42:1243–1249.

Hoenig, J. M., M. J. Morgan, and C. A. Brown.
1995. Analysing differences between two age determination methods by tests of symmetry. Can. J. Fish. Aquat. Sci. 52:364–368.

Ismen, A.
2003. Age, growth, reproduction and food of common stingray (*Dasyatis pastinaca* L., 1758) in Iskenderun Bay, the eastern Mediterranean. Fish. Res. 60:169–176.

Licandeo, R. R., J. G. Lamilla, P. G. Rubilar, and R. M. Vega.
2006. Age, growth, and sexual maturity of the yellownose skate *Dipturus chilensis* in the south-eastern Pacific. J. Fish Biol. 68:488–506.

Katsanevakis, S.
2006. Modelling fish growth: model selection, multi-model inference and model selection uncertainty. Fish. Res. 81:229–235.

Kimura, D. K.
1980. Likelihood methods for the von Bertalanffy growth curve. Fish. Bull. 77:765–774.

Klimley, A. P.
2013. Diet and growth. *In* The biology of sharks and rays, p. 339–372. Univ. Chicago Press, Chicago, IL.

Kume, G., K. A. Furumitsu, and A. Yamaguchi.
2008. Age, growth and age at sexual maturity of fan ray *Platyrhina sinensis* (Batoidea: Platyrhinidae) in Ariake Bay, Japan. Fish. Sci. 74:736–742.

Lessa, R., F. M. Santana, and P. Duarte-Neto.
2006. A critical appraisal of marginal increment analysis for assessing temporal periodicity in band formation among tropical sharks. Environ. Biol. Fish. 77:309–315.

Matta, M. E., and D. R. Gunderson.
2007. Age, growth, maturity, and mortality of the Alaska skate, *Bathyraja parmifera*, in the eastern Bering Sea. Environ. Biol. Fish. 80:309–323.

Mejía-Falla, P. A.
2012. Historia de vida y demografía de la raya espinosa *Urotrygon rogersi* en dos áreas con distintos niveles de presión pesquera. Ph.D. diss., 132 p. Univ. Valle, Cali, Colombia.

Mejía-Falla, P. A., E. Cortés, A. F. Navia, and F. A. Zapata.
2014. Age and growth of the round stingray *Urotrygon rogersi*, a particularly fast-growing and short-lived elasmobranch. PLoS ONE 9(4):e96077.

Montes-Domínguez, H. M., and M. González-Isáis.
2017. Skeleton anatomy of five species of genus *Urotrygon* (Chondrichthyes: Urotrygonidae). Int. J. Morphol. 35:831–839.

Morales-Azpeitia, R., J. López-Martínez, C. H. Rábago-Quiroz, M. O. Nevárez-Martínez, and E. Herrera-Valdivia.
2013. Growth and mortality rates of *Pseudupeneus grandisquamis* and *Urobatis halleri* bycatch species in the shrimp fishery. Hidrobiológica 23:386–393.

Natanson, L. J., G. B. Skomal, S. L. Hoffmann, M. E. Porter, K. J. Goldman, and D. Serra.
2018. Age and growth of sharks: do vertebral band pairs record age? Mar. Freshw. Res. 69:1440–1452.

Navarro-González, J. A., J. Bohórquez-Herrera, A. F. Navia, and V. H. Cruz-Escalona.
2012. Diet composition of batoids on the continental shelf off Nayarit and Sinaloa, Mexico. Cienc. Mar. 38:347–362.

Navarro-González, J. A., U. Rubio-Rodríguez, P. A. Mejía-Falla, and V. H. Cruz-Escalona.
2018. Morphological description of adult mouthparts of *Urotrygon nana* and *U. rogersi* (Urotrygonidae): interspecific and intraspecific differences. Hidrobiológica 28:219–222.

Navia, A. F., and P. A. Mejía-Falla.
2016. Fishing effects on elasmobranchs from the Pacific Coast of Colombia. Univ. Sci. 21:9–22.

Navia, A. F., P. A. Mejía-Falla, L. A. Zapata, S. Bessudo, G. Soler, and E. Rubio.
2009. Estado del conocimiento de tiburones y rayas del Pacífico colombiano. *In* Avances en el conocimiento de tiburones, rayas y quimeras de Colombia (V. Puentes, A. F. Navia, P. A. Mejía-Falla, J. P. Caldas, M. C. Diazgranados, and L. A. Zapata-Padilla, eds.), p. 131–194. Fundación SQUALUS, Cali, Colombia.

Neer, J. A., and G. M. Cailliet.
2001. Aspects of the life history of the Pacific electric ray, *Torpedo californica* (Ayres). Copeia 2001:842–847.

Neer, J. A., and B. A. Thompson.
2005. Life history of the cownose ray, *Rhinoptera bonasus*, in the northern Gulf of Mexico, with comments on geographic variability in life history traits. Environ. Biol. Fish. 73:321–331.

O'Shea, O. R., M. Braccini, R. McAuley, C. W. Speed, and M. G. Meekan.
2013. Growth of tropical dasyatid rays estimated using a multi-analytical approach. PLoS ONE 8(10):e77194.

Pilling, G. M., G. P. Kirkwood, and S. G. Walker.
2002. An improved method for estimating individual growth variability in fish, and the correlation between von Bertalanffy growth parameters. Can. J. Fish. Aquat. Sci. 59:424–432.

Ricker, W. E.
1979. Growth rates and models. *In* Fish physiology, vol. 8 (W. S. Hoar, D. J. Randall, and J. R. Brett, eds.), p. 677–743. Academic Press, New York.

Rico-Mejía, F., and M. Rueda.
2007. Evaluación experimental bioeconómica de cambios en la tecnología de captura de camarón con redes de arrastre en aguas someras del Pacífico colombiano. Bol. Invest. Mar. Cost. 36:79–109.

Robertson, D. R., and G. R. Allen.
2015. Shorefishes of the Tropical Eastern Pacific: online information system, vers. 2.0. Smithsonian Tropical Research Institute, Balboa, Panama. [Available from website, accessed May 2018.]

Rueda, M., J. A. Angulo S., N. Madrid, F. Rico, and A. Girón.
2006. La pesca industrial de arrastre de camarón en aguas someras del Pacífico colombiano: su evolución, problemática y perspectivas hacia una pesca responsable, 60 p. INVEMAR, Santa Marta, Colombia.

Santander-Neto, J.
2015. Dinâmica populacional da raia *Urotrygon microphthalmum* Delsman, 1941 no nordeste do Brasil. Ph.D. diss., 135 p. Univ. Fed. Pernambuco, Recife, Brazil. [Available from website.]

Simpfendorfer, C. A.
1993. Age and growth of the Australian sharpnose shark, *Rhizoprionodon taylori*, from north Queensland, Australia. Environ. Biol. Fish. 36:233–241.

Skomal, G. B., and L. J. Natanson.
2003. Age and growth of the blue shark (*Prionace glauca*) in the North Atlantic Ocean. Fish. Bull. 101:627–639.

Smart, J. J., A. V. Harry, A. J. Tobin, and C. A. Simpfendorfer.
2013. Overcoming the constraints of low sample sizes to produce age and growth data for rare or threatened sharks. Aquat. Conserv. 23:124–134.

Smart, J. J., A. Chin, A. J. Tobin, C. A. Simpfendorfer, and W. T. White.
2015. Age and growth of the common blacktip shark *Carcharhinus limbatus* from Indonesia, incorporating an improved approach to comparing regional population growth rates. Afr. J. Mar. Sci. 37:177–188.

Smart, J. J., A. Chin, A. J. Tobin, and C. A. Simpfendorfer.
2016. Multimodel approaches in shark and ray growth studies: strengths, weaknesses and the future. Fish Fish. 17:955–971.

Smith, W. D., G. M. Cailliet, and E. M. Melendez.
2007. Maturity and growth characteristics of a commercially exploited stingray, *Dasyatis dipterura*. Mar. Freshw. Res. 58:54–66.

Smith, W. D., J. A. Miller, and S. S. Heppell.
2013. Elemental markers in elasmobranchs: effects of environmental history and growth on vertebral chemistry. PLoS ONE. 8(10):e62423.

Soriano, M., J. Moreau, J. M. Hoenig, and D. Pauly.
1992. New functions for the analysis of two-phase growth of juvenile and adult fishes, with application to Nile perch. Trans. Am. Fish. Soc. 121:486–493.

Spieler, R. E., D. P. Fahy, R. L. Sherman, J. A. Sulikowski, and T. P. Quinn.
2013. The yellow stingray, *Urobatis jamaicensis* (Chondrichthyes: Urotrygonidae): a synoptic review. Caribb. J. Sci. 47:67–97.

Valenti, S. V., and R. Robertson.
2009. *Urotrygon aspidura*. The IUCN Red List of Threatened Species 2009: e.T161689A5480775. [Available from website.]

von Bertalanffy, L.
1938. A quantitative theory of organic growth (Inquiries on growth laws. II). Hum. Biol. 10:181–213.

White, W. T., and I. C. Potter.
2005. Reproductive biology, size and age compositions and growth of the batoid *Urolophus paucimaculatus*, including comparisons with other species of the Urolophidae. Mar. Freshw. Res. 56:101–110.

White, W. T., and E. Sommerville.
2010. Elasmobranchs of tropical marine ecosystems. *In* Sharks and their relatives II (J. C. Carrier, J. A. Musick, and M. R. Heithaus, eds.), p. 159–240. CRC Press, Boca Raton, FL.

White, W. T., M. E. Platell, and I. C. Potter.
2001. Relationship between reproductive biology and age composition and growth in *Urolophus lobatus* (Batoidea: Urolophidae). Mar. Biol. 138:135–147.

White, W., N. Hall, and I. C. Potter.
2002. Reproductive biology and growth during pre- and postnatal life of *Trygonoptera personata* and *T. mucosa* (Batoidea: Urolophidae). Mar. Biol. 140:699–712.

White, J., C. A. Simpfendorfer, A. J. Tobin, and M. R. Heupel.
2014. Age and growth parameters of shark-like batoids. J. Fish Biol. 84:1340–1353.

National Marine
Fisheries Service
NOAA

Fishery Bulletin
established in 1881

Spencer F. Baird
First U.S. Commissioner
of Fisheries and founder
of *Fishery Bulletin*

An exploration of factors that relate to the occurrence of multiple brooding in rockfishes (*Sebastes* spp.)

Anna M. Holder (contact author)[1]
John C. Field[2]

Email address for contact author: aholder@csumb.edu

[1] California State University, Monterey Bay
100 Campus Center
Seaside, California 93955

[2] Fisheries Ecology Division
Southwest Fisheries Science Center
National Marine Fisheries Service, NOAA
110 Shaffer Road
Santa Cruz, California 95060

Abstract—The phenomenon of multiple brooding, the production of more than one brood within a reproductive season, is a poorly understood process in rockfishes (*Sebastes* spp.). Most species produce a single brood, and all stock assessment models for *Sebastes* species assume the reproductive output (fecundity) of a single annual brood. We evaluated how well this life history trait could be predicted by both oceanographic (mean latitude, ocean temperature, dissolved oxygen levels, and depth) and demographic (maximum length, maximum age, and natural mortality rate) factors for 24 species of rockfish found on the continental shelf along the West Coast of the United States. Our results indicate that multiple-brooding species are considerably more common in lower latitudes (32–36°N) or in warmer waters (>9°C at depth) and that the other environmental and demographic factors analyzed were not empirically informative. This work provides a more comprehensive understanding of the reproductive ecology of shelf rockfishes, could contribute to assessments of climate change vulnerability, and should eventually lead to improvements in stock assessment models for economically and ecologically important rockfishes.

Manuscript submitted 20 October 2018.
Manuscript accepted 19 July 2019.
Fish. Bull. 117:180–188 (2019).
Online publication date: 31 July 2019.
doi: 10.7755/FB.117.3.5

The views and opinions expressed or implied in this article are those of the author (or authors) and do not necessarily reflect the position of the National Marine Fisheries Service, NOAA.

Population dynamics models that inform management decisions require an understanding of the reproductive biology of the fish species that are being managed. Rockfishes (*Sebastes* spp.) of the northeast Pacific Ocean tend to be long-lived species (maximum ages of some species are between 50 and 150 years) that can reach marketable size before maturity (Love et al., 1990). In addition to being long lived, slow growing, and late to mature, they have internal fertilization, are live-bearing, and usually develop a single brood annually (Love et al., 2002). Given these traits, which tend to be associated with high standing stock biomass and low productivity, rockfishes tend to be among the stocks that are more vulnerable to fishing pressure and presumably to future climate change (Parker et al., 2000; Berkeley et al., 2004; Cope et al., 2011).

Despite the report of multiple brooding, the production of more than one brood within a reproductive season, in some rockfishes over 50 years ago (Moser, 1966), multiple brooding continues to be poorly understood. Multiple brooding can be identified through macroscopic or histological examination of the ovaries. In macroscopically examined ovaries, multiple broods can be identified when ovaries contain residual larvae or fertilized eggs (primary brood) and developing oocytes (upcoming secondary brood) (Beyer et al., 2015; Lefebvre et al., 2018). Lefebvre et al. (2018) identified multiple brooding through histological examination when ovaries contained postovulatory follicle complexes, residual larvae or eyed larvae (primary brood) and late-stage developing vitellogenic oocytes (upcoming secondary brood). Although many rockfish species have been identified as having the capacity to produce multiple broods (Moser, 1967; Love et al., 1990; Beyer et al., 2015; Lefebvre et al., 2018), the potential for multiple brooding is unknown for a great many remaining species for which little data on their reproductive ecology exists.

Traditional stock assessment metrics, such as estimates of spawning stock biomass, depend on the reproductive strategies and annual fecundity of species. When data are not available, assumptions are made that

can result in bias and misspecification of stock status and associated parameters. For example, if size-dependent fecundity cannot be quantified in an assessment but such a relationship exists in a real population, assessment models will be biased toward estimating a stock status that is more optimistic than actually exists (He et al., 2015a; Barneche et al., 2018). There has been a growing awareness in recent years that the biological processes that determine a population's productivity are much more complicated than previously understood. For example, some *Sebastes* species exhibit skipped spawning (Rideout et al., 2005; Conrath, 2017), prolonged adolescent periods (Thompson and Hannah, 2010), and multiple brooding (Moser, 1967; Love et al., 1990; Beyer et al., 2015; Lefebvre et al., 2018). Accounting for all of these factors is critical in the understanding of a species' life history and in specifying life history characteristics in stock assessment models, climate vulnerability assessments, and other evaluations.

Previous studies indicate that multiple brooding more commonly occurs in southerly distributed rockfish species (32–36°N), as well as in individuals residing in the southern extent of the range of their species (Love et al., 1990; Beyer et al., 2015). For example, bocaccio (*S. paucispinis*) range from the Southern California Bight to British Columbia, Canada; individuals in the Southern California Bight frequently exhibit multiple brooding and those in Central California occasionally exhibit multiple brooding, but the phenomenon has never been reported in individuals north of Cape Mendocino (He et al., 2015b). Multiple brooding has not been reported in northern stocks (Love et al., 2002; Conrath, 2017), nor in species typically found in deeper water (on the continental slope at depths >400 m), other than the bank rockfish (*S. rufus*) in Southern California. However, beyond these general observations, the phenomenon of multiple brooding has never been empirically evaluated in relation to environmental or life history factors, and we have yet to determine if multiple brooding can be robustly predicted on a species level to allow estimation of the implications to stock assessments and climate vulnerability assessments.

We sought to quantitatively document the relationship between the phenomenon of multiple brooding in West Coast rockfishes with latitude or other demographic (maximum length, maximum age, and natural mortality rate) and environmental (temperature and dissolved oxygen [DO] at depth, and average depth) factors and to determine which of these factors would be the best predictors of multiple brooding. Specifically, we hypothesized that rockfish species of the continental shelf of the West Coast of the United States that are able to produce multiple broods would be statistically more likely to inhabit lower latitudes (32–36°N) or warmer waters (>9°C at depth). The results of this research are intended to provide a more comprehensive understanding of the reproductive biology of rockfish species and to improve the information available for their sustainable management.

Materials and methods

Study area and data collection

Researchers at the Fisheries Ecology Division of the NOAA Southwest Fisheries Science Center have been collecting fecundity samples of a range of rockfishes to improve our understanding of size-dependent fecundity and carefully noting the presence or absence of multiple broods (Beyer et al., 2015; Lefebvre et al., 2018). On the basis of these efforts and previous reports (Moser, 1966, 1967; MacGregor, 1970; Wyllie Echeverria, 1987; Love et al., 1990; Ralston and MacFarlane, 2010), we classified 13 rockfish species found on the continental shelf of the West Coast as being multiple brooders and 11 shelf rockfish species as single brooders (n=24; Table 1).

The NOAA Northwest Fisheries Science Center has conducted a fishery-independent groundfish bottom-trawl survey along the U.S. West Coast annually since 2003, in an area extending from the U.S.–Mexico border (latitude 32°30′N) to the U.S.–Canada border (latitude 48°10′N) and including depths from 55 m to 1280 m (Keller et al., 2012). We downloaded physical (trawl location, temperature, DO concentration at depth, and trawl depth) and biological (species and sex) data for shelf rockfishes (as defined in PFMC, 2016) for trawl tows conducted from 2004 through 2015 (FRAM Data Warehouse, Northwest Fisheries Science Center, available from website). It is important to note that the DO concentration at depth was not collected until 2007 and was not collected consistently until 2010. We downloaded commercial landings over the same time period from the Pacific Fisheries Information Network (PacFIN, available from website) and assigned port code latitudes based on port locations. We acquired the maximum length (i.e., asymptotic average fork length in centimeters; see Francis, 1988), maximum age (in years), and natural mortality rate of the species of interest from published stock assessments by the Pacific Fishery Management Council (available from website), Dick and MacCall (2010), and Love et al. (2002) (Table 1). Estimates of the natural mortality rate for shortbelly rockfish (*Sebastes jordani*) were used for halfbanded and pygmy rockfishes (*S. semicinctus* and *S. wilsoni*, respectively) because natural mortality had not been estimated for those 2 species and all 3 species are small, rapidly growing dwarf species. Species were excluded from our analyses if fewer than 20 individuals were collected over all the trawl samples; trawl samples were excluded if the tow of the trawl was conducted deeper than the depth range of continental shelf habitat (depths >400 m).

Data analysis

To provide some context to our analyses, we explored how cumulative survey and commercial catch (measured as weight in kilograms) varied by latitude for each species by plotting the cumulative distribution of the survey and commercial catch data, and the arithmetic mean

Table 1

Multiple brooder classification (MB; Y=yes, N=no), mean latitude (in decimal degrees), maximum fork length (L_∞, cm), observed maximum age (A_{MAX}, years), and natural mortality rate (M) for each species of rockfish (*Sebastes* spp.) collected by the Pacific Fishery Management Council and NOAA Southwest Fishery Science Center between 2004 and 2015 on the continental shelf along the West Coast of the United States. For species for which parameters varied by sex, values for females are given.

Common name	Scientific name	MB	Mean latitude	L_∞	A_{MAX}	M
Bocaccio	*Sebastes paucispinis*	Y	35.87	75.90	37	0.15
Canary	*Sebastes pinniger*	N	44.78	62.00	84	0.05
Chilipepper	*Sebastes goodei*	Y	37.82	52.00	35	0.16
Cowcod	*Sebastes levis*	Y	35.50	87.00	55	0.06
Flag	*Sebastes rubrivinctus*	N	34.24	51.00	38	0.12
Greenblotched	*Sebastes rosenblatti*	Y	34.06	57.99	50	0.09
Greenspotted	*Sebastes chlorostictus*	Y	36.53	44.20	51	0.09
Greenstriped	*Sebastes elongatus*	Y	42.86	37.26	54	0.08
Halfbanded	*Sebastes semicinctus*	N	34.57	18.14	15	0.26
Pink	*Sebastes eos*	Y	34.00	56.00	66	0.07
Pygmy	*Sebastes wilsoni*	N	42.67	23.00	26	0.26
Redstripe	*Sebastes proriger*	N	45.53	61.00	55	0.08
Rosethorn	*Sebastes helvomaculatus*	N	43.78	28.66	87	0.05
Rosy	*Sebastes rosaceus*	Y	33.87	32.90	18	0.27
Shortbelly	*Sebastes jordani*	Y	36.00	28.50	32	0.26
Silvergray	*Sebastes brevispinis*	N	45.78	71.00	82	0.05
Speckled	*Sebastes ovalis*	Y	33.67	49.99	37	0.13
Squarespot	*Sebastes hopkinsi*	Y	34.82	25.25	19	0.26
Starry	*Sebastes constellatus*	Y	35.64	45.00	32	0.15
Stripetail	*Sebastes saxicola*	N	38.30	33.05	38	0.12
Swordspine	*Sebastes ensifer*	Y	33.76	17.60	43	0.11
Vermilion	*Sebastes miniatus*	N	34.73	62.40	60	0.07
Widow	*Sebastes entomelas*	N	42.90	50.34	60	0.08
Yellowtail	*Sebastes flavidus*	N	46.37	52.20	64	0.15

of both data sources, for each species. We then pooled data from the respective data sets over the study period (2004–2015) and summarized them by calculating the arithmetic mean to provide estimates of mean latitude (in decimal degrees), mean temperature at depth (in degrees Celsius), mean DO concentration at depth (in milliliters per liter), mean survey depth (in meters) for each species in the study (n=1, for each species). We fit binomial generalized linear models to the probability of each species being identified as a multiple brooder. The capacity to produce multiple broods was the response variable, and the environmental and demographic metrics were predictor variables.

Because temperature and latitude were likely highly correlated, we analyzed the collinearity between all explanatory variables using scatterplots and conducted a variance inflation factor (VIF) analysis. In the VIF analysis, we used an a priori cutoff of 10 (Craney and Surles, 2002) to assess whether collinearity between the variables was problematic. If variables had a VIF greater than 10, they were not used in the same model. Using the results of the VIF analysis, we created 23 candidate models that represented hypothesized potential predictor–response relationships. We compared models using an information-theoretic approach using Akaike information criterion corrected for small sample sizes (AIC_c) (Burnham and Anderson, 2002). Following the general method used by Kowalski et al. (2015), we computed the maximized log-likelihood, AIC and AIC_c scores, ΔAIC_c values (difference between the AIC_c of model i and the smallest AIC_c among the considered models), and the AIC weight (AIC_w) for each model. A priori, we decided to describe the level of empirical support for a model using the terms *substantial*, *considerably less*, and *essentially none* to correspond to ΔAIC_c values less than 2, between 4–7, and greater than 10, respectively (as advised by Burnham and Anderson, 2002).

We evaluated the relative importance of influence of each predictor by summing the product of AIC_w and frequency of occurrence of the variable for all models. We computed the log evidence ratio (LER) in support for each predictor by calculating the $\log_{10}$ of its evidence ratio (quotient of relative importance and its complement) and used LERs as the basis of inference for predictor comparisons. Following Kass and Raftery (1995), a priori, we decided to use the terms *minimal*, *substantial*, *strong*, and *decisive* to correspond approximately to LERs greater than 0, 0.5, 1, and 2, respectively. All analyses were executed by using R statistical software (vers. 3.4.4; R Core Team, 2018), including the glm, AIC, and ggplot functions of this software.

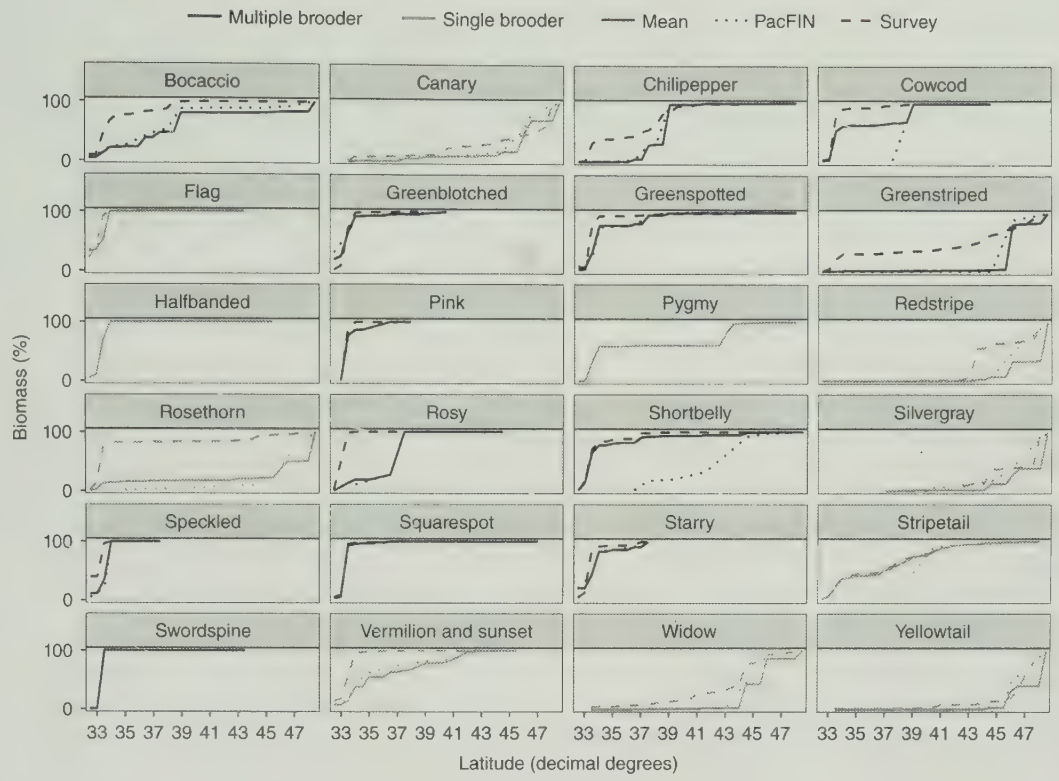

Figure 1

Contextual exploratory analysis of the cumulative distributions of biomass of rockfishes (*Sebastes* spp.) of the continental shelf in commercial landings based on data from the Pacific Fisheries Information Network (PacFIN, dotted line) and in a fishery-independent bottom-trawl survey (Survey, dashed line) along the West Coast of the United States in 2004–2015. Each graph shows the mean percentage of biomass from the 2 data sets (solid line) by latitude (decimal degrees). Black and dark gray lines indicate that the species was classified as a multiple-brooding or single-brooding species, respectively.

Results

The results of exploratory analysis of the cumulative distribution of all rockfishes of the continental shelf that were present in the trawl survey's catch data reveal distinct differences in latitude between single- and multiple-brooding species and similar trends between commercial and survey data (Fig. 1). There appears to have been substantial differences in both latitude and temperature between single and multiple-brooding species and slight differences in DO, depth, and all demographic variables between single-brooding and multiple-brooding species (Table 2).

Unsurprisingly, latitude and temperature were highly correlated (VIFs: 71 and 67, respectively). To address multicollinearity issues, latitude and temperature were included in separate models before retesting all VIF scores, and they remained separate in the rest of the models. Of the 23 models considered, we found substantial support for those models that included latitude and found considerably less support for models that included temperature: (model 1 [M1]: ΔAIC_c=0.0; model 2 [M2]: ΔAIC_c=0.7; and model 4 [M4]: ΔAIC_c=3.2; Table 3). There was marginal support for models that included some demographic variables (model 3 [M3]: ΔAIC_c=2.7; Table 3). The poorest performing models had essentially no support and were those for which latitude and temperature were separate (as required by the VIF results) but included all other variables (model containing all variables except temperature: ΔAIC_c=11.6; model containing all variables except latitude: ΔAIC_c=14.1; not shown).

Latitude and temperature were the strongest predictors of whether a shelf rockfish species could be a multiple brooder. There was substantial support for M1, which contained latitude and DO, and for M2, which contained only latitude, and there was considerably less support for M4 and M5, both of which include temperature (Table 3). When comparing the coefficients of M1 and M4, which contain DO and latitude (M1) or temperature (M4), the estimate for the latitude coefficient indicates that when DO is fixed and latitude increases by 1°, the odds of a shelf rockfish species being a multiple brooder is 0.6 times that of being a single brooder (for coefficients, see Table 3). Correspondingly,

Table 2

Comparison of the arithmetic mean and standard deviation (SD) of environmental and demographic variables between single- and multiple-brooding rockfish species (*Sebastes* spp.): latitude (decimal degrees), temperature (°C), dissolved oxygen (DO) concentration (mL/L), depth (m), maximum fork length (L_∞, cm), observed maximum age (A_{MAX}, years), and natural mortality rate (M). Data are provided for fish collected along the West Coast of the United States.

	Single brooding		Multiple brooding	
Variable	Mean	SD	Mean	SD
Latitude	41.24	4.83	35.72	2.49
Temperature	8.11	1.29	9.09	0.50
DO	1.94	0.44	1.91	0.46
Depth	157.44	28.18	161.35	34.33
L_∞	46.62	17.96	46.89	19.70
A_{MAX}	55.36	23.96	40.69	14.19
M	0.12	0.08	0.14	0.08

Table 3

Top 5 generalized linear models as defined by the Akaike information criterion (AIC) analysis. Models were used to evaluate the probability of each rockfish species (*Sebastes* spp.) being a multiple brooder; all variables were continuous. The number of parameters in the model (K), maximum log-likelihood (LL), AIC, AIC corrected for small sample sizes (AIC_c), difference between the AIC_c of model i and the smallest AIC_c among the considered models (ΔAIC_c), and AIC weights (AIC_w) are provided for each model (models 1–5 [M1–M5]). Variables include those for latitude (Lat), dissolved oxygen (DO) concentration, maximum fork length (L_∞, cm), and temperature (Temp).

Model name	Model ($\log(\hat{y}) =$)	K	LL	AIC	AIC_c	ΔAIC_c	AIC_w
M1	$25.27 - 0.51X_{Lat} - 2.78X_{DO}$	3	−9.95	25.91	27.11	0.00	0.39
M2	$13.32 - 0.35X_{Lat}$	2	−11.61	27.22	27.79	0.68	0.28
M3	$25.14 - 0.52X_{Lat} - 2.85X_{DO} + 0.01X_{L_\infty}$	4	−9.87	27.73	29.84	2.73	0.10
M4	$-10.55 + 1.98X_{Temp} - 3.25X_{DO}$	3	−11.54	29.07	30.27	3.16	0.08
M5	$-9.02 + 1.06X_{Temp}$	2	−13.68	31.36	31.93	4.82	0.04

the estimate for the temperature coefficient indicates that when DO is fixed and temperature increases by 1°C, the odds of a shelf rockfish species being a multiple brooder is 7.2 times that of being a single brooder. Finally, the results of evaluation of relative importance of influence of each predictor indicate that there was substantial evidence that species in lower latitudes had a higher probability of being a multiple brooder (LER for latitude=0.63; Table 4). There was minimal evidence indicating that any of the other variables affected the probability of a species being a multiple brooder (all other LERs were <0.5; Table 4).

Discussion

Our results indicate that species with the capacity for multiple brooding were more likely to occur in lower latitudes (32–36°N) or in warmer waters (>9°C at depth). This finding agrees with the established knowledge on differing distributions and community assemblages of rockfishes regionally (e.g., by latitude) (Love et al., 2002; Williams and Ralston, 2002; Gunderson and Vetter, 2006). Oceanographic conditions in waters of Southern California and Central California are characterized by warmer conditions and more variable, less seasonal upwelling patterns relative to conditions in the northern part of the California Current (e.g., north of Cape Mendocino), where ocean temperatures tend to be cooler and upwelling is both stronger and more strongly seasonal, conditions that result in higher primary and secondary productivity (Parrish et al., 1981; Ware and Thomson, 2005; Checkley and Barth, 2009). Consequently, rockfish species in waters of Southern California, where primary and secondary productivity and therefore presumably forage availability are both lower and characterized by greater interannual variability, may have an

Table 4

Summary of predictor variables considered in generalized linear models used to evaluate the probability of a rockfish species (*Sebastes* spp.) being a multiple brooder. Predictor variables include latitude (decimal degrees), temperature (°C), dissolved oxygen (DO) concentration (mL/L), depth (m), maximum fork length (L_∞, cm), maximum age (A_{MAX}, years), and natural mortality rate (M). Relative importance (RI), evidence ratio (ER), log evidence ratio (LER), and direction of effect (Direction) on the probability of a species being a multiple brooder for each predictor are shown.

Predictor variable	RI	ER	LER	Direction
Latitude	0.81	4.27	0.63	–
DO	0.64	1.79	0.25	–
L_∞	0.18	0.21	−0.67	+
Temperature	0.15	0.17	−0.76	+
A_{MAX}	0.07	0.08	−1.10	–
M	0.03	0.03	−1.58	+
Depth	0.01	0.01	−2.19	+

evolutionary advantage in producing multiple broods over those species constrained to a single brood. The presumed mechanism for such an advantage would be to increase the probability of post-parturition larvae to encounter appropriate foraging conditions in this more variable, less seasonal region of the California Current. This is consistent with the notion of Cushing's match-mismatch hypothesis in which the effect of highly variable prey abundance for early life history stages of marine fish species may be partially mitigated by spreading spawning effort across a broader time period (Cushing, 1990).

Temperature affects individuals directly by influencing their growth and metabolism (Boehlert and Yoklavich, 1983; Boehlert et al., 1991). Temperature also influences egg and larval development; for example, recent laboratory studies have shown that multiple-brooding rosy rockfish (*S. rosaceus*) produced and released broods more quickly in warm water (relative to cool water) treatments, indicating faster development of eggs and larvae (Beyer[1]), and that faster development could result in the production of multiple broods during potentially narrow environmental windows for spawning. Temperature may tend to covary with other oceanographic variables that drive ocean productivity and consequently the availability of food resources, given that past studies have shown that the condition and reproductive output of some rockfish species can degrade during the warmer ocean conditions associated with El Niño–Southern Oscillation events (VenTresca et al., 1995; Harvey et al., 2011).

The importance of depth in this study is consistent with other studies that demonstrate that depth is a key driver of benthic community structure (Gunderson and Vetter, 2006; Tolimieri and Anderson, 2010). We did not include rockfish species of the continental slope in this analysis because of our desire to focus on the multiple-brooding phenomenon, which is largely limited to species found on the continental shelf of the West Coast. However, we recognize that depth may more generally drive a broader range of reproductive strategies for rockfishes, such that species in deeper waters (>400 m) may respond to variable conditions by abortive maturity, skipped spawning, or atresia (Nichol and Pikitch, 1994; Lefebvre and Field, 2015; Conrath, 2017), rather than the production (or lack thereof) of multiple broods. Although we did not formally evaluate the phylogeny of rockfish species relative to the capacity to produce multiple broods, it would appear that there are examples of both single and multiple brooders across the phylogenetic range of the genus *Sebastes* (Hyde and Vetter, 2007).

The similar predictive ability of temperature and latitude reflects the prominence of the influence of these variables on current probability of shelf rockfish species being multiple brooders. However, ocean conditions are changing. As the effects of climate change become more pronounced, the environmental conditions that are associated with certain regions (i.e., latitudes) will also change. Additionally, we did not find any evidence indicating that demographic variables are substantially associated with the phenomenon of multiple brooding. Although the maximum length and maximum age of species did not serve as a substantial predictor of multiple brooding among species, within species the occurrence of multiple brooding has been shown to increase with both size and age (Beyer et al., 2015; Lefebvre et al., 2018). Our results are also relevant to consideration of how observations of multiple brooding within a stock or species may vary with future warming or with the increasingly variable ocean conditions expected, and potentially already being observed, as a result of climate change (Rykaczewski et al., 2015; McCabe et al., 2016). For example, Lefebvre et al. (2018) found that during

[1] Beyer, S. 2018. Unpubl. data. Dep. Ecol. Evol. Biol., Univ. Calif. Santa Cruz., 130 McAllister Way, Santa Cruz, CA 95060.

atypically warm years, when upwelling and forage conditions were above average, the frequency of occurrence of multiple brooding in chilipepper (*S. goodei*) was common and nearly equal in both Southern and Central California, whereas previous studies had not detected multiple broods in chilipepper of Central California (Wyllie Echeverria, 1987; Stafford et al., 2014). This finding might indicate that species capable of producing multiple broods do so more frequently under warmer ocean conditions when food resources are sufficient, potentially providing some advantage over single-brooding species in the face of warming trends.

Fisheries managers are beginning to prepare for the effects of climate change on fisheries by incorporating climate variables (such as ocean temperature trends) into harvest policies (Hill et al., 2017) and by conducting climate vulnerability assessments (Morrison et al., 2015; Hare et al., 2016). Climate vulnerability assessments evaluate which species will be at the greatest risk (or most vulnerable) to the effects of climate change, and these assessments consequently are intended to inform and prioritize research and management actions. Spawning frequency is 1 of 12 biological attributes used in the current criteria for evaluating vulnerability to climate change, with species that spawn in one single event per year considered to be more vulnerable than those that spawn several times per year (Hare et al., 2016). Therefore, multiple-brooding species may have an evolutionary advantage relative to single-brooding species in the face of either warming or more variable ocean conditions, necessitating an accurate assessment of the reproductive ecology of all *Sebastes* species in evaluating the vulnerability of different species to climate change.

Accounting for multiple brooding as a maternal effect in population models can substantially affect stock assessments, particularly if the likelihood of producing multiple broods (increasing overall reproductive output) is size dependent, as demonstrated for chilipepper (Lefebvre et al., 2018). Currently, stock assessment models of multiple-brooding species do not account for such factors in estimating reproductive output and stock status, potentially biasing assessment results if the effect is to nominally increase reproductive output of larger, older individuals. Taking multiple brooding into account in general, as well as in the context of climate change, will improve stock assessments and help managers develop appropriate management responses to climate variability and change now and into the future (Barneche et al., 2018). Our results provide robust predictions of this likelihood and provide context to the observed distribution of multiple-brooding species relative to single-brooding shelf rockfish species. However, our insights are not strictly mechanistic and are only the first step toward understanding the mechanisms and evolution of multiple brooding in rockfish species of the continental shelf. Future research should explicitly explore the mechanisms that drive multiple versus single brooding to aid in closing the knowledge gap for multiple-brooding rockfish species.

Acknowledgments

We would like to thank S. Sogard, S. Beyer, L. Lefebvre, N. Kashef, and D. Stafford at the Fisheries Ecology Division of the Southwest Fisheries Science Center and the University of California's Cooperative Institute for Marine Ecosystems and Climate because their combined efforts were critical to inform and guide this effort. Additionally, we are deeply appreciative of the detailed comments provided by 3 anonymous reviewers and feel that incorporating their recommendations has greatly improved this manuscript.

Literature cited

Barneche, D. R., D. R. Robertson, C. R. White, and D. J. Marshall.
2018. Fish reproductive-energy output increases disproportionately with body size. Science 360:642–645.

Berkeley, S. A., M. A. Hixon, R. J. Larson, and M. S. Love.
2004. Fisheries sustainability via protection of age structure and spatial distribution of fish populations. Fisheries 29:23–32.

Beyer, S. G., S. M. Sogard, C. J. Harvey, and J. C. Field.
2015. Variability in rockfish (*Sebastes* spp.) fecundity: species contrasts, maternal size effects, and spatial differences. Environ. Biol. Fish. 98:81–100.

Boehlert, G. W., and M. M. Yoklavich.
1983. Effects of temperature, ration, and fish size on growth of juvenile black rockfish, *Sebastes melanops*. Environ. Biol. Fish. 8:17–28.

Boehlert, G. W., M. Kusakari, and J. Yamada.
1991. Oxygen consumption of gestating female *Sebastes schlegeli*: estimating the reproductive costs of livebearing. Environ. Biol. Fish. 30:81–90.

Burnham, K. P., and D. R. Anderson.
2002. Model selection and multimodel inference: a practical information theoretic approach, 2nd ed., 488 p. Springer, New York.

Checkley, D. M., and J. A. Barth.
2009. Patterns and processes in the California Current System. Prog. Oceanogr. 83:49–64.

Conrath, C. L.
2017. Maturity, spawning omission, and reproductive complexity of deepwater rockfish. Trans. Am. Fish. Soc. 146:495–507.

Cope, J. M., J. DeVore, E. J. Dick, K. Ames, J. Budrick, D. L. Erickson, J. Grebel, G. Hanshew, R. Jones, L. Mattes, et al.
2011. An approach to defining stock complexes for US West Coast groundfishes using vulnerabilities and ecological distributions. N. Am. J. Fish. Manage. 31:589–604.

Craney, T. A., and J. G. Surles.
2002. Model-dependent variance inflation factor cutoff values. Qual. Eng. 14:391–403.

Cushing, D. H.
1990. Plankton production and year-class strength in fish populations: an update of the match/mismatch hypothesis. Adv. Mar. Biol. 26:249–293.

Dick, E. J., and A. D. MacCall.
2010. Estimates of sustainable yield for 50 data-poor stocks in the Pacific Coast groundfish fishery management plan. NOAA Tech. Memo. NMFS-SWFSC-460, 208 p.

Francis, R. I. C. C.
1988. Are growth parameters estimated from tagging and age–length data comparable? Can. J. Fish. Aquat. Sci. 45:936–942.

Gunderson, D. R., and R. D. Vetter.
2006. Temperate rocky reef fishes. *In* Marine metapopulations (J. P. Kritzer and P. F. Sale, eds.), p. 69–118. Elsevier, San Diego, CA.

Hare, J. A., W. E. Morrison, M. W. Nelson, M. M. Stachura, E. J. Teeters, R. B. Griffis, M. A. Alexander, J. D. Scott, L. Alade, R. J. Bell, et al.
2016. A vulnerability assessment of fish and invertebrates to climate change on the Northeast U.S. continental shelf. PLoS ONE 11(2):e0146756.

Harvey, C. J., J. C. Field, S. G. Beyer, and S. M. Sogard.
2011. Modeling growth and reproduction of chilipepper rockfish under variable environmental conditions. Fish. Res. 109:187–200.

He, X., J. C. Field, S. G. Beyer, and S. M. Sogard.
2015a. Effects of size-dependent relative fecundity specifications in fishery stock assessments. Fish. Res. 165:54–62.

He, X., J. C. Field, D. E. Pearson, L. Lefebvre, and S. Lindley.
2015b. Status of bocaccio, *Sebastes paucispinis*, in the Conception, Monterey and Eureka INPFC areas for 2015. Pacific Fishery Management Council stock assessment and fishery evaluation. Pac. Fish. Manage. Counc., Portland, OR. [Available from website.]

Hill, K. T., P. R. Crone, and J. P. Zwolinski.
2017. Assessment of the Pacific sardine resource in 2017 for U.S. management in 2017-18. NOAA Tech. Memo. NMFS-SWFSC-576, 262 p.

Hyde, J. R., and R. D. Vetter.
2007. The origin, evolution, and diversification of rockfishes of the genus *Sebastes* (Cuvier). Mol. Phylogenet. Evol. 44:790–811.

Kass, R. E., and A. E. Raftery.
1995. Bayes factors. J. Am. Stat. Assoc. 90:773–795.

Keller, A., J. R. Wallace, B. H. Horness, O. S. Hamel, and I. J. Stewart.
2012. Variations in eastern North Pacific demersal fish biomass based on the U.S. west coast groundfish bottom trawl survey (2003–2010). Fish. Bull. 110:63–80.

Kowalski, B., F. Watson, C. Garza, and B. Delgado.
2015. Effects of landscape covariates on the distribution and detection probabilities of mammalian carnivores. J. Mamm. 96:511–521.

Lefebvre, L. S., and J. C. Field.
2015. Reproductive complexity in a long-lived deepwater fish, the blackgill rockfish. Trans. Am. Fish. Soc. 144:383–399.

Lefebvre, L. S., S. G. Beyer, D. M. Stafford, N. S. Kashef, E. J. Dick, S. M. Sogard, and J. C. Field.
2018. Double or nothing: plasticity in reproductive output in the chilipepper rockfish (*Sebastes goodei*). Fish. Res. 204:258–268.

Love, M. S., P. Morris, M. McCrae, and R. Collins.
1990. Life history aspects of 19 rockfish species (*Scorpaenidae: Sebastes*) from the southern California Bight. NOAA Tech. Rep. NMFS 87, 44 p.

Love, M. S., M. Yoklavich, and L. Thorsteinson.
2002. The rockfishes of the Northeast Pacific, 416 p. Univ. Calif. Press, Berkeley, CA.

MacGregor, J. S.
1970. Fecundity, multiple spawning, and description of the gonads in *Sebastodes*. U.S. Fish Wildl. Serv., Spec. Sci. Rep. Fish. 596, 12 p.

McCabe, R. M., B. M. Hickey, R. M. Kudela, K. A. Lefebvre, N. G. Adams, B. D. Bill, F. M. Gulland, R. E. Thomson, W. P. Cochlan, and V. L. Trainer.
2016. An unprecedented coastwide toxic algal bloom linked to anomalous ocean conditions. Geophys. Res. Lett. 43:10–366.

Morrison W. E., M. W. Nelson, J. F. Howard, E. J. Teeters, J. A. Hare, R. B. Griffis, J. D. Scott, and M. A. Alexander.
2015. Methodology for assessing the vulnerability of marine fish and shellfish species to a changing climate. NOAA Tech. Memo. NMFS-OSF-3, 48 p.

Moser, H. G.
1966. Reproductive and developmental biology of the rockfishes (*Sebastodes* spp.) off California Ph.D. diss., 561 p. Univ. South. Calif., Los Angeles, CA.
1967. Reproduction and development of *Sebastodes paucispinis* and comparison with other rockfishes off southern California. Copeia 1967:773–797.

Nichol, D. G., and E. K. Pikitch.
1994. Reproduction of darkblotched rockfish off the Oregon-Coast. Trans. Am. Fish. Soc. 123:469–481.

PFMC (Pacific Fishery Management Council).
2016. Status of the Pacific coast groundfish fishery: stock assessment and fishery evaluation, 309 p. Pac. Fish. Manage. Counc., Portland, OR 97220. [Available from website.]

Parker, S. J., S. A. Berkeley, J. T. Golden, D. R. Gunderson, J. Heifetz, M. A. Hixon, R. Larson, B. M. Leaman, M. S. Love, J. A. Musick, et al.
2000. Management of Pacific rockfish. Fisheries 25:22–30.

Parrish, R. H., C. S. Nelson, and A. Bakun.
1981. Transport mechanisms and reproductive success of fishes in the California Current. Biol. Oceanogr. 1:175–203.

R Core Team.
2018. R: a language and environment for statistical computing. R Foundation for Statistical Computing, Vienna, Austria. [Available from website, accessed April 2018.]

Ralston, S., and B. R. MacFarlane.
2010. Population estimation of bocaccio (*Sebastes paucispinis*) based on larval production. Can. J. Fish. Aquat. Sci. 67:1005–1020.

Rideout, R. M., G. A. Rose, and M. P. M. Burton.
2005. Skipped spawning in female iteroparous fishes. Fish Fish. 6:50–72.

Rykaczewski, R. R., J. P. Dunne, W. J. Sydeman, M. García-Reyes, B. A. Black, and S. J. Bograd.
2015. Poleward displacement of coastal upwelling-favorable winds in the ocean's eastern boundary currents through the 21st century. Geophys. Res. Lett. 42:6424–6431.

Stafford, D. M., S. M. Sogard, and S. A. Berkeley.
2014. Maternal influence on timing of parturition, fecundity, and larval quality in three shelf rockfishes (*Sebastes* spp.). Aquat. Biol. 21:11–24.

Tolimieri, N., and M. J. Anderson.
2010. Taxonomic distinctness of demersal fishes of the California Current: moving beyond simple measures of diversity for marine ecosystem-based management. PLoS One 5:e10653.

Thompson, J. E., and R. W. Hannah.
2010. Using cross-dating techniques to validate ages of aurora rockfish (*Sebastes aurora*): estimates of age, growth and female maturity. Environ. Biol. Fish. 88:377–388.

VenTresca, D. A., R. H. Parrish, J. L. Houk, M. L. Gingras, S. D. Short, and N. L. Crane.
1995. El Niño effects on the somatic and reproductive condition of blue rockfish, *Sebastes mystinus*. CalCOFI Rep. 36:167–174.

Ware, D. M., and R. E. Thomson.
2005. Bottom-up ecosystem trophic dynamics determine fish production in the Northeast Pacific. Science 308:1280–1284.

Williams, E. H., and S. Ralston.
2002. Distribution and co-occurrence of rockfishes (family: *Sebastidae*) over trawlable shelf and slope habitats of California and southern Oregon. Fish. Bull. 100: 836–855.

Wyllie Echeverria, T.
1987. Thirty-four species of California rockfishes: maturity and seasonality of reproduction. Fish. Bull. 85:229–250.

National Marine
Fisheries Service
NOAA

Fishery Bulletin
established in 1881

Spencer F. Baird
First U.S. Commissioner
of Fisheries and founder
of *Fishery Bulletin*

Efficacy of 2 common bait types in reducing bycatch of coastal sharks on bottom longline gear in the absence of choice

William B. Driggers III (contact author)[1]
Kristin M. Hannan[2]

Email address for contact author: william.driggers@noaa.gov

[1] Mississippi Laboratories
Southeast Fisheries Science Center
National Marine Fisheries Service, NOAA
3209 Frederic Street
Pascagoula, Mississippi 39567-4112

[2] Riverside Technology Inc.
Mississippi Laboratories
Southeast Fisheries Science Center
National Marine Fisheries Service, NOAA
3209 Frederic Street
Pascagoula, Mississippi 39567-4112

Abstract—A recent study determined that when simultaneously exposed to 2 different commonly used baits, certain shark species demonstrate preferences for a specific bait on bottom longlines. To further investigate the value of bait type to reduce shark bycatch, we conducted single-bait-type bottom longline sets with standardized gear baited with either mackerel or squid. For 4 of the 5 shark species captured, there was no significant difference in catch rates with bait type. However, catch rates of Atlantic sharpnose sharks (*Rhizoprionodon terraenovae*) were significantly higher on mackerel-baited hooks. Our results indicate that the use of squid as bait can reduce the catch of at least one shark species in the northern Gulf of Mexico while not reducing the catch of a targeted species, in this case, the red snapper (*Lutjanus campechanus*). However, because some protected species, most notably sea turtles, have been shown to have higher catch rates on squid-baited hooks, it is necessary to assess the effect of a specific bait across all taxa directly or indirectly affected by a particular gear type before adopting any bycatch reduction measure.

Manuscript submitted 25 March 2019.
Manuscript accepted 24 July 2019.
Fish. Bull. 117:189–195 (2019).
Online publication date: 1 August 2019.
doi: 10.7755/FB.117.3.6

The views and opinions expressed or implied in this article are those of the author (or authors) and do not necessarily reflect the position of the National Marine Fisheries Service, NOAA.

Globally, shark populations are widely reported to be in decline (for a recent review, see Dulvy et al., 2014). Although a number of factors contribute to this trend, bycatch of sharks is a primary factor (Oliver et al., 2015). A number of potential shark bycatch mitigation measures have been considered, including time or area closures, gear modifications, adaptive fishing practices, and use of repellents (Molina and Cooke, 2012). Several studies have investigated the efficacy of bait type in reducing shark bycatch rates (e.g., Broadhurst and Hazin, 2001; Watson et al., 2005; Yokota et al., 2009); however, results of studies examining the relationship between catch rates and bait type on longline gear are often conflicting. For example, in studies with comparable gear comparing squid and mackerel baits, Watson et al. (2005) and Foster et al. (2012) found that catch of blue sharks (*Prionace glauca*) was highest on pelagic longlines when squid (*Illex* spp.) was used compared with when bait of Atlantic mackerel (*Scomber scombrus*) was used, whereas Coelho et al. (2012) reported a higher catch of blue sharks on mackerel (*Scomber* spp.) bait than on squid bait. All 3 studies used a single bait type on each longline set. However, none addressed potential biasing factors of this experimental design in assessing bait preference of blue sharks, most notably the propensity for this shark species to form large aggregations in discrete locations (e.g., Kenney et al., 1985; Litvinov, 2006) where only a single bait type would have been used.

Driggers et al. (2017) examined catch rates and bait preferences of fish species captured on bottom longline gear in the northern Gulf of Mexico using an experimental design alternating 2 bait types on individual bottom longline sets. The results of this study indicate that several shark species, including the little gulper shark (*Centrophorus uyato*), smooth dogfish (*Mustelus canis*), blacknose shark (*Carcharhinus acronotus*), sandbar shark (*C. plumbeus*), and Atlantic sharpnose shark (*Rhizoprionodon terraenovae*), showed a preference for Atlantic mackerel over northern shortfin

squid (*Illex illecebrosus*). Conversely, teleosts commonly targeted with bottom longline gear in the northern Gulf of Mexico, such as red snapper (*Lutjanus campechanus*), yellowedge grouper (*Hyporthodus flavolimbatus*), and tilefish (*Lopholatilus chamaeleonticeps*), showed no preference. The authors acknowledged that the use of alternating bait types could have biased results because of potential interaction effects of baits, a possibility suggested by Watson et al. (2005) and Foster et al. (2012). To address this issue and further investigate the efficacy of bait type in reducing shark bycatch, the objective of this study was to assess if the preference of sharks for Atlantic mackerel over northern shortfin squid baits reported by Driggers et al. (2017) would be evident in a single-bait experimental design.

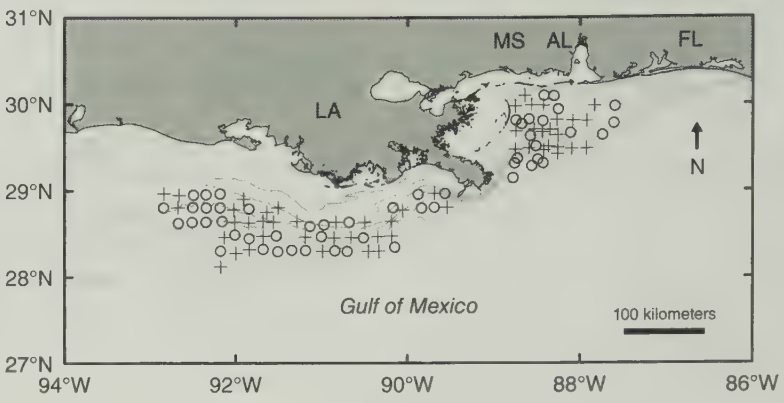

Figure 1

Map of sampling locations where bottom longline gear was set in the northern Gulf of Mexico during March–April 2017. Crosses indicate longline sets baited with northern shortfin squid (*Ilex illecebrosus*), and circles represent longline sets baited with Atlantic mackerel (*Scomber scombrus*). Gear was set in waters off Louisiana (LA), Mississippi (MS), Alabama (AL), and Florida (FL). Gray lines indicate the 10-, 20-, 30-, 40-, 50-, and 100-m isobaths.

Materials and methods

Bottom longline gear was deployed from the NOAA Ship *Oregon II* in the northern Gulf of Mexico from 26 March through 19 April 2017. All sets were made within an area bounded by 87.50°W to 93.00°W longitude at depths between 15 and 85 m (Fig. 1). Stations were preselected on the basis of a random starting point and subsequent stations being spaced 18.5 km apart in a grid to maximize sampling effort and minimize effects of sampling sites being in close proximity to one another. On several occasions, preselected stations were moved to avoid hazards to navigation (e.g., vessels, petroleum platforms, and shipping lanes) or excessively fast currents (>1 m/s). Sampling gear consisted of 1.8 km of 4-mm diameter monofilament mainline and 100 gangions. Each gangion was constructed of a size 148-8/0 snap, 3.2 m of 3-mm diameter monofilament, 0.5 m of 2.4-mm diameter fishing wire, and a hook (#15/0 non-offset, circle, Mustad #39960D[1], O. Mustad & Søn A.S., Gjøvik, Norway) and was identical to that used in Driggers et al. (2017). Each hook was baited with Atlantic mackerel or northern shortfin squid cut to fit the circle hooks. Bait consisted either entirely of Atlantic mackerel or northern shortfin squid for each longline set with bait randomly assigned at the beginning of each set.

Bottom temperature (in degrees Celsius) and salinity were measured at each sampling location, while the longline gear was in the water, by using an SBE 911plus CTD water profiler (Sea-Bird Scientific, Bellevue, WA). Soak time, defined as the time elapsed from completing deployment of the gear to beginning retrieval of the gear, was limited to 1 h in an effort to minimize mortality rates of captured organisms and to maximize the number of longline sets conducted during the allotted sampling period. Further, the relatively short soak time reduced data loss associated with shark depredation and potential bias associated with capturing large sharks feeding upon smaller captured fish, a behavior that would not reflect preference for Atlantic mackerel or northern shortfin squid. Upon capture, each fish was identified to species and its fork length was measured to the nearest millimeter on a straight line along the axis of the body from the tip of the rostrum to the caudal notch.

Depth, temperature, salinity, soak-time, and fish-length data associated with sampling locations where each bait was used were assessed for normality and homoscedasticity by calculating kurtosis, skewness, and F-ratio. Data were considered normally distributed when kurtosis and skewness were between −2 and 2. For data that adhered to the assumptions of parametric statistics, t-tests were used to compare mean values; for data that did not meet assumptions, median values were compared by using a Mann–Whitney W test. To determine if the number of individuals captured on each bait was significantly different from 1:1, a chi-square test with Yates correction for continuity was used on a species-specific basis. Sharks that were captured on hooks occupied by a smaller captured fish were removed from all analyses (2 blacktip sharks, *Carcharhinus limbatus*), and fish not measured because of shark-inflicted damage were excluded from comparisons of body length.

To account for the possibility that catch data were biased because of schooling behavior or areas of high abundance (i.e., high catch in limited cases because of habitat specificity or aggregations), catch data for each species were examined to determine if an unusually high number of individuals were caught on any specific set.

[1] Mention of trade names or commercial companies is for identification purposes only and does not imply endorsement by the National Marine Fisheries Service, NOAA.

The mean number of a given species captured on all sets, regardless of bait, was calculated. All sets where the total number of individuals captured was greater than 3 standard deviations from the mean were considered outliers and removed from analyses. For those species for which outliers were identified, chi-square tests based on revised expected values were conducted. Revised expected values were calculated by subtracting sets with identified outliers from the total number of sets conducted with the corresponding bait and then dividing the remaining number of sets with Atlantic mackerel bait by the number of sets with northern shortfin squid bait. All statistical tests were considered significant at an α level of 0.05.

Results

Of the 104 longline sets conducted for this study, 52 sets used northern shortfin squid as bait and 52 sets used Atlantic mackerel as bait (Fig. 1). There was no significant difference in the mean depth (t=–0.58, P=0.56) or temperature (t=–0.30, P=0.77) between sets that used the 2 types of bait (Table 1). Similarly, there was no significant difference in the median bottom salinity (W=1426.0, P=0.40) among sampling locations where the 2 baits were used (Table 1). Soak times ranged from 57 to 65 min, and there was no significant difference between soak times on sets that used mackerel or squid for bait (t=0.28, P=0.78) (Table 1). Among all sets, regardless of bait, 1572 fish from 25 species were captured; however, 6 of these species made up 91.3% of the total catch. Those species were the Gulf smoothhound (*Mustelus sinusmexicanus*), Atlantic sharpnose shark, blacknose shark, blacktip shark, scalloped hammerhead (*Sphyrna lewini*), and red snapper (Table 2). Species that constituted less than 1% of the total catch or were caught on fewer than 10 sets were not considered in subsequent analyses.

All captured fish had corresponding body length measurements with the exception of 23 specimens damaged by sharks (14 red snapper and 9 Atlantic sharpnose sharks). The mean or median fork length (FL) of all species examined did not differ by bait, with the exception of those for the Atlantic sharpnose shark, specimens of which were larger on sets with bait of Atlantic mackerel (median: 806 mm FL) than on sets with bait of northern shortfin squid (median: 781 mm FL) (W=49994.4, P<0.01) (Fig. 2, Table 2). However, there was a greater size range (323–970 mm FL) of Atlantic sharpnose sharks captured on sets baited with Atlantic mackerel compared with the size range on sets baited with northern shortfin squid (487–961 mm FL).

The total catch of all species on each bait was not different from the expected ratio of 1:1, with the exception of the catch of Atlantic sharpnose sharks, which were more frequently captured on sets baited with Atlantic mackerel (n=488) than on northern shortfin squid-baited sets (n=302) (χ^2=43.32, P<0.01) (Table 2). Outliers indicating unusually large catches were detected for Atlantic sharpnose sharks, blacknose sharks, blacktip sharks, and scalloped hammerheads (Table 3). After removing outliers, Atlantic sharpnose sharks (χ^2=12.14, P<0.01) and blacknose sharks (χ^2=4.92, P=0.03) were caught more frequently on sets baited with Atlantic mackerel. However, there remained no significant relationship between bait type and catch rates of blacktip sharks (χ^2=0.02, P=0.87) or scalloped hammerheads (χ^2=0.01, P=0.92).

Discussion

Results of our study indicate that for Gulf smoothhounds, blacktip sharks, scalloped hammerheads, and red snapper, there was no difference in capture rates related to bait. However, preference for Atlantic mackerel bait over

Table 1

Comparison of abiotic variables and soak times associated with bottom longline sets conducted with baits of Atlantic mackerel (*Scomber scombrus*) or northern shortfin squid (*Ilex illecebrosus*) in the northern Gulf of Mexico during March–April 2017. Means are given with standard errors of the mean (SEs). Results from t-tests and Mann–Whitney (M-W) W tests are provided with their associated P-values in parentheses.

Variable	Bait type	Range	Mean (SE)	Median	t-value (P)	M-W test (P)
Depth (m)	Mackerel	15.3–83.1	40.51 (2.22)	39.0	–0.58 (0.56)	1425.5 (0.64)
	Squid	15.9–77.3	42.41 (2.34)	37.3		
Temperature (°C)	Mackerel	19.8–23.0	21.48 (0.13)	21.4	–0.30 (0.77)	1369.5 (0.64)
	Squid	19.5–23.1	21.53 (0.13)	21.5		
Salinity	Mackerel	31.3–36.4	35.74 (0.14)	36.2	–	1426.0 (0.40)
	Squid	32.5–36.5	35.90 (0.10)	36.2		
Soak time (min)	Mackerel	57.0–65.0	60.61 (0.25)	60.5	0.28 (0.78)	1308.0 (0.77)
	Squid	57.0–65.0	60.52 (0.24)	61.0		

Table 2

Number of individuals (n), size range (millimeters fork length [FL]), mean size (mm FL), median size (mm FL), and test statistics for species caught on longline sets baited with Atlantic mackerel (*Scomber scombrus*) or northern shortfin squid (*Ilex illecebrosus*) in the northern Gulf of Mexico during March–April 2017. Statistics from t-tests, Mann–Whitney W tests, and chi-square tests are presented with associated P-values in parentheses. An asterisk (*) indicates data that did not meet the assumptions of normality or homoscedasticity.

Species	Bait type	n	Size range	Mean (SE)	Median	t-value (P)	W test (P)	Chi-square test (P)
Gulf smoothhound	Mackerel	51	573–1207	902.4 (19.8)	900.0	1.70 (0.08)	769.0 (0.07)	1.34 (0.25)
	Squid	39	402–1143	867.7 (21.3)	819.0			
Atlantic sharpnose shark	Mackerel	488	323–970	793.8 (3.1)	806.0	6.22 (<0.01)*	49,994.4 (<0.01)	43.32 (<0.01)
	Squid	302	487–961	759.5 (5.0)	781.0			
Blacknose shark	Mackerel	33	584–1057	861.1 (21.8)	884.0	0.14 (0.89)	363.0 (0.78)	2.24 (0.13)
	Squid	21	589–1015	855.6 (33.8)	922.0			
Blacktip shark	Mackerel	18	990–1214	1100.3 (62.1)	1115.0	−0.98 (0.33)	148.5 (0.58)	0.52 (0.47)
	Squid	13	1015–1250	1125.9 (23.7)	1096.0			
Scalloped hammerhead	Mackerel	46	643–1880	1254.5 (45.8)	1237.0	0.17 (0.86)	1177.0 (0.77)	0.36 (0.55)
	Squid	53	646–1820	1243.5 (43.5)	1210.0			
Red snapper	Mackerel	198	530–880	708.1 (4.4)	706.0	0.49 (0.62)*	17,554.0 (0.33)	0.02 (0.88)
	Squid	202	605–881	705.3 (3.4)	699.5			

northern shortfin squid bait was evident for Atlantic sharpnose sharks both when not accounting for and when accounting for sets with unusually high catches. This result, in agreement with the findings of Driggers et al. (2017), demonstrates that bait type is a viable option for shark bycatch reduction albeit on a species-specific basis. Further, the catch of red snapper was not affected by bait type in this study or in Driggers et al. (2017), indicating that shark catch can be reduced without affecting the catch of target species when bait type is used as a bycatch mitigation measure.

For blacknose sharks, there was no difference in catch rates between bait types unless unusually high catch rates identified as outliers were removed from the data set. Driggers et al. (2017) reported that, when both baits were alternated on a single set, the catch of blacknose sharks was over 5 times greater when Atlantic mackerel was used for bait compared with catch when northern shortfin squid was used. This finding is consistent with past reports that the diet of blacknose sharks is primarily piscivorous (e.g., Castro, 2011). For example, Dodrill (1977) reported that stomach contents of all blacknose sharks he examined contained teleost prey. Similarly, Cortés (1999) reported that the diet of blacknose sharks consisted of 98.2% teleosts, with less than 2% consisting of crustaceans and noncephalopod mollusks. Ford (2012), on the basis of a sample size larger than the combined sample size reported in the Dodrill (1977) and Cortés (1999) studies, found that fish compose 63.4% of the diet of blacknose sharks off the East Coast of the United States, with the remainder composed of invertebrates, including squid and octopods (11.4%).

Results of our study and those of Ford (2012) indicate that blacknose sharks are more opportunistic than previously thought. Additionally, when considered in conjunction with the findings of Driggers et al. (2017), although the species shows a clear preference for teleosts, blacknose sharks will opportunistically prey on other organisms when their preferred prey is not present. Although there were fewer blacknose sharks captured on sets baited with northern shortfin squid during our study, the difference in capture rates between the 2 baits was not significantly different. Therefore, on the basis of the data from our study, bait choice does not appear to be an efficient bycatch mitigation measure for the blacknose shark. However, it is important to note that only 54 blacknose sharks were captured during this study, and if a real effect was present, it could have been obfuscated by the relatively low sample size.

Like blacknose sharks, blacktip sharks are reported to feed primarily on teleosts (e.g., Castro, 1996; Bethea et al., 2004; Barry et al., 2008). For example, Hoffmayer and Parsons (2003) examined the diet of blacktip sharks in the Mississippi Sound and determined that 95% of the diet of this species was composed of teleosts. Results of this study demonstrate that blacktip sharks are opportunistic and, although they specialize in feeding on teleosts, they will feed on both squid and teleost baits, negating the value of bait type as a bycatch mitigation measure for this species. A similar conclusion was reached for the effect of bait type on catch rates of the Gulf smoothhound, scalloped hammerhead, and red snapper. This result was not unexpected because scalloped hammerheads and red snapper are known to have relatively wide dietary breadths, including teleosts and cephalopods (Stevens and Lyle, 1989; Szedlmayer and Lee, 2004; Wells et al., 2008; Vaske et al., 2009; Torres-Rojas et al., 2010). Further, to our knowledge, no species-specific diet studies have been conducted for the

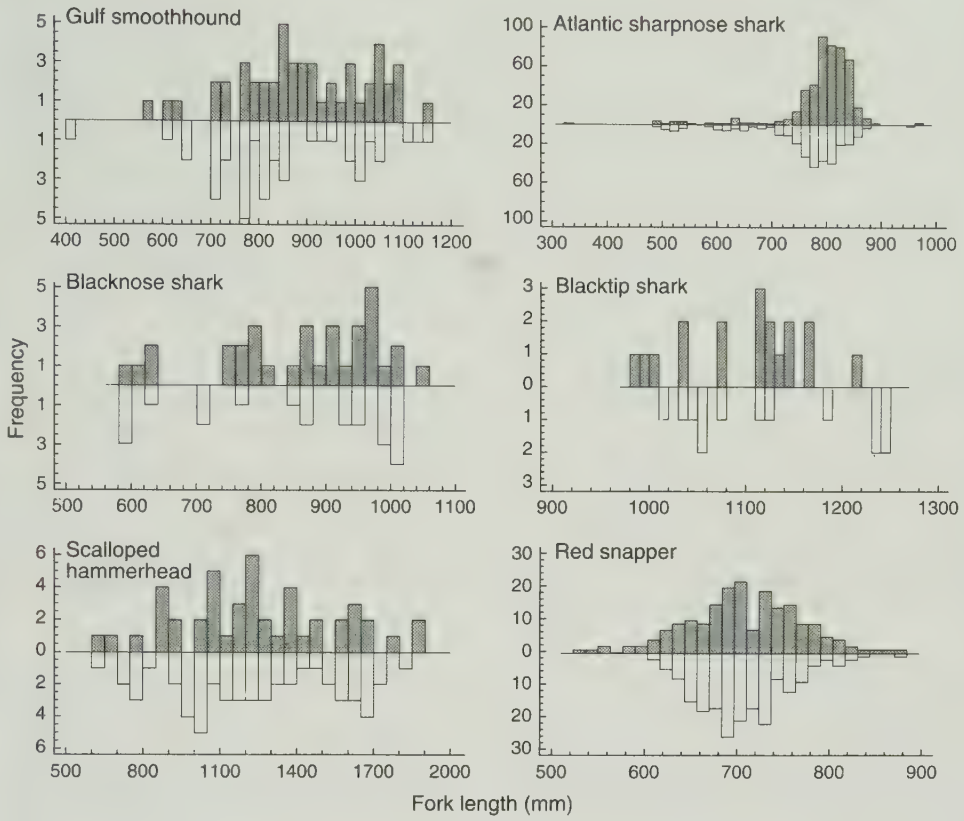

Figure 2

Length–frequency distributions of sharks captured on longline sets baited with Atlantic mackerel (*Scomber scombrus*) (gray bars) and northern shortfin squid (*Ilex illecebrosus*) (white bars) in the northern Gulf of Mexico during March–April 2017. There were no significant species-specific differences in the median fork length (FL) of sharks caught on the 2 bait types, with the exception of Atlantic sharpnose sharks (*Rhizoprionodon terraenovae*), which had a larger median FL on mackerel-baited hooks. Note that the scales of x- and y-axes differ among species.

Gulf smoothhound; however, Cortés (1999) summarized the diet of 13 species within the morphologically conservative genus *Mustelus* and demonstrated that these fishes have a diverse diet. For example, dietary studies of the smooth dogfish, which is sympatric with and has the same dental morphology as the Gulf smoothhound, indicate that its diet consists of decapod crustaceans, teleosts, and non-decapod invertebrates in decreasing order (Cortés, 1999).

Pitcher et al. (1982) empirically tested the effect of shoal size on the amount of time it took goldfish (*Carassius auratus*) and minnows (*Phoxinus phoxinus*) to locate a food source, and they found that foraging efficiency increased with shoal size for both species. Among coastal shark species captured during 3500 fishery-independent bottom longline sets conducted throughout the northern Gulf of Mexico as part of a survey by the National Marine Fisheries Service, Southeast Fisheries Science Center, Mississippi Laboratories, the Atlantic sharpnose shark is not only the most commonly caught species (n=15,494 individuals) but also the species most commonly caught in schools of 10 individuals or larger (number of sets=513, school size range of 10–72 sharks). If there is a link between shoal size and preferred bait detection for Atlantic sharpnose sharks, as our results indicate, it is possible that other species have a preference for a specific bait when shoaling. Because individuals of some shark species, such as the blacktip shark, spinner shark (*Carcharhinus brevipinna*), and scalloped hammerhead, form large shoals within the Gulf of Mexico during certain times of the year (senior author, unpubl. data), it is possible that bait preference could be exhibited during those periods but absent at other times when individuals are more dispersed. Future research should examine this hypothesis and test how the use of bait type as a bycatch mitigation measure can vary seasonally.

The combined results of this study and Driggers et al. (2017) provide the first comparison, as far as we are aware of, between the effect of bait type on catch rates of sharks caught on standardized longline gear with single-bait-type

Table 3

Range of number of individuals caught per set, mean number caught per set, and number of sets identified as outliers for species caught on longline sets baited with Atlantic mackerel (*Scomber scombrus*) or northern shortfin squid (*Ilex illecebrosus*) in the northern Gulf of Mexico during March–April 2017. Values provided in parentheses represent number of individuals caught in longline sets identified as outliers or *P*-values associated with χ^2 values from chi-square tests. Note that no catches of Gulf smoothhounds (*Mustelus sinusmexicanus*) or red snapper (*Lutjanus campechanus*) were identified as outliers. Therefore, no associated expected ratios or χ^2 values are presented for either species. SD=standard deviation.

Species	Bait type	No. per set	Mean + 3 SD	No. of outliers	Expected ratio	χ^2
Gulf smoothhound	Mackerel	1–8	9.81	0	–	–
	Squid	1–7		0		
Atlantic sharpnose shark	Mackerel	1–50	42.22	2 (43, 50)	0.96:1	12.14 (<0.01)
	Squid	1–31		0		
Blacknose shark	Mackerel	1–4	4.77	0	1.02:0	4.92 (0.03)
	Squid	1–5		1 (5)		
Blacktip shark	Mackerel	1–7	5.90	1 (7)	0.98:1	0.02 (0.87)
	Squid	1–3		0		
Scalloped hammerhead	Mackerel	1–5	5.15	0	1.02:0	0.01 (0.92)
	Squid	1–6		1 (6)		
Red snapper	Mackerel	1–15	22.50	0	–	–
	Squid	1–18		0		

sets and alternating-bait-type sets. A valid criticism of Driggers et al. (2017) is related to possible interaction effects when bait type is alternated on a single set, as suggested by Watson et al. (2005) and Foster et al. (2012). Although this concern is reasonable, if an interaction effect occurred, a statistically equal number of individuals of a given species would be expected to be caught on each bait. The results of Driggers et al. (2017) indicate significant bait type preference for 5 shark species and a clear trend for 3 other species; therefore, we believe the concern is unwarranted. However, the results of our study, for which we used a single-bait approach, indicate that in the absence of choice, most, but not all, species that Driggers et al. (2017) found demonstrated a bait preference will ingest whichever bait is available. Therefore, we conclude that studies examining the effect of bait type on catch rates with longline gear should use both single-bait and alternating bait approaches to determine the degree of bait preference and if a specific bait affects catch rates in such a way that would warrant management measures. Further, bait comparison studies that employ a single-bait approach must demonstrate that all bait types were fished in comparable abiotic and biotic conditions.

Results of our study indicate that it is important that bait type be accounted for when analyzing fishery-dependent and fishery-independent catch data rather than assuming there is no difference in catch rates among different baits. Although this assumption would have little to no effect when examining a species with no bait preference, in certain cases, such as when examining trends in abundance of Atlantic sharpnose sharks, significant bias would be introduced. Additionally, there can be a cascading effect whereby captured fish become bait themselves, therefore introducing unexpected biases for other species showing preferences. For example, during the Mississippi Laboratories survey, Atlantic mackerel has been the sole bait used since 1995. During this time, 26% of all bull sharks (*C. leucas*) have been caught on hooks occupied by captured Atlantic sharpnose sharks (senior author, unpubl. data). If a change were made from Atlantic mackerel bait to northern shortfin squid bait, on the basis of the results of this study, fewer Atlantic sharpnose sharks would be expected to be captured, and in turn fewer bull sharks, a species whose diet has been reported to consist to a large extent (35.4%) of smaller sharks (Cortés, 1999), would be captured.

In addition to indicating the importance of considering bait type in analyses of catch data, the results of this study demonstrate that the use of squid as bait can reduce the catch of at least one shark species in the northern Gulf of Mexico and could be employed as a bycatch reduction measure. However, some protected species, such as the loggerhead (*Caretta caretta*) and leatherback (*Dermochelys coriacea*) sea turtles, have been shown to have higher bycatch rates on squid-baited hooks (e.g., Watson et al., 2005). Therefore, the effect of a specific bait across all taxa that are directly or indirectly affected by a particular gear type must be assessed before adopting any bycatch reduction measure.

Acknowledgments

We thank the crew of the NOAA Ship *Oregon II*, P. Felts, E. Hoffmayer, N. Hopkins, C. Jones, L. Jones, K. Rademacher, C. Stepongzi, and T. Wallace for their field assistance.

Literature cited

Barry, K. P., R. E. Condrey, W. B. Driggers III, and C. M. Jones.
2008. Feeding ecology of neonate and juvenile blacktip sharks *Carcharhinus limbatus* in the Timbalier-Terrebone Bay complex, LA, U.S.A. J. Fish Biol. 73:650–662.

Bethea, D. M., J. A. Buckel, and J. K. Carlson.
2004. Foraging ecology of the early life stages of four sympatric shark species. Mar. Ecol. Prog. Ser. 268:245–264.

Broadhurst, M. K., and F. H. V. Hazin.
2001. Influences of type and orientation of bait on catches of swordfish (*Xiphias gladius*) and other species in an artisanal sub-surface longline fishery off northeastern Brazil. Fish. Res. 53:169–179.

Castro, J. I.
1996. Biology of the blacktip shark, *Carcharhinus limbatus*, off the southeastern United States. Bull. Mar. Sci. 59:508–522.
2011. The sharks of North America, 613 p. Oxford Univ. Press, New York.

Coelho, R., M. N. Santos, and S. Amorim.
2012. Effects of hook and bait on targeted and bycatch fishes in an equatorial Atlantic pelagic longline fishery. Bull. Mar. Sci. 88:449–467.

Cortés, E.
1999. Standardized diet compositions and trophic levels of sharks. ICES J. Mar. Sci. 56:707–717.

Dodrill, J. W.
1977. A hook and line survey of the sharks found within five hundred meters of shore along Melbourne Beach, Brevard County, Florida. M.S. thesis, 304 p. Fla. Inst. Technol., Melbourne, FL.

Driggers, W. B., III, M. D. Campbell, K. M. Hannan, E. R. Hoffmayer, C. M. Jones, L. M. Jones, and A. G. Pollack.
2017. Influence of bait type on catch rates of predatory fish species on bottom longline gear in the northern Gulf of Mexico. Fish. Bull. 115:50–59.

Dulvy, N. K., S. L. Fowler, J. A. Musick, R. D. Cavanagh, P. M. Kyne, L. R. Harrison, J. K. Carlson, L. N. K. Davidson, S. V. Fordham, M. P. Francis, et al.
2014. Extinction risk and conservation of the world's sharks and rays. eLife 3:e00590.

Ford, R. M.
2012. Diet and reproductive biology of the blacknose shark (*Carcharhinus acronotus*) from the southwestern Atlantic Ocean. M.S. thesis, 43 p. Univ. N. Fla., Jacksonville, FL.

Foster, D. G., S. P. Epperly, A. K. Shah, and J. W. Watson.
2012. Evaluation of hook and bait type on the catch rates in the western North Atlantic Ocean pelagic longline fishery. Bull. Mar. Sci. 88:529–545.

Hoffmayer, E. R., and G. R. Parsons.
2003. Food habits of three shark species from the Mississippi Sound in the northern Gulf of Mexico. Southeast. Nat. 2:271–280.

Kenney, R. D., R. E. Owen, and H. W. Winn.
1985. Shark distributions off the northeast United States from marine mammal surveys. Copeia 1985:220–223.

Litvinov, F. F.
2006. On the role of dense aggregations of males and juveniles in the functional structure of the range of the blue shark *Prionace glauca*. J. Ichthyol. 46:613–624.

Molina, J. M., and S. J. Cooke.
2012. Trends in shark bycatch research: current status and research needs. Rev. Fish Biol. Fish. 22:719–737.

Oliver, S., M. Braccini, S. J. Newman, and E. S. Harvey.
2015. Global patterns in the bycatch of sharks and rays. Mar. Policy 54:86–97.

Pitcher, T. J., A. E. Magurran, and I. J. Winfield.
1982. Fish in larger shoals find food faster. Behav. Ecol. Sociobiol. 10:149–151.

Stevens, J. D., and J. M. Lyle.
1989. Biology of three hammerhead shark (*Eusphyra blochii*, *Sphyrna mokarran* and *S. lewini*) from northern Australia. Aust. J. Mar. Freshw. Res. 40:129–146.

Szedlmayer, S. T., and J. D. Lee.
2004. Diet shifts of juvenile red snapper (*Lutjanus campechanus*) with changes in habitat and fish size. Fish. Bull. 102:366–375.

Torres-Rojas, Y. E., A. Hernández-Herrera, F. Galván-Magaña, and V. G. Alatorre-Ramírez.
2010. Stomach content analysis of juvenile, scalloped hammerhead shark *Sphyrna lewini* captured off the coast of Mazatlán, Mexico. Aquat. Ecol. 44:301–308.

Vaske, T., Jr., C. M. Vooren, and R. P Lessa.
2009. Feeding strategy of the night shark (*Carcharhinus signatus*) and scalloped hammerhead shark (*Sphyrna lewini*) near seamounts off northeastern Brazil. Braz. J. Oceanogr. 57:97–104.

Watson, J. W., S. P. Epperly, A. K. Shah, and D. G. Foster.
2005. Fishing methods to reduce sea turtle mortality associated with pelagic longlines. Can. J. Fish. Aquat. Sci. 62:965–981.

Wells, R. J. D., J. H. Cowan Jr., and B. Fry.
2008. Feeding ecology of red snapper *Lutjanus campechanus* in the northern Gulf of Mexico. Mar. Ecol. Prog. Ser. 361:213–225.

Yokota, K., M. Kiyota, and H. Okamura.
2009. Effect of bait species and color on sea turtle bycatch and fish catch in a pelagic longline fishery. Fish. Res. 97:53–58.

National Marine
Fisheries Service
NOAA

Fishery Bulletin
established in 1881

Spencer F. Baird
First U.S. Commissioner
of Fisheries and founder
of *Fishery Bulletin*

Use of parasites to clarify residency and migration patterns of Pacific sardine (*Sardinops sagax*) in the California Current

Kym Jacobson (contact author)[1]
Rebecca Baldwin[2]
Michael Banks[2]
Robert Emmett[1]

Email address for contact author: kym.jacobson@noaa.gov

[1] Newport Research Station
Northwest Fisheries Science Center
National Marine Fisheries Service, NOAA
2032 SE OSU Drive
Newport, Oregon 97365

[2] Cooperative Institute for Marine Resources Studies
Hatfield Marine Science Center
Oregon State University
2030 SE Marine Science Drive
Newport, Oregon 97365

Abstract—Migration patterns of the northern subpopulation of the Pacific sardine (*Sardinops sagax*) were examined by using parasites as biological tags. This approach has been employed on marine fish species worldwide, but it had not yet been used to investigate the migratory behavior of this ecologically and commercially valuable species in the California Current. In 2005–2008, 14 taxa of parasites were recovered from 1388 Pacific sardine collected between British Columbia, Canada, and Southern California. The results of multivariate analyses indicate significant differences in parasite communities among all size classes of Pacific sardine caught off Vancouver Island, British Columbia, compared with those caught off Washington and Oregon and regions off California. Significant differences in parasite communities also were identified between size classes of Pacific sardine: <210, 210–219, and ≥220 mm in standard length. Our results support a high degree of residency in all size categories of Pacific sardine off Vancouver Island during the study period, and they indicate that individual sardine behavior is not limited to completing an annual migration between British Columbia or the Pacific Northwest and Southern California. These data indicate that using parasites as biological tags could help clarify annual migration patterns of individual Pacific sardine.

Manuscript submitted 10 September 2018.
Manuscript accepted 26 July 2019.
Fish. Bull. 117:196–210 (2019).
Online publication date: 15 August 2019.
doi: 10.7755/FB.117.3.7

The views and opinions expressed or implied in this article are those of the author (or authors) and do not necessarily reflect the position of the National Marine Fisheries Service, NOAA.

The Pacific sardine (*Sardinops sagax*) is an ecologically important pelagic fish in upwelling systems that transfers energy from lower trophic levels (phytoplankton and zooplankton) to upper trophic predators, including fish, marine mammals, and birds (Cury et al., 2000). The Pacific sardine fishery is also economically important, providing for bait, aquaculture feed, and human consumption (Herrick et al., 2009). In the 1930s and 1940s, the Pacific sardine fishery in the California Current was the largest fishery in the Western Hemisphere (reviewed in Wolf, 1992). The fishery collapsed and was closed off the Pacific Northwest (PNW, Oregon and Washington) in 1947 and off Central California in 1967 (Radovich, 1981). Heavily influenced by ocean conditions, the biomass of the Pacific sardine in the California Current System (CCS) fluctuates widely. After a substantial biomass increase in the late 1980s and 1990s (Hargreaves et al., 1994; Emmett et al., 2005), a purse seine fishery reopened in California, the PNW, and off Vancouver Island in British Columbia, Canada, followed by a formal closure in 2015.

Three subpopulations of the Pacific sardine are currently recognized in the CCS (reviewed in Smith, 2005). One spawns in the Gulf of California, one spawns in inshore waters of southern Baja California, Mexico, and a northern subpopulation spawns primarily off Southern and Central California. For the management of Pacific sardine, the governments of both the United States and Canada assume all Pacific sardine of the northern subpopulation belong to one northerly migrating stock (Hill et al.[1]). Pacific sardine have also spawned successfully further north in some years, indicating either a possible separate spawning population

[1] Hill, K. T., P. R. Crone, E. Dorval, and B. J. Macewicz. 2015. Assessment of the Pacific sardine resource in 2015 for U.S.A. management in 2015–16, 116 p. Agenda item G.1.a. Pacific Fish. Manage. Counc., Portland, OR. [Available from website.]

or repeated spawning by migrants (Emmett et al., 2005; Lo et al., 2010). If the Pacific sardine commercially landed off British Columbia is from a portion of the northern subpopulation that does not return to California to spawn in certain years, it could have management considerations for how quotas are determined for both Canada and the United States.

The results of tagging studies conducted between 1936 and 1942, during the peak of the California fishery, indicate that Pacific sardine routinely migrated from spawning grounds off San Diego, California, to feeding grounds off the PNW and Vancouver Island (Hart, 1943; Clark and Janssen, 1945). In recent years, without a sufficient biomass or a reduction fishery to collect tags, repeating large-scale tagging studies has not been feasible. Financial costs of such studies have been prohibitive because thousands of tagged fish are needed to increase the probability of recovery of tagged individuals (Jacobsen and Hansen, 2005).

The recent use of techniques to examine potential stock discrimination and migration patterns of the northern stock, such as genetics (Hedgecock et al., 1989; Lecomte et al., 2004), size composition (Lo et al., 2011), otolith morphometrics (Javor et al., 2011; Javor, 2013), and stable oxygen isotopic signatures (Javor and Dorval, 2014), have had mixed results. No genetic differences have been identified between the Pacific sardine captured in any region of the CCS (Hedgecock et al., 1989; Lecomte et al., 2004). Lo et al. (2011) used biomass estimates of different size classes to estimate migration of different size classes between the PNW and California in 2003–2005. Otolith morphometrics differentiated age-1 Pacific sardine collected from Monterey, California, from those collected off San Diego in 2006–2007 (Javor et al., 2011). Stable oxygen isotopic signatures of otoliths showed some north–south trends for juvenile Pacific sardine but no regional differentiation among otoliths of adult Pacific sardine (Javor and Dorval, 2014).

One method that has successfully identified or confirmed migration patterns and stocks of marine fish species worldwide is the use of parasite species as biological tags (Thomas et al., 1996; MacKenzie and Abaunza, 1998; MacKenzie, 2002). Many parasite taxa can serve as biological tags because a fish can become infected with a parasite only within that parasite's endemic area (where all conditions for transmission exist). The presence of a parasite in a fish host caught outside of that parasite's endemic area, therefore, indicates that the fish host had previously been in the parasite's endemic area. Parasites of fish can be acquired by direct transmission or through trophic transmission, meaning the consumption of infected prey including crustaceans and other fish. Once in a fish host, parasites can be relatively long lived, remaining in or on the host from months to years, depending on the host–parasite association (Rohde, 1984). The technique of using parasites has limitations, such as time-consuming examination of hosts for internal parasites, a potential need for molecular techniques for correct identification, and a lack of adequate information on a parasite's ecology and biology (reviewed in MacKenzie and Abaunza, 1998, 2014). Despite these limitations, this technique has often been used by scientific and fisheries agencies (Pita et al., 2016), and by 2014 more than 290 peer-reviewed manuscripts had been published on the topic (Timi and MacKenzie, 2015).

The objective of our research was to determine if parasites infecting the northern stock of Pacific sardine could be used to identify migration patterns of the northern stock of Pacific sardine within the CCS. Our approach included comparing 1) the parasite communities of Pacific sardine collected from 5 regions along the west coast of North America and 2) the parasite communities of Pacific sardine to those of the central and northern subpopulations of non-migratory northern anchovy (*Engraulis mordax*), which are infected with many of the same parasite species (Love and Moser, 1983; Zorica et al., 2015). The parasites of northern anchovy could help confirm distributions of parasites recovered from migratory Pacific sardine in the northern CCS.

Materials and methods

Fish samples

From March through November 2005–2008, 1388 Pacific sardine were opportunistically collected by research and commercial fishing personnel in the CCS, between Vancouver Island (32° to 51°N) and Southern California (119–128°W) (Fig. 1). Pacific sardine from British Columbia were caught with a modified Cantrawl[2] (Cantrawl Nets Ltd., Richmond, Canada), a model 240-rope trawl (for details, see Morris et al.[3]). All other Pacific sardine and northern anchovy (except for northern anchovy collected off Southern California with a seine net) were caught using a Nordic 264-rope trawl (for details, see Baldwin et al., 2008). Fish collected for this study were immediately frozen onboard the vessel and later stored at −80°C in the laboratory until processed for parasites.

Pacific sardine ranged in size from 100.6 to 285.7 mm fresh standard length (SL). Of 1388 collected specimens, 562 fish were classified as non-migrants (<200 mm SL) and 826 fish were classified as migrants (≥200 mm SL) (Table 1). Following Lo et al. (2011), Pacific sardine <200 mm SL are non-migratory. Therefore, we hypothesized that parasite communities in this size category of Pacific sardine would differ among regions of the CCS. In contrast, migratory-sized Pacific sardine (≥200 mm SL) would have similar parasite communities throughout the CCS, if the entire population of the northern stock was migrating annually from Southern or Central California to British Columbia and then returning to California to spawn.

[2] Mention of trade names or commercial companies is for identification purposes only and does not imply endorsement by the National Marine Fisheries Service, NOAA.

[3] Morris, J. F. T., M. Trudel, M. E. Thiess, T. B. Zubowski, H. R. Maclean, J. M. R. Curtis, and L. Felli. 2009. CCGS *W.E. Ricker* Gulf of Alaska salmon survey, June 20–July 5, 2007. Dep. Fish. Oceans, Can. Data Rep. Fish. Aquat. Sci. 1221, 178 p. [Available from website.]

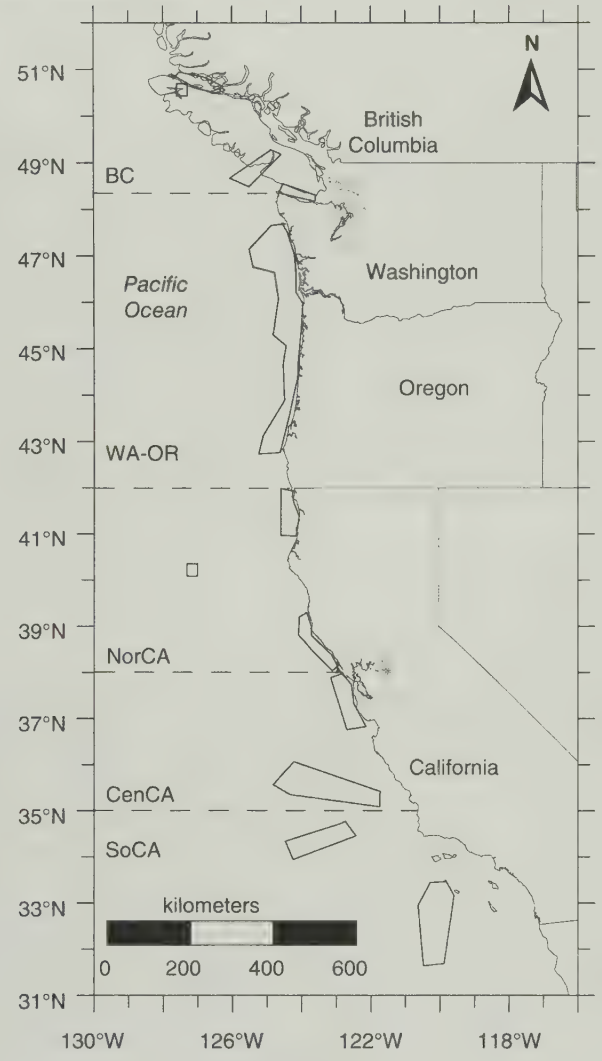

Figure 1

Map of the 5 regions of the California Current System where Pacific sardine (*Sardinops sagax*) were sampled from 2005 through 2008 for analyses of parasite communities. The regions are Vancouver Island, British Columbia (BC), Canada, Washington and Oregon (WA-OR), Northern California (NorCA), Central California (CenCA), and Southern California (SoCA). Boxes outlined with a black line represent areas within each region in which opportunistic samples were taken.

Although not all Pacific sardine were aged, we estimated ages to vary from 0 to 10 years, on the basis of Hill et al. (2010) and by using a relationship between age and SL (Javor[4]). A subset of the Pacific sardine caught off California during this period was aged. The median age of this subset ranged from 2 years in 2005 and 2006 to 3 years and 4 years in 2007 and 2008 (Dorval et al., 2015).

[4] Javor, B. 2008. Personal commun. Southwest Fish. Sci. Cent., Natl. Mar. Fish. Serv., 8901 La Jolla Shores Dr., La Jolla, CA 92037.

However, analyses did not focus on fish age because it was not possible to age all individual Pacific sardine in our study.

During 2007 and 2008, 168 northern anchovy (98.0–143.0 mm SL) were collected to serve as non-migratory sample controls. In June–July 2007, 20 northern anchovy (104–125 mm SL) were collected off Grays Harbor, Washington (47.00°N), and 97 fish (100–143 mm SL) were captured off Willapa Bay, Washington (46.67°N). In June 2008, 51 northern anchovy (98–142 mm SL) were collected off Point Hueneme, California (34.15°N).

Each fish was thawed in the laboratory, weighed to the nearest 0.1 g, and measured (as SL in millimeters). To account for shrinkage due to freezing, lengths of thawed Pacific sardine were adjusted by using the following regression (Lo et al., 2007):

$$Fresh\ SL = 2.89 + 1.0286\ (Thawed\ SL).$$

No length regression formula was available for the northern anchovy to estimate fresh SL; therefore, SL values are reported from fish that were frozen and then thawed.

Parasite recovery

Standard necropsy procedures were followed to examine fish for parasites (Arthur and Albert, 1994; Baldwin and Goater, 2003), with the body cavity and external surface of the viscera examined for parasites during removal of the stomach and intestine. Gills were examined only in Pacific sardine caught in 2005 because only one unknown monogenean was recovered from gills examined in 2005. Eyes were also not examined because no parasites were recovered from the eyes of Pacific sardine by us in a previous study; nor were they reported in other studies in the CCS (Love and Moser, 1983). When possible, recovered parasites were identified morphologically to species by using dissection and compound microscopes; then they were preserved in 95% ethanol. Most parasites were identified to species, but those in poor condition were classified only to phylum or class. Because we found no difference in geographic distributions among 5 anisakid nematode taxa from a subset of these Pacific sardine in a previous study (Baldwin et al., 2011), all anisakids (identified genetically or morphologically) were combined into one category for this study and referred to herein as *Anisakis* spp.

Statistical analyses

We divide the study area of the CCS into 5 regions to best define where fish were sampled: 1) Vancouver Island (hereafter, referred to as *British Columbia* (from 52.0°N to 48.3°N), 2) Washington and Oregon (48.3°N to 42.0°N), 3) Northern California (from the Oregon–California border at 42.0°N to 38.0°N), 4) Central California (38.0°N to 35.0°N), and 5) Southern California (south of 35.0°N to 32.0°N) (Fig. 1). We describe the parasite communities as defined by Bush et al. (1997) by using parasite prevalence (the percentage of infected fish) and mean intensity (the number of individual parasites per infected fish).

Because Lo et al. (2011) reported different migration rates (estimated percentages of the total biomass) of the northern subpopulation of Pacific sardine on the basis of size, we initially analyzed non-migrant Pacific sardine (<200 mm SL) and different size categories of potential migrants separately. Pacific sardine ≥200 mm SL (potential migrants) were split into 3 size categories: 200–209, 210–219, and ≥220 mm SL.

We used multivariate methods to explore variation in the parasite community data. Multivariate analyses of parasite communities were performed by using the multivariate statistics package PRIMER, vers. 7 (PRIMER-e Ltd., Auckland, New Zealand) (Clarke and Gorley, 2015) that includes the PERMANOVA+ module (Anderson et al., 2008). Only infected fish were included in multivariate analyses. Sample sizes of infected Pacific sardine per size category per region are provided in Table 2. Some individual fish harbored few parasites; therefore, parasite intensity data were averaged among 3–5 fish with the greatest similarity in length. Parasite intensity data were square-root transformed to reduce skewness due to any dominant parasite species and to stabilize the variance (Clarke et al., 2014a). Unidentifiable parasites (41 of the 2451 parasites recovered, <2% of the total) were not included in the multivariate analysis.

We constructed resemblance matrices based upon Bray–Curtis similarity with a dummy parasite value of 1 included to reduce the variability of some of the sparsely infected samples (Clarke et al., 2006). We then used these matrices to construct nonmetric multidimensional scaling (MDS) ordinations on region×fish size centroids to graphically explore spatial patterns of differences among the parasite communities of fish groups (Clarke et al., 2014a).

To quantitatively evaluate variation in parasite communities, multivariate parasite data were modeled for main effects by using a 3-way permutational multivariate analysis of variance (PERMANOVA) based on Bray–Curtis similarities (Bray and Curtis, 1957). The PERMANOVA test applies a nonparametric discriminative method based on permutation tests that do not rely on assumptions (e.g., normality, equal variance) commonly too stringent for most ecological data sets (Anderson, 2001). Main factors in the model include region, fish size category, and haul nested in region as a random factor. Year was included as a random factor in the initial model, but it was not a significant factor and was removed. The models were run for 9999

Table 1

General information on Pacific sardine (*Sardinops sagax*) classified as either non-migratory (<200 mm in standard length [SL]) or migratory (≥200 mm SL). Fish were caught by using a modified rope trawl or purse seine in 5 regions of the California Current System from 2005 through 2008 and analyzed for parasites. H=total number of hauls; *n*=number of fish caught; and SE=standard error.

		Mean SL						
		<200 mm				≥200 mm		
Region	H	*n*	Years	(SE)	Min.	*n*	Years	(SE)	Max.
Vancouver Island, Canada	6	43	05–07	175.8 (2.68)	148.1	176	05–07	223.1 (1.14)	285.7
Washington and Oregon	19	113	05–07	184.6 (1.55)	100.6	419	05–08	219.4 (0.83)	279.6
Northern California	10	142	06–07	191.8 (0.78)	120.2	139	06–07	208.2 (0.82)	260.4
Central California	5	152	05–07	175.4 (1.23)	106.8	36	06–07	211.3 (1.88)	267.2
Southern California	4	112	06–07	178.3 (0.93)	157.2	56	06–08	220.8 (1.53)	257.9

Table 2

Number of Pacific sardine (*Sardinops sagax*) caught from 2005 through 2008 in 5 regions of the California Current System and infected with at least 1 parasite to be included in multivariate community analyses. SL=standard length.

Size category (mm SL)	British Columbia	Washington and Oregon	Northern California	Central California	Southern California	Total
<200	29	40	87	79	87	322
200–209	20	55	59	7	7	148
210–219	40	72	13	11	9	145
≥220	78	101	6	2	21	208
Total	167	268	165	99	124	823

permutations. The PERMANOVA F-ratio test statistic is based on the expectations of mean squares and is directly analogous to the construction of the F-statistic for multifactorial univariate models but should be thought of as a pseudo F-test statistic because it does not have a known distribution under a true null hypothesis (Anderson et al., 2008). To estimate statistical significance between regions and between size categories, pairwise PERMANOVA tests were run. These tests included a Type II (conditional) sum of squares, with fixed effects summed to zero for mixed terms, and permutation of residuals under a reduced model. The pairwise PERMANOVA pseudo t-test statistic is a direct multivariate analogue to the univariate t-statistic (Anderson et al., 2008). Exact permutation P-values are reported.

Canonical analysis of principal coordinates (CAP) was used to further examine differences among parasite communities by measuring the distinctiveness of groups through cross validation (Anderson et al., 2008). Overparameterization was prevented by choosing the number of principal coordinate analysis (PCO) axes that maximized a leave-one-out allocation success to groups (Anderson and Robinson, 2003). The CAP analyses were based on abundance data and used a Bray–Curtis dissimilarity coefficient. A permutation "trace" (tr) test (sum of squared canonical eigenvalues) was used to test for significant differences.

We determined which parasite taxa contributed the greatest percent contributions to distinctiveness of parasite communities by using the similarity percentage (SIMPER) procedure in PRIMER and performed a shade plot analysis (Clarke et al., 2014b) on the 7 most abundant parasite taxa to provide a visual display of the parasite taxa most responsible for differences or trends among sizes of Pacific sardine and regions of collection.

For the parasite communities of northern anchovy, for which a less complex data set was available, a one-way multivariate analysis of similarities (ANOSIM) permutation test was used to identify differences in parasite mean abundances among regions. The ANOSIM test, based on rank similarities, provides R values. An R value close to or equal to one indicates that all communities within a group are more similar to each other than to communities from different groups, and an R value approximating zero indicates that similarities within and between groups are the same (Clarke and Green, 1988).

Results

Pacific sardine: parasite taxa recovered

A total of 14 trophically transmitted parasite taxa were recovered from Pacific sardine (Table 3). We recovered

Table 3

Prevalence (P) and mean intensity (I), with 95% confidence intervals (95% CIs), of parasites recovered from 1388 Pacific sardine (*Sardinops sagax*) caught in 5 regions of the California Current System from 2005 through 2008. n=sample size. Asterisks (*) denote that only 2 infected fish were collected.

	British Columbia (n=219)		Washington and Oregon (n=532)		Northern California (n=281)		Central California (n=188)		Southern California (n=168)	
Parasite taxa	P (%)	I (95% CI)	P (%)	I (95% CI)	P (%)	I (95% CI)	P (%)	I (95% CI)	P (%)	I (95% CI)
NEMATODA										
Anisakis spp.	25.1	1.4 (1.2–1.6)	24.2	1.7 (1.4–2.0)	11.4	1.0 (0.9–1.1)	6.4	1.3 (0.7–1.6)	12.0	2.3 (1.3–3.3)
Contracaecum margolisi	0.0		0.0		0.0		0.0		1.2	1.5*
C. rudolphii	0.0		0.0		0.0		0.0		1.8	1.0
Hysterothylacium sp.	18.7	1.3 (1.1–1.5)	19.0	1.5 (1.3–1.7)	24.9	1.4 (1.2–1.6)	9.6	1.2 (0.9–1.5)	31.5	1.5 (1.3–1.7)
Unknown nematode	0.9	1.0	2.4	1.2 (1.0–1.4)	3.2	1.2 (0.9–1.5)	2.1	1.0	3.0	1.0
TREMATODA										
Lampritrema sp.	0.0		0.0		0.0		0.5	1.0	0.0	
Lecithaster gibbosus	48.4	4.9 (3.7–6.1)	8.1	2.9 (1.8–3.0)	1.1	1.0	0.0		0.0	
Myosaccium ecaude	5.0	1.6 (0.6–2.6)	8.1	1.2 (0.8–1.6)	28.8	2.2 (1.6–3.0)	29.8	2.1 (1.6–2.6)	41.7	2.3 (1.5–3.1)
Parahemiurus merus	25.1	1.8 (1.4–2.2)	5.3	1.0 (0.9–1.1)	5.3	1.3 (0.9–1.7)	16.0	1.1 (0.9–1.3)	19.0	1.3 (1.1–1.5)
Pronoprymna petrowi	8.7	7.0 (2.8–11.2)	0.4	1.5*	0.0		0.0		0.0	
Unknown trematode	0.5	1.0	0.0		0.4	1.0	0.0		0.6	1.0
ACANTHOCEPHALA										
Rhadinorhynchus sp.	0.5	2.0	1.9	1.3 (0.9–1.7)	0.7	1.0	1.6	1.0	1.8	1.0
CESTODA										
Tetraphyllidea	0.0		0.2	1.0	0.0		0.0		0.0	
Unknown cestode	0.5	5.0	0.0		0.0		0.0		0.0	

parasites from 59.3% of the Pacific sardine sampled. The prevalence of infection (percentage of samples infected) of any parasite taxa ranged from less than 1.0% to 48.4%, and mean intensities of infection ranged from 1.0 to 7.0 individual parasites of a taxon per infected fish (Table 3).

The most abundant parasite (greatest prevalence and intensity) recovered from the Pacific sardine from any region was the trematode *Lecithaster gibbosus*. Its prevalence was highest in Pacific sardine caught off British Columbia at 48.4% infected. The highest intensity of *L. gibbosus* was 51 individual parasites in a single Pacific sardine caught off British Columbia. Although abundant in the north, this parasite was not recovered from any Pacific sardine caught off Central or Southern California. Another commonly recovered trematode, *Myosaccium ecaude*, was found at a high prevalence of 41.7% off Southern California, as well as at relatively high prevalences off Central and Northern California (29.8% and 28.8%, respectively). This trematode was also recovered in the region off Washington and Oregon and off British Columbia but at prevalences of only 8.1% and 5.0%, respectively.

Nematodes from 2 genera, *Hysterothylacium* sp. and *Anisakis* spp., were also recovered at relatively high prevalences (but low intensities) throughout the study area (Table 3). *Hysterothylacium* sp. was recovered in highest prevalence (31.5%) in Southern California. *Anisakis* spp. were recovered in highest prevalence off British Columbia and in the region off Washington and Oregon (25.1% and 24.2%, respectively), but mean intensity was slightly higher for *Anisakis* spp. in Southern California.

Northern anchovy: parasite taxa recovered and distribution patterns

A total of 7 parasite taxa were recovered from the northern anchovy (Table 4). Parasites were recovered from 60% of the northern anchovy caught off Grays Harbor, Washington, 21% of fish caught off Willapa Bay, Washington, and 69% of fish caught off Port Hueneme, California. Mean intensities of all parasite taxa were low, ranging from 1.0 to 2.0 individual parasites per infected anchovy. Although the nematodes *Anisakis* spp. and *Hysterothylacium* sp. were recovered from northern anchovy from all 3 locations, the parasite communities were significantly different (ANOSIM: global R=0.88, P<0.01). The trematode *Parahemiurus merus* was also found in all locations but at higher prevalence off Southern California at 33% infected, compared with 5% and 2% in both northern groups. An unidentified trematode belonging to the Didymozoidae was recovered exclusively from northern anchovy collected off Southern California at a prevalence of 41%. In contrast, the trematode *L. gibbosus* was recovered exclusively, and at a high prevalence of 45%, from the most northern samples collected off Grays Harbor. Pairwise ANOSIM showed that the parasite communities from the two collections of anchovy from different locations off Washington were also significantly different (ANOSIM: R=0.75, P=0.01).

Multivariate community analyses: parasites of Pacific sardine

A nonmetric MDS ordination of parasite community data averaged by size category and region shows the differences in parasite communities of all size categories of Pacific sardine from British Columbia compared with

Table 4

Prevalence (P) and mean intensity (I), with 95% confidence intervals (95% CI), of parasites recovered from northern anchovy (*Engraulis mordax*) caught off Washington (WA) in 2007 and Southern California (CA) in 2008. n=sample size. An asterisk (*) denotes that only 2 infected fish were collected.

	Grays Harbor, WA (n=20)		Willapa Bay, WA (n=97)		Port Hueneme, CA (n=51)	
Parasite taxa	P (%)	I (95% CI)	P (%)	I (95% CI)	P %	I (95% CI)
NEMATODA						
Anisakis spp.	10.0	1.5*	5.2	1.0	5.9	1.0
Hysterothylacium sp.	5.0	1.0	7.2	1.3 (0.8–1.8)	17.6	1.2 (0.7–1.7)
Unknown nematode	0.0		11.3	1.3 (0.9–1.7)	10.0	1.2 (0.6–1.8)
TREMATODA						
Lecithaster gibbosus	45.0	2.0 (0.8–3.2)	0.0		0.0	
Parahemiurus merus	5.0	1.0	2.1	1.0	33.3	1.3 (1.1–1.5)
Didymozoidae	0.0		0.0		41.2	1.8 (1.2–2.2)
CESTODA						
Tetraphyllidea	5.0	1.00	0.0		0.0	

those from all size categories from all other regions (Fig. 2A). This nonmetric MDS plot also shows the trend of the differences in parasite communities among size categories of Pacific sardine within each region, except for those from Central and Southern California.

An additional nonmetric MDS ordination includes the parasite communities of the 3 northern anchovy collections with those of Pacific sardine (Fig. 2B). Figure 2B shows the high similarity of the parasite community of northern anchovy collected off Grays Harbor to those of Pacific sardine collected off British Columbia. The parasite community of northern anchovy collected off Willapa Bay was most similar to parasite communities of Pacific sardine 200–209 and 210–219 mm SL from Washington and Oregon and of Pacific sardine 210–219 mm SL from Northern and Central California. The sample of northern anchovy collected off Port Hueneme was most similar to Pacific sardine 200–209 mm SL collected off Southern California. The overlays on this nonmetric MDS plot show clustering of all parasite communities south of British Columbia at 60% similarity and clustering in 4 groups of parasite communities at 70% similarity. The 4 groups are composed of communities recovered from 1) Pacific sardine from British Columbia and northern anchovy from off Grays Harbor, 2) northern anchovy from Southern California and Pacific sardine 200–209 mm SL from Southern California, 3) Pacific sardine <200 mm SL from all California regions and Pacific sardine 200–209 mm SL from Central California, and 4) all Pacific sardine collected from Washington and Oregon, Pacific sardine 200–209 mm SL from Northern California, all Pacific sardine 210–219 mm SL and ≥220 mm SL from California, and northern anchovy from Willapa Bay.

A 2-way PERMANOVA on Pacific sardine parasite communities showed that both region (pseudo-F=4.75) and fish size category (pseudo-F=5.12) were significant factors (P<0.01) in the main effects model. There was not a significant interaction between region and fish size (pseudo-F=0.97, P=0.50). A PERMANOVA for pairwise comparison of parasite communities showed that there was no significant difference between the parasite communities of Pacific sardine <200 mm SL and 200–209 mm SL (pseudo t=1.43, P=0.11) (data not shown). Thus, these size categories were combined into one category (<210 mm SL) in further analyses. In contrast, parasite communities from the 2 larger size categories were significantly different from those of the smaller Pacific sardine and from each other (all comparisons P<0.05) (data not shown).

Pairwise regional comparisons with PERMANOVA between the parasite communities

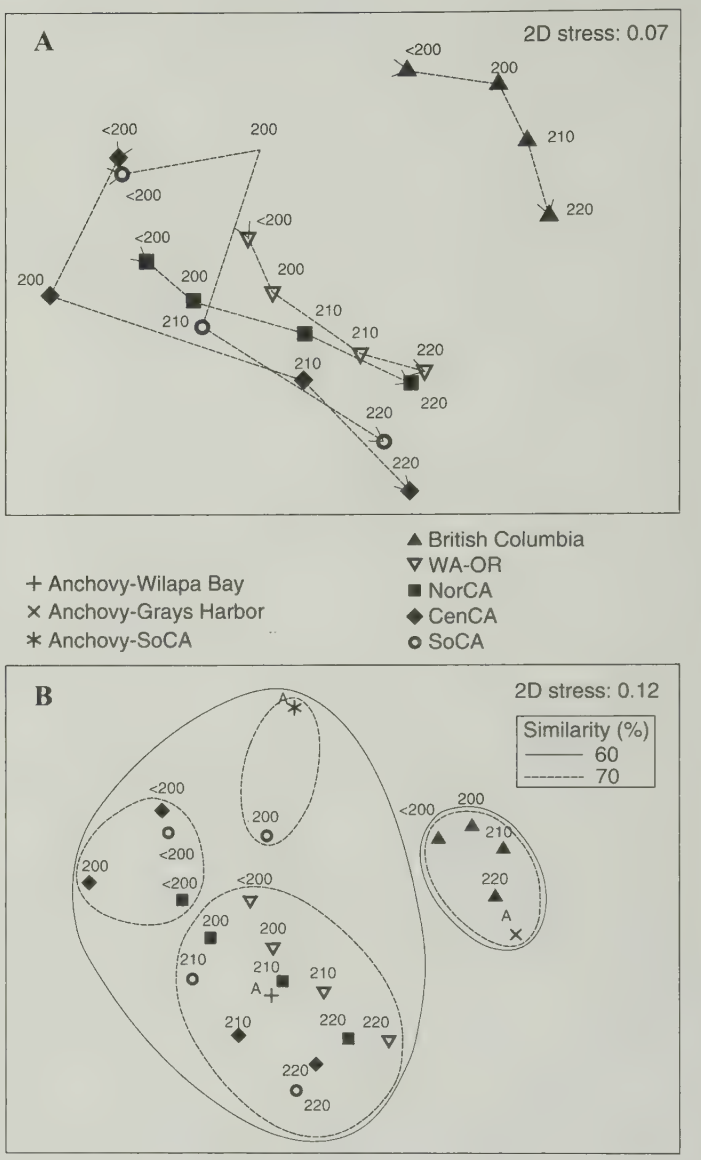

Figure 2

Nonmetric multidimensional scaling (MDS) plots of distance from centroids calculated from square-root transformed data of parasite abundance from (**A**) Pacific sardine (*Sardinops sagax*) sampled in the California Current System from 2005 through 2008, averaged by size category and region of collection (lines connect size categories within a region), and (**B**) Pacific sardine caught in 2005–2008 and northern anchovy (*Engraulis mordax*) caught off Washington in 2007 (2 sites) and Southern California in 2008 (1 site), averaged by collection location. Results of a hierarchical agglomerative clustering with similarity values of 60% and 70% are overlaid onto the plot. Symbol shapes represent regions where Pacific sardine were sampled. Sample collection occurred in 5 regions: Vancouver Island, British Columbia, Canada, Washington and Oregon (WA-OR); Northern California (NorCA), Central California (CenCA), and Southern California (SoCA). The labels *<200*, *200*, *210*, and *220* indicate the size category: <200, 200–209, 210–219, and ≥220 mm in standard length. The 2D stress value is a measure of the representation of interrelationships in a 2-dimensional ordination space, with stress <0.1 corresponding to a good interpretation and stress <0.2 providing a useful 2-dimensional picture.

of Pacific sardine from the 5 different regions were analyzed separately for the different size categories, following the results of the pairwise comparison on size categories described above. For Pacific sardine <210 mm SL (the combination of the 2 smallest size categories), the parasite communities collected off British Columbia were significantly different from those from all other sampled regions of the CCS (all comparisons: $P<0.01$) (Table 5). No other regional comparisons were statistically significant for this size category of Pacific sardine. For Pacific sardine 210–219 mm SL, the parasite communities of fish from British Columbia were significantly different from those collected off Washington and Oregon (pseudo-t=2.41, $P<0.01$) and off Northern California (pseudo-t=1.89, P=0.01). P-values for pairwise regional comparisons with PERMANOVA between Pacific sardine in this size category from British Columbia and Central and Southern California were 0.08. For Pacific sardine ≥220 mm SL, a significant difference between parasite communities was found between fish caught off British Columbia and those collected off Washington and Oregon (pseudo-t=1.71, P=0.04) (Table 5).

Because the pairwise PERMANOVA for regions showed no differences among our regions of California, we performed a CAP analysis with those regions condensed into one California region. The CAP analysis further supported significant differences among all regions for the Pacific sardine <210 mm SL (tr=0.63182, P=0.0001). The selected orthonormal PCO axes (m=3 axes) described 89% of the variation in the data cloud. Cross-validation results of this CAP model show the distinctiveness of the Pacific sardine <210 mm SL collected off British Columbia with correct allocation to their own group at 76.5% and of the Pacific sardine <210 mm SL collected off California with correct allocation to California at 82.2% (Table 6). Similar results of CAP analysis were observed with Pacific sardine 210–219 mm SL (tr=0.67626, P=0.0001) and ≥220 mm SL (tr=0.50237, P=0.0001). Correct allocations to British Columbia were 80% and 70% for these 2 size categories of large Pacific sardine when the m=3 and m=4 orthonormal PCO axes, respectively, were used. The correct allocation of Pacific sardine ≥220 mm SL back to California was also high at 80%. Correct allocations to Washington and Oregon were fewer, with assignments also going to both British Columbia and California, but were greater than the 33.3% that would be expected from chance alone, except for fish ≥220 mm SL (Table 6).

Regional differences in abundance of specific parasites observed among Pacific sardine played a differential role in defining regional parasite communities. For example, 3 trematode species, *L. gibossus*, *Pronoprymna petrowi*, and *Parahemiurus merus*, were more abundant in samples from British Columbia than in those from other regions (see shade differences presented in Figure 3). In contrast, another trematode, *M. ecaude*, had high abundance in Pacific sardine from California regions. Abundance of *Anisakis* spp. increased in concert with increasing size of Pacific sardine from all regions, but especially among large sardines collected off Central and Southern California.

In all size categories of Pacific sardine caught off British Columbia, the trematode *L. gibossus* provided the highest percent contribution to the parasite communities, from 71.5% in the Pacific sardine <210 mm SL to

Table 5

Results of pairwise comparisons with permutational multivariate analysis of variance (PERMANOVA) between parasite communities of Pacific sardine (*Sardinops sagax*) caught from 2005 through 2008 in 5 regions of the California Current System and analyzed separately by size category: <210 mm standard length (SL), 210–219 mm SL, and ≥220 mm SL. The regions are British Columbia (1), Washington and Oregon (2), Northern California (3), Central California (4), and Southern California (5). The pairwise PERMANOVA pseudo-t test statistic is a direct multivariate analogue to the univariate t-statistic. This value is provided with a permutation P-value.

	<210 mm SL		210–219 mm SL		≥220 mm SL	
Regional comparisons	Pseudo-t	P (perm)	Pseudo-t	P (perm)	Pseudo-t	P (perm)
1, 2	2.60	<0.01	2.41	<0.01	1.71	0.04
1, 3	3.69	<0.01	1.89	0.01	1.50	0.12
1, 4	3.08	<0.01	1.52	0.08	1.36	0.20
1, 5	2.85	<0.01	1.67	0.08	1.40	0.95
2, 3	1.32	0.17	0.59	0.77	0.38	0.95
2, 4	1.25	0.06	0.75	0.55	0.47	0.83
2, 5	1.66	0.22	1.18	0.24	0.53	0.75
3, 4	1.36	0.17	0.77	0.66	0.60	0.75
3, 5	1.35	0.17	0.85	0.67	0.71	0.50
4, 5	0.81	0.50	0.57	0.90	0.63	0.85

Table 6

Percentage of correct allocations of parasite communities of Pacific sardine (*Sardinops sagax*), caught from 2005 through 2008, to 3 regions of the California Current System based on cross-validation results of canonical analysis of principal coordinates. SL=standard length.

Collection location	Size category (mm SL)	British Columbia	Washington and Oregon	California	No. of sample groups	% correct
British Columbia	<210	13	3	1	17	76.5
	210–219	8	1	1	10	80.0
	≥220	14	5	1	20	70.0
Washington and Oregon	<210	5	15	14	34	44.1
	210–219	2	12	10	24	50.0
	≥220	8	9	12	29	31.0
California	<210	0	18	83	101	82.2
	210–219	1	5	5	11	45.5
	≥220	0	2	8	10	80.0

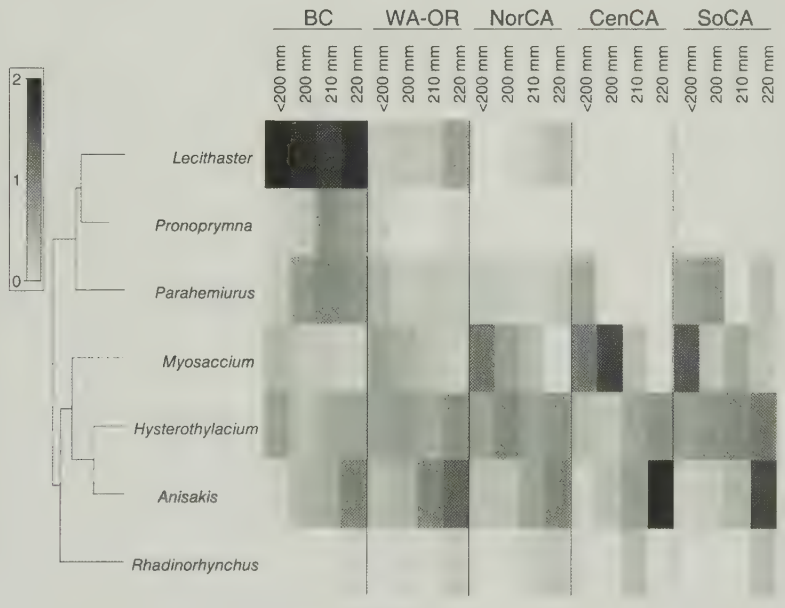

Figure 3

Shade plot of abundance of the 7 most abundant taxa of trophically transmitted parasites from Pacific sardine (*Sardinops sagax*), illustrating differences among fish size categories and regions of the California Current where Pacific sardine were sampled from 2005 through 2008. Shading intensity increases with parasite intensity on the dispersion-weighted scale (numeric values in the shade key represent the square-root of intensity). The grayscale shading in plot cells are proportional to square-rooted intensity: from white (taxon not recovered) to black (maximum intensity). Parasite taxa, displayed on the y-axis, are ordered by a cluster analysis of their mutual associations across size and region groups. Therefore, taxa exhibiting similar patterns of abundance across the averaged fish groups were clustered on the displayed y-axis dendrogram. The labels *<200 mm*, *200 mm*, *210 mm*, and *220 mm* indicate the size category: <200, 200–209, 210–219, and ≥220 mm in standard length. There are 5 regions: Vancouver Island, British Columbia (BC), Canada, Washington and Oregon (WA-OR), Northern California (NorCA), Central California (CenCA), and Southern California (SoCA).

35.9% and 40.5% in the 2 larger size categories. This parasite contributed 85.3% to the parasite communities of northern anchovy collected off Grays Harbor, and the high contribution of this parasite was responsible for the high similarity among these northern anchovy and the Pacific sardine from British Columbia.

In contrast to the Pacific sardine caught off British Columbia, Pacific sardine 210–219 mm SL and ≥220 mm SL caught off Washington and Oregon and in the regions off California had parasite communities dominated by nematodes. *Anisakis* spp. contributed over 50% to the parasite communities in both size categories of large Pacific sardine in all regions south of British Columbia. The only exception was that Pacific sardine 210–219 mm SL from Southern California were dominated by the nematode *Hysterothylacium* sp. (51.5% contribution) and the trematode *M. ecaude* (48.4% contribution).

The parasite communities from small (<210 mm SL) Pacific sardine from Washington and Oregon and northern anchovy collected off Willapa Bay were also dominated by *Hysterothylacium* sp. (44.5% and 62.6% contribution, respectively). In contrast, the small Pacific sardine collected off all regions of California were dominated by *M. ecaude*. The one exception was that Pacific sardine <210 mm SL from Southern California were dominated by another trematode, *P. merus* (63.2% contribution). The high abundance

of *P. merus* in this size category made them cluster with the northern anchovy from Southern California, where *P. merus* had a 31.2% contribution to the parasite community.

Discussion

Regional comparisons

The paradigm that when the northern stock of Pacific sardine is large and ocean conditions are favorable all Pacific sardine >200 mm SL, or some other length, migrate to northern waters and then all return to Central and Southern California seasonally each year to spawn may no longer be supported. We found that Pacific sardine were not uniformly infected with the same trophically transmitted parasite communities throughout the CCS, indicating that not all Pacific sardine of the northern subpopulation made the complete round-trip migration during the years studied. The parasite communities of all size categories of Pacific sardine collected off British Columbia were more similar to each other than to all sizes collected from any other region. The correct allocation in the CAP analysis of 70–80% of these parasite communities to British Columbia indicates that, during the years studied, a large proportion of Pacific sardine in British Columbia remained as residents, not returning to Central or Southern California to spawn. Differences among parasite communities from the region off Washington and Oregon and the 3 regions in California were not statistically significant, although a north–south trend was apparent in the nonmetric MDS plot (Fig. 2A).

Several taxa of parasites contributed to differences in the parasite communities among regions and size categories of Pacific sardine. Among these, the trematode *L. gibbosus* was recovered primarily off British Columbia from all sizes of Pacific sardine and not from any sardines examined from Central and Southern California. In contrast, the trematode *M. ecaude* was recovered in greatest abundances in small Pacific sardine from California regions and only from 5% of Pacific sardine collected in British Columbia. The parasite communities recovered from California regions also had higher abundances of the nematode *Hysterothylacium* sp. than those collected off British Columbia. Distinct distributional patterns of these parasites indicate that not all Pacific sardine of the northern stock make an annual roundtrip migration connecting the terminal regions of their habitat.

Regional differences in the parasite communities of Pacific sardine are supported by observed regional differences among parasite communities of northern anchovy. This other small, pelagic species generally harbors parasite species known to infect the Pacific sardine (Love and Moser, 1983), and, as a non-migratory species (Bakun, 1996), northern anchovy should host parasite species present in a local geographical area. We found a significant difference among the parasite communities of all 3 northern anchovy collections, a finding that agrees with the distributions of parasites recovered from Pacific sardine. The parasite community of northern anchovy collected from Grays Harbor had high similarity to those of Pacific sardine from British Columbia and supported a restricted northern distribution of *L. gibbosus* in the CCS. The northern anchovy from Southern California (part of the central subpopulation of northern anchovy) had a higher prevalence of *Hysterothylacium* sp., similar to the Pacific sardine collected there.

Parasites as biological tags

Parasite life span and life history are important considerations for selecting parasite taxa as biological tags (MacKenzie and Abaunza, 1998, 2014). The parasite communities of Pacific sardine in this study included both long-lived nematodes and shorter-lived trematodes. The maximum life span of the trematode *L. gibbosus* was reported to be 1–9 months in pink (*Oncorhynchus gorbuscha*) and chum (*O. keta*) salmon captured off central British Columbia (Margolis and Boyce, 1969). We recovered both mature and immature *L. gibbosus* in Pacific sardine off British Columbia from March through November, but we recovered none off Southern California, not even among April samples that were thought to include returns from British Columbia. The complete absence of *L. gibbosus* in our samples of large Pacific sardine caught off Southern California could be interpreted 3 ways: 1) our samples from Southern California were not representative of the Pacific sardine in the region at the time, 2) Pacific sardine did not return from British Columbia to Southern California, or 3) the life span of *L. gibbosus* is too short to be recovered after a return migration south. However, given that some of the *L. gibbosus* specimens recovered off British Columbia in November were still immature, their life span would have to be less than 5–6 months if this was the only reason for their absence from Pacific sardine caught in Southern California the following April.

The other trematode that contributed to differences in parasite communities among regions was *M. ecaude*. Unfortunately, little information is available on the distribution and life history of this species in the CCS. However, we have confidence that this trematode and *L. gibbosus* have sufficiently long life spans to evaluate seasonal movements of their fish hosts. In the CCS, *M. ecaude* has been previously reported from Pacific sardine caught off Baja California, Mexico (Sánchez-Serrano and Cáceres-Martínez, 2017), off Southern California (Montgomery, 1957; Kunnenkeri, 1962), and off southern Oregon (Jacobson et al., 2012). These reports and our observations of the high abundance of this parasite in small Pacific sardine in Central and Southern California compared to other regions and size classes of Pacific sardine suggest that the southern region of the CCS is likely the primary region of parasite transmission. However, the recovery of *M. ecaude* from a small percentage of Pacific sardine <200 mm SL caught off British Columbia (9%) and off Washington and Oregon

(10%) indicates that either transmission of the parasite occurs on a small scale in northern regions of the CCS or a very small number of Pacific sardine <200 mm SL made the migration north. Moreover, the recovery of only 7 Pacific sardine infected with both *L. gibbosus* and *M. ecaude* and of only 3 Pacific sardine ≥200 mm SL in Northern California infected with *L. gibbosus* indicates that a complete migration to and from British Columbia, or even Washington and Oregon, for all migratory-size Pacific sardine did not occur during the years of our study.

Other parasites recovered from Pacific sardine that contributed to differences among regions include the nematodes and the acanthocephalan that are both long-lived taxa. For example, *Anisakis* nematodes, which mature in cetaceans, accumulate as long-lived larvae in fish intermediate hosts and have been successfully used as biological tags for many fish populations (MacKenzie, 2002; Mattiucci et al., 2008; Mattiucci and Nascetti, 2008). In our study, there was also a greater abundance of *Anisakis* spp. in large Pacific sardine recovered off Central and Southern California, possibly because of a greater abundance of the definitive whale hosts in these regions of the CCS (Calambokidis and Barlow, 2004). Genetic identification of larval anisakids from a subset of Pacific sardine used in our study revealed a panmictic distribution of 3 populations of *Anisakis* spp., but these populations could not help inform stock structure or migration behavior of Pacific sardine in the CCS (Baldwin et al., 2011). The acanthocephalan *Rhadinorhynchus trachuri*, also longer-lived than the trematodes, is known to be a parasite of offshore fish species (George-Nascimento, 2000; Jacobson et al., 2012). Although less commonly recovered than the nematodes, it was recovered more often from the large Pacific sardine caught south of British Columbia. Its low abundance in large Pacific sardine from British Columbia indicates that fewer of these fish had been offshore compared with those from other regions, another line of evidence for residency in waters of British Columbia.

The spatial distributions of parasites in marine fish species have often reflected large geographical patterns such as latitudinal gradients (Blaylock et al., 1998; González and Poulin, 2005; González et al., 2006). A combination of environmental gradients and dispersal limitation of hosts and different developmental stages of parasites contribute to the latitudinal distribution of marine parasites (Oliva and González, 2005; González et al., 2006; González et al., 2008; Timi et al., 2010). For Pacific halibut (*Hippoglossus stenolepis*), a general north–south cline of parasite species distributions has been described from the Aleutian Islands, Alaska, to Northern California (Blaylock et al., 1998). Separate stocks of Pacific halibut, with some overlapping migration patterns, were confirmed by using their parasite communities, but one continuous stock was identified south of the Queen Charlotte Islands of British Columbia (Blaylock et al., 2003). Similarly, in our study, the distributional patterns of parasites showed high residency in British Columbia and an overlapping migration pattern for Pacific sardine south of British Columbia with a potential latitudinal gradient (Fig. 2A).

In the eyes of fish collected off South Africa, where this species is known as the South African sardine, Weston et al. (2015) found a significant difference in the abundance of a "tetracotyle" type larval trematode, tentatively identified as *Cardiocephaloides* sp. (Reed et al., 2012), and that difference supports the existence of a putative western and a putative southern stock with some degree of mixing. After 6 years of continuous data on the prevalence of this larval trematode from the west and south coasts of South Africa, de Moor et al. (2017) fit a sardine stock assessment model directly to parasite prevalence-by-length data and found that this inclusion of parasitological data improved estimates of annual movement and mixing between these semi-discrete stocks.

Migration north

Following the early tagging studies (Clark and Janssen, 1945), it has been assumed that Pacific sardine ≥200 mm SL, which are capable of migrating (Lo et al., 2011), migrate north from Southern California in the spring when ocean conditions in the north are favorable. We found no significant differences between the parasite communities of Pacific sardine <200 mm SL and those of Pacific sardine 200–209 mm SL, indicating that there is not a clear cut off at 200 mm SL at which a Pacific sardine will migrate. A recent paper by McDaniel et al. (2016) that included size and age data for Pacific sardine from British Columbia, Oregon and Washington, and Central and Southern California during 1981–2010 described a pattern of increasing age at length with distance from Southern California. They concluded that their results provide evidence that the migration of the northern subpopulation of the Pacific sardine to the northern reaches of their range in summer is age based, instead of length based.

Sardine biomass and length data from surveys that combined data from acoustic and trawl sampling and were conducted in the spring and summer of 2008 indicate that most, if not the entire, northern stock of Pacific sardine migrated from offshore waters of Southern California to inshore waters of the PNW and British Columbia (Demer et al., 2012). Unfortunately, we did not collect Pacific sardine from British Columbia in 2008, but our results from other years do not support the conclusion that the entire stock migrates that far north. Although our parasite community analysis was suggestive of a statistically significant difference only between the Washington and Oregon region and the Central California region for Pacific sardine <210 mm SL (pairwise PERMANOVA: P=0.06), the greater abundance of *M. ecaude* in Pacific sardine <210 mm SL in all California regions compared with that of the Pacific sardines from Washington and Oregon (Fig. 3) indicates that a proportion of Pacific sardine up to 210 mm SL may remain as residents in their natal regions. In addition, our samples of Pacific sardine ≥220 mm SL caught off Central and

Southern California in the spring had a greater abundance of the long-lived nematodes *Hysterothylacium* sp. and *Anisakis* spp. than those caught off Washington and Oregon and British Columbia in summer and fall. If the entire biomass of large Pacific sardine were migrating north, we would have expected to see the same abundance of these long-lived parasites throughout the CCS.

Return migration south

Lo et al. (2011) estimated different length-specific migration rates in 2003–2005 between the PNW and California and estimated that close to 50% of Pacific sardine 200–210 mm SL and close to 100% of Pacific sardine ≥220 mm SL migrated back to California in the fall and winter of 2003 and 2004. Similar to our conclusions, they questioned whether fish <200 mm SL remained as residents in the PNW because they had only weak evidence that some of these small fish returned to California. They concluded that not all Pacific sardine migrate and that some stay in the PNW and California (their study did not include British Columbia). Our results indicate that a high proportion of Pacific sardine of all size classes remained in waters of Canada during the period of our study and that waters off Washington and Oregon could be an area of mixing between regions for large Pacific sardine but could also support local recruitment.

In the McDaniel et al. (2016) study, Pacific sardine from British Columbia and from Oregon and Washington collected from July through December were older than those from Central and Southern California. They did not have data from January through March, and age and length data from April through June were presented only for California catches, but the ages of the largest and oldest Pacific sardine from California at all seasons were still younger than those from Oregon and Washington and from British Columbia. Although they state that their work assumed a single migrating population and that subpopulation structure could compromise their results of an age-based migration, they do not account for the difference in maximum ages between locations except for the unlikelihood of gear selectivity or different aging techniques. Our results indicate not only that they could indeed have documented age-based migration but also that their results could additionally reveal residency of fish in northern regions of the CCS, in contrast to the notion of a single migrating population. Similarly, Dorval et al. (2015) reported a reduction in the size distribution of Pacific sardine caught off California during 2005–2010 compared with that in 1996–2004. The larger size classes (250 and 260 mm SL) present in the survey conducted in spring 2004 off California were not recorded again during the 2005–2010 survey (Dorval et al., 2015). They speculated that Pacific sardine >250 mm SL that did not return after a northern migration either remained in the north or were removed by fishing. These observations are not the first to suggest overwintering of Pacific sardine in northern regions of the CCS, as spawning had previously been reported in 1998 and 2004 in waters of Canada (McFarlane et al., 2005) and during 1994–1998 and 2003–2004 in the PNW (Bentley et al., 1996; Emmett et al., 2004).

Management implications

Migration rates (the percentages of the population moving into other regions) are an important factor for managing transboundary fish stocks like the northern stock of Pacific sardine. Schweigert et al.[5] estimated annual migration rates to British Columbia on the basis of differences in biomass of Pacific sardine caught during surveys conducted off the west coast of Vancouver Island and the total biomass estimate for the coast-wide population as presented by Hill et al.[6] in the annual U.S. sardine assessment. During the years of our study, Schweigert et al.[5] estimated an average migration rate of 27.2% in 2006 and 34.7% in 2008. Their survey was not conducted in 2007, and in 2005 it was an incomplete survey from which they estimated a 13.2% annual migration rate. The significant differences among parasite communities of Pacific sardine from British Columbia and of those from all other regions indicate that the relatively large biomass (>200,000 metric tons, Schweigert et al.[5]) found off the coast of Vancouver Island in those years consisted of a large proportion of Pacific sardine that remained as residents of British Columbia waters as well as migrants from the southern regions.

The examination of allozymes among Pacific sardine from regions of Mexico and California (Hedgecock et al., 1989) and of mitochondrial DNA throughout the CCS (Lecomte et al., 2004) and among Mexican regions (García-Rodríguez et al., 2011) provides evidence for no genetic stock structure in the CCS. However, although Lecomte et al. (2004) state that their mitochondrial DNA data support a basin modal for the Pacific sardine in which a species distribution contracts to a central optimal range during population crashes, they also state that on shorter time scales local recruitment may dominate. At this time, our parasite data from Pacific sardine cannot provide quantitative information on migration rates, nor do they indicate distinct stock structure, but they do elucidate patterns of migration, residency, and periodic local recruitment and indicate that a greater variability in annual migratory behavior of Pacific sardine should be considered. A holistic inclusion of multidisciplinary approaches and techniques (as reviewed in Baldwin et al., 2012; Catalano et al., 2014; Pita et al., 2016) that advances our understanding of economically and ecologically important species should improve management of Pacific sardine, even in the

[5] Schweigert, J., G. McFarlane, and V. Hodes. 2010. Pacific sardine (*Sardinops sagax*) biomass and migration rates in British Columbia. Dep. Fish. Oceans, Can. Sci. Advis. Secr. Res. Doc. 2009/088, 13 p. [Available from website.]

[6] Hill, K. T., E. Dorval, N. C. H. Lo, B. J. Macewicz, C. Show, and R. Felix-Uraga. 2008. Assessment of the Pacific sardine resource in 2008 for U.S. management in 2009, 147 p. Agenda item G.2.b., Suppl. attach. 1. Pacific Fish. Manage. Counc., Portland, OR. [Available from website.]

absence of genetically distinct stock isolation. Examination of multiple biological metrics of Pacific sardine with testing of habitat prediction models should help elucidate migration patterns and improve estimates of migration. A new perspective of greater interannual and seasonal variability in behavior of Pacific sardine will also likely benefit future research efforts and fisheries management.

Acknowledgments

We dedicate this manuscript to our inspirational coauthor and good friend B. Emmett, who lost a battle against cancer prior to publication. We thank, for their assistance, individuals from the NOAA Northwest and Southwest Fisheries Science Centers, Oregon State University, the Scripps Institution of Oceanography, Fisheries and Oceans Canada, and the Pacific sardine fishing industry. Funding was provided by the National Marine Fisheries Service and by the Mamie Markham Research and Walter G. Jones Fisheries Development Awards to R. Baldwin.

Literature cited

Anderson, M. J.
2001. A new method for non-parametric multivariate analysis of variance. Austral Ecol. 26:32–46.

Anderson, M. J., and J. Robinson.
2003. Generalized discriminant analysis based on distances. Aust. N.Z. J. Stat. 45:301–318.

Anderson, M. J., R. N. Gorley, and K. R. Clarke.
2008. PERMANOVA+ for PRIMER: guide to software and statistical methods, 214 p. PRIMER-e, Plymouth, UK.

Arthur, J. R., and E. Albert.
1994. A survey of the parasites of Greenland halibut (*Reinhardtius hippoglossoides*) caught off Atlantic Canada, with notes on their zoogeography in this fish. Can. J. Zool. 72:765–778.

Bakun, A.
1996. Patterns in the ocean: ocean processes and marine population dynamics, 323 p. Calif. Sea Grant Coll. Syst., Univ. Calif., La Jolla, CA.

Baldwin, R. E., and C. P. Goater.
2003. Circulation of parasites among fishes from lakes in the Caribou Mountains, Alberta, Canada. J. Parasitol. 89:215–225.

Baldwin, R. E., T. W. Miller, R. D. Brodeur, and K. C. Jacobson.
2008. Expanding the foraging history of juvenile Pacific salmon: combining stomach-content and macroparasite-community analyses for studying marine diets. J. Fish Biol. 72:1268–1294.

Baldwin, R. E., M. B. Rew, M. L. Johansson, M. A. Banks, and K. C. Jacobson.
2011. Population structure of three species of *Anisakis* nematodes recovered from Pacific sardines (*Sardinops sagax*) distributed throughout the California Current System. J. Parasitol. 97:545–554.

Baldwin, R. E., M. A. Banks, and K. C. Jacobson.
2012. Integrating fish and parasite data as a holistic solution for identifying the elusive stock structure of Pacific sardines (*Sardinops sagax*). Rev. Fish Biol. Fish. 22:137–156.

Bentley, P. J., R. L. Emmett, N. C. H. Lo, and H. G. Moser.
1996. Egg production of Pacific sardine (*Sardinops sagax*) off Oregon in 1994. CalCOFI Rep. 37:193–200.

Blaylock, R. B., L. Margolis, and J. C. Holmes.
1998. Zoogeography of the parasites of Pacific halibut (*Hippoglossus stenolepis*) in the northeast Pacific. Can. J. Zool. 76:2262–2273.
2003. The use of parasites in discriminating stocks of the Pacific halibut (*Hippoglossus stenolepis*) in the northeast Pacific. Fish. Bull. 101:1–9.

Bray, J. R., and J. T. Curtis.
1957. An ordination of the upland forest communities of southern Wisconsin. Ecol. Monogr. 27:325–349.

Bush, A. O., K. D. Lafferty, J. M. Lotz, and A. W. Shostak.
1997. Parasitology meets ecology on its own terms: Margolis et al. revisited. J. Parasitol. 83:575–583.

Calambokidis, J., and J. Barlow.
2004. Abundance of blue and humpback whales in the eastern North Pacific estimated by capture-recapture and line-transect methods. Mar. Mamm. Sci. 20:63–85.

Catalano, S. R., I. D. Whittington, S. C. Donnellan, and B. M. Gillanders.
2014. Parasites as biological tags to assess host population structure: guidelines, recent genetic advances and comments on a holistic approach. Int. J. Parasitol: Parasites Wildl. 3:220–226.

Clark, F. N., and J. F. Janssen.
1945. Movements and abundance of the sardine as measured by tag returns. *In* Results of tagging experiments in California waters on the sardine (*Sardinops caerulea*). Calif. Dep. Fish Game, Fish Bull. 61, p. 7–42. [Available from website].

Clarke, K. R., and R. H. Green.
1988. Statistical design and analysis for a 'biological effects' study. Mar. Ecol. Prog. Ser. 46:213–226.

Clarke, K. R., and R. N. Gorley.
2015. PRIMER v7: user manual/tutorial, 296 p. PRIMER-e, Plymouth, UK.

Clarke, K. R., P. J. Somerfield, and M. G. Chapman.
2006. On resemblance measures for ecological studies, including taxonomic dissimilarities and a zero-adjusted Bray–Curtis coefficient for denuded assemblages. J. Exp. Mar. Biol. Ecol. 330:55–80.

Clarke, K. R., R. N. Gorley, P. J. Somerfield, and R. M. Warwick.
2014a. Change in marine communities: an approach to statistical analysis and interpretation, 3rd ed., 260 p. PRIMER-e, Plymouth, UK.

Clarke, K. R., J. R. Tweedley, and F. J. Valesini.
2014b. Simple shade plots aid better long-term choices of data pre-treatment in multivariate assemblage studies. J. Mar. Biol. Assoc. U.K. 94:1–16.

Cury, P., A. Bakun, R. J. M. Crawford, A. Jarre, R. A. Quiñones, L. J. Shannon, and H. M. Verheye.
2000. Small pelagics in upwelling systems: patterns of interaction and structural changes in "wasp-waist" ecosystems. ICES J. Mar. Sci. 57:603–618.

de Moor, C. L., D. S. Butterworth, and C. D. van der Lingen.
2017. The quantitative use of parasite data in multistock modelling of South African sardine (*Sardinops sagax*). Can. J. Fish. Aquat. Sci. 74:1895–1903.

Demer, D. A., J. P. Zwolinski, K. A. Byers, G. R. Cutter, J. S. Renfree, T. S. Sessions, and B. J. Macewicz.
2012. Prediction and confirmation of seasonal migration of Pacific sardine (*Sardinops sagax*) in the California Current Ecosystem. Fish. Bull. 110:52–70.

Dorval, E., J. D. McDaniel, B. J. Macewicz, and D. L. Porzio.
2015. Changes in growth and maturation parameters of Pacific sardine *Sardinops sagax* collected off California during a period of stock recovery from 1994 to 2010. J. Fish Biol. 87:286–310.

Emmett, R. L., R. D. Brodeur, and P. M. Orton.
2004. The vertical distribution of juvenile salmon (*Oncorhynchus* spp.) and associated fishes in the Columbia River plume. Fish. Oceanogr. 13:392-402.

Emmett, R. L., R. D. Brodeur, T. W. Miller, S. S. Pool, P. J. Bentley, G. K. Krutzikowsky, and J. McCrae.
2005. Pacific sardine (*Sardinops sagax*) abundance, distribution, and ecological relationships in the Pacific Northwest. CalCOFI Rep. 46:122–143.

García-Rodríguez, F. J., S. A. García-Gasca, J. De La Cruz-Agüero, and V. M. Cota-Gómez.
2011. A study of the population structure of the Pacific sardine *Sardinops sagax* (Jenyns, 1842) in Mexico based on morphometric and genetic analyses. Fish. Res. 107:169–176.

George-Nascimento, M.
2000. Geographical variations in the jack mackerel *Trachurus symmetricus murphyi* populations in the southeastern Pacific Ocean as evidenced from the associated parasite communities. J. Parasitol. 86:929–932.

González, M. T., and R. Poulin.
2005. Nested patterns in parasite component communities of a marine fish along its latitudinal range on the Pacific coast of South America. Parasitology 131:569–577.

González, M. T., C. Barrientos, and C. A. Moreno.
2006. Biogeographical patterns in endoparasite communities of a marine fish (*Sebastes capensis* Gmelin) with extended range in the Southern Hemisphere. J. Biogeogr. 33:1086–1095.

González, M. T., R. Vásquez, and E. Acuña.
2008. Biogeographic patterns of metazoan parasites of the bigeye flounder, *Hippoglossina macrops*, in the Southeastern Pacific coast. J. Parasitol. 94:429–435.

Hargreaves, N. B., D. M. Ware, and G. A. McFarlane.
1994. Return of Pacific sardine (*Sardinops sagax*) to the British Columbia coast in 1992. Can. J. Fish. Aquat. Sci. 51:460–463.

Hart, J. L.
1943. Tagging experiments on British Columbia pilchards. J. Fish. Res. Board Can. 6 b:164–182.

Hedgecock, D., E. S. Hutchinson, G. Li, F. L. Sly, and K. Nelson.
1989. Genetic and morphometric variation in the Pacific sardine, *Sardinops sagax caerulea*: comparisons and contrasts with historical data and with variability in the northern anchovy, *Engraulis mordax*. Fish. Bull. 87:653–671.

Herrick, S. F., J. G. Norton, R. Hannesson, U. R. Sumaila, M. Ahmed, and J. Pena-Torres.
2009. Global production and economics. *In* Climate change and small pelagic fish (D. Checkley, J. Alheit, Y. Oozeki, and C. Roy, eds.), p. 256–284. Cambridge Univ. Press, New York.

Hill, K. T., N. C. H. Lo, B. J. Macewicz, P. R. Crone, and R. Felix-Uraga.
2010. Assessment of the Pacific sardine resource in 2010 for U.S. management in 2011. NOAA Tech. Memo. NMFS-SWFSC-469, 137 p.

Jacobsen, J. A., and L. P. Hansen.
2005. Internal and external tags. *In* Stock identification methods: applications in fishery science (S. X. Cadrin, K. D. Friedland, and J. R. Waldman, eds.), p. 415–433. Elsevier, Burlington, MA.

Jacobson, K. C., R. E. Baldwin, and D. C. Reese.
2012. Parasite communities indicate effects of cross-shelf distributions, but not mesoscale oceanographic features on northern California Current mid-trophic food web. Mar. Ecol. Prog. Ser. 454:19–36.

Javor, B.
2013. Do shifts in otolith morphology of young Pacific sardine (*Sardinops sagax*) reflect changing recruitment contributions from northern and southern stocks? CalCOFI Rep. 54:85–96.

Javor, B., and E. Dorval.
2014. Geography and ontogeny influence the stable oxygen and carbon isotopes of otoliths of Pacific sardine in the California Current. Fish. Res. 154:1–10.

Javor, B., N. Lo, and R. Vetter.
2011. Otolith morphometrics and population structure of Pacific sardine (*Sardinops sagax*) along the west coast of North America. Fish. Bull. 109:402–415.

Kunnenkeri, J. K.
1962. Preliminary report on the parasites of the California sardine and the parasitic distribution in Clupeidae. J. Parasitol. 48:149.

Lecomte, F., W. S. Grant, J. J. Dodson, R. Rodríguez-Sánchez, and B. W. Bowen.
2004. Living with uncertainty: genetic imprints of climate shifts in East Pacific anchovy (*Engraulis mordax*) and sardine (*Sardinops sagax*). Mol. Ecol. 13:2169–2182.

Lo, N. C. H., B. J. Macewicz, and R. L. Charter.
2007. Spawning biomass of Pacific sardine (*Sardinops sagax*) off California in 2007. NOAA Tech. Memo. NMFS-SWFSC-411, 31 p.

Lo, N. C. H., B. J. Macewicz, and D. A. Griffith.
2010. Biomass and reproduction of Pacific sardine (*Sardinops sagax*) off the Pacific northwestern United States, 2003–2005. Fish. Bull. 108:174–192.
2011. Migration of Pacific sardine (*Sardinops sagax*) off the west coast of the United States in 2003–2005. Bull. Mar. Sci. 87:395–412.

Love, M. S., and M. Moser.
1983. A checklist of parasites of California, Oregon, and Washington marine and estuarine fishes. NOAA Tech. Rep. NMFS SSRF-777, 576 p.

MacKenzie, K.
2002. Parasites as biological tags in population studies of marine organisms: an update. Parasitology 124:153–163.

MacKenzie, K., and P. Abaunza.
1998. Parasites as biological tags for stock discrimination of marine fish: a guide to procedures and methods. Fish. Res. 38:45–56.
2014. Parasites as biological tags. *In* Stock identification methods, 2nd ed. (S. X. Cadrin, L. A. Kerr, and S. Mariani), p. 185–203. Elsevier, London.

Margolis, L., and N. P. Boyce.
1969. Life span, maturation, and growth of two Hemiurid trematodes, *Tubulovesicula lindbergi* and *Lecithaster gibbosus*, in Pacific salmon (Genus *Oncorhynchus*). J. Fish. Res. Board Can. 26:893–907.

Mattiucci, S., and G. Nascetti.
2008. Chapter 2. Advances and trends in the molecular systematics of anisakid nematodes, with implications for their evolutionary ecology and host—parasite co-evolutionary processes. Adv. Parasitol. 66:47–148.

Mattiucci, S., V. Farina, N. Campbell, K. MacKenzie, P. Ramos, A. L. Pinto, P. Abaunza, and G. Nascetti.
2008. *Anisakis* spp. larvae (Nematoda: Anisakidae) from Atlantic horse mackerel: their genetic identification and use as biological tags for host stock characterization. Fish. Res. 89:146–151.

McDaniel, J., K. Piner, H.-H. Lee, and K. Hill.
2016. Evidence that the migration of the northern subpopulation of Pacific sardine (*Sardinops sagax*) off the West Coast of the United States is age-based. PLoS ONE 11(11):e0166780.

McFarlane, G. A., J. Schweigert, L. MacDougall, and C. Hrabok.
2005. Distribution and biology of Pacific sardines (*Sardinops sagax*) off British Columbia, Canada. CalCOFI Rep. 46:144–160.

Montgomery, W. R.
1957. Studies on digenetic trematodes from marine fishes of La Jolla, California. Trans. Am. Microsc. Soc. 76:13–36.

Oliva, M. E., and M. T. González.
2005. The decay of similarity over geographical distance in parasite communities of marine fishes. J. Biogeogr. 32:1327–1332.

Pita, A., J. Casey, S. J. Hawkins, M. R. Villarreal, M.-J. Gutiérrez, H. Cabral, F. Carocci, P. Abaunza, S. Pascual, and P. Presa.
2016. Conceptual and practical advances in fish stock delineation. Fish. Res. 173:185–193.

Radovich, J.
1981. The collapse of the California sardine fishery. *In* Resource management and environmental uncertainty: lessons from coastal upwelling fisheries (M. H. Glantz and J. D. Thompson, eds.), p. 107–136. John Wiley & Sons, New York.

Reed, C., K. MacKenzie, and C. D. Van der Lingen.
2012. Parasites of South African sardines, *Sardinops sagax*, and an assessment of their potential as biological tags. Bull. Eur. Assoc. Fish Pathol. 32:41–48.

Rohde, K.
1984. Zoogeography of marine parasites. Helgol. Meeresunters. 37:35–52.

Sánchez-Serrano, S., and J. Cáceres-Martínez.
2017. First helminthological record of the Monterey sardine *Sardinops sagax* from Baja California, Mexico, gathered during two seasons. Hidrobiológica 27:1–11.

Smith, P. E.
2005. A history of proposals for subpopulation structure in the Pacific sardine (*Sardinops sagax*) population off western North America. CalCOFI Rep. 46:75–82.

Thomas, F., O. Verneau, T. de Meeûs, and F. Renaud.
1996. Parasites as host evolutionary prints: insights into host evolution from parasitological data. Int. J. Parasitol. 26:677–686.

Timi, J. T., and K. MacKenzie.
2015. Parasites in fisheries and mariculture. Parasitology 142:1–4.

Timi, J. T., A. L. Lanfranchi, and J. L. Luque.
2010. Similarity in parasite communities of the teleost fish *Pinguipes brasilianus* in the southwestern Atlantic: infracommunities as a tool to detect geographical patterns. Int. J. Parasitol. 40:243–254.

Weston, L. F., C. C. Reed, M. Hendricks, H. Winker, and C. D. van der Lingen.
2015. Stock discrimination of South African sardine (*Sardinops sagax*) using a digenean parasite biological tag. Fish. Res. 164:120–129.

Wolf, P.
1992. Recovery of the Pacific sardine and the California sardine fishery. CalCOFI Rep. 33:76–86.

Zorica, B., V. Čikes Keč, O. Vidjak, I. Mladineo, and D. Ezgeta Balič.
2015. Feeding habits and helminth parasites of sardine (*S. pilchardus*) and anchovy (*E. encrasicolus*) in the Adriatic Sea. Mediterr. Mar. Sci. 17:216–229.

National Marine Fisheries Service
NOAA

Fishery Bulletin
established in 1881

Spencer F. Baird
First U.S. Commissioner of Fisheries and founder of *Fishery Bulletin*

Experimental analyses of the mechanisms leading to American lobster (*Homarus americanus*) ventless trap saturation

Winsor H. Watson III (contact author)[1]
Elizabeth Morrissey[2]
Stephanie Sykes[1]
Abigail S. Clark[3]
Steven Jury[4]

Email address for contact author: win@unh.edu

[1] Department of Biological Sciences
School of Marine Sciences and Ocean Engineering
University of New Hampshire
46 College Road
Durham, New Hampshire 03824

[2] Marine Institute
Memorial University of Newfoundland
155 Ridge Road
St. John's, Newfoundland, Canada A1C 5R3

[3] International Center for Coral Reef Research and Restoration
Mote Marine Laboratory
24244 Overseas Highway
Summerland Key, Florida 33042

[4] Department of Biology
Saint Joseph's College
278 Whites Bridge Road
Standish, Maine 04084

Abstract—Ventless lobster traps are now widely used to assess the abundance of American lobsters (*Homarus americanus*). However, catch in ventless traps plateaus after 24 h (trap saturation), possibly influencing abundance estimates. This study addressed 3 mechanisms that may cause ventless trap saturation: 1) traps retain so many lobsters that, over time, fewer lobsters are available to catch; 2) as lobsters accumulate in traps, they inhibit entry of additional lobsters and; 3) bait quality deteriorates over time and loses its attractiveness. We found that 1) the number of lobsters in the vicinity of traps did not change after a 24-h soak; 2) stocking traps with lobsters before deployment lowered subsequent catch, while removing the lobsters captured after 24 h led to an increase in catch after 48 h; 3) when fresh bait was added to traps that had been fished for 24 h, entry rate immediately increased; 4) if "old" bait was used, catch after 24 h was less than in traps fished with fresh bait; and 5) amino acid attractants in bait declined after the first 6–24 h. Thus, ventless traps appear to saturate due to a combination of loss of bait attractiveness and the interactions between lobsters as they accumulate in traps.

Manuscript submitted 6 September 2018.
Manuscript accepted 25 July 2019.
Fish. Bull. 117:211–219 (2019).
Online publication date: 15 August 2019.
doi: 10.7755/FB.117.3.8

The views and opinions expressed or implied in this article are those of the author (or authors) and do not necessarily reflect the position of the National Marine Fisheries Service, NOAA.

The American lobster (*Homarus americanus*) represents one of the most lucrative fisheries in the United States and Canada, and, therefore, effective management is imperative. This requires accurate monitoring of the abundance of lobsters, of all sizes and sexes, so that declines and distribution shifts, such as the changes that have recently occurred in Southern New England (ASMFC[1]), can be detected and management options can be considered. However, one of the challenges inherent in using the standard traps employed by the industry to assess resident lobster populations is that they are designed to capture the larger adults; thus, many of the animals that enter them ultimately escape, especially those that are sublegal (Jury et al., 2001; Barber and Cobb, 2009; Boutson et al., 2009; Weiss, 2010; Sturdivant and Clark, 2011; Broadhurst, et al., 2014).

To address this problem, and improve the quality of the data used for stock assessments, in 2006 the coast-wide ventless trap survey was initiated (see ASMFC, 2015, for details). Ventless traps retain most of the sublegal lobsters that would otherwise escape because the escape vents that are typically present in standard (vented)

[1] ASMFC (Atlantic States Marine Fisheries Commission). 2010. Recruitment failure in the Southern New England lobster stock, 30 p. [Available from website.]

traps are covered or disabled. As a result, the number of lobsters captured per unit of time by these traps can be significantly greater than standard traps, and the size distribution more accurately represents the population on the seafloor (Courchene and Stokesbury, 2011). This leads to a better relationship between catch in ventless traps and the density of lobsters on the bottom than with standard, vented traps (Watson and Jury, 2013). Nevertheless, we recently demonstrated that the catch in ventless traps reaches a plateau, or "saturates," after soak times of ≤24 h, even though survey soak times are typically >3 days (Clark et al., 2015). This could influence estimates of lobster abundance, especially in areas where the density is high. In their 2015 report, in recognition of this concern, the Atlantic States Marine Fisheries Commission (ASMFC) stated that it was a high priority to conduct further research to help "calibrate" the relationship between ventless trap catch and the density of lobsters on the bottom because "ventless traps may be limited in their ability to differentiate between moderately high and extremely high abundance" (ASMFC, 2015).

Trap saturation, defined by Miller (1979) as a decrease in catch rate with increasing numbers of lobsters in a trap, is a common phenomenon for many types of traps used in a variety of fish and crustacean fisheries (Miller, 1990; Fogarty and Addison, 1997; Stoner, 2004; Hedgärde et al., 2016). In one of the first studies addressing this phenomenon, the "saturation effect" was observed in squirrelfish (*Holocentrus adscensionis*) and sablefish (*Anoplopoma fimbria*) pots, and it appeared to be due to a decrease in entry rate as soak time increased (High and Beardsley, 1970). In 1985, Auster demonstrated the asymptotic nature of catch of American lobsters in standard traps over 6–7-day soaks. In 1996, Miller and Rodger reported that standard lobster traps saturated within 12 h of being deployed. Furthermore, Fogarty and Addison (1997) modeled the effects of multiple variables on standard trap saturation and these models, which included variables associated with entry rate, escape rate, and changes in these variables over time, yielded data that compared favorably with Auster's (1985) data. More recently, using a trap-mounted time-lapse video system, we demonstrated that ventless traps saturate in ≤24 h because they reach a dynamic equilibrium where entry and escape rates are equivalent (Clark et al., 2018). Because the escape rate is low in ventless traps, variability in entry rate is likely a key factor that leads to trap saturation.

Mechanisms that might be responsible for ventless lobster trap saturation, or a plateau in catch after a certain period of time, include 1) deterioration of the bait and/or a decrease in its attractiveness; 2) removal/capture of most of the animals in the area fished; and 3) interactions between lobsters in, and around, the trap. The distance of bait attraction for lobsters to standard traps has been previously estimated as approximately 11 m from the odorant source (Watson et al., 2009), and we expect that ventless traps fish similarly in terms of bait attraction. While the fishable area of a trap will depend upon habitat conditions (e.g., current, temperature, bottom type), lobsters that are already in, or move into, the area of bait attraction will likely to be drawn to the trap. However, as bait is removed by the feeding activity of lobsters and other species, it may deteriorate and this will lead, in part, to a decline in the release of amino acids (and other potential attractants) from the bait over time (Mackie et al., 1980; Løkkeborg, 1990; Kamio and Derby, 2017). Moreover, as bait quality deteriorates, the catch rate of lobsters is also expected to decline because the area of attraction will be reduced, fewer lobsters will be attracted to the trap, and entry rate will decrease.

Although loss of bait attractiveness is a likely factor affecting trap saturation in both standard and ventless traps, it is possible that, at least for ventless traps, capture and retention of many of the lobsters in the effective fishing area (EFA) (Miller, 1975) is another factor. Some of the single-parlor ventless traps fished by the Massachusetts Division of Marine Fisheries have been shown to retain up to 50 lobsters (MADMF[2]). Therefore, depending on the initial density of lobsters on the bottom, after a 24-h soak most of the lobsters within the fishing area of the trap might be retained in the trap, and so there would be few lobsters remaining in the vicinity that could be captured. As a result, approach and entry rates would be reduced, catch rate would plateau, and traps would become "saturated."

Standard and ventless trap saturation is also likely a function of behavioral interactions, with animals in the trap inhibiting the entry of subsequent animals, as Barber and Cobb (2009) demonstrated with Dungeness crabs (*Cancer magister*). Similar interactions have been observed in and around American lobster traps (Richards et al., 1983; Jury et al., 2001; Watson and Jury, 2013), blue crab (*Callinectes sapidus*) traps (Sturdivant and Clark, 2011), and cod pots (Anders et al., 2017). It has been proposed that, as traps fill, these antagonistic interactions increase, reducing the further entry of lobsters and increasing the likelihood that lobsters will escape. This phenomenon might be even more pronounced for ventless traps, given their overall greater tendency to rapidly fill with lobsters.

The overall goal of this study was to test 3 possible mechanisms underlying saturation of ventless lobster traps: 1) so many of the lobsters in the fishable area of a trap get captured after 24 h that entry and exit rates equalize and subsequent catch plateaus; 2) catch levels off because the bait loses its attractiveness; and 3) the presence of lobsters in the trap inhibits the entry of additional lobsters.

Materials and methods

Overview

We conducted the following 4 types of experiments to test the hypotheses stated above: 1) quantifying the number of lobsters in the vicinity of ventless lobster traps before,

[2] MADMF (Massachusetts Division of Marine Fisheries). 2017. Unpubl. data. Mass. Div. Mar. Fish., 251 Causeway St., Ste. 400, Boston, MA 02114.]

and after, a soak time of 24 h to determine if ventless traps captured enough lobsters to reduce the local population, resulting in fewer entries on the second day of fishing; 2) either pre-stocking ventless traps with lobsters before deploying them, or removing the lobsters captured after the first 24 h, to determine if lobsters in a ventless trap reduce the rate of entry of additional lobsters; 3) fishing ventless traps with new bait, versus 1-day-old "pre-soaked" bait, to determine if bait loses attractiveness after 24 h; and 4) measuring the rate of leaching of putative lobster attractants from bait to determine if this might explain the reduced entry of lobsters into traps after 24 h of fishing. Some of these experiments involved deploying traps for 24 h, and in others we soaked traps for 48 h. The methods below, and the results, are organized according to both the type and duration of each experiment.

Study area

All of the experiments were carried out just off Wallis Sands State Beach in New Hampshire at depths of 7–12 m. This location was chosen based upon previous, comparable studies of lobster trap dynamics that also occurred at this site (Jury et al., 2001; Watson and Jury, 2013; Clark et al., 2015, 2018). Furthermore, the bottom substrate in this location is mostly sand, which makes it easier to conduct replicated, large-scale, transect surveys without having to disturb either the habitat or the lobsters. This habitat type also facilitates analysis of time-lapse videos of lobsters in and around traps. Finally, most commercial lobstermen do not fish in this area, so there was less chance of traps that were not part of our experiment being unexpectedly deployed and influencing the results.

Most of the lobsters captured at this site were below the minimum legal size limit (83 mm in carapace length [CL]), with an average CL of 64.6 mm (standard deviation [SD] 10.3; range: 34–117 mm; n=3005; see Clark et al., 2015, for the size-frequency distribution of lobsters captured by ventless traps and observed during scuba surveys at this same study site). In the 12-week period (mid-July–early October, 2013) during which we conducted this study, the catch per unit of effort remained relatively consistent (Fig. 1).

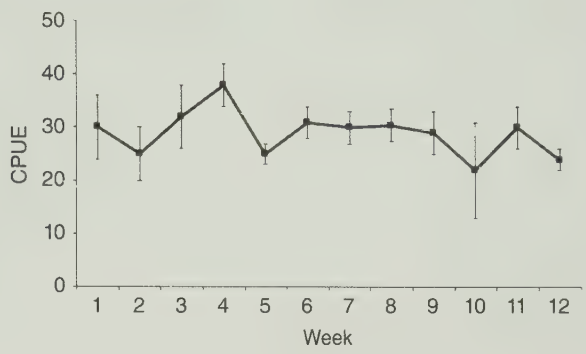

Figure 1

Mean catch per unit of effort of American lobsters (*Homarus americanus*) in ventless traps deployed off Wallis Sands State Beach in New Hampshire for a 12-week period in 2013 (15 July–9 October). All data presented are based on 48-h soak times (n=12, with 8–13 traps deployed per week). Error bars denote standard errors of the mean.

Traps

All of the traps used in this study were identical to the single-parlor ventless traps used by the Massachusetts Division of Marine Fisheries and the New Hampshire Fish and Game Department for their ventless trap stock assessment surveys, and they were deployed in the same manner as during their surveys (for details, see Clark et al., 2015). Typically, we used single-parlor traps that were set ~30 m apart, baited with 3–4 newly thawed Atlantic herring (*Clupea harengus*) (with a combined weight of approximately 1 kg), unless otherwise stated. For a subset of experiments, we used a ventless trap equipped with a lobster trap video (LTV) system (see Jury et al., 2001; Clark et al., 2015, 2018) to observe lobster behaviors in and around traps over the course of the soak period. The LTV system in these experiments consisted of a time-lapse digital video camera and recorder (Brinno BCC200[3], Brinno, Inc., Taipei City, Taiwan) secured inside an Ikelite clear plexiglass case (Ikelite, Indianapolis, IN) that was mounted above the trap on a PVC frame. Video frames were captured every 5 s, and video recordings were played back at 15 frames/s during analysis. The videos were taken only during the daylight hours of a typical 48-h soak because no supplemental light source was used in order to avoid the potential influence of artificial lights on lobster behavior.

Density of lobsters around traps before and after a 24-h soak

This experiment was designed to determine if ventless traps temporarily reduce the number of American lobsters in the vicinity of a trap after deployment for 24 h. On day 1 of the experiment, a single trap without bait was deployed, and then a pair of scuba divers conducted a transect survey of lobster abundance around the trap as described below. During each survey, divers swam 4 transects of 30 m each, extending out from the trap in the 4 cardinal directions. This distance was chosen because the fishable area of a trap is an estimated 2600 m^2, or a circle with a radius of 28.8 m, based upon data from a study by Watson et al. (2009). The width of each transect was typically 2–4 m, depending on visibility, yielding a survey area of 240–480 m^2 for each experiment. Immediately after completing the survey, the divers opened a watertight container of bait and placed it in a previously empty bait bag, in the trap. Lobsters were not handled during

[3] The mention of trade names or commercial companies is for identification purposes only and does not imply endorsement by the National Marine Fisheries Service, NOAA.

the surveys conducted on day 1 because handling often leads to an escape response or other aberrant behavior, which might have caused them to leave the area (senior author, personal observ.). After the trap had been deployed for 24 h, the dive survey described above was repeated to determine if the density of lobsters around the trap had changed. This experiment was repeated on 5 different occasions. A Wilcoxon matched-pairs signed rank test (n=5) was used to compare the density of lobsters present before and after the trap had soaked for 24 h.

Influence of lobsters in a trap on the entry of additional lobsters

American lobsters in a ventless trap may deter the entry of additional lobsters and thus reduce the rate of entry, leading to a plateau in catch (trap saturation). We conducted experiments with soak times of 24 h and 48 h to test this hypothesis and we both added lobsters to a trap (pre-stocked) and removed lobsters that were captured after 24 h from a trap, before redeploying it for another 24 h.

Pre-stocking experiment with 24-h soak Between 1 August 2013 and 2 October 2013, 6 different ventless traps were pre-stocked with all of the lobsters that were caught from 6 other ventless traps that had been deployed for 24 h. The number of lobsters used for pre-stocking was a function of the number of lobsters initially captured; lobsters were transferred directly from one ventless trap to another. The average number of lobsters used to pre-stock traps was 28.6 (SD 4.2; range: 21–33). Importantly, these lobsters had a size-frequency distribution that was typical for lobsters captured by ventless traps in this location. The lobsters used for pre-stocking were also marked, with a coded rubber band placed on the carpus of each of their claws (i.e., "knuckles"), so that they could be differentiated from any subsequently captured lobsters. We confirmed that the tags remained on lobsters for at least 1 week in a separate study conducted at the University of New Hampshire (UNH) Coastal Marine Laboratory (New Castle, New Hampshire). Pre-stocked ventless traps were provided with fresh bait and deployed in locations at least 0.5 km away from where the traps used to capture the lobsters for pre-stocking were fished, but in the same general fishing area. The pre-stocked ventless traps were then deployed for 24 h and catch was compared to the catch in the ventless traps that were initially used to capture the lobsters used for pre-stocking. The Mann–Whitney U test was used for this comparison, as well as for subsequent analyses when catch was compared between 2 groups of traps.

Trap emptying experiment with 48-h soak In this study, which was conducted between 1 August 2013 and 9 October 2013, ventless traps (n=9) were deployed for 24 h and then hauled. All captured lobsters were removed, but the used bait in each trap was retained. The lobsters were then released >0.5 km from where they were captured to minimize the chance of subsequent recapture. These traps, emptied of lobsters, were redeployed with the same 1-day-old bait for an additional 24-h soak. The catch from the initial 24-h deployment with fresh bait was compared with catch during the second 24-h soak of the same trap with the 1-day-old bait. The net catch for the entire soak time of 48 h, or the sum of the animals captured on day 1, plus those captured on the day 2, was also compared with catch from control ventless traps (n=27) that were deployed continuously for 48 h during the same time period, within the same study area.

Loss of bait attractiveness

Studies testing the hypothesis that bait loses at least some of its attractiveness over a soak were also conducted with traps deployed for both 24 h and 48 h.

Bait experiment 1: 24-h-old versus fresh bait Traps (n=33) were deployed for 24 h and then the used bait was removed and placed into different ventless traps. These traps were then then redeployed with the 1-day-old bait in a different location, >0.5 km away, but in the same general study area. Catch in the original traps, fished with fresh bait for 24 h, was compared with catch in the traps fished with 1-day-old bait for 24 h.

Bait experiment 2: 48-h soak with rebait Ventless traps (n=27) were deployed for 24 h and hauled, the used bait was removed, and then the traps were rebaited with the same amount of fresh bait. Lobsters in each trap were counted but *not* removed from the trap, and the traps were redeployed and fished for another 24 h. In a supplementary experiment using a ventless trap equipped with a LTV system (n=7), the fresh bait was added by scuba divers after a soak of 24 h so that video recordings would not be interrupted by hauling of the trap and any lobsters retained by the trap up to this point would not be startled, potentially influencing their behavior. After an additional 24-h soak with the new bait (48-h total soak time), the trap was hauled and the captured lobsters quantified. The catch for the traps that received fresh bait (n=27) was compared to the catch in control ventless traps (n=34) that were continuously deployed with the same bait for 48 h, in the same general area and during the same time period.

We also used data from the 7 trials with the LTV system, described above, to quantify the number of lobsters that entered and escaped from traps during experiments in which scuba divers added fresh bait. In addition, the videos obtained allowed us to determine the total number of lobsters in the trap each hour (i.e., accumulated catch), so that the time course of saturation could be plotted.

Bait experiment 3: leaching of amino acids This experiment was conducted to determine the relative rate at which amino acids leached out of bait over 24 h. Salted Atlantic herring (4 samples, each with a wet weight of 150 g) were put in individual bait bags, which were then placed into 1-L beakers containing clean artificial seawater with a practical salinity of 32 (Crystal Sea Marinemix, Marine Enterprises International, LLC, Baltimore, MD) and gently

mixed for 1 h on a shaker table in a temperature-controlled bath (20°C). The soaked bait and particulates were then allowed to settle for 15 min, and duplicate 15-mL aliquots of the supernatant were removed and frozen at −20°C for future analyses. The bait remaining after this 1-h period was weighed and then placed inside a bait bag and transferred to a ventless lobster trap that had the entries covered to minimize possible feeding on the bait by lobsters or other organisms too large to fit through the trap mesh. These traps were deployed in the field in Casco Bay, Maine (15°C, salinity of 32), for periods of 3, 6, and 24 h, and then the bait from each trap was weighed. After each time interval of soaking in the field, each bait bag with remaining bait was placed into 1 L of temperature-controlled, clean artificial seawater and shaken in the lab for another hour, after which duplicate leachate aliquots were removed and frozen. Thus, for each of the 4 bait samples tested, we had the wet weight of the bait and a leachate sample for 4 time periods: 0–1 h, 3–4 h, 6–7 h, and 24–25 h. For amino acid analyses, leachate samples were sent to SGS Analytical Services (Brookings, SD) for standard analyses via liquid chromatography–mass spectrometry.

Results

Density of lobsters around traps before and after a 24-h soak

There was no significant difference between the density of lobsters in the vicinity of ventless traps before and after a soak of 24 h (Fig. 2; 2-tailed Wilcoxon test: n=5, P=0.125). Even when the density of lobsters determined by scuba surveys was at its highest, there were more lobsters around the trap after 24 h than just after the trap was set. Therefore, with the possible exception of times of the year when, or locations where, densities of lobsters are very low, it appears that the reduction in the number of lobsters in the EFA of a trap, due to their accumulation in a ventless trap, is probably not a primary cause of trap saturation.

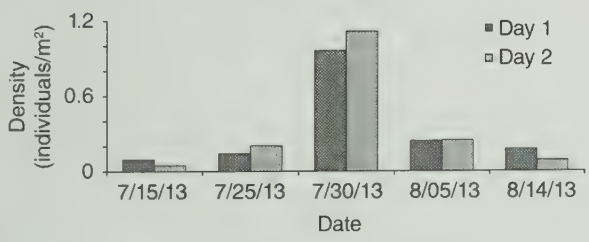

Figure 2

The abundance of American lobsters (*Homarus americanus*) in the vicinity of a trap prior to, and after, a soak of 24 h. Traps were deployed in 2013 off Wallis Sands State Beach in New Hampshire. There was no significant difference (n=5, P=0.125) in the density of lobsters before, and after, a trap had been deployed for 24 h. Therefore, traps did not reduce the number of lobsters in the area surrounding the traps significantly enough to influence catch on day 2 of a 48-h soak. Gray bars represent day 1, and black bars represent day 2.

Influence of lobsters in a trap on the entry of additional lobsters

Catch in pre-stocked traps versus control traps deployed for 24 h Pre-stocked traps captured significantly fewer additional lobsters than traps that were not pre-stocked (Fig. 3; Mann-Whitney U test: P=0.002). An average of 12.2 *new* lobsters entered the pre-stocked traps in 24 h, while 7.8 of the marked lobsters used for pre-stocking *escaped*, yielding a net increase in catch of only 4.4 lobsters (SD 3.7). This indicates that lobsters in ventless traps influence the subsequent entry of additional lobsters, as has been observed for standard traps (Jury et al., 2001). When taken together with the fact that a number of the pre-stocked lobsters escaped, it appears as if, at some point during a soak, as traps fill, a dynamic equilibrium between entries and escapes is reached, which plays an important role in causing catch to plateau, or saturate, in ventless traps.

Removal of captured lobsters after 24 h of a soak influences catch after 48 h Traps (n=9) deployed for 24 h captured an average of 25.7 lobsters (SD 6.1). After these lobsters were removed from the traps and the same traps were redeployed *without changing the bait* for a second 24 h, they captured significantly fewer lobsters in the second 24-h soak period (13.7 individuals [SD 8.6]; Mann-Whitney U test: P=0.004). Moreover, if the number of lobsters captured during each of the 2 days are added together, a net total of 39.3 lobsters (SD 12.9) were caught in the equivalent of a 48-h soak. This was significantly more than the

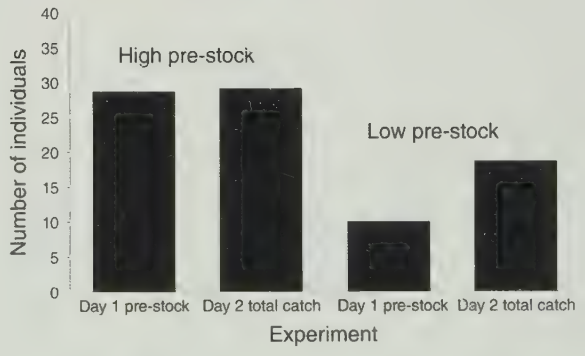

Figure 3

The effect of pre-stocking traps on subsequent catch. When traps (n=6) were pre-stocked with ~28 American lobsters (*Homarus americanus*) on day 1 (high pre-stock), the traps captured few additional lobsters after a soak of 24 h (day 2). When traps (n=3) were pre-stocked with only 10 lobsters (low pre-stock), they caught ~9 more lobsters during the next 24 h, for a total of ~19. Error bars in this figure denote standard errors of the mean.

catch in nearby ventless traps that were deployed for 48 h without the removal of lobsters (28.9 individuals [SD 9.4]; Mann–Whitney U test: P=0.035). These data indicate that 1) bait is less attractive after 24 h and 2) lobsters already in a trap influence the entry of new lobsters, so if they are removed, more lobsters will enter the trap.

Loss of bait attractiveness

Traps deployed for 24 h with fresh or old bait Ventless traps (n=33) that were fished for 24 h with "fresh" bait captured significantly more lobsters (unpaired t-test: P<0.006) than ventless traps (n=29) fished with bait that had been previously used for 24 h in a different set of traps (i.e., 1-day-old bait) (Fig. 4A). These results indicate that the old bait was less attractive than the new bait. It should be noted that, although this old bait had been in a trap for 24 h, much of the Atlantic herring, by weight, was still intact (on average, 62% of the bait by wet weight remained).

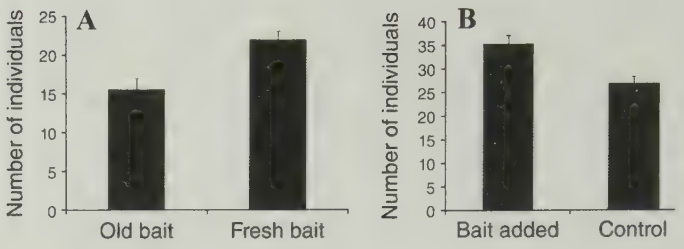

Figure 4

The effect of bait "age" on catch per unit of effort. (**A**) Twenty-nine traps were deployed for 24 h with bait that had already been used in different traps in the same location for 24 h (old bait), and 33 other traps were deployed for 24 h with the same amount of fresh bait. The traps with fresh bait captured significantly more American lobsters (*Homarus americanus*) (P<0.006). (**B**) Control traps (n=34) were deployed for 48 h with the same bait. Experimental traps (n=34, bait added) were hauled after 24 h, the bait in each trap was replaced with fresh bait, and then the traps were redeployed for an additional 24 h. The traps with added bait caught significantly more lobsters (P=0.027). Error bars in this figure denote standard errors of the mean.

Traps deployed for 48 h Ventless traps (n=34) were deployed for 24 h and then the bait was replaced with new bait, and the traps were redeployed, without removing any of the captured lobsters, for a second 24 h. These traps with bait added captured a mean of 21.0 lobsters after the initial 24 h and 13.9 lobsters during the second 24 h, for a total of 34.9 lobsters after the total soak time of 48 h (Fig. 4B). This was significantly more than control traps (n=27) captured; control traps were fished over the same time period, but without new bait added after the initial 24 h (unpaired t-test: P<0.05) (Fig. 4B). Interestingly, the experimental traps with added bait captured ~50% fewer lobsters on day 2 than on day 1 in virtually every experiment, even though fresh bait was added, a result that was likely due to the influence of the lobsters retained from day 1 on the subsequent entry of new lobsters. Therefore, while loss of bait attractiveness appears to play a role in reducing the catch of lobsters during day 2 of a 48-h soak, other factors, such as the behavioral interactions between lobsters, also influence saturation of ventless traps.

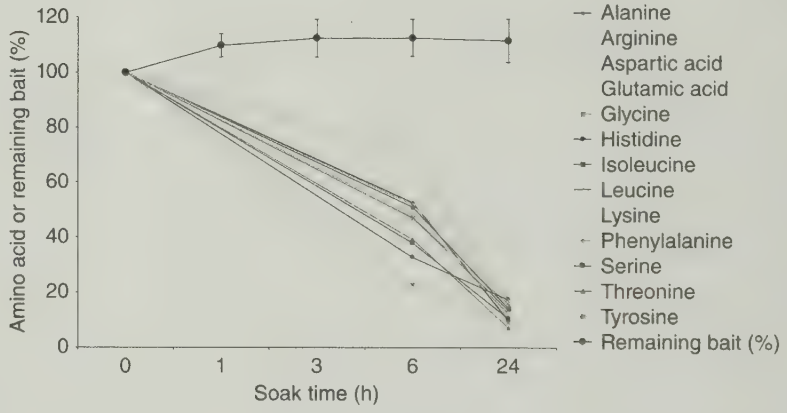

Figure 5

Bait degradation over time, by proportion of remaining weight (%) and relative concentration (%) of amino acids. Although wet weight of the bait (n=4, frozen salted Atlantic herring, *Clupea harengus*), was relatively unchanged over a 24-h simulated trap deployment, the concentrations of multiple amino acids rapidly decreased due to leaching. Note that the initial increase in weight is due to rehydration of the salted herring. Error bars in this figure denote standard errors of the mean.

Attractants leaching from bait To estimate the leaching of possible bait attractants from Atlantic herring within the first 24 h of trap deployment, we measured changes in the concentrations of various amino acids over time in simulated trap deployments (Fig. 5). Although the weight of the Atlantic herring that were used as bait was essentially unchanged after 24 h (note that lobsters were not allowed to feed on baits during the soak time; for details, see the "Materials and methods" section), the amino acid concentrations decreased by 30–80% after just 6 h and then decreased even further after 24 h. As a result, under the conditions tested, salted Atlantic herring after 24 h had

<20% of its initial concentration of potential attractants. In the field, the decrease in attractiveness would likely be even greater because feeding on the bait would reduce its quantity and increase the rate of leaching. These data add further support to the hypothesis that even though loss of bait attractiveness is not the only factor influencing ventless trap saturation, it is a key factor leading to a decrease in the rate of lobster entries into a trap even after a soak of just 24 h.

Time-lapse video observations of ventless traps For insight into the behavioral mechanisms underlying the effect of new versus old bait, time-lapse videos of ventless traps (n=7) were obtained before and after the addition of fresh bait (Fig. 6). Data from analysis of these videos indicate that the entry of lobsters typically leveled off on day 2 of a soak, but when fresh bait was added by divers on day 2 there was an immediate increase in the entry of lobsters into the trap (Fig. 6). As a result, while the entry rate of lobsters in control traps dropped 77% between day 1 and 2 (from 1.7 to 0.4 entries/h), it only dropped 38%, from 1.6 to 1.0 entries/h, for experimental traps with fresh bait added.

Discussion

Although the mechanisms underlying trap saturation in standard lobster traps have been addressed in a number of previous studies (Miller, 1979; Richards et al., 1983; Fogarty and Addison, 1997; Jury et al., 2001), the focus of this study was the testing of specific hypotheses concerning the potential causes of ventless trap saturation. Our results indicate that catch typically reaches a plateau after ~24 h for 2 main reasons: 1) a loss of bait attractiveness, which leads to a decrease in the rate of entries; and 2) behavioral interactions between American lobsters, which become more prevalent as traps fill and cause both a decrease in the entry of new lobsters and an increase in the rate of escapes. These conclusions are supported by data showing that, if fresh bait was added, or lobsters in a trap were removed, catch was higher than in control traps, and if old bait was used, or lobsters were pre-stocked in traps, catch declined relative to catch in control traps (Fig. 7). These same mechanisms are likely to come into play with standard traps as well, but the relative rates of entry and escape differ, leading to different behavioral dynamics.

In a previous study, Clark et al. (2015) demonstrated that ventless traps saturate before they reach capacity (i.e., they reach the maximum biomass they can hold) and

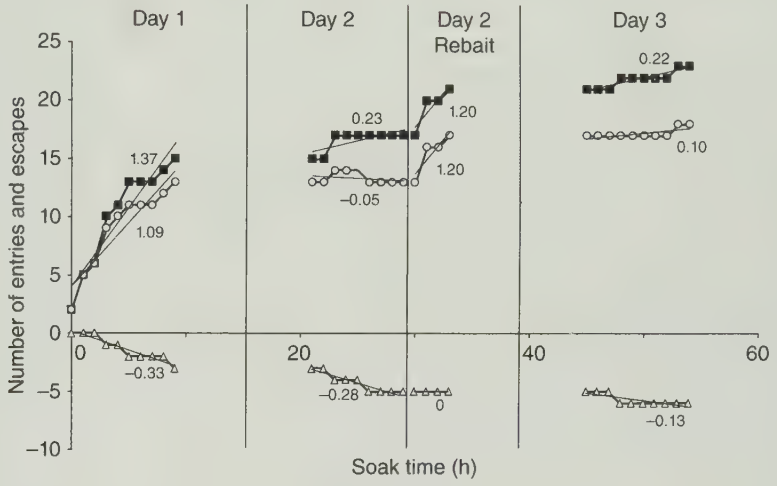

Figure 6

The effect of fresh bait on the entry rate of American lobsters (*Homarus americanus*) into traps deployed off New Hampshire in 2013, based on video observations. The accumulated rates of entry (black squares), catch (white circles), and escapes (white triangles) are shown for one representative 72-h soak of a ventless trap. Lines that best fit the data are overlaid on each segment of data points. Note that on day 2 (after traps already had been fished for 24 h), rates of entry and catch reached a plateau. Then scuba divers added fresh bait to the trap (vertical line labelled *Day 2 rebait*), which led to an immediate increase in entries and catch. Also note that, when escapes were equivalent to entries, catch reached a plateau. Missing data are the result of night hours when observations were not possible because lights were not used on traps.

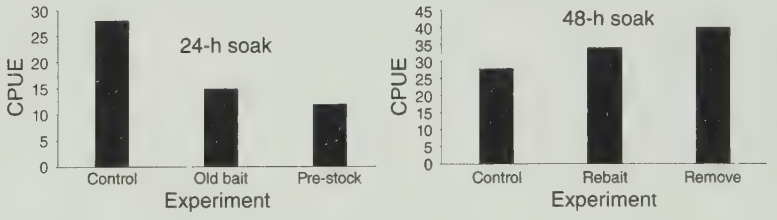

Figure 7

Summary overview of the effects of various experiments on the catch per unit of effort (CPUE) of American lobsters (*Homarus americanus*) in ventless traps. These data are presented in summary for comparison; therefore, error bars have been omitted. Note that pre-stocking traps and using 1-day-old bait reduces catch, compared with catch of control traps (24-h soak), and that removing the lobsters captured on day 1, or adding fresh bait after 24 h, led to an increase in catch. The CPUE data for the "remove experiment" includes the lobsters that were removed on day 1 and the new lobsters captured on day 2.

that catch at the point of saturation is correlated with the density of American lobsters on the bottom. Saturation tended to occur when the rate of entry of lobsters into ventless traps became equal to their rate of escape, so lobsters stopped accumulating in the trap, and the catch rate reached a plateau (Clark et al., 2018). Importantly, these data indicate that ventless traps probably saturate before they reach some upper physical capacity, or maximum number of lobsters the trap could hold. Therefore, ventless traps seem to provide a fairly accurate index of the number of lobsters on the bottom, at least when the density of lobsters on the bottom is not very high (Watson and Jury, 2013; Clark et al., 2015).

Previously, Clark et al. (2018) determined, using video cameras mounted above traps, that the number of lobsters within 1 m of both standard and ventless traps was less on day 2 of a 48-h soak than on day 1. Given that ventless traps typically capture ≥30 lobsters in the area studied by Clark et al. (2018) (i.e., same site used in the present study) during a 48-h soak (Fig. 1), the ventless traps may have accumulated enough lobsters to reduce the density of lobsters in the EFA surrounding the traps. In this study, we surveyed a much larger area around traps and found that there were no significant differences in the densities of lobsters in the EFA after the traps were deployed for 24 h. These findings do not support the hypothesis that ventless traps saturate because they accumulate enough lobsters to reduce the density in their vicinity.

One reason why some American lobsters do not enter traps is that conspecifics already inside the traps keep them out (Richards et al., 1983). During 2 previous studies (Jury et al., 2001; Watson and Jury, 2013), time-lapse videos were used to investigate this phenomenon with standard lobster traps, and, in both cases, it was clear that lobsters in the kitchen portion of the trap, where lobsters enter and the bait is located, would often prevent other lobsters from entering. However, it should be noted that in all previous studies of this type the lobsters used for pre-stocking were large adults that might be more aggressive than the sublegal lobsters that typically accumulate in ventless traps.

In this study, ventless traps were pre-stocked with the same number, and size composition, of lobsters that were typically captured in ventless traps on day 1 of a soak, in the same location (see Clark et al., 2015), and despite this modification in protocol, pre-stocking traps still reduced catch. Also, the removal of the lobsters captured on day 1 increased the number of lobsters captured on day 2, most likely because of reduced agonistic interactions. Moreover, when the lobsters captured and removed on day 1 of a 48-h soak were added to those captured on day 2, the total net catch was greater than that for traps that were deployed continuously for 48 h (Fig. 7). This result indicates that as a trap fills over the course of the soak time, fewer lobsters enter, and more lobsters leave, leading eventually to a dynamic equilibrium in which catch plateaus. However, although it appears as if the reduction in the rate of entry is, in part, due to the presence of lobsters in the trap, loss of bait attractiveness also appears to play an important role.

Bait attractiveness was reduced after 24 h, as indicated by a number of different results. First, catch of traps with 1-day-old bait was significantly less than catch of identical traps deployed for 24 h with fresh bait (Fig. 4). Second, when scuba divers replaced old bait with fresh bait, there was an immediate increase in the rate of entries observed on video recordings made with the LTV system. This finding strongly indicates that the new bait was significantly more attractive than the old bait (Fig. 6). Moreover, traps that had new bait added after 24 h captured more lobsters than control traps (Fig. 4). Finally, after 6–24 h, there was a significant reduction in the amount of amino acids released from Atlantic herring bait, even though the bait itself, in terms of weight, was mostly intact. These results are consistent with those of a previous study of the rate of leaching from mackerel bait (Løkkeborg, 1990). Therefore, a change in the attractiveness of bait over time also plays a key role in lobster trap dynamics and the onset of ventless trap saturation. It should be noted that the initial amount and type of bait, along with environmental factors such as temperature and current velocity, will likely affect catch and trap saturation by altering the rate at which bait loses its attractiveness.

The findings from this study have several practical implications. First, ventless traps saturate after approximately 24 h because of a combination of factors related to bait deterioration and behavioral interactions between lobsters that inhibit further entries and enhance escapes. Therefore, in areas with high densities of lobsters, soak times of ~24 h might be best for ventless trap surveys. However, longer soak times might be appropriate in areas where the density of lobsters is lower or where the size-frequency distribution is different. Second, even though there is a correlation between catch in ventless traps and the density of lobsters on the bottom (Clark et al., 2015), the accuracy of catch in ventless trap surveys as an indicator of abundance might be affected in areas with higher densities of lobsters or, as mentioned previously, in habitats with a higher density of larger, more aggressive lobsters. In these areas, one possible solution might be to use double-parlor ventless traps, which might saturate at a higher capacity, or after a longer soak time. Finally, it would be prudent to consider standardization of the amount and type of bait used in ventless traps and to consider bait or bait delivery systems that do not deteriorate as fast as Atlantic herring, so that lobsters will continue to approach and enter traps at a high rate throughout a longer soak time.

Acknowledgments

We thank the staff at the UNH Coastal Marine Laboratory, including W. Howell, N. Rennels. and the late N. Carlson, as well as UNH students, J. Goldstein, N. Copp, H. Cheng, B. Dubofsky, and T. Langley and Southern Maine Community College students under the supervision of B. Tarbox. We also thank the Massachusetts Division of Marine Fisheries, J. Carloni, and T. Pugh. This work was supported by a faculty development grant from

St. Joseph's College to S. Jury and funding from New Hampshire Sea Grant (NOAA award R/SSS-3) to W. Watson.

Literature cited

ASMFC (Atlantic States Marine Fisheries Commission).
2015. American lobster benchmark stock assessment and peer review report, 417 p. Atlantic States Mar. Fish. Comm., Arlington, VA. [Available from website.]

Anders, N., A. Fernö, O.-B. Humborstad, S. Løkkeborg, G. Rieucau, and A. C. Utne-Palm.
2017. Size-dependent social attraction and repulsion explains the decision of Atlantic cod *Gadus morhua* to enter baited pots. J. Fish Biol. 91:1569–1581.

Auster, P.
1985. Factors affecting catch of American lobster, *Homarus americanus,* in baited traps. Univ. Conn. Sea Grant Program, Tech. Bull. Ser. CT-SG-85-1, 46 p.

Barber, J. S., and J. S. Cobb.
2009. Qualitative observations of Dungeness crabs, *Cancer magister*, in and around traps: evidence of resource guarding and clustering. Mar. Freshw. Behav. Physiol. 42:135–146.

Boutson, A., C. Mahasawasde, S. Mahasawasde, S. Tunkijjanukij, and T. Arimoto.
2009. Use of escape vents to improve size and species selectivity of collapsible pot for blue swimming crab *Portunus pelagicus* in Thailand. Fish. Sci. 75:25–33.

Broadhurst, M. K., P. A. Butcher, and B. R. Cullis.
2014. Effects of mesh size and escape gaps on discarding in an Australian giant mud crab (*Scylla serrata*) trap fishery. PLoS ONE 9(9):e106414.

Clark, A. S., S. H. Jury, J. S. Goldstein, T. G. Langley, and W. H. Watson III.
2015. A comparison of American lobster size structure and abundance using standard and ventless traps. Fish. Res. 167:243–251.
2018. Underwater video surveillance of American lobsters (*Homarus americanus*) to understand saturation levels in lobster traps. Fish. Bull. 116:161–170.

Courchene, B., and K. D. E. Stokesbury.
2011. Comparison of vented and ventless trap catches of American lobster with scuba transect surveys. J. Shellfish Res. 30:389–401.

Fogarty, M. J., and J. T. Addison.
1997. Modelling capture processes in individual traps: entry, escapement and soak time. ICES J. Mar. Sci. 54:193–205.

Hedgärde, M., C. W. Berg, L. Kindt-Larsen, S. G. Lunneryd, and S. Königson.
2016. Explaining the catch efficiency of different cod pots using underwater video to observe cod entry and exit behaviour. J. Ocean Technol. 11(4):67–90.

High, W. L., and A. J. Beardsley.
1970. Fish behavior studies from an undersea habitat. Commer. Fish. Rev. 32:31–37.

Jury, S. H., H. Howell, D. F. O'Grady, and W. H. Watson III.
2001. Lobster trap video: in situ video surveillance of the behavior of *Homarus americanus* in and around traps. Mar. Freshw. Res. 52:1125–1132.

Kamio, M., and C. D. Derby.
2017. Finding food: how marine invertebrates use chemical cues to track and select food. Nat. Prod. Rep. 34:514–528.

Løkkeborg, S.
1990. Rate of release of potential feeding attractants from natural and artificial bait. Fish. Res. 8:253–261.

Mackie, A. M., P. T. Grant, R. G. J. Shelton, B. T. Hepper, and P. R. Walne.
1980. The relative efficiencies of natural and artificial baits for the lobster, *Homarus gammarus*: laboratory and field trials. ICES J. Mar. Sci. 39:123–129.

Miller, R. J.
1975. Density of the commercial spider crab (*Chionoecetes opilio*), and calibration of effective area fished per trap using bottom photography. J. Fish. Res. Board Can. 32:761–768.
1979. Saturation of crab traps: reduced entry and escapement. ICES J. Mar. Sci. 38:338–345.
1990. Effectiveness of crab and lobster traps. Can. J. Fish. Aquat. Sci. 47:1228–1251.

Miller, R. J., and R. S. Roger.
1996. Soak times and fishing strategy for American lobster. Fish. Res. 26:199–205.

Richards, R. A., J. S. Cobb, and M. J. Fogarty.
1983. Effects of behavioral interactions on the catchability of American lobster, *Homarus americanus*, and two species of *Cancer* crab. Fish. Bull. 81:51–60.

Stoner, A. W.
2004. Effects of environmental variables on fish feeding ecology: implications for the performance of baited fishing gear and stock assessment. J. Fish Biol. 65:1445–1471.

Sturdivant S. K., and K. L. Clark.
2011. An evaluation of the effects of blue crab (*Callinectes sapidus*) behavior on the efficacy of crab pots as a tool for estimating population abundance. Fish. Bull. 109:48–55.

Watson, W., and S. H. Jury.
2013. The relationship between American lobster catch, entry rate into traps and density. Mar. Biol. Res. 9:59–68.

Watson, W. H. III, W. Golet, D. Scopel, and S. Jury.
2009. Use of ultrasonic telemetry to determine the area of bait influence and trapping area of American lobster, *Homarus americanus*, traps. N.Z. J. Mar. Freshw. Res. 43:411–418.

Weis, J. S.
2010. The role of behavior in the success of invasive crustaceans. Mar. Freshw. Behav. Physiol. 43:83–98.

National Marine
Fisheries Service
NOAA

Fishery Bulletin
established in 1881

Spencer F. Baird
First U.S. Commissioner
of Fisheries and founder
of *Fishery Bulletin*

Evaluation of the stock structure of cobia (*Rachycentron canadum*) in the southeastern United States by using dart-tag and genetics data

Matt Perkinson (contact author)[1]
Tanya Darden[1]
Maggie Jamison[1]
Matt J. Walker[1]
Michael R. Denson[1]
James Franks[2]
Read Hendon[2]
Susanna Musick[3]
Eric S. Orbesen[4]

Email address for contact author: perkinsonm@dnr.sc.gov

[1] Marine Resources Research Institute
South Carolina Department
of Natural Resources
217 Fort Johnson Road
Charleston, South Carolina 29412

[2] Gulf Coast Research Laboratory
University of Southern Mississippi
703 East Beach Drive
Ocean Springs, Mississippi 39564

[3] Virginia Institute of Marine Science
College of William and Mary
P.O. Box 1346
Gloucester Point, Virginia 23062

[4] Southeast Fisheries Science Center
National Marine Fisheries Service, NOAA
75 Virginia Beach Drive
Miami, Florida 33149

Abstract—Available tag-recapture and population genetics data for cobia (*Rachycentron canadum*) in the southeastern United States were evaluated to provide information on population structure and determine the geographic boundary between stocks in the Gulf of Mexico and the Atlantic Ocean. The movements of 1750 cobia were evaluated on the basis of assigned tagging and recapture zones. Genetic samples from an additional 2796 cobia collected during the presumed spawning season were genotyped at 10 microsatellite loci, and standard population genetic statistical analyses were applied to the resulting sample data set. Tag-recapture results indicate that cobia tagged south of Cape Canaveral, Florida, primarily move between that area and the Gulf of Mexico and that cobia tagged north of Georgia have little interaction with the area south of Cape Canaveral. Cobia tagged at Cape Canaveral distributed widely throughout the entire southeastern coast of the United States. Genetic analysis results agree, indicating separate stocks that occur from Texas through Hobe Sound on the east coast of Florida and from Savannah, Georgia, to the Chesapeake Bay in Virgina, with distinct genetic groupings within the Atlantic Ocean stock. The results indicate a transition area that occurs from Cape Canaveral through northern Georgia, and additional data from this region are necessary to further refine the stock boundary.

Manuscript submitted 5 November 2018.
Manuscript accepted 13 August 2019.
Fish. Bull. 117:220–233 (2019).
Online publication date: 23 August 2019.
doi: 10.7755/FB.117.3.9

The views and opinions expressed or implied in this article are those of the author (or authors) and do not necessarily reflect the position of the National Marine Fisheries Service, NOAA.

The cobia (*Rachycentron canadum*) is a large, migratory pelagic species found throughout most of the world's tropical and subtropical waters, with the exception of the eastern Pacific Ocean (Shaffer and Nakamura, 1989). In the United States, the species is found throughout the Gulf of Mexico (GOM) and Atlantic Ocean from Texas through Massachusetts (Briggs, 1960), although catches north of the Chesapeake Bay in Virginia are less frequent. Life-history characteristics differ between cobia from the GOM and those from the western North Atlantic Ocean, with a faster growth rate in the GOM and a greater maximum age in the Atlantic Ocean (Burns et al.[1]). In the GOM, cobia undertake seasonal migrations from overwintering grounds in South Florida to spawning grounds in the northern GOM during spring and summer (Burns and Neidig[2]; Ditty and Shaw, 1992; Biesiot et al., 1994; Franks and Brown-Peterson, 2002; Dippold et al., 2017), although some cobia may migrate from deeper offshore overwintering grounds to coastal areas as well (Hendon and Franks[3]). In the western North Atlantic Ocean, cobia enter high-salinity estuaries as well as nearshore locations in Georgia, South

[1] Burns, K. M., C. Neidig, J. Lotz, and R. Overstreet. 1998. Cobia (*Rachycentron canadum*) stock assessment study in the Gulf of Mexico and in the South Atlantic. Mote Mar. Lab. Tech. Rep. 571, 108 p. [Available from website.]

[2] Burns, K. M., and C. L. Neidig. 1992. Cobia (*Rachycentron canadum*), amberjack (*Seriola dumerili*), and dolphin (*Coryphaena hipurus*) migration and life history study off the southwest coast of Florida. Mote Mar. Lab. Tech. Rep. 267, 58 p. [Available from website.]

[3] Hendon, J. R., and J. S. Franks. 2010. Sport fish tag and release in Mississippi coastal waters and the adjacent Gulf of Mexico, 13 p. Final Rep., Proj. F-132, Segments 7–9. Gulf Coast Res. Lab., Univ. South. Miss., Ocean Springs, MS. [Available from website.]

Carolina, North Carolina, and Virginia as water temperatures approach 20°C (Richards, 1967; Smith, 1995; Lefebvre and Denson, 2012). The results of work that involved the collection of eggs and larvae, as well as ovarian histology, indicate that spawning occurs in these inshore locations during the spring and summer (Smith, 1995; Franks and Brown-Peterson, 2002; Lefebvre and Denson, 2012), although spawning may also occur with fish aggregating on the continental shelf (Hassler and Rainville, 1975). When estuarine and nearshore waters drop below 20°C in the fall, cobia move out of these areas, although overwintering locations are not well known. Because cobia are a popular target for recreational anglers throughout their range, state and federal regulations have been established to promote sustainable fishing.

Formal management measures for cobia in the United States began with the implementation of the coastal migratory pelagic resources fishery management plan (FMP) in 1983 (GMFMC and SAFMC, 1983), which established a single stock of cobia extending from Texas through the border of North Carolina and Virginia (later extended through New York) and established a size limit of 838 mm fork length (FL). Management authority was shared by the Gulf of Mexico and South Atlantic Fishery Management Councils. In 2012, Amendment 18 to the FMP (GMFMC and SAFMC, 2011) established GOM and Atlantic Ocean migratory groups of cobia. Although early genetic analysis revealed no differences between GOM and western North Atlantic Ocean cobia (Hrincevich, 1993), differences in life-history characteristics, such as maximum age and growth rate, required the change. The stock boundary was established in Monroe County, Florida, at the current demarcation of jurisdiction between the management councils. The Monroe County stock boundary was chosen on the basis of the documented seasonal migration of GOM cobia from overwintering grounds in the Florida Keys to the northern GOM and the presumption that Atlantic Ocean migratory group cobia overwinter in the Florida Keys as well (Williams, 2001). Initial genetic and conventional tagging data analyzed in preparation for Southeast Data, Assessment, and Review 28 (SEDAR, 2013a, 2013b) refuted the Florida Keys as an overwintering location for western North Atlantic Ocean cobia and, as a result, Amendment 20B to the FMP (GMFMC and SAFMC, 2014) established a new boundary between GOM and western North Atlantic Ocean stocks at the border of Georgia and Florida. Data that led to the new stock delineation are presented herein.

Identification of fish stocks is necessary to properly allocate catch among multiple user groups and effectively manage the species under the requirements of the Magnuson-Stevens Fishery Conservation and Management Act (MSFCMA, 2007). Successful stock delineation is also critical to the stock assessment process, as most population models assume that the stock will have homogeneous life-history characteristics and a closed life cycle in which recruitment occurs from within that stock (Cadrin et al., 2005). Because these characteristics differ between GOM and western North Atlantic Ocean cobia, an appropriate delineation of the stock boundary is essential to accurately assigning life-history parameters such as growth rate, fecundity, and age structure for each stock. Stock identification methods include analyzing a variety of characteristics, such as meristics, reproduction, morphometrics, otolith composition and shape, parasite tags, and fatty acid profiles (Hilborn and Walters, 1992; Izzo et al., 2017); however, mark-recapture and genetic analysis are 2 of the most commonly used methods of identifying stocks.

Mark-recapture methods that involve external tags have been used for over a century to provide information on fisheries (Ricker, 1948). Tagging studies have been used to determine migratory patterns and stock structure of species such as the Atlantic salmon (*Salmo salar*) (Hansen and Jacobsen, 2003), billfish (Istiophoridae) (Orbesen et al., 2008), Queensland school mackerel (*Scomberomorus queenslandicus*), Australian spotted mackerel (*S. munroi*) (Begg et al., 1997), and pollock (*Pollachius virens*) (Neilson et al., 2006). In contrast to the use of tag-recapture methods in studies of stock structure, the use of genetic analysis in stock identification is a relatively recent and rapidly evolving field. Over the last 2 decades, genetic methods have been more frequently employed to distinguish population structure of fish; genetic analyses have included the use of random amplified polymorphic DNA in species such as the striped bass (*Morone saxatilis*) (Bielawski and Pumo, 1997), Pacific cod (*Gadus microcephalus*) (Saitoh, 1998), and Antarctic toothfish (*Dissostichus mawsoni*) (Parker et al., 2002). More recently, microsatellite markers have been used to differentiate stock structure in Atlantic cod (*Gadus morhua*) (Knutsen et al., 2011), steelhead (*Oncorhynchus mykiss*) (Campbell et al., 2012), and eulachon (*Thaleichthys pacificus*) (Flannery et al., 2013). Our study combined the more traditional tag-recapture analysis with modern genetic methods.

Preliminary genetic and tag-capture analyses of cobia stock structure in the southeastern United States conducted in preparation for the 2012 benchmark stock assessment (Perkinson and Denson[4]; Darden[5]) cast doubt on the accepted stock boundary in the Florida Keys. Recently, Dippold et al. (2017) examined cobia migratory patterns by using tag-recapture data; however, the study focused primarily on 5 zones within the GOM. All regions north of the Florida Keys were combined into a single zone, making a thorough evaluation of the stock boundary delineation between the GOM and Atlantic Ocean stocks difficult. To identify the most biologically appropriate delineation, we conducted a meta-analysis of all available tag-recapture data, adding additional zones to the east coast of Florida to provide greater resolution of movement. Additionally, we analyzed microsatellite genetic data from cobia to compare the genotypes of fish collected in locations throughout the GOM and western North Atlantic Ocean. Our combination of data sources provided a complementary

[4] Perkinson, M., and M. Denson. 2012. Evaluation of cobia movements and distribution using tagging data from the Gulf of Mexico and South Atlantic coast of the United States. SEDAR28-DW05, 17 p. Southeast Data Assessment and Review (SEDAR), North Charleston, SC. [Available from website.]

[5] Darden, T. 2012. Cobia preliminary data analyses—US Atlantic and GOM genetic population structure. SEDAR28-DW01, 2 p. Southeast Data Assessment and Review (SEDAR), North Charleston, SC. [Available from website.]

approach to stock boundary identification (Begg and Waldman, 1999) with results that are more robust than those from the use of either method alone.

Materials and methods

Tagging methods

Tag-recapture data for cobia from 7 tagging programs were included in the analysis: the Virginia Game Fish Tagging Program, North Carolina Division of Marine Fisheries, South Carolina Department of Natural Resources (SCDNR), Hilton Head Reef Foundation, NOAA Southeast Fisheries Science Center Cooperative Tagging Center, Mote Marine Laboratory, and the Sport Fish Tag and Release Program of the Gulf Coast Research Laboratory, University of Southern Mississippi (Table 1). All 7 programs employed similar methods, including the use of nylon or stainless-steel-tipped dart tags and reliance on a trained group of recreational anglers and charter boat captains to tag and release cobia. Anglers were asked to submit a data card for each tagged fish that included the following information: tag number, date, release location, fish length (converted to millimeters in FL where necessary), and weight (converted to kilograms), as well as other pertinent information that differed by tagging program. Upon recapture of a tagged fish, anglers reported similar data, including whether the fish was released or harvested. In this study, we determined general migratory trends over a large geographic area on the basis of recapture data. There were minor differences in tag types (stainless versus nylon anchors) and incentive structure between programs and within programs during different time periods that could affect tag retention and reporting rates and could, therefore, influence estimates of mortality or other quantitative measures. However, these difference are unlikely to influence the analysis of large-scale migratory patterns based on capture and recapture location. Therefore, recapture data were pooled into a comprehensive data set. Tag and recapture locations were assigned a GPS coordinate on the basis of location description, if latitude and longitude were not otherwise provided. In those instances, we assigned latitudes and longitudes by using the best available information. These coordinates were assigned solely for the purpose of graphical depiction of recapture locations and not for analyses; all analyses were based on zone assignment. Only cobia at large for greater than 30 d were included in the final analysis to minimize the location bias of fish that were tagged and immediately recaptured. Where programs reported total length (TL), rather than FL of fish tagged, the formula $FL=13.52399+(0.878671\times TL)$ (SEDAR, 2013b) was used to transform data.

Table 1

Number of cobia (*Rachycentron canadum*) tagged and recaptured by each of 7 tagging programs throughout the Gulf of Mexico and Atlantic Ocean off the southeastern United States between 1988 and 2017. The tagging programs were those of the following organizations: Virginia Game Fish Tagging Program (VGTP), North Carolina Division of Marine Fisheries (NCDMF), South Carolina Department of Natural Resources (SCDNR), Hilton Head Reef Foundation (HHRF), NOAA Southeast Fisheries Science Center (SEFSC), Mote Marine Laboratory (MOTE), and Gulf Coast Research Laboratory, University of Southern Mississippi (GCRL).

Data source	Number tagged	Number recaptured	Recapture rate (%)	Years active
VGFTP	3899	433	11.1	1995–2017
NCDMF	73	5	6.8	2017
SCDNR	1194	216	18.1	1990–2014
HHRF	95	14	14.7	2007–2012
SEFSC	1557	159	10.2	1986–2014
MOTE	920	100	10.9	1991–2001
GCRL	18,129	1197	6.6	1988–2017
Total	25,867	2124	8.2	1986–2017

Data partitioning

Tagging areas and recapture areas were partitioned into 10 different zones for analysis of movement patterns (Fig. 1). The East Coast of the United States north of Florida was segmented into 5 zones: the areas within and extending offshore of states north of Virginia, Virginia, North Carolina, South Carolina, and Georgia. All tagging and recapture events that occurred within the Chesapeake Bay were assigned to the Virginia zone. Because preliminary genetic results (Darden[5]) indicated a break along the east coast of Florida, the area was segmented into 3 zones: north of Brevard County, encompassing the area from the Florida–Georgia border south to the border of Volusia and Brevard Counties; Brevard County, including Cape Canaveral; and south of Brevard County, encompassing the area from the border of Brevard and Indian River Counties to Biscayne Bay. County lines were chosen because of their congruency with recreational and commercial catch data used in the stock assessment process. To the south, the Florida Keys zone covered the area from Biscayne Bay around to Marco Island in southwest Florida. Although genetic structure and movements of fish between locations in the GOM to the Atlantic Ocean were evaluated, specific movements of fish solely within the GOM were beyond the scope of this paper, resulting in the entire GOM from Marco Island to the Texas–Mexico border being assigned a single zone. Dippold et al. (2017) provide a thorough analysis of cobia movements within the GOM. Analyses of movement between zones as well as recaptures within a zone were largely qualitative and focused on identifying seasonal trends and broad patterns in movement that indicate potential breaks in biological stocks.

Genetics

The SCDNR Genetic Tissue Collection currently houses more than 5050 archived genetic samples of cobia collected by numerous researchers and anglers around the

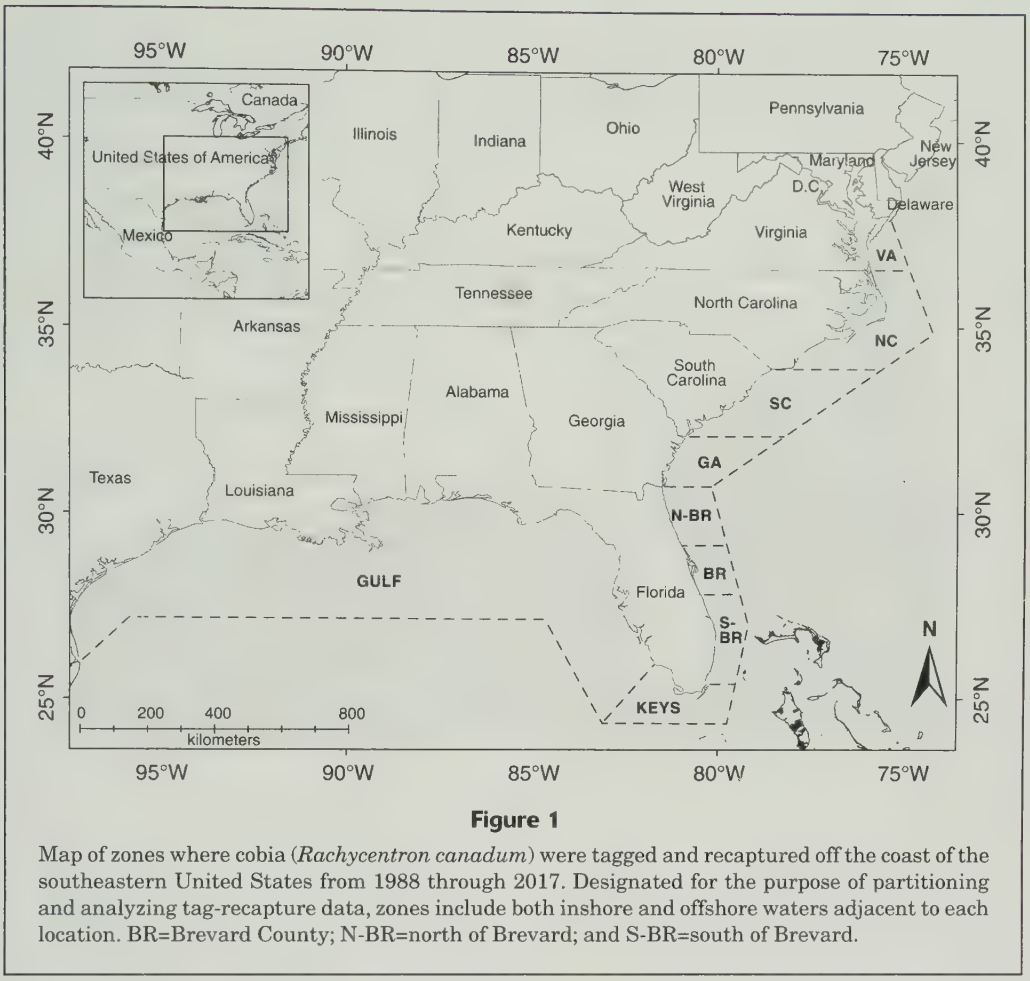

Figure 1

Map of zones where cobia (*Rachycentron canadum*) were tagged and recaptured off the coast of the southeastern United States from 1988 through 2017. Designated for the purpose of partitioning and analyzing tag-recapture data, zones include both inshore and offshore waters adjacent to each location. BR=Brevard County; N-BR=north of Brevard; and S-BR=south of Brevard.

globe. In all cases, small tissue samples were collected from the anal or caudal fin and stored in either 95% non-denatured ethanol (EtOH) or a sarkosyl-urea preservation solution (8 M urea, 1% sarkosyl, 20 mM sodium phosphate, 1 mM EDTA) until processed. For the current project, sample selection included those collected along the U.S. coast in the GOM and western North Atlantic Ocean during cobia spawning season defined by each state on the basis of temperature-based patterns and gonadosomatic indices (SEDAR, 2013b). Available samples ranged from Virginia south along the Atlantic coast around the Florida peninsula into the GOM and westward to Texas. Spawning season was defined for each state in this way: Virginia, June–August; North Carolina, May–July; South Carolina and Georgia, April–July; Florida, March–August; Mississippi, May (only samples available); and Texas, April–August.

The sarkosyl-urea preservative simultaneously stabilizes sample DNA and serves as a preliminary cell lysis solution. The EtOH-stored samples were subjected to a proteinase K cell lysis prior to DNA isolation. All DNA isolation, microsatellite amplification, and genotyping methods followed the method of Darden et al. (2014). Briefly, DNA was isolated from all samples by using a magnetic bead isolation procedure. Ten polymorphic microsatellite loci were then amplified through polymerase chain reaction (PCR) in 3 multiplexed groupings. These loci have been optimized and multiplexed previously and were used to document both global and local population structure in cobia. PCR was conducted in 11-µL reactions with 1× 5PRIME[6] HotMaster buffer kit (5PRIME HotMaster *Taq* DNA Polymerase and 10× 5PRIME HotMaster Buffer, 5000 U [5 u/µL]; Qiagen Beverly, Inc., Beverly, MA) and with 2.5 mM Mg^{2+}, 0.2 mM dNTPs, 0.3 units 5PRIME HotMaster *Taq* DNA Polymerase, 0.5 mM $MgCl_2$, 0.20 mg/mL BSA, 0.3 µM forward and reverse primers, and 1 µL of 1:10 diluted DNA template. Individual primer concentrations differ among loci and are given in Darden et al. (2014). Forward primers for all loci were labeled with WellRED fluorescent dyes (Beckman Coulter, Inc., Fullerton, CA). Thermal cycling for PCR used a modified 60°C touchdown protocol (Renshaw et al., 2006) consisting of an initial denaturation step at 94°C for 2 min, followed by 34 cycles of denaturing at 94°C for 30 s, annealing at 60°C, 57°C,

[6] Mention of trade names or commercial companies is for identification purposes only and does not imply endorsement by the National Marine Fisheries Service, NOAA.

and 54°C (7, 7, and 20 cycles, respectively) for 1 min, and extension at 64°C for 2 min, followed by a final extension step at 64°C for 60 min (as in Darden et al., 2014). Both size standards (GenomeLab DNA Size Standard Kit 400, Beckman Coulter, Inc.) and reaction products were separated with a Beckman Coulter CEQ 8000 Genetic Analysis System, with fragment size analysis performed with CEQ 8000 software. All chromatograms were scored manually by 2 independent readers. Discrepancies between readers were resolved in conference, or samples were rerun to obtain an unambiguous genotype for all individuals.

In 2004, researchers at SCDNR began a cobia stock enhancement research program, releasing discrete numbers of cobia juveniles into the wild. Therefore, all hatchery-produced fish were removed from the data set prior to further analysis. We used a maximum likelihood parentage approach as implemented in the software Cervus, vers. 3.0.3 (Kalinowski et al., 2007), to provide a statistical evaluation of parentage taking into account mutation rates, population allele frequencies, and lab error rates. The power of the loci suite to correctly identify hatchery fish as well as individual fish is high, with average parent-pair and identity non-exclusion probabilities of 1.7×10^{-7} and 7.8×10^{-12}, respectively, indicating very low probabilities of incorrectly identifying hatchery fish or individuals. Parentage simulations (number of simulations [n]=20) were run with known sex parentage analysis by using allele frequencies from individuals collected from 2007 through 2009 (n=1407). All simulations were conducted with 10,000 offspring, 8 candidate parent pairs (with all parents sampled), 95% genotyping, and low mistyping error (0.01) and mutation (0.001) rates. Critical delta scores were determined by using 99.0% and 99.9% confidence levels for the relaxed and strict criteria, respectively. Parentage analyses for the juvenile samples were conducted with the modal simulation file from the simulation runs. All parental assignments were designated at the strict confidence level (99.9%).

All remaining individuals that were successfully genotyped at 8 or more loci were subjected to sibship analyses as implemented in the software COLONY, vers. 2.0.6.4 (Jones and Wang, 2010), to identify any potential large family groups within the data set that could confound further genetic structure analyses. Two simulations were run by using settings of polygamous breeding, weak prior, updating allele frequencies, no genotyping error, and full likelihood and pairwise likelihood combined method for a medium run length. Any identified duplicate samples were removed from the data set prior to further analyses. Results were evaluated for consistency among runs for individual fullsib relationships as well as family sizes present.

For the initial analyses, the data set was partitioned into 18 geographic sections based on natural latitudinal breaks in the collection data (Table 2, Fig. 2). Standard population genetic statistical analyses were applied to the resulting sample data set. Population genetic structure throughout the collection range was assessed through evaluations of Hardy–Weinburg equilibrium (HWE) in GenAlEx, vers. 6.5 (Peakall and Smouse, 2006, 2012), analysis of molecular variance (AMOVA) in Arlequin, vers. 3.5.1.2 (Excoffier and Lischer, 2010), pairwise F_{ST}-style statistics calculated in GenAlEx and Arlequin, and the clustering algorithms implemented in STRUCTURE, vers. 2.3.4 (Pritchard et al., 2000). Iterative AMOVAs (R_{ST}-based) were conducted to evaluate areas of genetic discontinuity in the data set with potential location groupings under 2- and 3-population scenarios. Pairwise comparisons of sample locations and HWE were conducted initially at the smallest geographic scale, and locations were combined sequentially to represent the smallest number of homogenous groupings. Estimates of R_{ST}, F_{ST}, G_{ST}, G'_{ST} (Nei, 1973), G''_{ST}, and D_{EST} were initially calculated to verify consistency across metrics. Because patterns of all estimates were consistent, only R_{ST} metrics are reported. The clustering model assignment employed in the program STRUCTURE by using a hierarchical approach with the assistance of the web-based software STRUCTURE HARVESTER, vers. 0.6.94 (Earl and vonHoldt, 2012), was used to identify the most appropriate number of distinct populations (K) of each run. Simulations were run by using the locprior parameter, with 5 replicates for each K, the length of the burn-in period was 20,000 runs, and the number of Markov chain Monte-Carlo reps after burn-in was 20,000. Sites that were strongly assigned to one population were removed from the data set, and STRUCTURE was run iteratively until K=1 was the most appropriate assignment for each cluster. The effective numbers of migrants per generation and year (based on generation time of 5–7 years for cobia) were calculated for each resulting homogenous cluster in Arlequin.

Results

Tag-recapture data

The tagging data analyzed covers a 29-year period, with the first fish tagged in 1988 and the last recapture occurring in 2017. During that period, 25,867 cobia were tagged cumulatively by all 7 tagging programs (Table 1), and 2124 cobia were subsequently recaptured and reported (8%) with the highest recapture rates occurring in South Carolina (18%) and Virginia (11%) and the lowest in the GOM (7%). After removing recaptures that were missing location or date information (n=110) as well as those that occurred less than 30 d after tagging (n=264), the combined data set consisted of 1750 recaptures. Mean FL at tagging was largest in Virginia, South Carolina, and North Carolina (Table 3) and was smaller along the coast of Florida and in the GOM. Overall, mean FL at tagging was 786 mm, indicating that most tagging efforts were focused on sublegal cobia because the minimum legal size was 838 mm FL until September 2017 in federal waters in the western North Atlantic Ocean and until 2016 in North Carolina and Virginia state waters. Minimum legal size in the GOM remains 838 mm FL. Mean FL at recapture (Table 4) was largest from cobia recaptured in North Carolina, South Carolina, and Virginia but did not vary greatly

Table 2

Details about collection of samples of cobia (*Rachycentron canadum*) captured in the Gulf of Mexico and Atlantic Ocean in the southeastern United States during 2005–2017 and successfully genotyped for inclusion in genetic data analyses. Sample sizes are given for both the initial partitioned data set and the final grouped data set.

Code	Location	Collection years	Sample size		Final group code
			Initial	Final	
TX	Texas (Corpus Christi)	2010–2011	51		
MS	Mississippi	2010	6		
FLW	Florida panhandle	2008, 2017	45		
FLS	Florida Keys	2010, 2015	9	385	GOM
FLE1	Boynton Beach to Jupiter Beach	2016–2017	36		
FLE2	Hobe Sound to Ft. Pierce	2011, 2015–2017	238		
FLE3	Canaveral/Sebastian	2014–2017	77	77	FLE3
FLGA	Jacksonville, FL, to Brunswick, GA	2009–2010, 2016–2017	16	50	FLGA
GA	Savannah	2008–2009, 2012, 2014–2016	34		
SCO1	Offshore Port Royal Sound, Betsy Ross Reef	2009–2016	430		
SCO2	Offshore Charleston, Murrels Inlet, Georgetown	2007–2011, 2015–2017	21		
SCO	All other SC offshore samples	2007–2009, 2014–2017	615	1291	Atlantic offshore
NCO1	Offshore south of Cape Hatteras	2010, 2013–2014, 2016–2017	35		
NOC2	Offshore at and north of Cape Hatteras	2008–2010, 2016–2017	190		
SCI	SC inshore	2005, 2007–2016	834	834	SC inshore
NC1	Inshore area around Cape Lookout	2010, 2016–2017	16		
NC2	Inshore area of Pamlico Sound	2010, 2016–2017	41	159	NCVA inshore
VA	VA inshore	2006–2008, 2017	102		

from zone to zone. For all cobia recaptures, the mean number of days between initial tagging and recapture (days at large) was 463 d and varied slightly depending on tagging zone (Table 5). The results from the 4 main tagging zones, Virginia, South Carolina, Brevard County in Florida, and the Florida Keys, generated a large number of recaptures (n=90–351), provided information relevant to assessing the stock boundary between GOM and western North Atlantic Ocean cobia, and are reported herein. The remaining 6 zones provided supplementary data that are reflected in overall summaries of movement. References to the number of cobia tagged in a specific region or time of year will henceforth refer only to tagging events with a subsequent recapture in excess of 30 d.

Virginia

All cobia in the Virginia zone were tagged within the Chesapeake Bay or immediately adjacent as part of an annual spawning aggregation (Richards, 1967) that occurs during summer (n=351). Peak interactions occur over a relatively brief period, and most fish were captured during June–August, when 91% (n=321) of tagging events and 88% (n=277) of recaptures took place. In contrast, only 1% (n=4) of cobia tagging events and 2% (n=6) of recaptures occurred during October–April. Cobia tagged in this zone were largely recaptured in the same zone (n=293, 84%) in subsequent years and often in close proximity to the tagging location (Fig. 3). There was considerable exchange between the Chesapeake Bay and the North Carolina Outer Banks, with Chesapeake Bay fish tagged during July–September being recaptured in North Carolina during April–July (n=34) or October–December (n=8). In total, 95% of cobia tagged in Virginia were recaptured in the Virginia or North Carolina zones. A similar pattern occurred with cobia tagged off North Carolina, where 86% (n=18) were eventually recaptured in the Chesapeake Bay. A small subset of cobia tagged in the Chesapeake Bay during summer were also recaptured off the east coast of Florida (north of Brevard/Brevard zones) during late fall–winter (n=2) or spring (n=6). Three cobia were also recaptured in the GOM, after 2–4 years at large. The furthest of these recaptures represents a movement of at least 2500 km from the tagging location. Although unexpected, these long distance movements are consistent with genetic data that indicate some level of gene flow between GOM and western North Atlantic Ocean stocks.

South Carolina

Historically, cobia annually aggregate in 3 South Carolina estuaries, Port Royal, Calibogue, and St. Helena Sounds, along with coastal waters from roughly 0–30 km offshore during April–June. The majority of South Carolina cobia (n=128) were tagged within Port Royal Sound during these aggregations (n=112, 88%). Peak interactions in South Carolina coastal waters are brief. Over 90% of tagging (n=117) and recaptures (n=111) occurred during April–July, whereas only 2% (n=2) of tagging and 3% (n=3) of recaptures occurred in October–March. As in Virginia, the

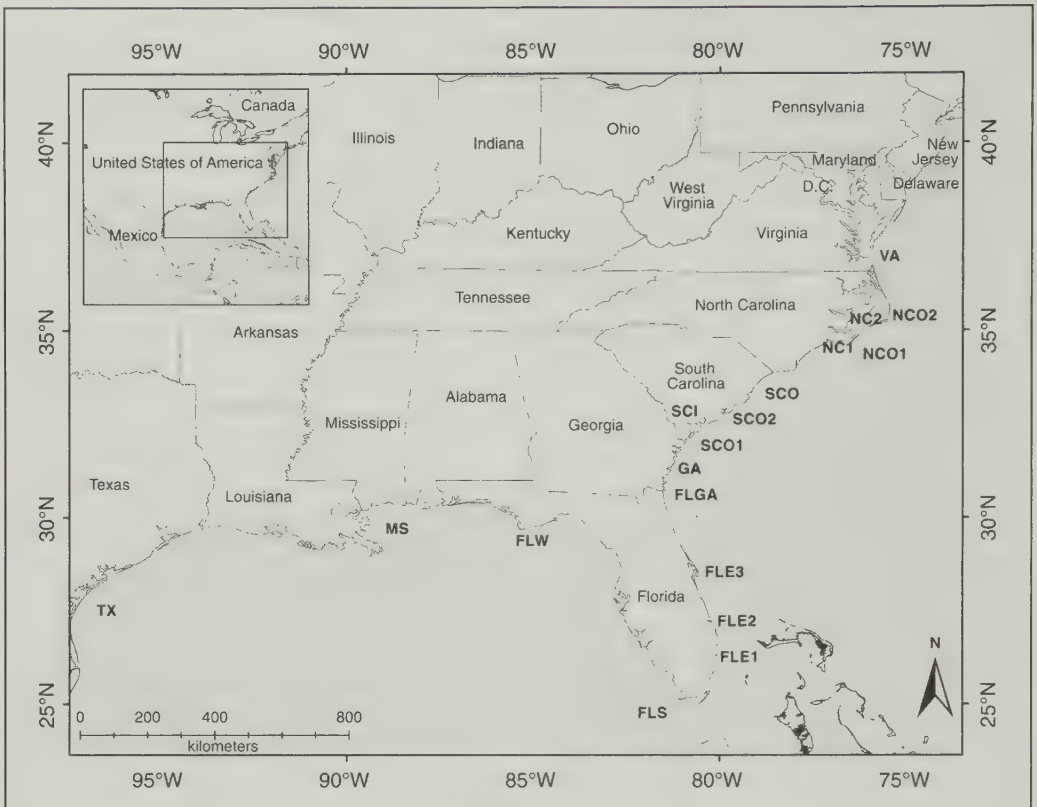

Figure 2

Map of study area showing the 18 genetic sample groupings used in analyses for cobia (*Rachycentron canadum*) collected in the Atlantic Ocean off the southeastern United States during 1988–2017. Groupings were determined on the basis of natural latitudinal breaks in the collection data. Abbreviations for group locations are given in Table 2.

Table 3

Mean fork length (FL) at tagging, by tagging zone, of cobia (*Rachycentron canadum*) sampled from 1988 through 2017. The tagging zones of Georgia (n=1) and north of Brevard County, Florida (n=2), were excluded because of small sample sizes. Standard deviations (SDs) are given for means. GOM=Gulf of Mexico.

Tagging zone	Mean FL (mm)
Virginia	853 (SD 9)
North Carolina	803 (SD 19)
South Carolina	825 (SD 10)
Brevard County	774 (SD 15)
South of Brevard	740 (SD 30)
Florida Keys	750 (SD 6)
GOM	764 (SD 25)
Total	786 (SD 19)

Table 4

Mean fork length (FL) at recapture, by recapture zone, of cobia (*Rachycentron canadum*) sampled from 1988 through 2017. The recapture zones of north of Virginia (sample size [n]=2) and Georgia (n=5) were excluded because of small sample sizes. Standard deviations (SDs) are given for means. GOM=Gulf of Mexico.

Recapture zone	Mean FL (mm)
Virginia	964 (SD 10)
North Carolina	1008 (SD 29)
South Carolina	985 (SD 13)
North of Brevard	957 (SD 19)
Brevard	921 (SD 21)
South of Brevard	972 (SD 20)
Florida Keys	903 (SD 8)
GOM	935 (SD 6)

majority of South Carolina cobia were recaptured within the South Carolina zone (n=112, 87.5%) in subsequent years and in close proximity to the tagging location (Fig. 3). Cobia tagged in South Carolina were also recaptured off the east coast of Florida (north of Brevard/Brevard), primarily during November–April (n=12). In total, 98% of cobia tagged in South Carolina were recaptured there or in the north of Brevard/Brevard zones. One cobia tagged within Port Royal Sound was recaptured in the GOM off the central coast of Florida after 2 years at large.

Table 5

Mean number of days between initial tagging and recapture (days at large), by tagging zone, for cobia (*Rachycentron canadum*) captured and tagged between 1988 and 2017. Standard deviations (SDs) are given for means. GOM=Gulf of Mexico.

Tagging zone	Mean days at large
Virginia	539 (SD 25)
North Carolina	766 (SD 190)
South Carolina	496 (SD 33)
Brevard County	400 (SD 38)
South of Brevard	430 (SD 86)
Florida Keys	362 (SD 22)
GOM	449 (SD 13)
Total	464 (SD 10)

Brevard County, Florida

Of the 90 recaptures from the Brevard zone, the majority (n=56, 62%) were tagged during March–April, and 31% (n=18) of recaptures occurred then as well. However, in contrast to the Virginia and South Carolina zones, cobia were available over a long period, and tagging occurred in every month of the year excluding September. Additionally, recaptures occurred in the Brevard zone during every month of the year. Cobia tagged in the Brevard zone were also recaptured over a very wide geographic area, from Texas to New Jersey, and recaptures of Brevard-tagged cobia occurred in every zone (Fig. 3). Recaptures in the Brevard zone occurred from cobia tagged from Louisiana to Virginia. Unlike in Virginia and South Carolina, where the majority of cobia were recaptured in the same zone where tagging occurred, only 37% (n=33) of the cobia tagged in the Brevard zone were also recaptured in the Brevard

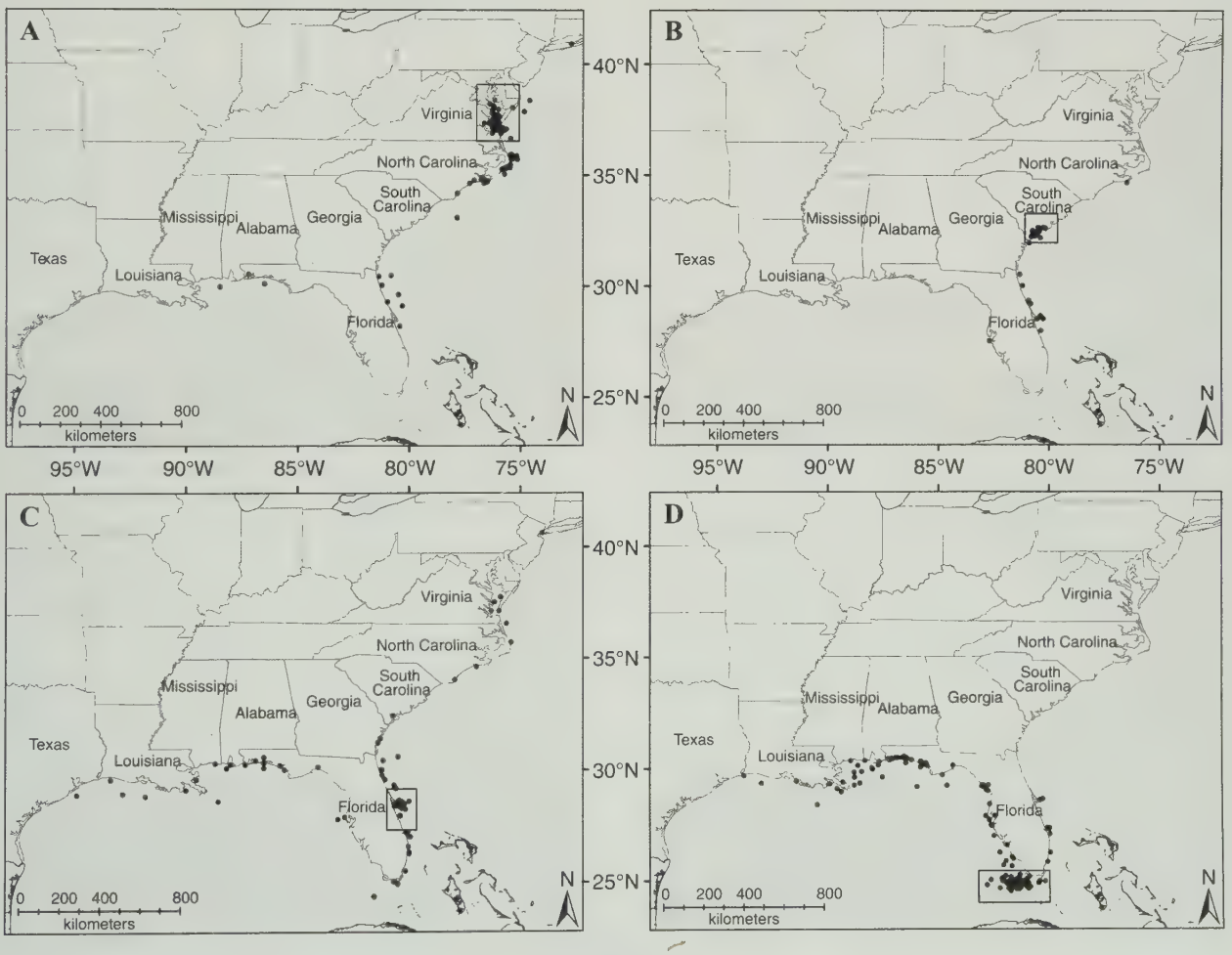

Figure 3

Maps of study area showing the sites where cobia (*Rachycentron canadum*) were recaptured after being tagged in 1988–2017 in 4 zones: (**A**) Virginia, including all waters of the Chesapeake Bay, (**B**) South Carolina, (**C**) Brevard County, Florida, and (**D**) Florida Keys. A rectangle indicates the general tagging location in each zone.

zone. The next largest group of exchange was the GOM, where 22% (n=20) of recaptures occurred. Cobia tagged in Brevard in January–March were largely recaptured in the GOM during April–May. Exchange also occurred with the south of Brevard and Florida Keys zones (n=14, 16% collectively), north of Brevard (n=10, 11%), and the zones north of the Florida border (n=13, 14% collectively).

Florida Keys

In a pattern similar to that of the Brevard zone, cobia were tagged (n=181) and recaptured during every month of the year in this zone. The majority of tagging events (n=109, 60%) and recaptures (n=113, 56%) occurred during December–March. Only 18% (n=32) of tagging events and 21% (n=43) of recaptures occurred during June–October. Most fish tagged in the Florida Keys zone were recaptured in the same zone (n=104, 57%), often in close proximity to the tagging location (Fig. 3). The next greatest area of exchange was the GOM zone (n=66, 37%), with most recaptures occurring during April and May. Conversely, of the 201 cobia recaptured in the Florida Keys zone, 45% (n=90) were originally tagged in the GOM. Cobia tagged in the Florida Keys zone were recaptured in the GOM from Texas to the west coast of Florida, and recaptures from the Florida Keys and GOM zones collectively account for 94% of all recaptures for this group. The remaining 6% (n=10) were recaptured on the east coast of Florida (Brevard/south of Brevard zones). To date, no cobia tagged in the Florida Keys zone have been recaptured north of Cape Canaveral, and no cobia tagged north of Florida on the East Coast have been recaptured in the Florida Keys zone.

Tagging summary

Cobia tagged in the GOM were captured in the western North Atlantic Ocean (n=59, 6%) and cobia tagged in the western North Atlantic Ocean were recaptured in the GOM (n=26, 4%) in relatively small numbers. However, most of this exchange occurred between the GOM and the east coast of Florida. Movements of cobia tagged north of Florida to the GOM (n=4, 0.6%) and from the GOM to north of Florida (n=4, 0.4%) were very rare. Movements of fish tagged above the current stock delineation at the border of Florida and Georgia to the north of Brevard and Brevard zones in northern and central Florida (n=21, 4%) and vice versa (n=14, 14%) were somewhat more common. Evaluating the frequency of recaptures by recapture location can provide information on the seasonal availability and susceptibility of cobia to the fishery during the period of the study. In the northern area, from Georgia through the Mid-Atlantic region, cobia were mostly recaptured during May–August (n=434, 88%) with a peak in June (n=144, Table 6). In the GOM, cobia were present for a slightly longer period with recaptures mostly occurring between April and September (n=767, 84%), peaking in April (n=164). In contrast to the areas from Georgia to the north and the GOM, cobia recaptures along the east coast of Florida and the Florida Keys occurred throughout the year, with no clear temporal peaks.

Table 6

Number of cobia (*Rachycentron canadum*) recaptured by month from 1988 through 2017 for 3 regions along the southeastern coast of the United States. GOM=Gulf of Mexico.

Month	GOM	East Florida and Florida Keys	North of Florida
January	11	41	2
February	12	39	1
March	28	61	1
April	165	35	18
May	141	24	103
June	139	15	144
July	127	23	112
August	111	20	75
September	85	10	26
October	58	18	7
November	26	20	3
December	11	34	3

Genetics

A total of 2796 samples meeting our selection criteria were successfully genotyped for inclusion in data analyses; collection years for samples included 2005 through 2017 (Table 2). Only a single duplicate sample and 39 hatchery-produced fish occurred within the original data set. No large family groups (>3 siblings) were present within the data set, and only 12 fullsib pairs were identified (P=1.0); therefore, no confounding effects from family structure are anticipated in further analyses.

Results from multiple rounds of hierarchical STRUCTURE, initial pairwise F_{ST}, and HWE analyses support the notion of a genetically distinct South Carolina inshore population and a homogenous GOM population ranging from Texas through the Ft. Pierce, Florida, area (FLE2) (Fig. 4). Additionally, the Virginia and inshore North Carolina (NC1, NC2) samples represented a distinct genetic grouping, as did the combined offshore South Carolina and North Carolina samples (SCO, SCO1, SCO2, NCO1, NCO2) (Fig. 4). Samples from Cape Canaveral, Florida, through Savannah, Georgia, had genetic similarities with samples from collection locations both to the north (SCOs) and to the south (FLE2) and appeared to reflect a geographic transition zone in the STRUCTURE analyses (Fig. 4). As such, the iterative AMOVA were employed to evaluate potential breaks in gene flow within the area, including all potential locations from those of Atlantic Ocean offshore (SCOs, NCOs) and Savannah (GA) samples through those of Jupiter Beach (FLE1) and Hobe Sound (FLE2) in Florida. Results indicate that the strongest significant break (R_{ST}=0.0073, P=0.001) among the groupings occurred with the separation between the Cape Canaveral (FLE3) and Jacksonville, Florida/Brunswick, Georgia (FLGA) locations, explaining 0.73% of the variation in the data set. However, grouping scenarios between

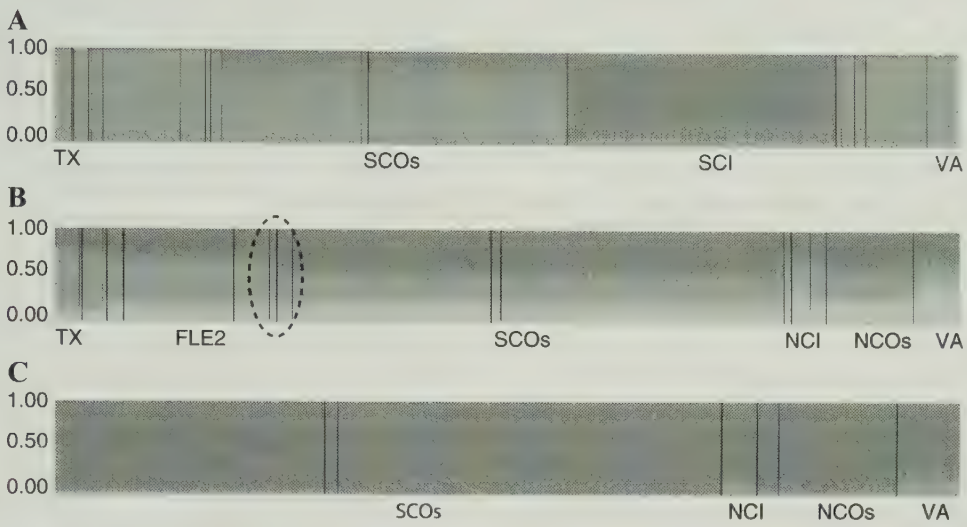

Figure 4

Genetically determined population ancestry plots for cobia (*Rachycentron canadum*) collected in the Gulf of Mexico (GOM) and Atlantic Ocean off the southeastern United States in 2006–2017, produced by using the program STRUCTURE. Each vertical bar represents an individual in the plot with shades or colors indicating percent ancestry to each genetic group. Genetic groupings or collections, as presented in Table 2, are geographically oriented from Texas (TX) on the left to Virginia inshore (VA) on the right. (**A**) Results for the complete data set when the number of distinct populations (K) was 2, with the South Carolina inshore (SCI) collection identified as distinct from the remaining data. (**B**) Results for the data set that excludes the SCI samples, indicating distinct populations (K=4) for the GOM and Florida groupings (TX–FEL2) and the North Carolina inshore (NCI) and VA groupings. Analyses of samples from South Carolina and North Carolina offshore collections (SCOs and NCOs) indicate a homogenous population, and the Cape Canaveral, Florida, through Savannah, Georgia, collections represent a transition zone as indicated by the dashed oval. (**C**) Results for the data set that excludes SCI, GOM, and east coast of Florida and Georgia groupings (K=2), with the NCI and VA collections grouped together and with a distinct population (K=1) indicated for an Atlantic Ocean offshore group consisting of the remaining SCOs and NCOs.

the Atlantic Ocean offshore (SCOs, NCOs) and Savannah (GA) samples, between Savannah (GA) and Jacksonville–Brunswick (FLGA) samples, and between Ft. Pierce (FLE2) and Cape Canaveral (FLE3) samples were also significant but not as strong (R_{ST}=0.0067–0.0069, P=0.004–0.006), explaining 0.67–0.69% of the variation. The last AMOVA scenario (break between Jupiter Beach and Hobe Sound) did not partition a significant amount of variation among groupings (P=0.450). Therefore, the AMOVA also support the occurrence of a transition zone from Cape Canaveral through Savannah.

Guided by these analyses, final sample groupings included GOM, South Carolina inshore, North Carolina–Virginia inshore, and Atlantic Ocean offshore populations, as well as the Cape Canaveral and Jacksonville–Savannah groupings (Table 2). Due to the lower sample sizes from some of the GOM and North Carolina inshore collection locations, deviations from HWE were evaluated to verify no substructure was being masked within these regions. No loci were out of HWE within the GOM population and only a single locus was out of HWE (P<0.001) in the combined North Carolina inshore and Virginia data set, supporting the groupings. Pairwise comparisons among these groupings confirmed significant differences between all groupings (P<0.00001–0.04), except comparisons with the Cape Canaveral and Jacksonville–Savannah groupings with GOM and Atlantic Ocean offshore populations (P=0.07–0.96). Significant genetic differentiation ranged from an R_{ST} of 0.020 between South Carolina inshore and GOM populations to an R_{ST} of 0.006 between the South Carolina inshore and Atlantic Ocean offshore populations (Table 7). The levels of genetic differentiation detected translated into effective number of migrants ranging from 0.2 to 10.0 individuals/year between these populations. Therefore, the results indicate that the cobia stock boundary is occurring somewhere within a range from Cape Canaveral to northern Georgia, a location that is consistent with that of the current management stock boundary along the coast of the southeastern United States.

Discussion

A few major patterns became apparent when tagging data were evaluated together. Cobia in the area north of Florida were seasonally available as a pulse fishery in close proximity

Table 7

Ranked R_{ST} values from significant pairwise comparisons among final genetic sample groupings of cobia (*Rachycentron canadum*) with effective number of migrants (N_{em}). Annual calculations are based on a generation time of 5–7 years. Examined regions include South Carolina inshore (SC inshore), North Carolina–Virginia inshore (NCVA inshore), Gulf of Mexico (GOM), Jacksonville, Florida, and Savannah, Georgia (FLGA), Cape Canaveral, Florida (FLE3), and Atlantic Ocean offshore.

Pairwise comparison	R_{ST}	N_{em} per generation	N_{em} per year
SC inshore–GOM	0.020	1.0	0.2–0.6
SC inshore–NCVA inshore	0.019	12.9	1.8–2.6
SC inshore–FLE3	0.015	20.5	2.9–4.2
NCVA inshore–GOM	0.012	20.6	2.9–4.1
NCVA inshore–FLGA	0.011	22.5	3.2–4.5
NCVA inshore–FLE3	0.009	27.5	3.9–5.5
SC inshore–FLGA	0.009	27.5	3.9–5.5
Atlantic offshore–GOM	0.007	35.5	5.1–7.1
SC inshore–Atlantic offshore	0.006	41.4	5.9–8.3
NCVA inshore–Atlantic offshore	0.005	49.8	7.1–10.0

to the coast during spring and summer and are largely absent from harvest during cooler months. One group of cobia moves through coastal North Carolina waters in May–June and in October on their way to and from the Chesapeake Bay, although some cobia aggregate in North Carolina estuaries as well (Smith, 1995). Another group moves into the southern estuaries of South Carolina during May and June. Higher recapture rates in the Chesapeake Bay and South Carolina estuaries indicate that fish remain within these systems for extended periods of time and may have historically been subject to higher fishing pressure than other areas, such as the GOM, where recapture rates are lower. There is evidence of some exchange between cobia tagged in South Carolina and Virginia with the central and northeast coast of Florida, indicating that some level of seasonal migration from south to north occurs. However, Hendon and Franks[3] described potential inshore–offshore seasonal movements in the northern GOM, and the authors believe inshore–offshore movements occur in the western North Atlantic Ocean as well. A movement from estuarine or nearshore environments to deeper, warmer offshore waters in winter may explain why so few fish tagged in either South Carolina or Virginia are recaptured in other zones and are so frequently recaptured in the same locations in subsequent years. Cobia moving into deeper waters may be subject to reduced fishing pressure and therefore less likely to be recaptured until seasonally moving back into natal estuaries or nearshore waters where more concentrated fishing effort occurs. Commercial catch data (Wrege[7]) and pop-up satellite archival tagging data (Jensen and Graves[8]) provide evidence that cobia are present on the continental shelf waters of North Carolina, South Carolina, Georgia, and north Florida in winter. Additionally, cobia fitted with acoustic transmitters in South Carolina and Georgia were completely absent from detection in coastal receiver arrays in winter (Young et al.[9]), indicating movement into other areas (i.e., deeper water).

There is strong evidence that some cobia use the areas along the east coast of Florida and the Florida Keys as overwintering locations before undertaking a seasonal migration into the GOM during spring and summer, as also reported by Dippold et al. (2017). To a lesser extent, a similar migration occurs between central and north Florida to the north as described above. However, there is evidence that some cobia may be largely resident to these locations throughout the year. Many cobia tagged in winter have been recaptured in the same zone in summer and vice versa, representing fish that are not likely undertaking a seasonal migration to the GOM or north along the Atlantic coast.

Although it has been speculated that the Florida Keys serve as an overwintering location for both western North Atlantic Ocean and GOM cobia and a boundary between the 2 stocks, the available genetic and tagging data do not support that conclusion. A segment of the GOM cobia stock does appear to overwinter in the Florida Keys and migrate into the northern GOM during spring. However, despite movement into southeast and central Florida, no cobia tagged in the Florida Keys were recaptured north of Cape Canaveral. Franks et al. (1991), Hammond[10], and Dippold et al. (2017) describe routine movements of cobia between the GOM and western North Atlantic Ocean. However, virtually all of these movements occurred between the GOM and the southeast and central coasts of Florida. This finding is supported by the results of the genetic analysis, indicating that cobia collected from the Florida Keys and southeast coast of Florida were genetically similar to those collected throughout the GOM. Analyses of our robust microsatellite data set indicates that a genetic break occurs somewhere between Cape Canaveral and northern Georgia. Tagging results indicate that cobia tagged near Cape Canaveral distribute widely to both the GOM and north of Florida, with greater dispersal to the GOM. These results indicate that the area around Cape Canaveral serves as a transitional area for GOM and western North Atlantic Ocean cobia. Although we are confident

[7] Wrege, B. M. 2018. Spatial and temporal distribution of cobia, Southeast US and Gulf of Mexico. SEDAR58-SID-10, 18 p. Southeast Data Assessment and Review (SEDAR), North Charleston, SC. [Available from website.]

[8] Jensen, D., and J. Graves. 2018. Use of pop-up satellite archival tags (PSATs) to investigate the movements, habitat utilization, and post-release survival of cobia (*Rachycentron canadum*) that summer in Virginia waters. SEDAR58-SID-02, 12 p. Southeast Data Assessment and Review (SEDAR), North Charleston, SC. [Available from website.]

[9] Young, J., M. Perkinson, K. Brenkert, E. Reyier, and J. Whittington. 2018. Cobia telemetry working paper. SEDAR58-SID-08, 15 p. Southeast Data Assessment and Review (SEDAR), North Charleston, SC. [website.]

[10] Hammond, D. L. 2001. Status of the South Carolina fisheries for cobia. South Carolina Dep. Nat. Resour., Mar. Resour. Div., Tech. Rep. 89, 22 p.

that Cape Canaveral falls within this transitional area, genetic and tag-recapture data for northern Florida and Georgia are limited, making it difficult to determine how far this transition extends to the north.

The area around Cape Canaveral is a well-studied phylogeographic break for many species (Burton, 1998; Hellberg et al., 2002). Species that either terminate their southern range or show a divergence in genetics in this area include the Eastern oyster (*Crassostrea virginica*) (Reeb and Avise, 1990), Atlantic menhaden (*Brevoortia tyrannus*) and black sea bass (*Centropristis striata*) (Bowen and Avise, 1990), and American horseshoe crab (*Limulus polyphemus*) and oyster toadfish (*Opsanus tau*) (Avise, 1992). The region marks the transition from a temperate to a subtropical climate where the Gulf Stream diverges from the coastline (Avise, 1992), with potential implications for the distribution of eggs and larvae. Differences in water temperature between the areas north and south of Cape Canaveral may also have an impact on the migratory behavior of cobia. Oceanographic temperature data from the NOAA National Data Buoy Center indicate that the coastal waters at and just north of Cape Canaveral are the southernmost location along the U.S. Atlantic coast where coastal mean water temperatures routinely fall below 20°C during winter. The waters offshore or south of Cape Canaveral through the Florida Keys typically remain above 20°C throughout the year. These moderate winter water temperatures may explain why some cobia in these waters do not appear to make long migrations and may be found there year-round. By contrast, coastal waters north of Cape Canaveral regularly fall below 20°C and result in the movement of cobia into more southerly waters, deeper waters, or a combination of both.

The transitional area occurring within the range of Cape Canaveral to northern Georgia appears to serve as a major division between GOM and western North Atlantic Ocean stocks. The complete population structure and migratory patterns of GOM and Atlantic Ocean cobia is likely more complex. Tag-recapture data indicate multiple migratory behaviors and geographic partitioning of cobia in the Atlantic Ocean group underscored by the lack of exchange between cobia tagged in Virginia or North Carolina and cobia tagged in South Carolina. Hendon and Franks[3] suggested multiple migratory patterns from cobia tagged in the GOM as well. These complicated migratory patterns are further supported by genetic analysis. Darden et al. (2014) found evidence of distinct population segments within the western North Atlantic Ocean stock. Although our study found no genetic differences throughout the GOM stock, increased sample sizes in the Florida Keys and northern GOM locations could potentially provide greater resolution into the genetic population structure of cobia in these areas. Current projects that use acoustic and satellite telemetry, as well as additional genetic and conventional tagging data, when evaluated in concert, will increase our understanding of cobia structure on a regional level and benefit the assessment and management process moving forward.

Acknowledgments

We wish to thank the late K. Burns whose tagging data was integral to these analyses and the Mote Marine Laboratory for allowing their inclusion. We also thank the Hilton Head Reef Foundation, S. Poland at the North Carolina Division of Marine Fisheries, contributing anglers, and the NOAA Hollings Marine Laboratory. Funding for the analyses included South Carolina Saltwater Recreational License Funds and NOAA CRP project NA15NMF4540105. This manuscript represents SCDNR MRRI contribution number 807.

Literature cited

Avise, J. C.
1992. Molecular population structure and the biogeographic history of a regional fauna: a case history with lessons for conservation biology. Oikos 63:62–76.

Begg, G. A., and J. R. Waldman.
1999. An holistic approach to fish stock identification. Fish. Res. 43:35–44.

Begg, G. A., D. S. Cameron, and W. Sawynok.
1997. Movements and stock structure of school mackerel (*Scomberomorus queenslandicus*) and spotted mackerel (*S. munroi*) in Australian east-coast waters. Mar. Freshw. Res. 48:295–301.

Bielawski, J. P., and D. E. Pumo.
1997. Randomly amplified polymorphic DNA (RAPD) analysis of Atlantic Coast striped bass. Heredity 78:32–40.

Biesiot, P. M., R. E. Caylor, and J. S. Franks.
1994. Biochemical and histological changes during ovarian development of cobia, *Rachycentron canadum*, from the northern Gulf of Mexico. Fish. Bull. 92:686–696.

Bowen, B. W., and J. C. Avise.
1990. Genetic structure of Atlantic and Gulf of Mexico populations of sea bass, menhaden, and sturgeon: influence of zoogeographic factors and life-history patterns. Mar. Biol. 107:371–381.

Briggs, J. C.
1960. Fishes of worldwide (circumtropical) distribution. Copeia 1960:171–180.

Burton, R. S.
1998. Intraspecific phylogeography across the Point Conception biogeographic boundary. Evolution 52:734–745.

Cadrin, S. X., K. D. Friedland, and J. R. Waldman (eds.).
2005. Stock identification methods: applications in fishery science, 736 p. Elsevier, Burlington, MA.

Campbell, M. R., C. C. Kozfkay, T. Copeland, W. C. Schrader, M. W. Ackerman, and S. R. Narum.
2012. Estimating abundance and life history characteristics of threatened wild Snake River steelhead stocks by using genetic stock identification. Trans. Am. Fish. Soc. 141:1310–1327.

Darden, T. D., M. J. Walker, K. Brenkert, J. R. Yost, and M. R. Denson.
2014. Population genetics of Cobia *Rachycentron canadum*: implications for fishery management along the coast of the southeastern United States. Fish. Bull. 112:24–35.

Dippold, D. A., R. T. Leaf, J. S. Franks, and J. R. Hendon.
2017. Growth, mortality, and movement of cobia (*Rachycentron canadum*). Fish. Bull. 115:460–472.

Ditty, J. G., and R. F. Shaw.
1992. Larval development, distribution, and ecology of cobia *Rachycentron canadum* (Family: Rachycentridae) in the northern Gulf of Mexico. Fish. Bull. 90:668–677.

Earl, D. A., and B. M. vonHoldt.
2012. STRUCTURE HARVESTER: a website and program for visualizing STRUCTURE output and implementing the Evanno method. Conserv. Genet. Resour. 4:359–361.

Excoffier, L., and H. E. L. Lischer.
2010. Arlequin suite ver 3.5: a new series of programs to perform population genetics analyses under Linux and Windows. Mol. Ecol. Resour. 10:564–567.

Flannery, B. G., R. E. Spangler, B. L. Norcross, C. J. Lewis, and J. K. Wenburg.
2013. Microsatellite analysis of population structure in Alaska eulachon with application to mixed-stock analysis. Trans. Am. Fish. Soc. 142:1036–1048.

Franks, J. S., and N. J. Brown-Peterson.
2002. A review of age, growth, and reproduction of cobia, *Rachycentron canadum,* from U.S. waters of the Gulf of Mexico and South Atlantic Ocean. Proc. Gulf Caribb. Fish. Inst. 53:553–569.

Franks, J. S., M. H. Zuber, and T. D. McIlwain.
1991. Trends in seasonal movements of cobia *Rachycentron canadum* tagged and released in the northern Gulf of Mexico. J. Miss. Acad. Sci. 36(1):55.

GMFMC and SAFMC (Gulf of Mexico and South Atlantic Fishery Management Councils).
1983. Fishery management plan for coastal migratory pelagic resources in the Gulf of Mexico and South Atlantic Region, 311 p. Gulf Mex. Fish. Manage. Counc., Tampa, FL, and South Atl. Fish. Manage. Counc., North Charleston, SC.
2011. Final amendment 18 to the fishery management plan for coastal migratory pelagic resources in the Gulf of Mexico and Atlantic Region including environmental assessment, regulatory impact review, and regulatory flexibility act analysis, 373 p. Gulf Mex. Fish. Manage. Counc., Tampa, FL, and South Atl. Fish. Manage. Counc., North Charleston, SC.
2014. Final amendment 20B to the fishery management plan for the coastal migratory pelagic resources in the Gulf of Mexico and Atlantic Region including environmental assessment, fishery impact statement, regulatory impact review, and regulatory flexibility act analysis, 258 p. Gulf Mex. Fish. Manage. Counc., Tampa, FL, and South Atl. Fish. Manage. Counc., North Charleston, SC.

Hansen, L. P., and J. A. Jacobson.
2003. Origin and migration of wild and escaped farmed Atlantic salmon, *Salmo salar* L., in oceanic areas north of the Faroe Islands. ICES J. Mar. Sci. 60:110–119.

Hassler, W. W., and R. P. Rainville.
1975. Techniques for hatching and rearing cobia, *Rachycentron canadum*, through larval and juvenile stages. Univ. N.C. Sea Grant Coll. Program Rep. UNC-SG-75-30, 26 p. Sea Grant, Raleigh, NC.

Hellberg, M. E., R. S. Burton, J. E. Neigel, and S. R. Palumbi.
2002. Genetic assessment of connectivity among marine populations. Bull. Mar. Sci. 70(Suppl. 1):273–290.

Hilborn, R., and C. J. Walters (eds.).
1992. Quantitative fisheries stock assessment: choice, dynamics and uncertainty, 570 p. Chapman and Hall, New York.

Hrincevich, A. W.
1993. Mitochondrial DNA analysis of cobia *Rachycentron canadum* population structure using restriction fragment length polymorphisms and cytochrome *B* sequence variation. M.S. thesis, 91 p. Univ. South. Miss., Hattiesburg, MS.

Izzo, C., T. M. Ward, A. R. Ivey, I. M. Suthers, J. Stewart, S. C. Sexton, and B. M. Gillanders.
2017. Integrated approach to determining stock structure: implications for fisheries management of sardine, *Sardinops sagax*, in Australian waters. Rev. Fish Biol. Fish. 27:267–284.

Jones, O. R., and J. Wang.
2010. COLONY: a program for parentage and sibship inference from multilocus genotype data. Mol. Ecol. Resour. 10:551–555.

Kalinowski S. T., M. L. Taper, and T. C. Marshall.
2007. Revising how the computer program CERVUS accommodates genotyping error increases success in paternity assignment. Mol. Ecol. 16:1099–1106.

Knutsen, H., E. M. Olsen, P. E. Jorde, S. H. Espeland, C. André, and N. C. Stenseth.
2011. Are low but statistically significant levels of genetic differentiation in marine fishes 'biologically meaningful'? A case study of coastal Atlantic cod. Mol. Ecol. 20:768–783.

Lefebvre, L. S., and M. R. Denson.
2012. Inshore spawning of cobia (*Rachycentron canadum*) in South Carolina. Fish. Bull. 110:397–412.

MSFCMA (Magnuson-Stevens Fishery Conservation and Management Act).
2007. Public Law 94-265. [Available from website.]

Nei, M.
1973. Analysis of gene diversity in subdivided populations. Proc. Natl. Acad. Sci. U.S.A. 70:3321–3323.

Neilson, J. D., W. T. Stobo, and P. Perley.
2006. Pollock (*Pollachius virens*) stock structure in the Canadian Maritimes inferred from mark-recapture studies. ICES J. Mar. Sci. 63:749–765.

Orbesen E. S., J. P. Hoolihan, J. E. Serafy, D. Snodgrass, E. M. Peel, and E. D. Prince.
2008. Transboundary movement of Atlantic istiophorid billfishes among international and US domestic management areas inferred from mark-recapture studies. Mar. Fish. Rev. 70(1):14–23.

Parker, R. W., K. N. Paige, and A. L. Devries.
2002. Genetic variation among populations of the Antarctic toothfish: evolutionary insights and implications for conservation. Polar Biol. 25:256–261.

Peakall, R., and P. E. Smouse.
2006. GENALEX 6: genetic analysis in Excel. Population genetic software for teaching and research. Mol. Ecol. Notes 6:288–295.
2012. GenAlEx 6.5: genetic analysis in Excel. Population genetic software for teaching and research—an update. Bioinformatics 28:2537–2539.

Pritchard, J. K., M. Stephens, and P. Donnelly.
2000. Inference of population structure using multilocus genotype data. Genetics 155:945–959.

Renshaw, M. A., E. Saillant, S. C. Bradfield, and J. R. Gold.
2006. Microsatellite multiplex panels for genetic studies of three species of marine fishes: red drum (*Sciaenops ocellatus*), red snapper (*Lutjanus campechanus*), and cobia (*Rachycentron canadum*). Aquaculture 253:731–735.

Reeb, C. A., and J. C. Avise.
1990. A genetic discontinuity in a continuously distributed species: mitochondrial DNA in the American oyster, *Crassostrea virginica*. Genetics 124:397–406.

Richards, C. E.
1967. Age, growth and fecundity of the cobia, *Rachycentron canadum*, from Chesapeake Bay and adjacent Mid-Atlantic waters. Trans. Am. Fish. Soc. 96:343–350.

Ricker, W. E.
1948. Methods of estimating vital statistics of fish populations, 115 p. Indiana Univ. Publ., Bloomington, IN.
Saitoh, K.
1998. Genetic variation and local differentiation in the Pacific cod *Gadus macrocephalus* around Japan revealed by mtDNA and RAPD markers. Fish. Sci. 64:673–679.
SEDAR (Southeast Data Assessment and Review).
2013a. SEDAR 28—Gulf of Mexico cobia stock assessment report, 616 p. SEDAR, North Charleston, SC. [Available from website.]
2013b. SEDAR 28—South Atlantic cobia stock assessment report, 420 p. [Available from website.]
Shaffer, R. V., and E. L. Nakamura.
1989. Synopsis of biological data on the cobia *Rachycentron canadum* (Pisces: Rachycentridae). NOAA Tech. Rep. NMFS 82 [FAO Fish. Synop. 153], 21 p.
Smith, J. W.
1995. Life history of cobia, *Rachycentron canadum* (Osteichthyes: Rachycentridae), in North Carolina waters. Brimleyana 23:1–23.
Williams, E. H.
2001. Assessment of cobia, *Rachycentron canadum*, in the waters of the U.S. Gulf of Mexico. NOAA Tech. Memo. NMFS-SEFSC-469, 55 p.

National Marine
Fisheries Service
NOAA

Fishery Bulletin
established in 1881

Spencer F. Baird
First U.S. Commissioner
of Fisheries and founder
of *Fishery Bulletin*

Using otolith morphometric analysis to improve species discrimination of blackspotted rockfish (*Sebastes melanostictus*) and rougheye rockfish (*S. aleutianus*)

Jeremy P. Harris (contact author)[1]
Charles Hutchinson[1]
Sharon Wildes[2]

Email address for contact author: jeremy.harris@noaa.gov

[1] Alaska Fisheries Science Center
National Marine Fisheries Service, NOAA
7600 Sand Point Way NE
Seattle, Washington 98115-6349

[2] Auke Bay Laboratories
Alaska Fisheries Science Center
National Marine Fisheries Service, NOAA
17109 Point Lena Loop Road
Juneau, Alaska 99801

Abstract—Blackspotted rockfish (*Sebastes melanostictus*) and rougheye rockfish (*S. aleutianus*) are sympatric species found in the North Pacific Ocean. However, these species were not identified as separate taxa until the mid-2000s, and they remain difficult to differentiate in the field. These species are managed as a single mixed stock despite the fact that the North Pacific Fisheries Management Council rates them as Tier 3 species, meaning that an individual assessment including historical data is required for each. In this study, we developed a technique that distinguishes these species on the basis of otolith morphology and age, allowing both old and new collections to be identified to the correct species. Tissue samples and otoliths were collected from 1847 specimens during survey seasons in 2009 and 2013. Tissue samples were identified genetically to species by using the *Sma6* microsatellite locus. We used morphometrics, weight, and age from 859 otoliths to develop a logistic regression model that identified 97.3% of blackspotted rockfish and 86.2% of rougheye rockfish. Otolith shape analysis distinguishes rougheye rockfish and blackspotted rockfish and can allow for more focused management of these species.

Manuscript submitted 14 November 2018.
Manuscript accepted 15 August 2019.
Fish. Bull. 117:234–244 (2019).
Online publication date: 30 August 2019.
doi: 10.7755/FB.117.3.10

The views and opinions expressed or implied in this article are those of the author (or authors) and do not necessarily reflect the position of the National Marine Fisheries Service, NOAA.

The blackspotted rockfish (*Sebastes melanostictus*) and rougheye rockfish (*S. aleutianus*) are 2 of the largest and longest-lived rockfish species found in the North Pacific Ocean. The distribution of blackspotted rockfish stretches along the western coasts of the United States and Canada from Northern California to the Gulf of Alaska and across the Aleutian Islands and North Pacific Ocean to as far as Japan. The rougheye rockfish ranges from California to the Aleutian Islands (Orr and Hawkins, 2008). They are 2 of 72 rockfish species found in the North Pacific Ocean (Love et al., 2002). Although not targeted, rougheye rockfish and blackspotted rockfish occur as incidental catches in several major fisheries in the Gulf of Alaska, Bering Sea, and Aleutian Islands. Their slow population growth and late maturation make them vulnerable to overfishing (Ormseth and Spencer, 2011). These species are sympatric throughout the waters of Alaska, the coasts of British Columbia, Canada, and the West Coast of the United States, and they have only subtle morphological differences (Orr and Hawkins, 2008). Difficulties in accurately identifying these species have complicated research into their life history and ecology. Although both species are managed as a mixed stock at present, separation of the stock into individual species would be a major improvement in future assessments (Hicks et al., 2014; Shotwell et al., 2017).

Jordan and Evermann (1898) first described *S. aleutianus*, but it was not until 36 years later that Matsubara (1934) described a similar species, *S. melanostictus*. However, subsequent researchers reexamined the issue and found only 1 species with significant variation in body coloration (Barsukov, 1970; Kanayama and Kitagawa, 1982). A series of recent projects has since noted a genetic split within the species *S. aleutianus*, first on the basis of protein allozymes (Seeb, 1986; Hawkins et al., 2005) and subsequently by using mitochondrial DNA and microsatellites (Gharrett et al., 2005; Gharrett

et al., 2006). In this research, the 2 species, which were referred to as Type I and Type II, have a fixed difference at the *Sma6* microsatellite locus (Gharrett et al., 2005). Orr and Hawkins (2008) subsequently resurrected *S. melanostictus* for the blackspotted rockfish following a detailed morphological study. Orr and Hawkins (2008) also developed a discriminant model for identifying the 2 species with 97.8% total accuracy. Unfortunately, this method relies on careful caliper measurements of several morphological features, such as the gill rakers, dorsal spines, and pelvic fin rays. As such, this method has not been widely adopted for use with large-scale stock assessment surveys, and a quick and accurate method for distinguishing these species in the field remains elusive.

At sea, blackspotted rockfish can often be distinguished by black markings on the body, but these spots vary in number and intensity. Rougheye rockfish often have some minor spotting or dark coloration, such that there is considerable overlap in the color patterns of the species. Experienced field scientists can separate them with a moderate level of accuracy, but fishery observers and other personnel do not attempt to identify these species. The genus *Sebastes* has been found to have several cryptic species of similar appearance, but they have different habitat preferences and require different management measures (Hyde et al., 2008). Consequently, in some areas the fishery catch is predominantly blackspotted rockfish (Orr and Hawkins, 2008). If the catch is not evenly distributed, managing these species jointly runs the risk of causing detrimental effects to the more vulnerable population (Hawkins et al., 2005).

Otoliths are found as 3 paired sets of calcium carbonate structures in the inner ear of teleost fish species and function in hearing, balance, and orientation. In rockfish species, the sagittae are the largest of the otoliths and are most frequently collected for age determination. Age estimates are obtained by examining sectioned otoliths under a microscope, and ages obtained this way have been validated by using radiometric dating in a number of species (Hutchinson et al., 2007; Kastelle et al., 2008). Because otoliths from different populations may have unique shapes, the analysis of otolith data is a popular method for distinguishing similar species (Sadighzadeh et al., 2012) or different stocks within a species (Campana and Casselman, 1993; Hicks et al., 2003).

The purpose of this study was to develop a mathematical method that accurately separates the rougheye and blackspotted rockfish species on the basis of their otolith morphometrics and other data that are collected in the biennial fishery-independent surveys conducted by the NOAA Alaska Fisheries Science Center (AFSC) in the Gulf of Alaska. Because diagnostic genetic markers have been developed (Gharrett et al., 2005), it is possible to correctly identify a specimen to species and to use these genetically identified specimens to construct and validate a discrimination method based on otolith morphology. This model will be used to separate the 2 species in AFSC fishery-dependent collections and to verify field identifications made on stock assessment surveys. An otolith-based discrimination method would give scientists access to over 30 years of AFSC archived otolith collections that were not separated by species until 2006 and would greatly increase the data for each species.

Materials and methods

Sampling

Otoliths were collected from rougheye rockfish and blackspotted rockfish sampled from the Gulf of Alaska in the summers of 2009 and 2013 during AFSC survey cruises on contracted fishing vessels (Fig. 1). During 2009 and 2013, AFSC scientists collected 945 and 902 fish, respectively. At the time of capture, each sampled rockfish was measured and weighed, its sex was determined, and its otoliths were removed and stored in 50% glycerol-thymol solution. Fin clips were taken from each fish and stored in 20% dimethyl sulfoxide and 80% 0.25-M EDTA solution.

Genetic analysis

Fin clips were sent to the AFSC Auke Bay Laboratories in Juneau, Alaska, for genetic analysis. These samples were genotyped according to the methods published in Wimberger et al. (1999). The *Sma6* locus has been shown to clearly delineate rougheye and blackspotted rockfish species, with each species homozygous having a unique allele in more than 99.7% of all specimens (Gharrett et al., 2005). The field identifications were compared with the genetic

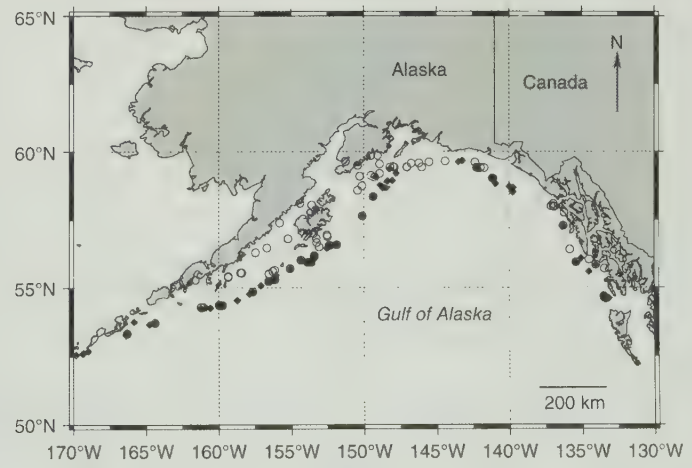

Figure 1

Map showing the locations where 859 rockfish were collected in 2009 and 2013 in the Gulf of Alaska. Data from sampled rougheye rockfish (*Sebastes aleutianus*) (open circles) and blackspotted rockfish (*S. melanostictus*) (black circles) were used for the models in this study.

identification to estimate the accuracy of survey personnel in field conditions. Specimens that could not be conclusively genetically identified were removed from further analysis.

Measurements and statistical analysis

Otoliths were prepared for measurements by blotting them dry and placing them under a dissecting microscope. The otoliths were viewed distal side facing up on a black background at a magnification of 6.3×. Image-Pro Plus[1] software (vers. 7; Media Cybernetics, Inc., Rockville, MD) was used to capture otolith images, calculate each otolith's area, perimeter, Feret length, and Feret width, and determine the length and width of each otolith from lines intersecting at the center of the otolith core (major and minor axes) (Tuset et al., 2003). Otolith weight was taken to the nearest thousandth of a gram by using a Sartorius milligram balance (Sartorius AG, Göttingen, Germany). Measurements were imported to Microsoft Excel 2010 (Microsoft Corp., Redmond, WA). The first 72 blackspotted rockfish and 90 rougheye rockfish were tested for asymmetry between their left and right otoliths. This test found no significant differences (multivariate analysis of variance: P=0.122), and during the remainder of the study no distinction was made between left or right otoliths. Otolith age was read by scientists from the AFSC Age and Growth Program in accordance with established protocols (Matta and Kimura, 2012).

Initial analysis of the data indicated potential differences between the species in terms of otolith size versus age. The significance of these trends in otolith shape or otolith weight were compared in each species through regression analysis of the form shown in this equation:

$$Variable = Intercept + \beta_1 Species + \beta_2 \log_{10} Age + \beta_3 Species \times \log_{10} Age + \varepsilon, \quad (1)$$

where β = the estimated coefficient for each model term;
Species = the genetic identification for each specimen as a categorical variable;
$\log_{10}Age$ = the log-transformed age of the specimen; and
ε = an error term with a normal distribution.

Seven variables were modeled: area, perimeter, otolith length, otolith width, major axis length, minor axis length, and otolith weight. A log transformation was applied to otolith ages to render these comparisons as a linear relationship. A t-test with a Bonferroni correction was applied to judge the significance of all regression parameters. Additionally, the von Bertalanffy growth function (von Bertalanffy, 1938) was used to model the relationship of age to fork length:

$$Fork\ length = L_\infty \left(1 - e^{-K(Age - t_0)}\right), \quad (2)$$

where L_∞ = mean asymptotic length;
K = the growth coefficient; and
t_0 = the time or age when mean length was zero.

[1] Mention of trade names or commercial companies is for identification purposes only and does not imply endorsement by the National Marine Fisheries Service, NOAA.

Linear models were fit by using the lm function in statistical software R (vers. 3.3.3; R Core Team, 2017), and parameters of the the von Bertalanffy growth function were estimated by using the nls function in R.

Logistic regression is a standard statistical tool that can be used to assign classification probabilities on the basis of a variety of parameters (McCullagh and Nelder, 1989). For otolith morphometrics, the function calculates a probability (P) between 0 and 1 that corresponds to the likelihood that a given otolith is from a rougheye rockfish and probability (1–P) that the otolith is from a blackspotted rockfish. The advantage of this method over other classification procedures (e.g., discriminant analysis) is that it is robust to deviations from normality and heteroscedasticity that are assumed for most other statistical models and is equally effective given a large sample size (McCullagh and Nelder, 1989). Growth-related differences in otolith measurements were accounted for by including age as an interaction for each variable in the model. The model contains 9 predictor variables: otolith area, otolith perimeter, otolith major axis length, otolith minor axis length, otolith length, otolith width, otolith weight, fish fork length, and fish $\log_{10}$-transformed age. The model also contains 8 interactions with $\log_{10}$-transformed age. Here is its abbreviated form:

$$\text{logit}(P_i) = \ln\left(\frac{P_i}{1 - P_i}\right) = Intercept + \beta_j \left[X_{ij}\right] + \varepsilon_i \quad (3)$$

where P_i = probability for specimen i;
X_{ij} = the matrix of j predictor variables, including interactions, for specimen i;
β_j = the regression coefficient for each j predictor variable; and
ε_i = an error term with a binomial distribution for specimen i.

Nonsignificant parameters were removed by using a stepwise backward elimination algorithm with Aikake information criterion (AIC). In addition to probabilities, the standard error of a prediction can be calculated on the basis of the linear combination of the standard errors in the parameter estimates. In this study, this standard error was used to calculate the 95% prediction interval around each specimen, and only specimens whose prediction interval did not cross the 0.5 threshold were classified as *rougheye* or *blackspotted*. Other specimens were assigned to an *uncertain* category, reflecting the fact that their prediction interval was not confined to a single species. This step removed specimens that may have been too close to call and improved the specificity of the model's predictions. This model was fit by using the glm function in R.

The practical validity of a classification model is best determined by examining its accuracy when given new data. With this in mind, we divided the data collected during surveys in the 2 years into a training data set and a second validation or testing data set (Table 1). Of the 945 specimens in the sample from 2009, 738 fish were included in the actual study. Specimens were excluded because they

Table 1

Division of data from blackspotted rockfish (*Sebastes melanostictus*) and rougheye rockfish (*S. aleutianus*) collected in the Gulf of Alaska in 2009 and 2013 into the 2 data sets used to construct and validate the logistic regression model. The model parameters were fit by using specimens from the training data set and then tested against a new set of specimens in the testing data set. The training data set includes 638 specimens, all from 2009, and the testing data set includes 221 specimens from both 2009 and 2013.

		Number of specimens		
Species	Year	Training data set	Testing data set	Total
Blackspotted rockfish	2009	434	50	484
	2013	0	62	62
Rougheye rockfish	2009	204	50	254
	2013	0	59	59
	Total	638	221	859

could not be genetically identified to species or because the corresponding otoliths were damaged and could not be measured. Of the fish used in the study, 50 specimens from each species were randomly assigned to the testing data set, and the remaining 638 fish were used to construct and fit the logistic regression function. Not all of the 902 specimens from the survey conducted in 2013 were necessary for an adequate test; therefore, 121 fish were randomly chosen and they were included in the testing data set. Overall, the training and testing sets covered similar ranges of age and length values, and the training and testing sets had similar mean ages and lengths (Table 2). In the testing data set, the predicted species of each otolith was compared with the genetically determined identity to yield the accuracy of this classification method.

This method relies heavily on otolith age to help discriminate between the blackspotted and rougheye rockfish species, but otolith age is typically more prone to measurement error than standard methods. Furthermore, these species frequently attain very old ages and are among the most difficult to read. Therefore, we simulated the potential effect of errors in the age reading process by generating a false age and using that age to estimate new classification probabilities. This simulation looks at 2 types of errors: bias and random noise. Bias is a systematic tendency to age an otolith higher or lower than its true age. With a −10% bias, a 10-year-old fish would be evaluated as if it were a 9 years old, and a 100-year-old fish would be evaluated as if it were 90 years old. Random noise was simulated by drawing from a normal distribution defined by the age and a coefficient of variation (CV) (standard deviation [SD]/mean). Hence, a 10-year-old fish with a CV of 0.1 will have its age adjusted in each simulation run by an amount drawn from a normal distribution with an SD of 1, and an SD of 10 would be used for a 100-year-old fish. These types of errors are combined to produce a simulated age by using this equation:

$$New\ Age \sim N(\mu = MeasuredAge(1 + bias), \sigma = MeasuredAge \times CV), \quad (4)$$

where N is the normal distribution with the mean equal to μ and the standard deviation equal to σ. This process was repeated 5000 times for each combination of error and bias, with the average classification accuracy measured for each run. All statistical analyses for this simulation were carried out by using R.

Results

Genetics

The results of the genetic analysis from the data collected during the survey in 2009 show that field identification accuracy was 92% for blackspotted rockfish and 66% for rougheye rockfish. Out of 945 samples, 540 fish were genetically identified as blackspotted rockfish and 318 fish were identified as rougheye rockfish. Additionally,

Table 2

Summary statistics for specimens of blackspotted rockfish (*Sebastes melanostictus*) and rougheye rockfish (*S. aleutianus*) sampled for the training data set used to construct the logistic regression model and for the testing data set used to validate the model's accuracy. Specimens were collected in the Gulf of Alaska in 2009 and 2013. All lengths are fork lengths in millimeters, and all ages are in years. n=number of specimens.

			Length			Age		
Species	Data set	n	Min.	Mean	Max.	Min.	Mean	Max.
Blackspotted rockfish	Training	434	70	355	570	2	22	113
	Testing	112	130	348	540	3	22	103
Rougheye rockfish	Training	204	130	396	670	3	20	135
	Testing	109	120	371	730	3	17	83

17 specimens were heterozygous at the *Sma6* locus and were identified as hybrids, and 70 samples were degraded or otherwise produced inconclusive results. The data collected in 2013 indicate an improvement to 94% and 68% accuracy in field identifications of blackspotted rockfish and rougheye rockfish, respectively. Of the 902 specimens, 428 were blackspotted rockfish, 429 were rougheye rockfish, 8 were *Sma6* hybrids, and 37 fish could not be identified to species.

Multivariate regression and length at age

Across all measurements examined, otoliths of rougheye rockfish tended to be a larger size for a given age than blackspotted rockfish, as shown by bivariate plots (Fig. 2). This pattern manifests as a small but significant differences in the initial size of otoliths and in the rate at which these structures grow with age. According to all 7 of the parameters, otoliths of rougheye rockfish are greater beginning in the first few years of life, as evidenced by a significant species effect on the intercept (Table 3). A more varied response is observed as the fish grow, with some characteristics like otolith length, major axis length, and perimeter tending to converge over time (Fig. 2). By comparison, otolith area becomes even more divergent. In most cases, the difference in slopes between the species is not significant (Table 3), indicating that most of the size difference in rougheye rockfish occurs in the early years of life. A very similar dynamic is observed in the von Bertalanffy growth curves (Fig. 3, Table 4). Rougheye rockfish have a much higher rate of growth early in life, leading to a significant gap in the length at age between the 2 species.

Classification success

Logistic regression found that several otolith parameters and age interactions were predictive of species between these 2 rockfish species. Several of the predictors used in this model are highly correlated; however, removal of these collinear predictors resulted in a worse fit to the data as measured by AIC. Removing collinear predictors had little effect on discrimination accuracy. Therefore, only nonsignificant parameters that did not increase AIC were eliminated from the final model. The full model that includes all 8 parameters and 7 interactions had an AIC of 143.35, and the reduced model that includes all 8 parameters and 2 interactions had an AIC of 139.93 (Table 5). Of the 638 specimens used to build the logistic regression, 94.7% of 434 blackspotted rockfish and 88.2% of 204 rougheye rockfish could be correctly identified, once uncertain cases were removed (Table 6). However, the best test of a classification method is its accuracy when confronted with new data. When used to classify 221 specimens from the testing data set, it was successful for 97.3% of 112 blackspotted rockfish and 86.2% of 109 rougheye rockfish (Fig. 4, Table 6). Overall, 11 of the 221 fish are classified as *uncertain* because their prediction intervals indicate both possibilities of species idenfitication are reasonably likely. Of these 11 specimens, 5 fish would have been assigned to the incorrect species, a result that would almost double the total number of misidentifications. When uncertain cases were excluded, only 0.9% of blackspotted rockfish and 5.5% of rougheye rockfish were misidentified (Table 6).

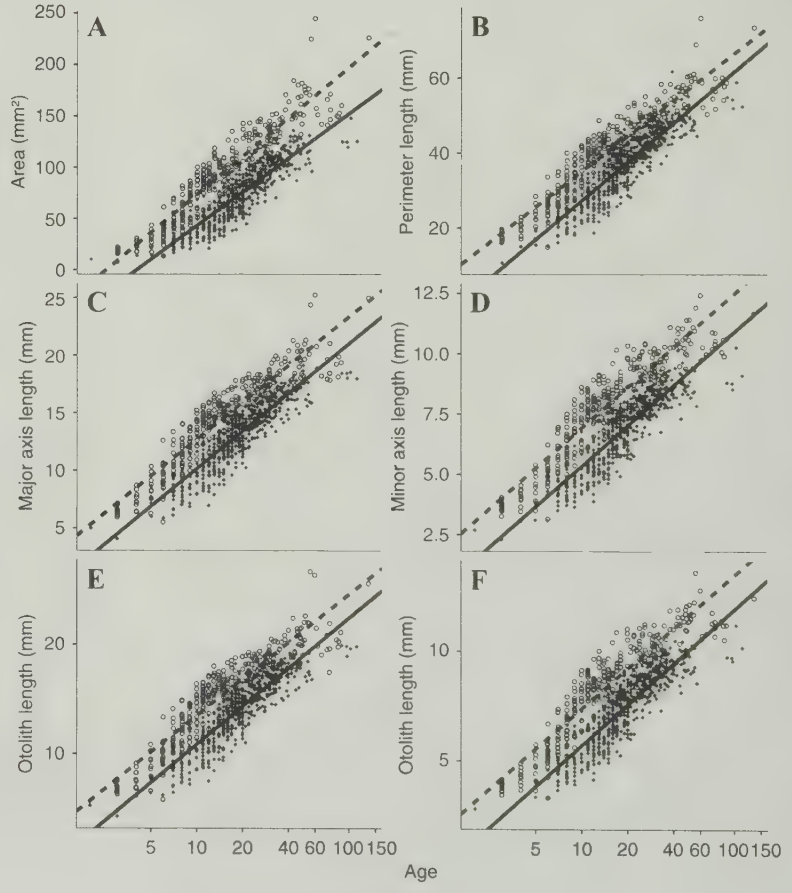

Figure 2

Bivariate plots with species-specific regression lines for the relationships of different otolith morphometrics with age from models based on data from rougheye rockfish (*Sebastes aleutianus*) (open circles, dashed lines) and blackspotted rockfish (*S. melanostictus*) (black circles, solid lines) collected in the Gulf of Alaska in 2009 and 2013. Note that age is shown on a logarithmic scale. Across all measurements, rougheye rockfish are larger at any given age than blackspotted rockfish.

Table 3

Regression statistics for each of 6 morphometric parameters and otolith weight. Each set of 2 rows provides the parameter versus $\log_{10}$-transformed age in blackspotted rockfish (*Sebastes melanostictus*) and rougheye rockfish (*S. aleutianus*), as well as the *t*-statistics and *P*-values used to examine whether the species have different slopes or intercepts. Because multiple tests were conducted, a Bonferroni correction was applied such that differences are considered significant only if $P<0.003$. Data used in the regression model are from specimens collected in the Gulf of Alaska in 2009 and 2013.

Otolith variable	Parameter	Blackspotted rockfish	Rougheye rockfish	Difference	*t*	*P*
Area	Intercept	−65.1	−49.2	15.9	3.61	<0.001
	Slope	108.5	123.0	14.4	4.09	<0.001
Perimeter	Intercept	−7.11	3.67	10.78	8.30	<0.001
	Slope	34.3	31.4	−2.9	−2.85	0.004
Major axis length	Intercept	−0.66	2.13	2.79	6.46	<0.001
	Slope	10.8	10.6	−0.2	−0.67	0.506
Minor axis length	Intercept	−0.22	1.37	1.59	6.91	<0.001
	Slope	5.55	5.55	−0.005	−0.004	0.979
Otolith length	Intercept	−0.71	2.41	3.12	6.68	<0.001
	Slope	11.56	11.08	−0.48	−1.28	0.202
Otolith width	Intercept	−0.50	1.30	1.80	7.11	<0.001
	Slope	6.20	6.08	−0.117	−0.58	0.563
Otolith weight	Intercept	−0.357	−0.456	−0.099	−4.49	<0.001
	Slope	0.463	0.695	0.232	13.15	<0.001

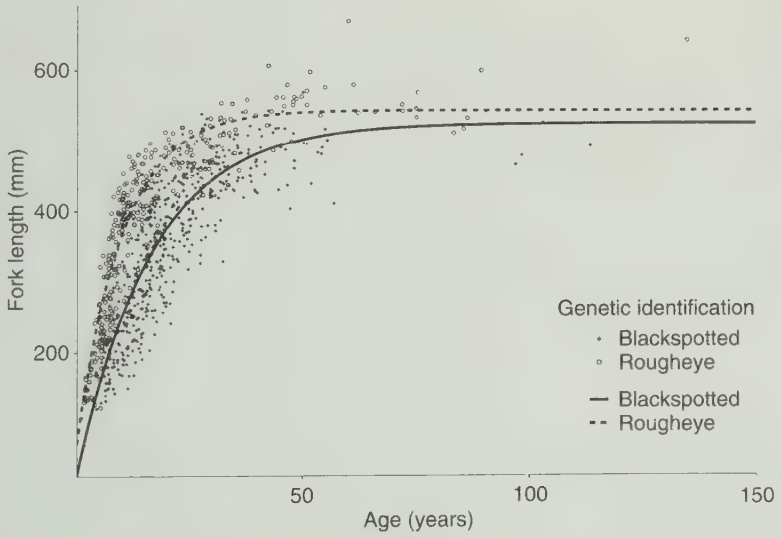

Figure 3

Estimated von Bertalanffy growth curves for rougheye rockfish (*Sebastes aleutianus*) (open circles, dashed line) and blackspotted rockfish (*S. melanostictus*) (black circles, solid line). Data used in the growth model come from specimens collected in the Gulf of Alaska in 2009 and 2013. Similar to the pattern predicted for otolith parameters, rougheye rockfish grow at a substantially faster rate and achieve a greater length at age than blackspotted rockfish.

Simulation

The classification process was found to be robust with respect to moderate errors in the age assigned to each specimen through otolith analysis (Fig. 5). Classification accuracy averaged across both species remained above 90% when bias and CV were each less than 10%. Random errors in the aging process (represented by CV) generally were not a severe concern unless they were particularly strong with overall accuracy exceeding 80% even with a CV of 0.2. In contrast, classification accuracy indicates a strong response to directional bias and particularly suffers if the assigned ages are too low.

Discussion

In this study, otolith data, fork length, and age were sufficient to correctly identify 97% of blackspotted rockfish and 86% of rougheye rockfish (Table 6). This model's accuracy provides a slight improvement compared with the 92–94% of blackspotted rockfish

Table 4

Results for parameters of the von Bertalanffy growth function for blackspotted rockfish (*Sebastes melanostictus*) and rougheye rockfish (*S. aleutianus*) collected in the Gulf of Alaska in 2009 and 2013. The parameters are the mean asymptotic length (L_∞), the growth coefficient (K) and the time or age when mean length was zero (t_0). n=number of specimens.

Parameter	Blackspotted rockfish	Rougheye rockfish
n	546	313
L_∞	526 mm	544 mm
K	0.062	0.102
t_0	0.2	−0.36

Table 5

Regression coefficients for the final form of the logistic regression model following stepwise elimination of parameters. Data used in the regression model are from blackspotted rockfish (*Sebastes melanostictus*) and rougheye rockfish (*S. aleutianus*) collected in the Gulf of Alaska in 2009. After stepwise elimination, all remaining parameters were significantly different from zero.

Parameter	Coefficient	Error	z-score	P
Intercept	−18.92	5.37	−3.53	<0.01
Area	1.07	0.25	4.29	<0.01
Perimeter	2.88	0.64	4.51	<0.01
Minor axis length	7.36	3.50	2.10	0.04
Otolith width	−7.96	3.12	−2.55	<0.01
Otolith length	−3.23	1.06	−3.06	<0.01
Otolith weight	−174.87	59.03	−2.96	<0.01
Fork length	−0.08	0.02	−4.60	<0.01
$\text{Log}_{10}(Age)$	32.74	10.82	3.03	<0.01
Perimeter × $\text{Log}_{10}(Age)$	−2.81	0.55	−5.15	<0.01
Otolith weight × $\text{Log}_{10}(Age)$	133.79	33.78	3.96	<0.01

that are correctly identified in the field. However, the model substantially improves identification of rougheye rockfish, for which field identifications are only 66–68% accurate. The results of a more recent study of field identifications from the season in 2015 indicate 75% accuracy (Shotwell et al., 2017), but this level of accuracy is still significantly worse than the results obtained in this study.

Most studies of this kind will assign a species to all specimens, even if the model indicates a high degree of uncertainty. We recommend a more conservative approach as a further defense against errors imposed by the process of otolith age determination. Our method trades a decrease in misclassifications (improved specificity) for the cost of fewer correct classifications

Table 6

Results of species classification from the logistic regression model comparing the agreement between the genetic identification and the species predicted by the model constructed and validated with data for blackspotted rockfish (*Sebastes melanostictus*) and rougheye rockfish (*S. aleutianus*) collected in the Gulf of Alaska in 2009 and 2013. Data are from the training data set used to fit the regression model and from the testing data set created when the regression model was used on new data. Values in the left columns provide the results when all specimens were classified and those in the right columns indicate the effect of removing specimens classified as *uncertain*. n=number of specimens; ID=identification.

	Number of specimens (successful ID [%])				
	Model ID (all classified)		Model ID (uncertain cases removed)		
Data set for genetic ID	Blackspotted rockfish	Rougheye rockfish	Blackspotted rockfish	Rougheye rockfish	Uncertain
Training data set					
Blackspotted rockfish n=434	424 (97.6%)	10 (2.3%)	411 (94.7%)	5 (1.2%)	18 (4.1%)
Rougheye rockfish n=204	11 (5.4%)	193 (94.6%)	7 (3.4%)	180 (88.2%)	17 (8.3%)
Testing data set					
Blackspotted rockfish n=112	110 (98.2%)	2 (1.8%)	109 (97.3%)	1 (0.9%)	2 (1.8%)
Rougheye rockfish n=109	10 (9.2%)	99 (90.8%)	6 (5.5%)	94 (86.2%)	9 (8.2%)

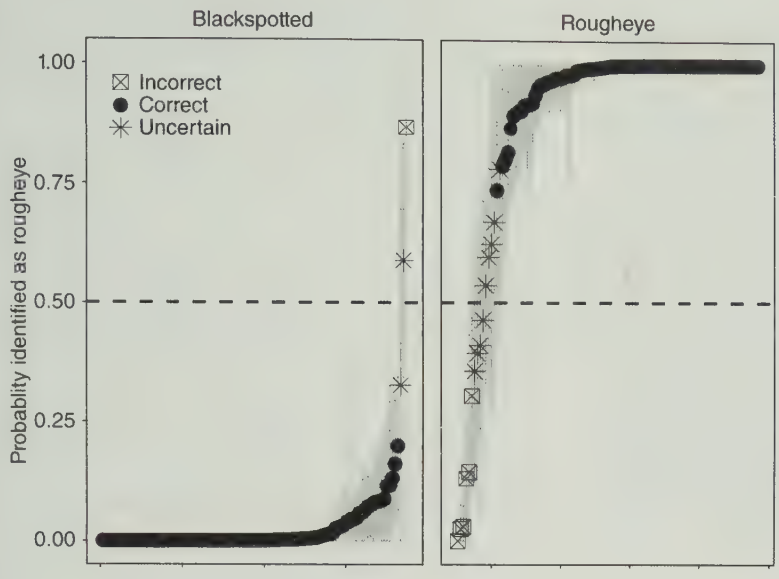

Figure 4

Plot showing how the logistic regression model assigns species identifications to each specimen in the testing data set collected in the Gulf of Alaska in 2009 and 2013. Values on the y-axis are calculated probabilities of each specimen being a rougheye rockfish (*Sebastes aleutianus*). If $P>0.5$, the specimen is identified as a rougheye rockfish, and if $P<0.5$, it is identified as a blackspotted rockfish (*S. melanostictus*). The left panel shows *P*-values for specimens that were genetically identified as blackspotted rockfish, and the right panel shows *P*-values for specimens that were genetically identified as rougheye rockfish. The error bars represent 95% prediction intervals for specimens, based on the standard error of the predictions. An identification is assigned only when the prediction interval does not cross the dashed line for probability of 0.5. Specimens classified as *uncertain* had a prediction interval that was not confined to a single species.

(decreased accuracy) caused by discarding a number of otoliths (approximately 5% overall) that are ruled *uncertain* on the basis of the estimated error around each prediction. Likewise, if the uncertain specimens had been classified, overall accuracy would have increased but the number of misidentifications would have increased as well (Table 6). The logistic regression method developed in this study allows the use of an algorithm to determine when specimens are too difficult or atypical to identify. Removal of the uncertain otoliths led to high specificity, with less than 5% of specimens misidentified. With both high accuracy and high specificity, this method ensures the highest quality data are available for use in managing the populations of these species. In contrast, if a simpler method that attempts to identify all specimens is used, some additional specimens will be correctly identified if they fall on the correct side of the threshold of $P=0.5$ (Fig. 4), but misidentifications double to as much as 9–10% in rougheye rockfish. In this study, no apparent pattern was observed with uncertain specimens with respect to age or location, meaning that the exclusion of uncertain specimens is unlikely to have caused a bias in this data set.

A key finding in this study is the importance of age in distinguishing the 2 species. A common practice in morphometric studies is to standardize all fish to a set size, usually determined by standard or fork length (Campana, 1999; Lleonart et al., 2000). For this study, age was included as an interaction effect with the other predictors, allowing the model to account for it directly. In this study, we observed that almost no difference existed between the species when their otolith measurements were compared with fork length, but a clear separation in the growth patterns emerged when age was considered (Figs. 2 and 3). Our findings are consistent with a growing understanding that, despite their similarities, the rougheye and blackspotted rockfish species have different rates of growth (Conrath, 2017; Shotwell et al., 2017) and specifically that rougheye rockfish grow faster and attain a larger size at age. The von Bertalanffy growth parameters obtained in this study indicate a strong divergence between the 2 species (Table 4). Given our findings, it is possible that using age alongside length or body size may help resolve other problems of difficult stock or species discrimination. Including measurements such as fork length and age into a model as an interaction carries the fewest overall assumptions, makes full use of all available information, and allows the difference in growth rate to inform the results and improve the predictions of the model.

The most significant disadvantage of this method is that reading the ages of otoliths is time consuming, and each specimen would not receive a final species identification for several weeks or months. Although measurements of age have a higher error than other data, the results of our simulations indicate that moderate age determination errors, consistent with commonly reported estimates, are unlikely to degrade the accuracy of this method. The AFSC reports an age determination CV of 0.08 for rougheye rockfish, meaning that otolith age readers tend to disagree by 8%. In the simulation conducted in our study, the logistic regression model maintains high overall accuracy (≈90%) in this simulation (Fig. 5). This method is somewhat more vulnerable to systematic bias in age estimates. The drop in classification accuracy from increasing directional bias is not greater than that from random noise, but it happens unevenly. The core observation on which this model is based is that otoliths of rougheye rockfish are larger and

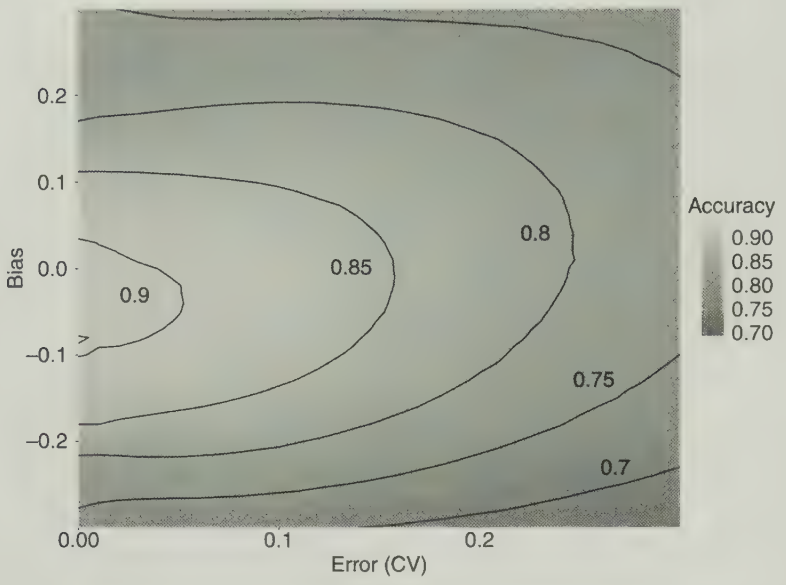

Figure 5

Heatmap showing the accuracy of the species prediction method used in this study, with simulated errors. Lighter shades of gray indicate higher accuracy. Contour lines highlight the gradual change in values of accuracy. Coefficients of variation (CVs) on the x-axis represent simulated random errors in the aging process, and values on the y-axis indicate bias in a specific positive or negative direction.

grow faster than otoliths of blackspotted rockfish. If ages are systematically biased upward, more fish will appear to be slower growing and the model will predict a greater number of blackspotted rockfish. Conversely, a bias toward lower ages will make specimens appear to be faster growing and will tend to predict more rougheye rockfish. With this in mind, it is imperative that the age determination process carefully police any nonrandom errors.

This model is not designed to identify hybrids or classify hybrids. Of the 1847 specimens that were genetically identified from the surveys conducted in 2009 and 2013, 25 (1.3%) fish were hybrids at the *Sma6* locus. With such a small sample, this study was unable to determine what potential effect these hybrids might have had on the accuracy of identifications. The best course of action may be to assume that hybrids represent a minor source of identification error. Furthermore, this model should not be expected to identify or remove miscellaneous rockfish species from a mixed sample of otoliths. All specimens must be correctly identified as part of the rougheye and blackspotted species complex in the field, and it will require that field personnel be adequately trained to identify other species.

All the specimens used in this study were collected from the Gulf of Alaska, but the rougheye and blackspotted rockfish species are found together off the western coasts of the United States and Canada, in the eastern Aleutian Islands, and in the southern Bering Sea. We have tried to account for any potential geographic and temporal differences by collecting specimens from different locations in the Gulf of Alaska (Fig. 1) and in 2 different years. The model was developed and fit by using data from 2009, but it was tested against additional data from 2009 as well as data from a second collection of specimens made in 2013. The model performed well with data from both years, with only 2–3% difference between years in overall accuracy. We think this result is a strong indication that attempts to apply this method in future years throughout the Gulf of Alaska and Bering Sea will be successful.

Considering the positive performance of this logistic regression model, we predict it will be useful to classify or reclassify historical otolith samples from mixed species catches. Applying these findings backward in time does rely on the assumption that the growth rates of these fish species in the present day are similar to those of the past and have not been altered by changes in climate, fishing, or other forces. However, given that both species have a rather long life span, many of the fish in this study did experience those past environmental conditions. Many of the specimens collected are 30 years old or older, and the oldest is a 135-year-old rougheye rockfish with an estimated birth year of 1878. Errors for the model were not correlated with increasing age, meaning that the model was capable of assigning the correct species whether the majority of a fish's growth occurred in present day conditions or those of decades past. This is a promising indication that the model will be reliable for archived specimens going back at least 20–30 years, making it invaluable for establishing individual stock assessments for each species.

The rougheye rockfish and the blackspotted rockfish are assessed as a complex in a single statistical age-structured model that assumes equal age compositions, growth rates, and many other parameters (Shotwell et al., 2017). However, it has been observed that the spatial and depth distributions of the 2 species are different (Orr and Hawkins, 2008) and that rougheye rockfish appear to grow faster and mature earlier (Conrath, 2017). Although Conrath's findings are consistent with our observations of growth at age, her study did not confirm species identifications with genetics, raising the possibility that her estimates are skewed by misidentifications. In the future, our method will allow researchers to more confidently identify these species and arrive at more accurate estimates of important population parameters. New studies,

along with disaggregating historically mixed samples, will allow for better estimates of age, growth, and abundance and will most likely lead to an improved assessment for each species and provide a long-term benefit to sustainable management.

Acknowledgments

We would like to thank everyone who assisted in collecting or archiving specimens during the surveys conducted in 2009 and 2013 in the Gulf of Alaska, especially J. Heifetz, who was instrumental in obtaining genetic samples paired to otoliths. We also thank the staff at the Auke Bay Laboratories for conducting all of the genetic tests. J. Orr and J. Heifetz provided much useful feedback on the initial manuscript, and we would like to thank the anonymous reviewers who provided many useful suggestions.

Literature cited

Barsukov, V. V.
1970. Specific structure of *Sebastes* genus in northern part of Pacific, with description of a new species. Dokl. Bot. Sci. 195:994–997.

Campana, S. E.
1999. Chemistry and composition of fish otoliths: pathways, mechanisms and applications. Mar. Ecol. Prog. Ser. 188:263–297.

Campana, S. E., and J. M. Casselman.
1993. Stock discrimination using otolith shape-analysis. Can. J. Fish. Aquat. Sci. 50:1062–1083.

Conrath, C. L.
2017. Maturity, spawning omission, and reproductive complexity of deepwater rockfish. Trans. Am. Fish. Soc. 146:495–507.

Gharrett, A. J., A. P. Matala, E. L. Peterson, A. K. Gray, Z. Z. Li, and J. Heifetz.
2005. Two genetically distinct forms of rougheye rockfish are different species. Trans. Am. Fish. Soc. 134:242–260.

Gharrett, A. J., C. W. Mecklenburg, L. W. Seeb, Z. Li, A. P. Matala, A. K. Gray, and J. Heifetz.
2006. Do genetically distinct rougheye rockfish sibling species differ phenotypically? Trans. Am. Fish. Soc. 135: 792–800.

Hawkins, S. L., J. Heifetz, C. M. Kondzela, J. E. Pohl, R. L. Wilmot, O. N. Katugin, and V. N. Tuponogov.
2005. Genetic variation of rougheye rockfish (*Sebastes aleutianus*) and shortraker rockfish (*S. borealis*) inferred from allozymes. Fish. Bull. 103:524–535.

Hicks, A. C., P. J. Smith, P. L. Horn, and D. J. Gilbert.
2003. Differences in otolith measurements and gill raker counts between the two major spawning stocks of hoki (*Macruronus novaezelandiae*) in new Zealand. N.Z. Fish. Assess. Rep. 2003/7, 23 p. Minist. Fish., Wellington, New Zealand.

Hicks, A. C., C. Wetzel, and J. Harms.
2014. The status of rougheye rockfish (*Sebastes aleutianus*) and blackspotted rockfish (*S. melanostictus*) as a complex along the U.S. West Coast in 2013, 250 p. Pac. Fish. Manage. Counc., Portland, OR. [Available from website.]

Hutchinson, C. E., C. R. Kastelle, D. K. Kimura, and D. R. Gunderson.
2007. Using radiometric ages to develop conventional aging methods from shortraker rockfish (*Sebastes borealis*). *In* Biology, assessment, and management of North Pacific rockfishes. Alaska Sea Grant Rep. AK-SG-07-01 (J. Heifetz, J. DiCosimo, A. J. Gharrett, M. S. Love, V. M. O'Connell, and R. D. Stanley, eds.), p. 237–249. Alaska Sea Grant Coll. Program, Univ. Alaska Fairbanks, Fairbanks, AK.

Hyde, J. D., C. A. Kimbrell, J. E. Budrick, E. A. Lynn, and R. D. Vetter.
2008. Cryptic speciation in the vermilion rockfish (*Sebastes miniatus*) and the role of bathymetry in the speciation process. Mol. Ecol. 17:1122–1136.

Jordan, D. S., and B. W. Evermann.
1898. The fishes of North and Middle America: a descriptive catalogue of the species of fish-like vertebrates found in the waters of North America, north of the Isthmus of Panama. Part II. Bull. U.S. Natl. Mus. 47:1241–2183.

Kanayama, T., and D. Kitigawa.
1982. Fishes in Iwate Prefecture Soi-Menukerui, 47 p. Iwate Fish. Exp. Stn., Iwate, Japan.

Kastelle, C. R., D. K. Kimura, and B. J. Goetz.
2008. Bomb radiocarbon age validation of Pacific ocean perch (*Sebastes alutus*) using new statistical methods. Can. J. Fish. Aquat. Sci. 65:1101–1112.

Lleonart, J., J. Salat, and G. J. Torres.
2000. Removing allometric effects of body size in morphological analysis. J. Theor. Biol. 205:85–93.

Love, M. S., M. M. Yoklavich, and L. K. Thorsteinson.
2002. The rockfishes of the northeast Pacific, 405 p. Univ. Calif. Press, Berkeley, CA.

Matsubara, K.
1934. Studies on the scorpaenoid fishes of Japan. I. Descriptions of one new genus and five new species. J. Imperial Fish. Inst. 30:199–210.

Matta, M. E., and D. K. Kimura.
2012. Age determination manual of the Alaska Fisheries Science Center Age and Growth Program. NOAA Prof. Pap. NMFS 13, 92 p.

McCullagh, P., and J. A. Nelder.
1989. Generalized linear models, 526 p. Chapman and Hall, New York.

Ormseth, O. A., and P. D. Spencer.
2011. An assessment of vulnerability in Alaska groundfish. Fish. Res. 112:127–133.

Orr, J. W., and S. Hawkins.
2008. Species of the rougheye rockfish complex: resurrection of *Sebastes melanostictus* (Matsubara, 1934) and a redescription of *Sebastes aleutianus* (Jordan and Evermann, 1898) (Teleostei: Scorpaeniformes). Fish. Bull. 106:111–134.

R Core Team.
2017. R: a language and environment for statistical computing. R Foundation for Statistical Computing, Vienna, Austria. [Available from website, accessed March 2017.]

Sadighzadeh, Z., V. M. Tuset, T. Valinassab, M. R. Dadpour, and A. Lombarte.
2012. Comparison of different otolith shape descriptors and morphometrics for the identification of closely related species of *Lutjanus* spp. from the Persian Gulf. Mar. Biol. Res. 8:802–814.

Seeb, L. W.
1986. Biochemical systematics and evolution of the Scorpaenid genus *Sebastes*. Ph.D. diss., 176 p. Univ. Wash., Seattle, WA.

Shotwell, S. K., D. H. Hanselman, and J. Heifetz.
2017. Assessment of the rougheye and blackspotted rockfish stock complex in the Gulf of Alaska. *In* Stock assessment and fishery evaluation report for the groundfish resources of the Gulf of Alaska, p. 1055–1148. N. Pac. Fish. Manage. Counc., Anchorage, AK. [Available from website.]

Tuset, V. M., A. Lombarte, J. A. Gonzalez, J. F. Pertusa, and M. J. Lorente.
2003. Comparative morphology of the sagittal otolith in Serranus spp. J. Fish Biol. 63:1491–1504.

von Bertalanffy, L.
1938. A quantitative theory of organic growth (inquiries on growth laws. II). Hum. Biol. 10:181–243.

Wimberger, P., J. Burr, A. Gray, A. López, and P. Bentzen.
1999. Isolation and characterization of twelve microsatellite loci for rockfish (*Sebastes*). Mar. Biotechnol. 1:311–315.

National Marine Fisheries Service
NOAA

Fishery Bulletin
established in 1881

Spencer F. Baird
First U.S. Commissioner
of Fisheries and founder
of *Fishery Bulletin*

Trophic ecology and ontogenetic shift in the diet of the sicklefin smoothhound (*Mustelus lunulatus*) in the southeastern Pacific Ocean

José S. Méndez-Macías[1]
Vanessa M. Velázquez-Chiquito[1]
Colombo Estupiñán-Montaño (contact author)[2]
Felipe Galván-Magaña[3]

Email address for contact author: goliathcem@gmail.com

[1] Facultad Ciencias del Mar
Universidad Laica "Eloy Alfaro" de Manabí
Avenida Circunvalación, Vía a San Mateo
Manta, Manabí, Ecuador

[2] Fundación Alium Pacific
Carrera 26 No. 5C-13
Santiago de Cali, Valle del Cauca, Colombia

[3] Centro Interdisciplinario de Ciencias Marinas
Instituto Politécnico Nacional
Avenida Instituto Politécnico Nacional s/n
Colonia Playa Palo de Santa Rita
23096 La Paz, Baja California Sur, Mexico

Abstract—The feeding habits of the sicklefin smoothhound (*Mustelus lunulatus*) were studied on the basis of analysis of stomach contents of 314 specimens, allowing the diet of this species to be determined by sex, size, and stage of sexual maturity and for changes in the dietary ontogeny to be identified. The prey-specific index of relative importance revealed that the sicklefin smoothhound is a crab predator. Female and male sicklefin smoothhounds consumed a swimming crab species, *Achelous iridescens*, in similar proportions. Adults and juveniles of both sexes complemented their diets with the Panama mantis shrimp (*Squilla panamensis*), the dart squid, *Lolliguncula (Loliolopsis) diomedeae*, and the crab species *Euphylax robustus*, indicating behavioral and habitat segregation. Ontogenetic changes in diet were identified, with juveniles feeding almost exclusively on *A. iridescens* and adults having a more varied diet. The diet of sicklefin smoothhounds also changed with size: sharks ≤90 cm in total length (TL) consumed more *A. iridescens*, and sharks >90 cm TL fed on a wider variety of prey. These results indicate that the sicklefin smoothhound is a selective mesopredator in the coastal marine food chain, having a significant influence on populations of benthic crustaceans in the southeastern Pacific Ocean.

Manuscript submitted 31 October 2018.
Manuscript accepted 21 August 2019.
Fish. Bull. 117:245–257 (2019).
Online publication date: 30 August 2019.
doi: 10.7755/FB.117.3.11

The views and opinions expressed or implied in this article are those of the author (or authors) and do not necessarily reflect the position of the National Marine Fisheries Service, NOAA.

Sharks generally occupy high positions in the food chain (Cortés, 1999), and some play an important role as regulators of lower trophic positions (Stevens et al., 2000; Heithaus et al., 2008; Ferretti et al., 2010). Such top-down control can be key to maintaining the health of the marine ecosystem because a decline in top-level predator populations can lead to trophic cascades, thereby changing the abundance of lower trophic-level populations (Ferretti et al., 2010). For example, some authors have hypothesized that the removal of sharks can cause a significant increase in the biomass of smaller sharks (mesopredators), sea turtles, sea birds, and fishes (Heithaus et al., 2010).

Understanding the ecological role of a species in an ecosystem depends mostly on knowing its trophic relationships (Braga et al., 2012). The trophic ecology of a species can in turn provide the information required for studies on resource sharing, competition, energy transfer, and food web dynamics (Navia et al., 2010; Bornatowski et al., 2014a). These more complex approaches rely on basic diet descriptions and are affected by the lack of basic knowledge of the diet of fish species (Bornatowski et al., 2014b). Understanding the trophic interactions and positions of large predators within food webs is a crucial step toward unraveling the dynamics of marine communities and the effect of sharks on different food web components (Lucifora et al., 2009; Heithaus et al., 2013).

The sicklefin smoothhound (*Mustelus lunulatus*) is an abundant species in warm temperate and tropical waters of the eastern Pacific Ocean (Compagno, 1984). This species typically inhabits muddy bottoms (Fernández, 1975) of the continental shelf and offshore areas (Compagno, 1984; Fischer et al., 1995) and feeds mainly

on benthic crustaceans (Gómez et al., 2003; Navia et al., 2007; Moreno-Sánchez et al., 2012). The sicklefin smoothhound is a placental viviparous species (Compagno, 1984) that reaches a maximum total length (TL) of approximately 170 cm (Compagno, 1984). Mature females and males typically have TLs of approximately 103.2 and 91.5 cm, respectively (Pérez-Jiménez and Sosa-Nishizaki, 2010), and the TL at birth is 32–35 mm (Compagno, 1984). Despite its abundance, little is known about the biology and ecology of the sicklefin smoothhound. Studies on the trophic ecology of sharks are scarce in Ecuador, and no research on the sicklefin smoothhound has been undertaken. Therefore, this study is the first to address the trophic ecology of this shark species in this region. The objectives of this study were 1) to collect quantitative dietary information for sicklefin smoothhounds, 2) to test for ontogenetic shifts in diet between stages of sexual maturity and size classes, and 3) to estimate the relative trophic position of sharks. Because of the rapid decline in the populations of several shark species (Bornatowski et al., 2014b), it is critical that we build our understanding of these patterns and processes to develop appropriate conservation strategies.

Materials and methods

We analyzed the stomach contents of 314 specimens of the sicklefin smoothhound. All sharks were caught by the artisanal fishery in Ecuador with gill nets and longlines in depths of 80–90 m along the continental platform and were landed in the port of Manta in Manabí, Ecuador, between November 2003 and October 2004 (Fig. 1).

For each specimen, natural TL (Francis 2006) was measured in centimeters and sex was determined before the digestive tract was extracted. Stomach contents were removed and filtered through a 1.5-mm mesh sieve, stored in plastic bags, and preserved on ice for transportation to the laboratory.

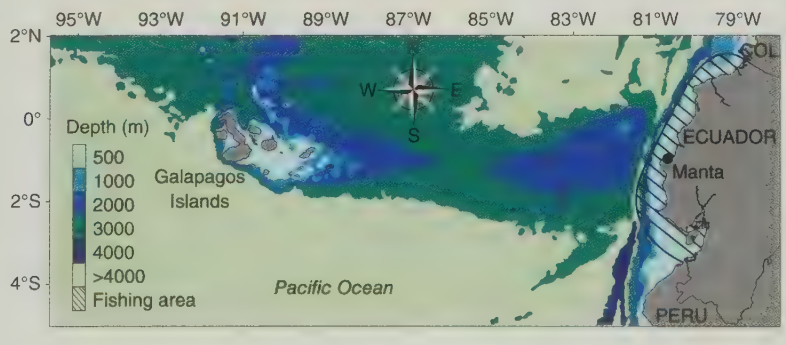

Figure 1

Map of the study area showing the port of Manta, Ecuador, where sicklefin smoothhounds (*Mustelus lunulatus*) were collected from landings of an artisanal fishery between November 2003 and October 2004. The fishing area of the artisanal fishery and depth zones are also indicated.

The prey were identified to the lowest taxon possible (on the basis of the digestion state of prey), counted, and weighed in grams. The prey species (i.e., complete organisms, skeletons, and otoliths) were identified according to Clothier (1950), Fischer et al. (1995), Chirichigno and Vélez (1998), and García-Godos (2001). The cephalopod species were identified by using their beaks (mandible) according to Wolff (1984) and Clarke (1986), and crustacean species were identified by their exoskeleton by using the keys from Garth (1973) and Fischer et al. (1995).

Cumulative prey curve

To determine whether the number of stomachs was sufficient to adequately describe the diet of sicklefin smoothhounds, a cumulative prey curve was constructed. The observed number of each prey item in the stomachs was used to estimate the value of the Shannon–Wiener diversity index for each stomach, and the samples were randomized 500 times with a sample-based rarefaction routine by using the software EstimateS, vers. 9 (Colwell, 2013). The coefficient of variation (0.05) was the basis for determining whether the number of stomachs was sufficient.

Dietary analyses

To assess the importance of the different prey taxa in the diet of sicklefin smoothhounds (overall and by sex, stage of sexual maturity, size class, and trimester), the prey-specific index of relative importance ($PSIRI_i$) (Brown et al., 2012), a modification of the index of relative importance (IRI) proposed by Pinkas et al. (1971) was used, according to this equation:

$$PSIRI_i = \frac{\%FO_i \times (\%PN_i + \%PW_i)}{2}, \quad (1)$$

where $\%FO_i$ is the percent frequency of occurrence of a specific prey in all samples and $\%PN_i$ and $\%PW_i$ are the substitution of IRI's prey percent number and prey percent weight with their corresponding prey-specific abundances. Unlike the IRI, the PSIRI is cumulative with respect to taxonomic levels. The PSIRI of a major taxon is equal to the sum of the PSIRI of the items belonging to that taxon (Brown et al., 2012).

Stages of sexual maturity were determined on the basis of Pérez-Jiménez and Sosa-Nishizaki (2010), who report that the average size of sicklefin smoothhounds at sexual maturity in their study was 103.2 cm TL for females and 91.5 cm TL for males. The specimens caught were between 63 and 142 cm TL. They were grouped into 3 size classes (of both sexes) with a constant length range: 60–90 cm TL (Size I), 90–120 cm TL (Size II), and 120–150 cm TL (Size III).

The specimens collected during November 2003–October 2004 were grouped by trimester in chronological order: November 2003–January 2004 (Trimester I), February 2004–April 2004 (Trimester II), May 2004–July 2004 (Trimester III), and August 2004–October 2004 (Trimester IV). The information was grouped in this way in order to obtain a significant quantity for each trimester of the year.

To test for ontogenetic shifts in diet, a Bray–Curtis similarity matrix was constructed by using standardized estimates of the contribution of each prey taxon to the diet based on abundance (number of samples [*n*]). A one-way analysis of similarities (ANOSIM) was then performed, by using individuals as samples and stages of sexual maturity (sexes separated) and size classes (sexes combined) as factors. This test is analogous to analysis of variance and was used to evaluate similarity (or difference) within predefined groups (factors) versus similarity between groups and to calculate the statistic R, which varies between −1 and +1 (Clarke and Gorley, 2006). A post-hoc multiple comparison test (Benfferroni test) was then performed to identify specific differences between categories.

A nonmetric multidimensional scaling analysis was used to determine the maturity differences by diet and to determine the size-class dietary changes that occurred. Similarity percentage (SIMPER) analysis was used to estimate the contribution of each prey category to ontogenetic differences in diet. The analyses were performed by using the software PAST, vers. 3.14 (Hammer, 2001).

Dietary niche breadth, overlap, and trophic position

Dietary niche breadth was estimated by using Levin's index (B_i) (Krebs, 1999):

$$B_i = \frac{1}{\Sigma P_j^2}, \quad (2)$$

where P_j is the fraction (in PSIRI) of each food item in the diet j (ΣP_j=1). The B_i values were standardized to B_A so that they ranged from 0 to 1 by using this equation: $B_A=(B_i-1)(N-1)^{-1}$, where N is the number of classes (Krebs, 1999). Low B_A values indicate diets dominated by few prey items (i.e., selective predators), and values close to 1 indicate opportunistic, generalist diets.

Trophic overlap was assessed by calculating the Morisita–Horn index ($C\lambda$) (Smith and Zaret, 1982) to detect possible differences in diet between sexes, stages of sexual maturity, and size classes:

$$C\lambda = 2\frac{\sum_{i=1}^{n}\left(P_{xi} \times P_{yi}\right)}{\sum_{i=1}^{n} P_{xi}^2 + \sum_{i=1}^{n} P_{yi}^2}, \quad (3)$$

where P_{xi} is the proportion of i^{th} prey with respect to all prey of predator x, P_{yi} is the proportion of the i^{th} prey with respect to predator y, and n is the total number of prey species. This index ranges from 0 to 1, with values close to 0 indicating dietary differences and values close to 1 indicating similarity in prey consumed.

Standardized trophic position (TP) was calculated by using the trophic index proposed by Cortés (1999):

$$TP_k = 1 + \left(\sum_{i=1}^{n} P_j \times TP_j\right), \quad (4)$$

where n is the number of prey, TP_j is the trophic position of each prey taxon j (Cortés, 1999), and P_j is the proportion of each prey category j in the predator's diet, based on IRI values (percentages) (Bornatowski, 2014a). The trophic positions of all prey were taken from Cortés (1999), Hobson and Welch (1992), Sea Around Us (Pauly and Zeller[1]), and FishBase (Froese and Pauly[2]).

For all analyses, the crustacean, fish, and squid remains and unidentified organic matter were not considered because it was not possible to identify them with precision.

Results

A total of 314 stomachs were collected from specimens of the sicklefin smoothhound measuring 63–142 cm TL, and 95.2% (n=299) of the stomachs contained food. Of these stomachs, 171 were taken from females (69–142 cm TL) and 143 were taken from males (63–118 cm TL), with 96.5% (n=165) and 93.7% (n=134) of the stomachs containing food, respectively.

Regarding the stages of sexual maturity, there were 90 juvenile females and 81 adult females, of which 96.7% and 96.3%, respectively, had food in their stomachs. Of the 54 juvenile males and 90 adult males, 88.9% and 96.7%, respectively, had food in their stomachs.

When examined by size class, 91.0% (n=100) of the Size-I sharks (60–90 cm TL), 97.3% (n=183) of the Size-II sharks (90–120 cm TL), and 96.9% (n=32) of the Size-III sharks (120–150 cm TL) had food in their stomachs.

In addition, of the specimens studied in Trimester I, Trimester II, Trimester III, and Trimester IV, 91.6% (n=87), 98% (n=58), 92% (n=73), and 100% (n=81), respectively, contained food in their stomachs.

Cumulative prey curve

The coefficient of variation indicates that all the cumulative prey curves approached their asymptote. This finding indicates that sample sizes were sufficient to adequately describe the diet of sicklefin smoothhounds (Fig. 2A). Indeed, the minimum number of stomachs required was 58 for females (51 for juveniles and 44 for adults; Fig. 2, B, D, and F) and 75 for males (44 for juveniles and 38 for adults; Fig. 2, C, E, and G).

[1] Pauly, D., and D. Zeller (eds.). 2015. Sea Around Us concepts, design, and data. [Available from website, accessed June 2016].

[2] Froese, R., and D. Pauly. 2016. FishBase, vers. 06/2016. World Wide Web electron. publ. [Available from website, accessed June 2016].

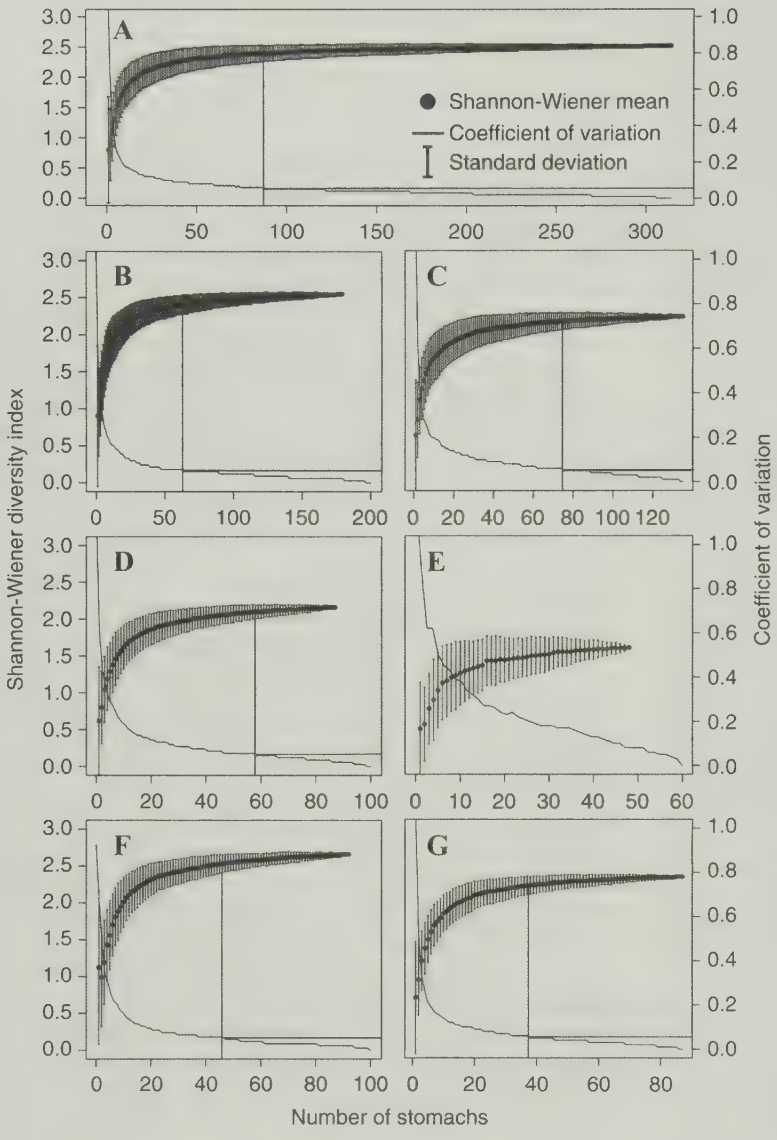

Figure 2

Cumulative prey curves for sicklefin smoothhounds (*Mustelus lunulatus*) caught in the southeastern Pacific Ocean between November 2003 and October 2004. Graphs plot Shannon–Wiener diversity index values and coefficients of variation against the numbers of stomachs analyzed for (**A**) all samples combined (number of stomachs analyzed [*n*]=87), (**B**) females (*n*=58), (**C**) males (*n*=75), (**D**) juvenile females (*n*=51), (**E**) juvenile males (*n*=44), (**F**) adult females (*n*=44), and (**G**) adult males (*n*=38).

Dietary analyses

The examination of stomachs revealed that the diet of sicklefin smoothhounds was composed mostly of crustaceans and, in a lower proportion, of mollusks and teleosts (Table 1). The main prey were a swimming crab, *Achelous iridescens*, and crab species of the genus *Iliacantha*. (Table 1). Both sexes fed mostly on *A. iridescens*, but the females also consumed a small proportion of Panama mantis shrimp (*Squilla panamensis*) and dart squid, *Lolliguncula (Loliolopsis) diomedeae*, and the males also consumed a small proportion of purse crabs (*Iliacantha* spp.) and small arched box crab (*Calappula saussurei*) (Table 2).

The dietary analysis by stage of sexual maturity revealed that the main prey of both juvenile and adult sicklefin smoothhounds was *A. iridescens*. Adult females, however, incorporated in their diet the dart squid, the small arched box crab, and a swimming crab, *Euphylax robustus*, and adult males complemented their diet with prey such as the small arched box crab, *Iliacantha* spp., and the crab *Acanthocarpus delsolari* (Fig. 3).

The dietary analysis of sicklefin smoothhounds also showed that Size-I sharks fed mostly on crustaceans: *Achelous iridescens* (PSIRI: 42.2%), *Iliacantha* spp. (4.8%), small arched box crab (3.9%), and Panama mantis shrimp (3.7%). In addition to *A. iridescens* (26.6%), Size-II sharks ate *Iliacantha* spp. (7.7%), small arched box crab (5.7%), Panama mantis shrimp (3.8%), and dart squid (3.4%). Size-III sharks had a more varied diet composed of *E. robustus* (11.9%), dart squid (10.9%), *Acanthocarpus delsolari* (9.3%), Panama mantis shrimp (8.6%), and *Achelous iridescens* (7.5%) (Fig. 4).

The dietary analysis by trimester indicated that crustaceans were the principal prey consumed by sicklefin smoothhounds throughout the year. By trimester, the importance of some species changed. The importance of the crustacean *A. iridiscens* increased from Trimester I to Trimester IV; however, the second crustacean in importance, the Panama mantis shrimp, decreased in importance throughout the year. For other crustaceans and for cephalopods, changes were minimal (Fig. 5).

Ontogenetic changes were identified in the diet of sicklefin smoothhounds, by stage of sexual maturity (global coefficient of multiple correlation [*R*]=0.035, *P*=0.002), because of dietary differences between female adults with respect to female juveniles and male adults (Benfferroni test, corrected: *P*=0.02) as well as between female juveniles and male adults (Benfferoni test, corrected: *P*=0.01) (Fig. 6A).

Likewise, ontogenetic changes were observed by size class (global *R*=0.043, *P*=0.006; Figs. 4 and 6B). The results of the SIMPER analysis by stage of sexual maturity and size class are given in Table 3.

Table 1

Diet composition for sicklefin smoothhounds (*Mustelus lunulatus*) in the southeastern Pacific Ocean, based on analysis of stomach contents of specimens collected from landings of an artisanal fishery at the port of Manta, Ecuador, between November 2003 and October 2004. Values provided for prey found in stomachs include percent abundance (percent number of samples [%N]), percent prey-specific abundance (percent number of samples for specific prey [%PN]), percent weight (%W), percent prey-specific weight (percent weight of specific prey [%PW]), percent frequency of occurrence (%FO), and prey-specific index of relative importance (PSIRI). Trophic position (TP) values are taken from Hobson and Welch (1992), Cortés (1999), Sea Around Us (2015), and FishBase (2016). A dash indicates that data were not available because a value was not estimated.

Prey	%N	%PN	%W	%PW	%FO	PSIRI (%)	TP
ARTHROPODA	88.17	90.59	89.03	91.48	97.32	88.60	2.52
Guyanacaris caespitosa	0.11	33.33	0.18	53.54	0.30	0.15	3.43
Acanthocarpus delsolari	4.29	64.17	4.20	62.74	6.70	4.25	2.52
Calappula saussurei	5.13	36.51	4.43	31.54	14.00	4.78	3.60
Cycloes bardii	0.17	50.00	0.23	67.90	0.30	0.19	2.52
Ethusa spp.	2.40	34.22	2.29	32.63	7.00	2.34	2.60
Euphylax robustus	1.99	37.28	2.77	51.84	5.30	2.36	4.00
Diogenidae	0.07	20.00	0.03	8.88	0.30	0.05	2.50
Penaeidae	0.02	6.67	<0.01	0.48	0.20	0.01	3.31
Goneplax spp.	0.44	26.38	0.51	30.79	1.70	0.49	2.82
Hemisquilla spp.	0.08	25.00	0.01	1.53	0.30	0.04	3.50
Hepatus kossmanni	0.08	25.00	0.10	30.35	0.30	0.09	2.60
Iliacantha spp.	46.00	41.05	46.00	40.33	15.40	6.27	2.60
Mesorhoea belli	0.83	31.15	0.47	17.38	2.70	0.66	2.52
Munida hispida	0.11	33.33	0.07	22.17	0.30	0.09	3.10
Munida refulgens	1.01	38.02	0.97	36.29	2.70	0.99	3.10
Panopeus spp.	1.09	29.55	0.98	26.62	3.70	1.04	3.38
Parasquilla similis	0.04	12.50	0.02	6.63	0.30	0.03	2.52
Parthenope spp.	0.84	25.24	0.68	20.46	3.30	0.75	2.52
Pilumnus fernandezi	0.87	43.52	0.85	42.34	2.00	0.86	2.52
Plesionika mexicana	0.17	50.00	0.06	17.77	0.30	0.10	2.70
Platymera gaudichaudii	1.52	64.76	1.53	65.37	2.30	1.50	2.52
Achelous iridescens	30.16	60.12	29.12	58.05	50.20	29.66	3.40
Portunus asper	0.84	83.33	0.91	90.99	1.00	0.87	3.40
Ranilia spp.	1.09	36.28	1.05	34.90	3.00	1.07	2.52
Sicyonia disdorsalis	0.06	16.67	0.04	11.24	0.30	0.05	2.40
Sicyonia picta	0.21	31.25	0.16	23.25	0.70	0.19	2.40
Solenocera agassizi	0.36	26.90	0.50	37.69	1.30	0.43	2.20
Solenocera spp.	0.17	25.89	0.14	21.38	0.70	0.17	2.20
Squilla biformis	0.81	48.33	0.80	48.02	1.70	0.82	3.50
Squilla hancocki	0.37	27.92	0.22	16.16	1.30	0.29	3.50
Squilla panamensis	4.22	40.08	4.36	43.46	10.00	4.29	3.50
Squilla spp.	2.82	38.26	2.31	31.41	7.40	2.58	3.50
Rimapenaeus pacificus	0.06	16.67	0.01	3.29	0.30	0.03	2.52
Trizocarcinus dentatus	0.22	22.22	0.16	5.74	1.00	0.19	2.52
Crustacean remains	19.18	48.19	22.66	56.93	39.80	20.92	2.52
OSTEICHTHYES	5.87	39.89	5.39	36.59	14.72	5.63	3.24
Anchoa spp.	0.26	77.78	0.14	43.02	0.33	0.20	3.25
Auxis spp.	0.94	40.36	1.07	45.54	2.34	1.01	4.24
Bollmannia chlamydes	0.17	50.00	0.28	82.23	0.33	0.22	3.50
Citharichthys gilberti	0.17	50.00	0.08	25.33	0.33	0.13	4.10
Citharichthys platophrys	0.08	25.00	0.03	10.29	0.33	0.06	3.50
Paralichthyidae	0.03	9.09	0.02	5.21	0.33	0.02	4.06
Pleuronectiformes	0.12	37.50	0.17	52.07	0.33	0.15	3.57
Unidentified fish	0.56	55.56	0.51	50.40	1.00	0.53	3.24
Symphurus spp.	0.15	22.92	0.05	6.99	0.67	0.10	3.30
Fish remains	3.38	38.89	3.04	34.93	8.70	3.21	3.24
MOLLUSCA	5.76	44.13	5.34	40.98	13.04	5.55	3.20
Gastropoda	0.29	28.89	0.07	6.49	1.00	0.18	2.10
Lolliguncula (Loliolopsis) diomedeae	4.01	45.36	3.69	40.83	9.03	3.89	3.90
Squid remains	1.37	45.49	1.59	52.89	3.01	1.48	3.20
Unidentified organic matter	0.20	20.37	0.23	23.28	1.00	0.22	–

Table 2

Diet composition, by sex (with size classes and maturity stages combined), for sicklefin smoothhounds (*Mustelus lunulatus*) caught in the southeastern Pacific Ocean during November 2003–October 2004. Values provided for prey include percent prey-specific abundance (percent number of samples for specific prey [%PN]), percent prey-specific weight (percent weight of specific prey [%PW]), percent frequency of occurrence (%FO), and prey-specific index of relative importance (PSIRI). A dash indicates that data were not available because the prey species was not consumed by both sexes.

	%PN		%PW		%FO		PSIRI (%)	
Prey	Females	Males	Females	Males	Females	Males	Females	Males
ARTHROPODA	89.12	92.39	90.21	93.04	96.90	97.70	86.94	90.64
Guyanacaris caespitosa	33.33	–	53.54	–	0.60	–	0.26	–
Acanthocarpus delsolari	62.50	64.88	60.69	63.62	3.60	10.40	2.24	6.71
Calappula saussurei	35.57	37.22	31.00	31.94	10.90	17.90	3.63	6.19
Cycloes bardii	50.00	–	67.90	–	0.60	–	0.36	–
Ethusa spp.	26.22	47.22	21.19	51.23	7.90	5.90	1.87	2.94
Diogenidae	–	20.00	–	8.88	–	0.70	–	0.11
Euphylax robustus	39.09	10.00	54.46	12.61	9.10	0.70	4.25	0.08
Penaeidae	6.67	–	0.48	–	0.60	–	0.02	–
Goneplax spp.	24.64	33.33	29.94	34.23	2.40	0.70	0.66	0.25
Hemisquilla spp.	25.00	–	1.53	–	0.60	–	0.08	–
Hepatus kossmanni	25.00	–	30.35	–	0.60	–	0.17	–
Iliacantha spp.	40.19	41.83	40.66	40.03	13.30	17.90	5.39	7.33
Mesorhoea belli	27.64	41.67	12.47	32.11	3.60	1.50	0.73	0.55
Munida hispida	–	33.33	–	22.17	–	0.70	–	0.21
Munida refulgens	22.50	43.19	22.32	40.95	1.20	4.50	0.27	1.88
Panopeus spp.	30.00	25.00	28.57	7.18	6.10	0.70	1.77	0.12
Parasquilla similis	12.50	–	6.63	–	0.60	–	0.06	–
Parthenope spp.	26.06	23.33	24.55	10.89	4.20	2.20	1.07	0.38
Pilumnus fernandezi	25.00	62.04	15.34	69.34	1.80	2.20	0.37	1.47
Platymera gaudichaudii	55.00	77.78	55.61	78.39	2.40	2.20	1.34	1.75
Plesionika mexicana	–	50.00	–	17.77	–	0.70	–	0.25
Achelous iridescens	58.25	62.44	54.97	61.87	50.30	50.00	28.48	31.08
Portunus asper	83.33	–	90.99	–	1.80	–	1.58	–
Ranilia spp.	31.63	40.00	24.88	42.92	2.40	3.70	0.68	1.55
Squilla biformis	–	48.33	–	48.01	–	3.70	–	1.79
Squilla hancocki	18.33	37.50	3.19	29.12	1.20	1.50	0.13	0.49
Squilla panamensis	43.43	36.67	46.63	30.80	14.50	4.50	6.55	1.51
Squilla spp.	32.61	53.33	26.67	44.06	9.70	4.50	2.87	2.18
Solenocera agassizi	14.29	31.11	12.95	45.94	0.60	2.20	0.08	0.86
Solenocera spp.	37.50	14.29	19.21	3.56	0.60	0.70	0.17	0.14
Sicyonia disdorsalis	16.67	–	11.24	–	0.60	–	0.08	–
Sicyonia picta	31.25	–	23.25	–	1.20	–	0.33	–
Rimapenaeus pacificus	16.67	–	3.29	–	0.60	–	0.06	–
Trizocarcinus dentatus	22.22	–	15.74	–	1.80	–	0.35	–
Crustacean remains	45.24	52.41	53.87	61.31	42.40	36.50	21.02	20.79
OSTEICHTHYES	41.44	38.05	34.70	38.88	14.50	14.90	5.54	5.74
Anchoa spp.	77.78	–	43.02	–	0.60	–	0.37	–
Auxis spp.	41.67	39.83	49.10	44.12	1.20	3.70	0.55	1.57
Bollmannia chlamydes	–	50.00	–	82.23	–	0.70	–	0.49
Citharichthys gilberti	50.00	–	25.33	–	0.60	–	0.23	–
Citharichthys platophrys	25.00	–	10.29	–	0.60	–	0.11	–
Paralichthyidae	–	9.09	–	5.21	–	0.70	–	0.05
Unidentified fish	58.33	50.00	52.47	46.26	1.20	0.70	0.67	0.36
Pleuronectiformes	37.50	–	52.07	–	0.60	–	0.27	–
Symphurus spp.	22.92	–	6.99	–	1.20	–	0.18	–
Fish remains	39.89	37.73	34.64	35.27	8.40	8.90	3.16	3.27
MOLLUSCA	43.92	44.65	43.85	33.66	16.90	8.20	7.45	3.21
Gastropoda	16.67	35.00	4.81	7.34	0.60	1.50	0.07	0.32
Lolliguncula (Loliolopsis) diomedeae	45.94	43.33	42.94	33.46	12.70	4.40	5.66	1.72
Squid remains	41.39	53.70	53.54	51.60	3.60	2.20	1.73	1.18
Unidentified organic material	16.67	22.22	6.56	31.64	0.60	1.50	0.07	0.40

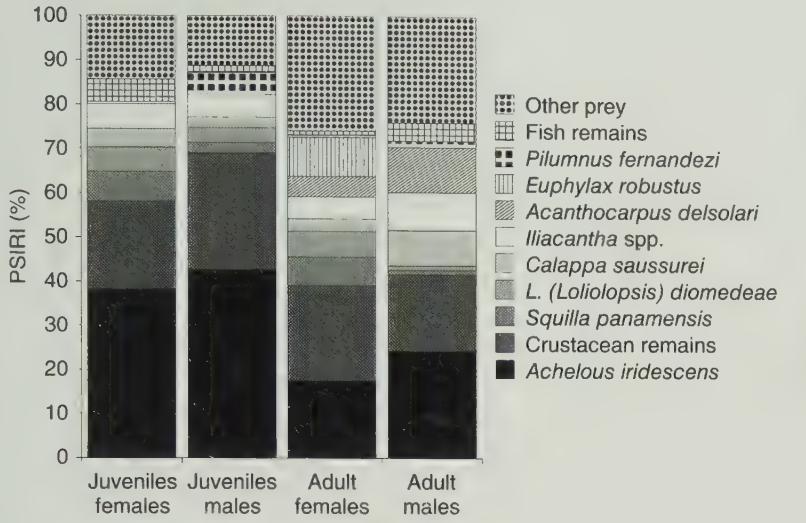

Figure 3

Diet composition of sicklefin smoothhounds (*Mustelus lunulatus*) caught in the southeastern Pacific Ocean between November 2003 and October 2004, by stage of sexual maturity (juvenile and adult).

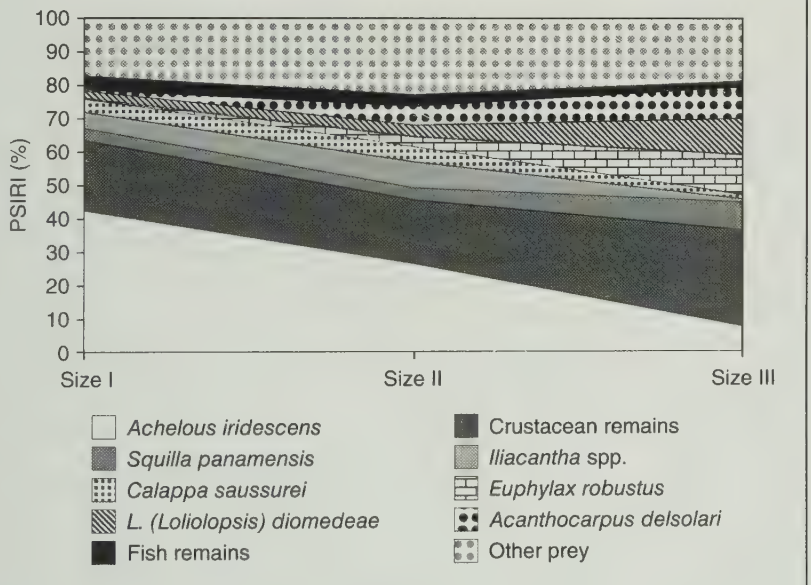

Figure 4

Diet composition of sicklefin smoothhounds (*Mustelus lunulatus*) caught in the southeastern Pacific Ocean between November 2003 and October 2004, by size class. The size classes are 60–90 cm in total length (TL, Size I, n=100), 90–120 cm TL (Size II, n=183), and 120–150 cm TL (Size III, n=32).

Dietary niche breadth, overlap, and trophic position

The standardized niche breadth index showed that the sicklefin smoothhound is a selective predator. This was the case for both females (B_A=0.06) and males (B_A=0.05), as well as for the different stages of sexual maturity (Table 4), size classes (Table 5), and trimesters. The B_i values were 0.50, 0.18, 0.06, and 0.05 for Trimesters I, II, III, and IV, respectively.

The trophic overlap index revealed high dietary overlap between the sexes ($C\lambda$=0.92, global R=0.009, P=0.072). When applied to the stages of sexual maturity, this index showed that the diet of adult females significantly overlaped with that of juveniles, both females and males (Table 4). However, there was little trophic overlap between size classes (Table 5).

The estimated trophic position (3.59 [standard deviation (SD) 0.24]) indicates that the sicklefin smoothhound is a secondary consumer. Also, by sex, maturity stage (Table 4), and size class (Table 5), this species is a secondary consumer.

Discussion

The few studies on the trophic ecology of the sicklefin smoothhound mention that its diet includes crustaceans (e.g., shrimps, blue crabs, and other crabs), small fishes (e.g., anchovies and sardines), and, occasionally, mollusks (Fernández, 1975; Gómez et al., 2003; Navia et al., 2006; Navia et al., 2007), with crustaceans being the most important prey group. These results are in line with those of this study, allowing the sicklefin smoothhound to be classified as a carcinophagous predator.

Dietary studies of other members of *Mustelus* have shown that this taxon prefers crustaceans. The humpback smoothhound (*M. whitneyi*), for example, eats crabs of the families Calappidae and Portunidae and shrimps of the family Squillidae and consumes small proportions of seaweed, annelids, mollusks, and fishes (Samame et al., 1989). The brown smoothhound (*M. henlei*) feeds mostly on crabs, shrimps (Squillidae), isopods, tunicates, cephalopods, and small fishes (e.g., Fischer et al., 1995; Gómez et al., 2003). These similarities in the diet of *Mustelus* species indicate that they prey on benthic crustaceans.

We found that the crabs *A. iridescens* and *Iliacantha* spp. were the main prey of sicklefin smoothhounds, similar to what was reported by Gómez et al. (2003) and Bohórquez-Herrera (2006) for Gorgona Island, Colombia. Our results are also consistent with those of studies

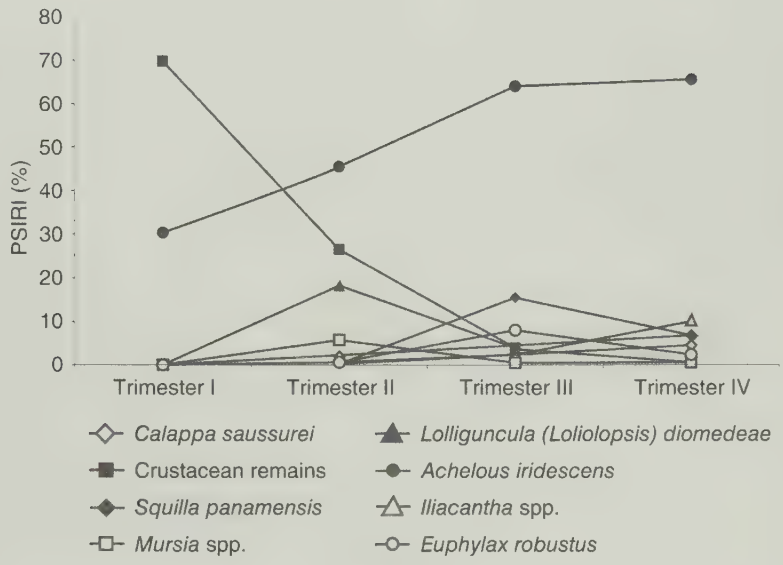

Figure 5

Diet composition of sicklefin smoothhounds (*Mustelus lunulatus*) caught in the southeastern Pacific Ocean between November 2003 and October 2004, by trimester of the year. The trimesters are November 2003–January 2004 (Trimester I), February 2004–April 2004 (Trimester II), May 2004–July 2004 (Trimester III), and August 2004–October 2004 (Trimester IV).

examining other species of the genus *Mustelus* that indicate that their principal prey are crustaceans (Ellis et al., 1996; Rojas, 2006). The results of our study, however, differ from the findings of Rojas (2000), Navia et al. (2006), and Navia et al. (2007), who reported that shrimps of the family Squillidae (e.g., Panama mantis shrimp and *Squilla parva*) were the main prey of sicklefin smoothhounds along the Pacific coast of Colombia. In contrast, the results of our study indicate that, although these shrimp species were present, they contributed little to the diet of sicklefin smoothhounds. This discrepancy can probably be attributed to the small number of stomachs (n=50, n=42) and size classes (mainly 50–70 cm TL) analyzed by Navia et al. (2006) and Navia et al. (2007), rather than to latitudinal variations that could affect the diversity and abundance of the main prey groups, because of the proximity of the localities studied. The distance between the location of this study (in Manta, Ecuador) and the location of the studies by Navia et al (2006) and Navia et al. (2007) (in Buenaventura, Colombia) is approximately 760 km.

Furthermore, Gomez et al (2003) and Bohórquez-Herrera (2006) conducted similar studies in areas close to the area studied by Navia et al. (2006) and Navia et al. (2007), and their results also differ from those obtained by Navia et al. (2006) and Navia et al. (2007). An example of latitudinal variation is the contrast in results obtained in the study by Moreno-Sánchez et al. (2012), who reported that in Baja California Sur, Mexico, sicklefin smoothhounds fed mostly on a squat lobster, *Munida tenella*, and the bigtooth rock crab (*Cancer amphioetus*), 2 species that are distributed from Southern California in the United States to the Gulf of California in Mexico (Nations, 1975; Hendrickx, 2000).

A likely explanation of the large presence of *A. iridescens* in the stomachs of sicklefin smoothhounds in waters of Ecuador is the abundance of this species in the region, as found by Mora et al. (2010). That study demonstrated that the most abundant macroinvertebrates along the coast of Ecuador were *A. iridescens*, followed by the arched swimming crab (*C. arcuatus*), dart squid, *C. toxotes*, and the pink shrimp (*Farfantepenaeus brevirostris*). These observations and results indicate that 1) sicklefin smoothhounds feed primarily at depths between 80 and 200 m (where there is the greatest abundance of *A. iridescens*, according to Mora et al., 2010) and 2) this species is a selective one, a trait that is associated with the abundance and availability of prey in the zones that it inhabits.

The dietary analysis by sex revealed that both female and male sicklefin smoothhounds have a preference for *A. iridescens*, a result that, together with the high dietary overlap between the sexes ($C\lambda$=0.92), indicates that there is no sexual segregation in this species. This finding agrees with the dietary overlap ($C\lambda$=0.96) estimated by Moreno-Sánchez et al. (2012), despite the geographical differences between the 2 studies. Nonetheless, these results must be interpreted with caution because they could represent "false positives," as occurred in our study with the analysis of the values of trophic overlap by stage of maturity for separate sexes (Table 4) indicating that sicklefin smoothhounds present behavioral and habitat segregation (Wearmouth and Sims, 2008). However, juveniles of both sexes and female adults complement their principal diet (*A. iridescens*) with coastal benthic prey that are typically associated with shallow waters and muddy–sandy seabeds, such as *E. robustus* (7–85 m) (Hendrickx, 1995a) and Panama mantis shrimp (18–102 m) (Hendrickx, 1995b) and with coastal pelagic species, such as the dart squid (50–200 m) (Sánchez, 2003).

The use of different feeding areas by juveniles of both sexes and female adults could be related to selection of breeding areas, abundance and availability of prey, development of hunting skills by juveniles, preferences for particular foraging zones pertaining to sex (McCord and Campana, 2003), size class, stage of maturity, and access to alternative sources of nutrition (e.g., pelagic prey; Eder and Lewis, 2005) related to specific stages of individual growth (Philips, 1969; Tytler and Calow, 1985).

In contrast, male adult sicklefin smoothhounds prefer to complement their diet with the consumption of benthic coastal prey that exhibit a greater range of distribution,

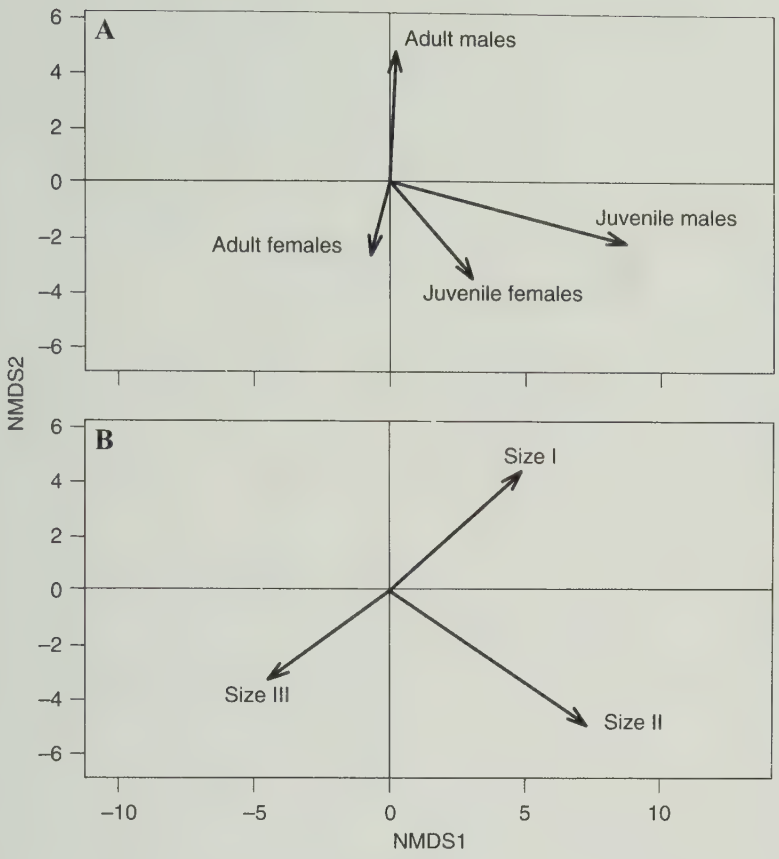

Figure 6

Nonmetric multidimensional scaling (MDS) ordination indicating the changes in diet of sicklefin smoothhounds (*Mustelus lunulatus*) caught in the southeastern Pacific Ocean between November 2003 and October 2004, for (**A**) maturity stages (juvenile and adult) and (**B**) size classes. The size classes are 60–90 cm in total length (TL, Size I), 90–120 cm TL (Size II), and 120–150 cm TL (Size III).

prey such as the small arched box crab, present at depths of 1–300 m (Hendrickx, 1997), and *Acanthocarpus desolari*, present at depths of 100–300 m (Del Rosario and Abele, 1976). These species typically inhabit seabeds formed from sand, mud, pebbles, stones, or dead coral (Hendrickx, 1997; Del Rosario and Abele, 1976).

Moreno-Sánchez et al. (2012) mentioned that juvenile and adult sicklefin smoothhounds fed on the same prey, but adults had a stronger preference for fish species. However, the authors analyzed juveniles and adults of both sexes combined, which may have obscured dietary patterns. In our study, for which the sexes were analyzed separately, both female and male juveniles were found to have a diet based on *Achelous iridescens* (>30% PSIRI; Fig. 3), a crustacean inhabiting sandy and muddy bottoms (Wehrtmann and Cortés, 2009) that can be easily captured by young sharks that are still developing their hunting skills. Adults (both female and male) ate less of this crustacean and complemented their diet with cephalopods (in the case of females) as well as other crustacean species (in the case of males). These results indicate that adult sharks, with their larger size and better hunting skills, explore new areas (i.e., the pelagic zone) while they search for food. The consumption of different foods by sharks at different stages of sexual maturity may be associated with 1) different energy requirements, 2) reproductive processes, 3) cost–benefit tradeoffs, 4) prey availability, and 5) hunting skills.

To date, no trophic study of the sicklefin smoothhound had analyzed feeding patterns throughout the year. Therefore, this study is the first to have conducted an analysis that took into account the trophic spectrum of the sicklefin smoothhound in 4 trimesters. The results of our study indicate that this species prefers *A. iridescens* throughout the year. However, between November 2003 and January 2004 the prey consumed was dominated by crustaceans (PSIRI: 69.7%), and in the other 3 trimesters the presence of *A. iridescens* increased in importance by 45–65% (PSIRI) and there was a corresponding reduction in the presence of crustaceans (Fig. 5).

These results are consistent with the abundance of crustaceans estimated by Mora et al. (2010), who identified 150 species of macroinvertebrates (120 crustaceans, 15 mollusks, 13 echinoderms, and 2 cnidarians), with the most abundant species being a swimming crab, *A. iridescens*, followed by a cephalopod, the dart squid. These observations support our results that indicate that the sicklefin smoothhound is a species that specializes in the consumption of crustaceans that are highly abundant in the zone they inhabit. Because of the substantial presence of crustaceans in stomachs of specimens during November–January (Trimester I) and the greater number of individuals in Size I (n=95) analyzed in the study period, we hypothesize that during this period juvenile individuals consume more small crustaceans that are easier to hunt and digest. Nonetheless, more studies are required, including research related 1) to abundance of prey species and (2) to other biological aspects of the sicklefin smoothhound (such as reproduction and growth) that would improve understanding of the spatial and temporal feeding behavior of this species.

The study of the diet of sicklefin smoothhounds by Moreno-Sánchez et al. (2012) may be the most detailed so far, and it found no ontogenetic changes in the diet of this species. Our study, in contrast, has revealed that the diet of sicklefin smoothhounds changes as they grow (Fig. 4) and become sexually mature (Fig. 3), from a diet composed

Table 3

Contribution of prey to the similarity of diet, by sex, stage of sexual maturity, and size class, for sicklefin smoothhounds (*Mustelus lunulatus*) caught in the southeastern Pacific Ocean during November 2003–October 2004, based on similarity percentage analysis. The maturity stages are juvenile (J.) and adult (A.), and the size classes are 60–90 cm in total length (TL, Size I), 90–120 cm TL (Size II), and 120–150 cm TL (Size III). A dash indicates that data were not available because the prey species was not shared between categories.

	Combination								
Prey	J. female vs. A. female	J. male vs. A. male	J. female vs. J. male	A. female vs. A. male	J. female vs. A. male	A. female vs. J. male	Size I vs. Size II	Size I vs. Size III	Size II vs. Size III
Dissimilarity (%)	86.28	84.00	80.40	88.48	82.67	85.23	82.37	89.30	90.92
Achelous iridescens	34.52	39.24	45.82	27.29	33.46	39.00	38.46	28.78	25.35
Lolliguncula (Loliolopsis) diomedeae	9.19	–	8.52	5.36	5.66	8.38	5.67	11.73	10.87
Squilla panamensis	8.43	–	7.11	5.25	5.34	7.11	5.41	10.16	9.11
Iliacantha spp.	7.76	10.47	8.97	9.46	10.93	7.38	9.99	–	6.20
Calappula saussurei	5.61	8.94	5.69	8.71	9.29	–	7.61	–	5.22
Mursia spp.	–	6.97	–	9.17	6.31	–	–	9.66	9.67
Euphylax robustus	–	–	–	–	–	–	–	6.39	6.54
Ethusa spp.	–	–	–	–	–	–	–	–	5.17
Mollusks	13.16	5.98	11.69	8.09	8.98	11.43	7.86	16.78	17.3
Crustaceans	82.18	90.2	84.48	87.21	85.72	85.34	87.63	77.16	77.49
Fishes	4.66	3.82	3.84	4.70	5.30	3.33	4.51	6.06	5.21

Table 4

Dietary overlap between stages of sexual maturity, dietary niche breadth (B_A), and trophic position (TP) for sicklefin smoothhounds (*Mustelus lunulatus*) caught in the southeastern Pacific Ocean during November 2003–October 2004. An asterisk (*) indicates high overlap. n=number of stomachs analyzed.

Maturity stage and sex	Juvenile male (n=54)	Adult male (n=90)	Juvenile female (n=90)	Adult female (n=81)	B_A	TP
Juvenile male	–				0.03	3.86
Adult male	0.34	–			0.15	3.49
Juvenile female	0.02	0.31	–		0.03	3.85
Adult female	0.60*	0.47	0.56*	–	0.29	3.30

almost exclusively of *A. iridescens* to one including other crustaceans, cephalopods, and fishes. This diet change may be related 1) to hunting ability and skill and 2) to the morphology of the mouth and jaw (Luczkovich et al., 1995). In addition, this change in diet is reflected in the narrow trophic niche and the low dietary overlap between organisms of different size classes of sicklefin smoothhounds considered in this study (Table 5).

Because sharks exhibit characteristics typical of top-level predators, they are thought to regulate prey communities through top-down control (e.g., Ferretti et al., 2010; Navia et al., 2010; Bornatowski et al., 2014b), together with habitat structure and ecosystem productivity (Estes et al., 2011; Ripple et al., 2014). Consequently, they are regarded as a key functional group (Frisch et al., 2016). Sharks are attributed important roles in marine food webs; however, few studies have provided evidence of the presumably high trophic positions of some shark species (Cortés, 1999).

Nonetheless, it is worth noting that not all sharks are top-level predators in a given ecosystem because the potential ecological functions of the species are related to a variety of factors, such as feeding habits, maximum body length, geographic and environmental range, the extent to which they are omnivorous, and vulnerability to predation by other sharks. Hence, the results of the study by Roff et al. (2016) indicate that sharks can exercise functions as high-level predators (maximum TL >300 cm, geographic

Table 5

Dietary overlap between size classes, dietary niche breadth (B_A), and trophic position (TP) in sicklefin smoothhounds (*Mustelus lunulatus*) caught in the southeastern Pacific Ocean during November 2003–October 2004. The size classes are 60–90 cm in total length (TL, Size I), 90–120 cm TL (Size II), and 120–150 cm TL (Size III). An asterisk (*) indicates high overlap. n=number of stomachs analyzed.

Size class	Size I (n=100)	Size II (n=182)	Size III (n=32)	B_A	TP
Size I	–			0.02	3.93
Size II	0.12	–		0.06	3.60
Size III	0.31	0.52*	–	0.13	2.73

range of 100–1000 km, highly omnivorous), intermediate mesopredators (maximum TL 150–300 cm, geographic range <10 km, high trophic position), or small mesopredators (maximum TL <100 cm, geographic range <10 km, generally not omnivorous).

In accordance with these groupings, this study classified the sicklefin smoothhound as an intermediate mesopredatory shark (mean trophic position: 3.59 [SD 0.24]). This finding is consistent with the trophic position estimated by Cortés (1999) for the sicklefin smoothhound (3.9) and for other species of the genus *Mustelus*, for example, the brown smoothhound (3.6) and the gray smoothhound (*M. californicus*, 3.5). Our results indicate that the sicklefin smoothhound could be an important factor if there is a substantial change in the populations of other large shark species (Bornatowski et al., 2014b).

In conclusion, the sicklefin smoothhound is an intermediate mesopredator that regulates the most abundant benthic crustacean populations along the coast of Ecuador. Generally, this species exhibits behavior and habitat segregation, and it is a selective predator that specializes in the consumption of highly abundant crustaceans off the coast of Ecuador. In this study, ontogenetic changes related to stage of maturity, size class, and time of year were observed in the diet of sicklefin smoothhounds. This study fills gaps in our knowledge of sharks in the waters of Ecuador and provides data for Ecuador's national plan of action for the conservation and management of sharks (MICIP, 2006).

Acknowledgments

The authors thank the fishermen and storekeepers of Tarqui Beach in Manta. C. Estupiñán-Montaño thanks the Fundación Alium Pacific, and F. Galván-Magaña thanks the Instituto Politecnico Nacional programs Estímulos al Desempeño de los Investigadores and Comisión de Operación y Fomento de Actividades Académicas. We thank I. Gambache and D. Edgar for editing our text for English.

Literature cited

Bohórquez-Herrera, J.
2006. Aspectos biológicos y pesqueros de los elasmobranquios capturados en el Parque Nacional Natural Gorgona y su área de influencia entre 2004 y 2005. B.S. thesis, 104 p. Univ. de Bogota Jorge Tadeo Lozano, Bogota, Colombia. [In Spanish.] [Available from website.]

Bornatowski, H., R. R. Braga, V. Abilhoa, and M. F. Corrêa.
2014a. Feeding ecology and trophic comparions of six shark species in coastal ecosystem off southern Brazil. J. Fish Biol. 85:246–263.

Bornatowski, H., A. F. Navia, R. R. Braga, V. Abilhoa, and M. F. M. Corrêa.
2014b. Ecological importance of sharks and rays in a structural foodweb analysis in southern Brazil. ICES J. Mar. Sci. 71:1586–1592.

Braga, R. R., H. Bornatowski, and J. R. Vitule.
2012. Feeding ecology of fishes: an overview of worldwide publications. Rev. Fish Biol. Fish. 22:915–929.

Brown, S. C., J. J. Bizarro, G. M. Cailliet, and D. A. Ebert.
2012. Breaking with tradition: redefining measures for diet description with a case study of the Aleutian skate *Bathyraja aleutica* (Gilbert 1896). Environ. Biol. Fish. 95:3–20.

Chirichigno F., N., and J. Vélez D.
1998. Clave para identificar los peces marinos del Peru, 2nd ed., 491 p. Publ. Espec. Inst. Mar Peru, Callao, Peru. [In Spanish.] [Available from website.]

Clarke, M. R.
1986. A handbook for identification of cephalopod beaks, 269 p. Clarendon Press, Oxford, UK.

Clarke, K. R., and R. N. Gorley.
2006. PRIMER v6: user manual/tutorial, 18 p. PRIMER-E, Plymouth, UK.

Clothier, C. R.
1950. A key to some Southern California fishes based on vertebral characters. Calif. Dep. Fish Game, Fish Bull. 79, 83 p.

Colwell, R. K.
2013. EstimateS: statistical estimation of species richness and shared species from samples. Vers. 9. User's guide and application. [Available from website.]

Compagno, L. J. V.
1984. FAO species catalogue. Vol. 4, Sharks of the world: an annotated and illustrated catalogue of shark species known to date. Parts 1 and 2 (Hexanchiformes to Lamniformes; Carcharhiniformes). FAO Fish. Synop. 125, vol. 4, 655 p. FAO, Rome.

Cortés, E.
1999. Standardized diet composition and trophic levels of sharks. ICES J. Mar. Sci. 56:707–717.

Del Rosario, J. B., and L. G. Abele.
1976. Description of the male and new distribution records for *Acanthocarpus delsolari* Garth 1973 (Decapoda, Calappidae) from de Pacific coast of Panama. Crustaceana 30:225–228.

Eder, E. B., and M. N. Lewis.
2005. Proximate composition and energetic value of demersal and pelagic prey species from the SW Atlantic Ocean. Mar. Ecol. Prog. Ser. 291:43–52.

Ellis, J. R., M. G. Pawson, and S. E. Shackley.
1996. The comparative feeding ecology on six species of shark and four species of ray (Elasmobranchii) in the north-east Atlantic. J. Mar. Biol. Assoc. U.K. 76:89–106.

Estes, J. A., J. Terborgh, J. S. Brashares, M. E. Power, J. Berger, W. J. Bond, S. R. Carpenter, T. E. Essington, R. D. Holt, J. B. C. Jackson et al.
2011. Trophic downgrading of planet Earth. Science 333:301–306.

Fernández, P.
1975. Estudio biológico y pesquero de algunas especies de tiburones carcharinidos del Pacífico colombiano. Ph.D. diss., 154 p. Univ. Jorge Tadeo Lozano, Bogota, Colombia. [In Spanish.]

Ferretti, F., B. Worm, G. L. Britten, M. R. Heithaus, and H. K. Lotze.
2010. Patterns and ecosystem consequences of shark declines in the ocean. Ecol. Lett. 13:1055–1071.

Fischer, W., F. Krupp, W. Schneider, C. Sommer, K. E. Carpenter, and V. H. Niem (eds.).
1995. Guía FAO para la identificación de especies para los Fines de Pesca. Pacífico centro-oriental: vertebrados, vols. 2 and 3, p. 647–1813. FAO, Rome. [In Spanish.]

Frisch, A. J., M. Ireland, J. R. Rizzari, O. M. Lönnstedt, K. A. Magnenat, C. E. Mirbach, and J.-P. A. Hobbs.
2016. Reassessing the trophic role of reef sharks as apex predators on coral reefs. Coral Reefs 35:459–472.

García-Godos, I.
2001. Patrones morfológicos del otolito sagitta de algunos peces óseos del mar Peruano. Bol. Inst. Mar Peru 20(1–2):1–83. [In Spanish.] [Available from website.]

Garth, J. S.
1973. New taxa of brachyuran crabs from deep water off western Peru and Costa Rica. Bull. South. Calif. Acad. Sci. 72:1–12.

Gómez, G. O., L. A. Zapata, R. Franke, and G. E. Ramos.
2003. Hábitos alimentarios de *Mustelus lunulatus* y *M. henlei* (Pisces: Triakidae) colectados en el Parque Nacional Natural Gorgona, Pacífico Colombiano. Bol. Invest. Mar. Cost. 32:219–229. [In Spanish.]

Hammer, Ø., D. A. T. Harper, and P. D. Ryan.
2001. PAST: paleontological statistics software package for education and data analysis. Palaeontol. Electron. 4(1), 9 p. [Available from website.]

Heithaus, M. R., A. Frid, A. J. Wirsing, and B. Worm.
2008. Predicting ecological consequences of marine top predator declines. Trends Ecol. Evol. 23:202–210.

Heithaus, M. R., A. Frid, J. J. Vaudo, B. Worm, and A. J. Wirsing.
2010. Unraveling the ecological importance of elasmobranchs. *In* Biology of sharks and their relatives II (J. C. Carrier, J. A. Musick, and M. R. Heithaus, eds.), p. 611–637. CRC Press, Boca Raton, FL.

Heithaus, M. R., J. J. Vaudo, S. Kreicker, C. A. Layman, M. Krützen, D. A. Burkholder, K. Gastrich, C. Bessey, R. Sarabia, K. Cameron et al.
2013. Apparent resource partitioning and trophic structure of large-bodied marine predators in a relatively pristine seagrass ecosystem. Mar. Ecol. Prog. Ser. 481:225–237.

Hendrickx, M. E.
1995a. Cangrejo. *In* Guía FAO para la identificación de especies para los fines de la pesca. Pacífico centro-oriental, vol. 1: plantas e invertebrados (W. Fischer, F. Krupp, W. Schneider, C. Sommer, K. E. Carpenter, and K. E. Niem, eds.), p. 565–636. FAO, Rome. [In Spanish.]
1995b. Estomatópodos. *In* Guía FAO para la identificación de especies para los fines de la pesca. Pacífico centro-oriental, vol. 1: plantas e invertebrados (W. Fischer, F. Krupp, W. Schneider, C. Sommer, K. E. Carpenter, and U. H. Niem, eds.), p. 355–382. FAO, Rome. [In Spanish.]
1997. Los cangrejos braquiuros (Crustacea: Brachyura: Dromiidae, hasta Leucosiidae) del Pacifico Mexicano, 178 p. Com. Nac. Conocim. Uso Biodivers., Inst. Cienc. Mar Limnol., Univ. Nac. Auton. Mex., Mexico City, Mexico. [In Spanish.]
2000. The genus *Munida* Leach (Crustacea, Decapoda, Galatheidae) in the eastern tropical Pacific, with description of two new species. Biologie 79:163–192.

Hobson, K. A., and H. E. Welch.
1992. Determination of trophic relationships within a high Arctic marine food web using $\delta^{13}C$ and $\delta^{15}N$ analysis. Mar. Ecol. Prog. Ser. 84:9–18.

Krebs, C. J.
1999. Ecological methodology, 745 p. Addison Wesley, Menlo Park, CA.

Lucifora, L. O., V. B. Garcia, R. C. Menni, A. H. Escalante, and N. M. Hozbor.
2009. Effects of body size, age and maturity stage on diet in a large shark: ecological and applied implications. Ecol. Res. 24:109–118.

Luczkovich, J. J., S. F. Norton, and R. G. Gilmore.
1995. The influence of oral anatomy on prey selection during the ontogeny of two percoid fishes, *Lagodon rhomboides* and *Centropomus undecimalis*. Environ. Biol. Fish. 44:79–95.

McCord, M. E., and S. E. Campana.
2003. A quantitative assessment of the diet of the blue shark (*Prionace glauca*) off Nova Scotia, Canada. J. Northwest Atl. Fish. Sci. 32:57–63.

MICIP (Ministerio de Comercio Exterior, Industrialización, Pesca y Competitividad).
2006. Plan de acción nacional para la conservación y manejo de tiburones de Ecuador (PAT-Ec), 44 p. MICIP, Quito, Ecuador. [In Spanish.]

Mora, E., V. Jurado, and W. Mendívez.
2010. Diversidad de macroinvertebrados en la plataforma continental de Ecuador. Rev. Cienc. Mar Limnol. 4(2):101–116. [In Spanish.]

Moreno-Sánchez, X. G., O. Escobar-Sánchez, L. A. Abitia-Cardenas, and V. H. Cruz-Escalona.
2012. Diet composition of the sicklefin smooth-hound shark *Mustelus lunulatus* caught off El Pardito Island, Baja California Sur, Mexico. Mar. Biodivers. Rec. 5:e67.

Nations, D. J.
1975. The genus *Cancer* (Crustacea: Brachyura): systematics, biogeography and fossil record. Nat. Hist. Mus. Los Ang. Cty., Sci. Bull. 23, 104 p.

Navia, A. F., A. Giraldo, and P. A. Mejía-Falla.
2006. Notas sobre la biología y dieta del toyo vieja (*Mustelus lunulatus*) en la zona central de pesca del Pacífico colombiano. Invest. Mar. 34:217–222. [In Spanish.]

Navia, A. F., P. A. Mejia-Falla, and A. Giraldo.
2007. Feeding ecology of elasmobranch fishes in coastal waters of the Colombian Eastern Tropical Pacific. BMC Ecology 7:8.

Navia, A. F., E. Cortés, and P. A. Mejía-Falla.
2010. Topological analysis of the ecological importance of elasmobranch fishes: a food web study on the Gulf of Tortugas, Colombia. Ecol. Model. 221:2918–2926.

Pérez-Jiménez, J. C., and O. Sosa-Nishizaki.
2010. Determining reproductive parameters for population assessments of two smoothhounds (*Mustelus californicus* and *Mustelus lunulatus*) from the northern Gulf of California, Mexico. Bull. Mar. Sci. 86:3–13.

Philips, A. M., Jr.
1969. Nutrition, digestion, and energy utilization. *In* Fish physiology, vol. 1 (W. S. Hoar and D. J. Randall, eds.), p. 391–431. Academic Press, London.

Pinkas, L., M. S. Olphant, and I. L. K. Iverson.
1971. Food habits of albacore, bluefin tuna, and bonito in California waters. Calif. Dep. Fish Game, Fish Bull. 152, 105 p.
Ripple, W. J., J. A. Estes, R. L. Beschta, C. C. Wilmers, E. G. Ritchie, M. Hebblewhite, J. Berger, B. Elmhagen, M. Letnic, M. P. Nelson et al.
2014. Status and ecological effects of the world's largest carnivores. Science 343:1241484.
Roff, G., C. Doropoulos, A. Rogers, Y.-M. Bozec, N. C. Krueck, E. Aurellado, M. Priest, C. Birrell, and P. J. Mumby.
2016. The ecological role of sharks on coral reefs. Trends Ecol. Evol. 31:395–407.
Rojas, P. A.
2000. Contribución al conocimiento biológico de *Mustelus lunulatus* un recurso potencial para el Pacífico Colombiano. M.S. thesis, 59 p. Univ. del Valle, Cali, Colombia. [In Spanish.]
Rojas, J. R.
2006. Reproducción y alimentación del tiburón enano *Mustelus dorsalis* (Pisces: Triakidae) en el golfo de Nicoya, Costa Rica: elementos para un manejo sostenible. Rev. Biol. Trop. 54:861–971. [In Spanish.]
Sánchez, P.
2003. Cephalopods from off the Pacific coast of Mexico: biological aspects of the most abundant species. Sci. Mar. 67:81–90.
Samame, M., J. Castillo, and M. Espino.
1989. El tollo un recurso demersal. Algunos aspectos de la biología y pesquería del *Mustelus whitneyi*. Ch. Com. Perm. Pac. Sur. Rev. Pac. Sur. 313–326. [In Spanish.]
Smith, E. P., and T. M. Zaret.
1982. Bias in estimating niche overlap. Ecology 63:1248–1253.
Stevens, J. D., R. Bonfil, N. K. Dulvy, and P. A. Walker.
2000. The effects of fishing on sharks, rays, and chimeras (chondrichthyans), and the implications for marine ecosystems. ICES J. Mar. Sci. 57:476–494.
Tytler, P., and P. Calow.
1985. Fish energetics: new perspectives, 349 p. Johns Hopkins Univ. Press, Baltimore, MD.
Wearmouth, V. J., and D. W. Sims.
2008. Chapter 2. Sexual segregation in marine fish, reptiles, bird and mammals: behaviour patterns, mechanisms and conservation implications. Adv. Mar. Biol. 54:107–170.
Wehrtmann, I. S., and J. Cortés (eds.).
2009. Marine biodiversity of Costa Rica, Central America, 538 p. Springer, San Jose, Costa Rica.
Wolff, C. A.
1984. Identification and estimation of size from the beaks of eighteen species of cephalopods from the Pacific Ocean. NOAA Tech. Rep. NMFS 17, 50 p.

National Marine
Fisheries Service
NOAA

Fishery Bulletin
established in 1881

Spencer F. Baird
First U.S. Commissioner
of Fisheries and founder
of *Fishery Bulletin*

Behavioral thermoregulation by adult Chinook salmon (*Oncorhynchus tshawytscha*) in estuary and freshwater habitats prior to spawning

Frederick A. Goetz (contact author)[1]
Thomas P. Quinn[2]

Email address for contact author: fred.goetz@usace.army.mil

[1] Seattle District
U.S. Army Corps of Engineers
P.O. Box 3755
Seattle, Washington 98124-3755

[2] School of Aquatic and Fishery Sciences
University of Washington
Box 355020
Seattle, Washington 98195

Abstract—The movements of maturing Pacific salmon (*Oncorhynchus* spp.) from marine waters into rivers pose challenges for their physiology, especially in basins affected by human structures and increasing temperatures. This study determined the thermal regimes experienced by maturing Chinook salmon (*O. tshawytscha*) entering the Lake Washington basin in western Washington through navigational locks and a ship canal and migrating through the lake to spawning grounds. Chinook salmon entered in mid-summer, when temperatures were warmest, but often moved back into the cool, marine waters of Puget Sound before travelling quickly through the ship canal and into Lake Washington. In Lake Washington, they swam above and below the thermocline and made little use of the available thermal refuge in deep water before ascending rivers to spawn. The migration timing and tactics of Chinook salmon indicate a greater tolerance for warm water than that of sympatric sockeye salmon (*O. nerka*, documented in an independent study), but in each species the ability to exploit thermal refuges may be essential for their survival in the face of the increasing temperatures seen in this basin in the past decades and those that are likely to continue rising in the future.

Manuscript submitted 24 October 2018.
Manuscript accepted 22 August 2019.
Fish. Bull. 117:258–271 (2019).
Online publication date: 6 September 2019.
doi: 10.7755/FB.117.3.12

The views and opinions expressed or implied in this article are those of the author (or authors) and do not necessarily reflect the position of the National Marine Fisheries Service, NOAA.

Most fish species live entirely in fresh or salt water, and only a small fraction, from many different evolutionary lineages, migrates regularly between these environments (McDowall, 1988). These diadromous fish species always experience a decrease in salinity and temperature changes when entering fresh water. In the summer and early fall at higher latitudes (>40°N), the marine waters are typically cooler than the rivers, but the reverse may be the case in winter. Estuaries are the transition zone for this shift between marine and riverine habitats, affording intermediate conditions of salinity and temperature. However, estuaries and their associated waterways are often altered by human development (Nichols et al., 1986; Emmett et al., 2000; Lotze et al., 2006).

The thermal transition that diadromous fish species experience in estuaries is important because temperature affects so many aspects of their biology (Magnuson, 2010) and has been called the abiotic "ecological master factor" (Brett, 1971). For example, temperatures that adult Pacific salmon (*Oncorhynchus* spp.) experience in coastal marine waters and during upriver migration can affect survival (Gilhousen, 1990; Hinch et al., 2012), maturation (Roscoe et al., 2010), and reproductive success (Minke-Martin et al., 2018). Consequently, adult Pacific salmon and Atlantic salmon (*Salmo salar*) show many behavioral responses to temperature, including changes in vertical distribution at sea (Quinn et al., 1989; Tanaka et al., 2000; Walker et al., 2000), holding in river plumes outside estuaries (Cooke et al., 2008; Strange, 2013), changing vertical distribution in estuaries (Olson and Quinn, 1993), delay in upriver migration (Kristinsson et al., 2015), use of cool tributaries or deep pools (Berman and Quinn, 1991; Goniea et al., 2006; Strange, 2010; Moore et al., 2012), or spending the summer below the thermocline in lakes (Newell and Quinn, 2005; Mathes et al., 2010).

Many Pacific salmon populations experiencing high water temperatures are at low levels of abundance, and salmon experience *en route* or prespawning mortality in some years (Gilhousen, 1990; Richter and Kolmes, 2005; Hinch et al., 2012). Temperatures are predicted to continue to increase in the future, exacerbating the problem (Yates et al., 2008; Mantua et al., 2010). The changing thermal regimes may be especially

stressful for populations migrating through estuaries and river corridors that have been modified through channelization, reducing suitable holding habitat, and where structures such as locks and dams have altered tidal regimes and hydrology (Hallock et al., 1970; Potter, 1988; Russell et al., 1998; Holbrook et al., 2009).

The combination of warming conditions and habitat alteration is exemplified by Lake Washington (Fig. 1), in Washington (Williamson et al., 2009), where adult Chinook salmon (*O. tshawytscha*) enter from July through September—the warmest period of the year (Fig. 2A). Temperatures in the lake and tributaries have been increasing, especially in summer (Quinn et al., 2002; Winder and Schindler, 2004; Fig. 2B). In contrast to large systems like the Columbia River, where salmonids use tributary junctions as thermal refuges (Keefer et al., 2018), and some small rivers apparently lacking thermal refuges (Hasler et al., 2012), the Lake Washington system's primary thermal refuge is stratification in the lake, but other small-scale thermal structures (i.e., river confluence and pools in rivers) also are available. The system also poses special challenges for salmon, including an abrupt change in salinity from Puget Sound to the migration corridor above the locks and low dissolved oxygen (DO) levels in parts of the corridor. Increasing temperatures may adversely affect migration rate and spawning success of Chinook and other salmon species in this system, and elsewhere (Connor et al., 2019), but the nature and extent of the effects may depend on the behavioral thermoregulation and other tactics used by salmon migrating through these altered waterways.

In this study, we used acoustic transmitters and archival temperature loggers to determine how adult Chinook salmon migrate through a complex sequence of structures and ambient water conditions from a small, marine-influenced estuary through a set of locks and a shallow, warm navigation canal into a large, stratified lake and then into tributaries for spawning. We sought to determine whether segments of the migration route have conditions that delay migration and expose salmon to thermal stress from elevated temperatures that might affect survival and reproductive success. We did so by posing the following questions: 1) do Chinook salmon move back and forth between marine and fresh water prior to upriver migration? 2) do water temperatures experienced in fresh water affect transit time? 3) do the salmon minimize exposure to warm water by moving to deeper, cooler water where available? and 4) is use of cool water affected by ambient DO concentration and salinity? In this context, we use the term *experience* to indicate the thermal and other environmental conditions in the water the fish occupied, without making any implication regarding preference or avoidance.

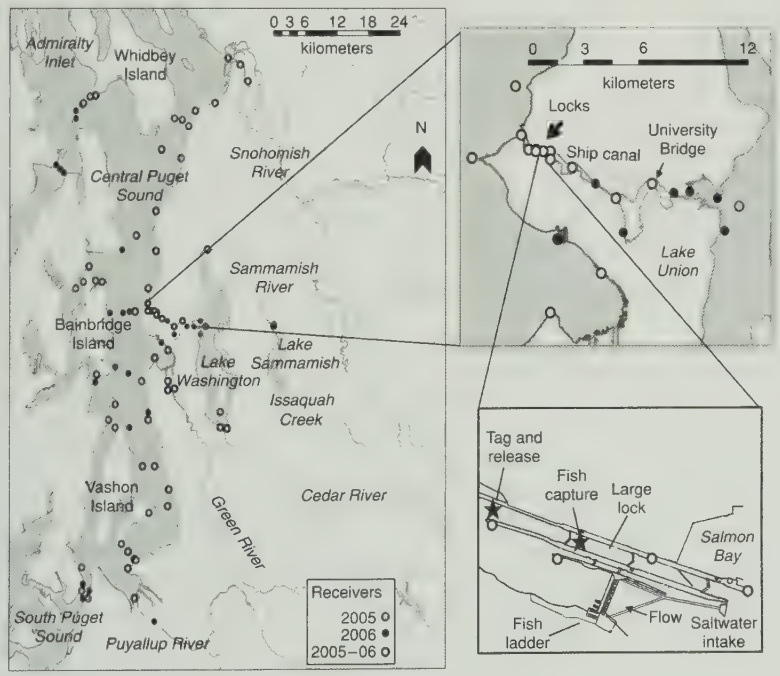

Figure 1

Map showing the acoustic monitoring network in coastal waters near Puget Sound, in western Washington, used to track the migration of tagged adult Chinook salmon (*Oncorhynchus tshawytscha*) in 2005 and 2006. The shade of circles indicates the year of deployment of acoustic receivers. The other maps show locations of receivers (circles) and of tagging and release events (stars) in the ship canal (top) and locks (bottom) in Lake Washington.

Materials and methods

Study area

Puget Sound is a large (3700 km^2) fjord system in western Washington bordered by British Columbia, Canada, to the north (Fig. 1). The Lake Washington watershed covers 1274 km^2 and flows from tributaries of Lakes Sammamish and Washington through a navigation channel (henceforth, the *ship canal*) through the north end of Lake Union, to the Hiram M. Chittenden Locks (henceforth, the *locks*), and into Shilshole Bay. Salmon Bay, immediately upstream of the locks, has a saltwater wedge, and we refer to this bay as the *upper estuary* and to the area from the locks down to Shilshole Bay as the *lower estuary*. The lower estuary has summer mean temperatures of 12–13°C and salinity of 15–30. The saltwater wedge intrudes up to 6 km into the ship canal above the locks, but the highest salinities (1–20) and most mixing are within 1 km of the locks (Fig. 1, insets). The ship canal is 12.5 km long from Shilshole Bay to Lake Washington (10.8 km from the

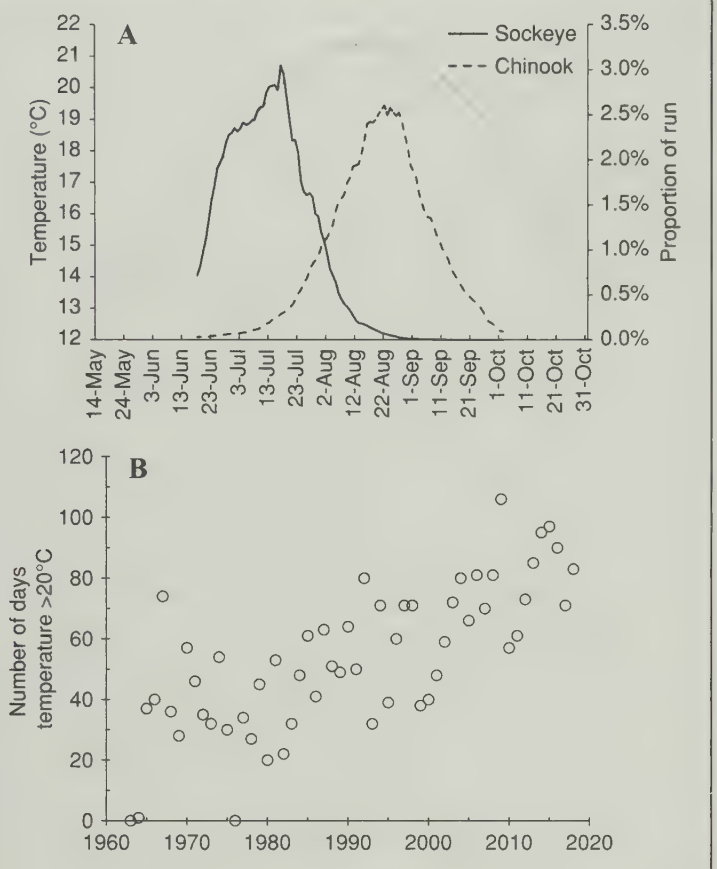

Figure 2

(**A**) Migration timing of sockeye (*Oncorhynchus nerka*) and Chinook (*O. tshawytscha*) salmon at the locks in the Lake Washington watershed in Washington (black lines) and mean lock temperature (gray line) during May–October in 2005 and 2006. The timing of migration (black lines) is presented as the proportion of the time of the run fish spent at various temperatures. (**B**) Number of days, by year, between the first and last days when the epilimnetic temperatures exceeded 20°C in Lake Washington. Data were provided by C. DeGasperi, King County Department of Natural Resources and Parks, Seattle, Washington.

locks to the lake) with a mean depth of 9 m and includes shallow Lake Union (mean depth: 10.5 m; maximum: 16 m). Lake Washington has a surface area of 87.6 km^2, a mean depth of 32.9 m (maximum: 65.2 m), and a summer epilimnion to about 10 m. Lake Washington's 2 largest tributaries are the Cedar River and the Sammamish River, which drains Lake Sammamish (surface area: 21 km^2; mean depth: 18 m).

The locks include a tidally influenced fish ladder, small (8 m deep) and large (16 m deep) lock chambers, a spillway bay (5 m deep), and a drain above the large lock to return salt water to Puget Sound. The large lock is used by migrating salmon and is included in the area defined as the lower estuary. The locks physically separate the freshwater system, without any tidal elevation changes, from the marine system where tidal amplitudes reach 4 m. The exchange of fresh and salt water occurs predominantly in localized pulses during locking events, resulting in unusual circulation patterns within the estuarine portion of the ship canal. Salt water enters when the locks lift vessels from Puget Sound up and into the ship canal; therefore, temperatures in the large lock chamber can change up to 9°C in less than 1 h. Salt water intrusion in spring and early summer is usually restricted to the lower 1.5 km of the ship canal, but by late summer it reaches Lake Union (4–6 km upstream), although at lower concentrations (salinity: 0–2) than near the locks (salinity up to 15). Vertical stratification in temperature and salinity occurs in Puget Sound, below the locks, within the large lock, in the saltwater wedge in Salmon Bay, in the ship channel (salinity only), and in Lake Union, and temperature stratification occurs in Lake Washington and Lake Sammamish. Low DO levels (<5 mg/L) occur near the bottom from the upper estuary starting in August until the end of September.

Fish capture and tagging

In 2005 and 2006, the Washington Department of Fish and Wildlife (WDFW) and R2 Resource Consultants[1] (R2, Redmond, WA) captured 368 Chinook salmon by using a purse seine in the lower half of the large lock from early August through early September, tagged, and immediately released them below the locks in the lower estuary. This net was designed for sampling and safely releasing juvenile salmonids (Durkin and Park, 1967; Ledgerwood et al., 1991), and only fish in good condition were used for tagging, in an effort to minimize the effects of handling on fish survival and behavior. Catch and release, from commercial, scientific, and recreational fisheries, can affect survival, physiology, and behavior of salmon, but the effects are context dependent (Candy et al., 1996; Donaldson et al., 2011; Raby et al., 2015). Given the nature of our study system, there was no way to know how salmon would have behaved had we not caught and tagged them, nor did it allow us to compare survival rates among salmon with different types of tags. However, our goal was not to assess survival, it was to examine thermoregulatory behavior, for which our approach was standard and appropriate.

The Chinook salmon had both archival temperature data loggers, implanted by using tagging techniques similar to those in Newell and Quinn (2005), and passive integrated transponder (PIT) tags; approximately 25% also received acoustic tags (Table 1). These types of tags yield different but complementary kinds of information. The fish ladder

[1] Mention of trade names or commercial companies is for identification purposes only and does not imply endorsement from the National Marine Fisheries Service, NOAA.

Table 1

Mean length of adult Chinook salmon (*Oncorhynchus tshawytscha*) captured and tagged in coastal waters near Puget Sound in Washington in 2005 and 2006, and associated tagging and recovery data for discrete weekly tagging events. Standard deviations of mean lengths are given in parentheses. PIT=passive integrated transponder.

Tag and release date	Mean fork length (mm)	No. of archival/PIT tags	No. of acoustic tags	No. of PIT detections	No. of archival recoveries	No. of archival and acoustic recoveries
11-Aug-05	780.7 (84.7)	19	15	5	4	3
17-Aug-05	738.1 (117.5)	57	7	11	9	1
24-Aug-05	735.1 (82.0)	72	10	17	27	3
31-Aug-05	750.1 (105.7)	50	10	7	19	4
Mean or total for 2005	744.1 (99.8)	198	42	40	59	11
9-Aug-06	795.7 (63.9)	50	19	12	13	7
16-Aug-06	768.4 (96.0)	32	11	3	8	4
23-Aug-06	820.3 (72.3)	29	9	2	11	2
30-Aug-06	789.7 (64.5)	32	7	4	13	3
6-Sep-06	796.7 (64.8)	21	5	0	6	1
13-Sep-06	842.0 (117.3)	10	2	2	3	0
Mean or total for 2006	794.2 (82.6)	174	53	23	54	17

had PIT tag detectors in a pool immediately upstream of the exit, indicating the proportion of fish using the ladder. Archival loggers attached externally, just behind the dorsal fin, recorded ambient temperatures experienced by the salmon. For data loggers, we used model iBCod (Alpha Mach, Ste-Julie, Quebec) type Z (high resolution ±0.125°C, precision ±1°C, temperature range of –5–26°C, weight of 12 g in air), a size appropriate for tagging fish 50–100 cm in fork length, and attached them to the salmon by using nickel pins and vinyl disks. The temperature loggers recorded data hourly for 95 d but had to be recovered to acquire the data. Moreover, the precise location of the fish had to be inferred from the thermal regime or detection of a transmitter in the fish (if it had one) when it passed a receiver.

Locations of 95 Chinook salmon were determined by using acoustic transmitters weighing ≤12 g. Vemco (Bedford, Canada) V13-1L (22) and V13P-1L pressure sensors (63) and V9-6L (11) acoustic tags, with 20–60 s and 30–90 s minimum and maximum pulse rates (or intervals between each signal transmission), were inserted into stomachs. The detection range of the tags in marine and deep areas in fresh water was about 100–400 m for the V9 and 200–600 m for the V13 tags. Detection ranges for all tags declined to about 10–100 m in shallow areas and were affected by proximity to the shoreline, fish depth, and other local features.

Data retrieval from tags and environmental monitors

Vemco VR2 acoustic receivers (16 in 2005 and 21 in 2006) were installed along the migration corridor (Fig. 1; see also Goetz, 2016) before the Chinook salmon were tagged and before they were retrieved after the spawning season. All detections were checked, and erroneous records, inconsistencies, and data anomalies were removed. Data from other researchers were obtained either through direct contact or from online databases (Hydraphone Data Repository, available from website; Ocean Tracking Network, available from website). Four sets of antennae and PIT tag readers were installed in the fish ladder; sequential detections indicated the direction of movement.

To characterize the conditions available to salmon, we obtained data on salinity, temperature, and DO concentration from fixed stations and from water-quality data collected by various agencies (Table 2), including data in the large lock during 1 d each year of the study by measuring temperature and salinity changes over a series of lock-filling events. We monitored temperature hourly in the large lock during the course of the study by using a thermometer at a depth of 10 m (in 2005) and near surface (in 2006).

Data analysis

Telemetry data indicating time and depth at fixed receivers were combined with hourly data from archival temperature loggers to reveal the thermal experience of individual fish along their route. This was done by constructing, for each fish, a chronology by merging the logger data (with temperature, date, and time) with the receiver data (with date, time, and depth, at fixed locations). Salmon were excluded from analysis if they apparently died, they were not detected upriver of the locks, or the date and location of the recovery of their archival tag could not be verified. Analyses were designed to describe the behavior and environmental experience of fish by recovery location and by segment of the migration route. The segments were as follows: 1) marine waters of Puget Sound to the locks, 2) upper estuary above the locks in Salmon Bay, 3) ship canal and Lake Union, 4) Lake Washington, including the deltas of the Sammamish River and the Cedar River, 5) the

Table 2

Information about the water-quality stations along the salmon migration corridor from Puget Sound to spawning streams in Washington, including the period of record considered for this study of adult Chinook salmon (*Oncorhynchus tshawytscha*), frequency of measurements, depth, and parameters used. Data sources are the U.S. Army Corps of Engineers, Muckleshoot Tribe, and King County Department of Natural Resources. Parameters include temperature (Temp), dissolved oxygen concentration (DO), salinity (Sal), and rate of flow (Flow).

Ship canal location	Year	Frequency	Depth (m)	Parameters	Latitude	Longitude
Marine, West Point	2000–09	Monthly	1–25+	Temp, DO, Sal	47.663	−122.448
Shilshole Bay	2005–06	Hourly	0.5, 1, 4	Temp, Sal	47.666	−122.400
Large lock	2005–06	Hourly	1, 10	Temp	47.665	−122.396
Salmon Bay 1	2005–06	Hourly	5.3, 8.3, 11, 13	Temp, Sal	47.665	−122.395
Salmon Bay 2	2005–06	Hourly	2, 5, 7, 9–13	Temp	47.665	−122.392
Salmon Bay	2006	Weekly	1–15	Temp, DO, Sal	47.665	−122.394
Ship Canal West	2005	Weekly	1–9	Temp, DO, Sal	47.656	−122.367
Lake Union North	2005–06	Weekly	1–12	Temp, DO, Sal	47.643	−122.336
Ship Canal East	2005–06	Weekly	1–8	Temp, DO	47.648	−122.312
Lake Washington	2005–06	Hourly	2, 6, 8, 10, 20	Temp	47.643	−122.271
Cedar River	2005–06	Hourly	1	Temp, Flow	47.482	−122.203
Sammamish River 1	2005–06	Hourly	1	Temp, Flow	47.703	−122.143
Sammamish River 2	2005–06	Hourly	1	Temp, Flow	47.662	−122.124
Cottage Creek	2005–06	Hourly	1	Temp, Flow	47.717	−122.088
Issaquah Creek	2005–06	Hourly	1	Temp	47.552	−122.048

Sammamish River, 6) Lake Sammamish, and 7) spawning tributaries, including the Cedar and Sammamish Rivers and Issaquah, Cottage, and Kelsey Creeks.

Telemetry data indicate the residence time (defined by the first and last detections) in each migration segment. For fish with only archival temperature data, we inferred the transitions between segments by comparing that fish's temperature record with those of fish carrying both archival and acoustic tags (Table 1, Fig. 3). Residence time by migration segment was evaluated through analysis of variance (ANOVA) with year and tagging week as factors, by using the duration of residence and also the proportion of the total time spent in a migration segment. For fish with acoustic tags, the depth recorded on the receiver was used to estimate the ambient temperature based on vertical thermal profiles at that location (Table 2). A 2-way ANOVA was used to test for significant differences between years and among weekly tagging groups for each metric.

Mean daily temperatures were calculated from archival tag records of temperatures experienced by individual fish. The accumulated degree days (DD, mean daily temperature exposure above 0°C) for each fish were calculated by summing the mean daily temperatures it experienced during the entire migration or in specific migratory segments. To assess possible cumulative stress, mean daily temperatures that exceeded thresholds of 18.0°C and 20.0°C were also summed for each migrant. These 2 thresholds are associated with stress response in Pacific salmon (McCullough et al., 2009; Eliason et al., 2011) and with potential changes in behavior for thermoregulation (e.g., Berman and Quinn, 1991; Goniea et al., 2006).

Results

Movements and residence time

All but 1 of the 95 acoustic-tagged Chinook salmon were detected at least once in the Lake Washington basin, and 63 PIT-tagged fish were detected in the fish ladder (40 in 2005 and 23 in 2006). Archival tags were recovered from 113 salmon, primarily in spawning streams and in the hatchery that raises Chinook salmon on Issaquah Creek. Data were also collected from 28 fish with both archival and acoustic tags (Table 1). The transmitters provided over 450,000 detections for up to 61 d. We reduced the number for analysis to 62 fish by removing fish that had transmitter failure or malfunction that limited the number of detections, died or had a regurgitated tag, left the watershed, or remained in the lower estuary. After entering the lower estuary following tagging, 51% of acoustic-tagged fish moved continuously upstream, 21% returned once to Puget Sound, 16% returned twice, and 13% returned 3 or more times. To reach the upper estuary, 17% of the fish used the fish ladder and 83% used the large lock, as indicated by PIT-tag detections. After reaching the upper estuary, 62% of the fish continued upstream, 21% returned once to the lower estuary, 9% returned twice, and 8% returned 3 or more times.

Individual Chinook salmon displayed diverse patterns of thermal experience, resulting from time spent in different areas along the migration route: cool in the lower estuary, warm in the upper estuary and ship canal, and cool in Lake Washington's deep waters. In addition to variation in thermal experience arising from horizontal movement patterns, some fish remained below the thermo-halocline,

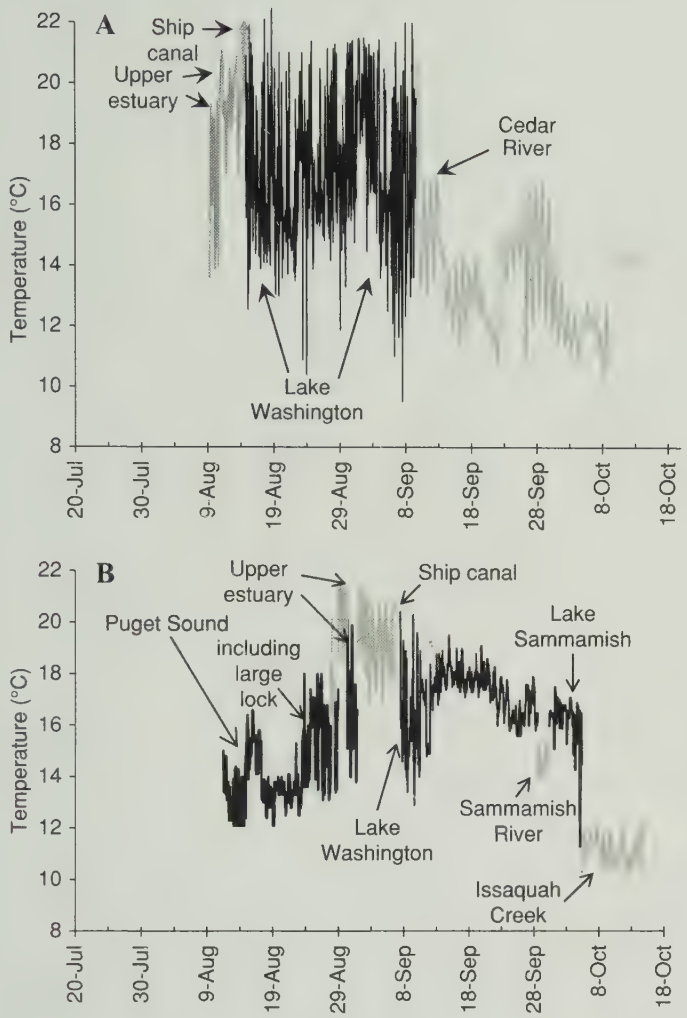

Figure 3

Typical hourly temperatures by location for Chinook salmon (*Oncorhynchus tshawytscha*) migrating from the upper estuary in the Lake Washington watershed, in western Washington, to their final capture location in (**A**) Cedar River and (**B**) Issaquah Creek during July–October in 2005 and 2006.

occupied cooler temperatures in the late afternoon and evening, and rose in the water column to shallower depths during the rest of the 24-h period.

The Chinook salmon reached the spawning grounds slightly faster in 2005 than in 2006 (mean: 34.1 and 36.0 d, respectively, F=6.5, P<0.01; Table 3), and fish tagged earlier in August were slower in 2005 and 2006 (mean: 41.5 and 37.1 d, respectively) than those tagged later in both years (mean: 31.0 and 33.8 d, respectively). The salmon took longer to move through the lower estuary (from Puget Sound to Salmon Bay) in 2005 than in 2006 but moved through the upper estuary faster in 2005 than in 2006; therefore, the overall time was similar between years. Once they exited the upper estuary, Chinook salmon moved quickly (mean: 0.6 d) through the 10.8 km from the ship canal to Lake Washington. Those migrating into the Lake Sammamish system spent, on average, 7.9 d in Lake Washington, 7.5 d in the Sammamish River, and 4.8 d in Lake Sammamish. Individuals returning to the Cedar River spent on average 20.2 d in Lake Washington before ascending the river—the same total period as those moving through to Lake Sammamish.

The proportion of total residence time in the estuary (lower and upper) was similar between years and tagging groups (mean: 47.1% [standard deviation (SD) 17.9], P=0.36; Table 3). However, there was an inverse relationship between time spent in the estuary and in Lake Washington (coefficient of correlation [r]=–0.350, df=91, P<0.001) that tended to conserve the overall transit time. This correlation was significant and stronger in 2006 (r=–0.546) than in 2005 (r=–0.118).

Environmental conditions available to Chinook salmon

The temperatures along the migration route were coolest in Puget Sound (range: 10–18°C), warmer in Salmon Bay (15.4–22.6°C) and the ship canal (17.3–22.5°C), and variable with depth in Lake Washington (8.5–22.5°C; Table 4). The estuary had a zone of dynamic short-term mixing of warm fresh water (20–23°C) and colder salt water (12–15°C) environments. The large lock and a small area of the upper estuary had a halocline at about 10 m; the upper estuary's halocline had warmer surface water in August than that of the large lock (19.5°C versus 15.5°C). The DO levels at lower depths (13–10 m) in the upper estuary ranged from 5.7 to 7.1 mg/L, whereas in Lake Washington DO concentration at similar depths ranged from 6.4 to 7.4 mg/L.

The upper estuary was slightly warmer than Lake Washington (20.8°C versus 20.2°C) at depths from 2 to 10 m, and more so at 12 m (just above the typical thermocline depth: 19.6°C versus 17.9°C; Table 4). In 2005, it was 1.3°C warmer than in 2006 at all depths above 12 m in the upper estuary and 0.4°C warmer in Lake Washington at depths above 10 m. Temperatures in the upper estuary were similar at depth between August and September in 2005, whereas in 2006 temperatures were more than 2.0°C cooler in August than in September at each depth. Lake Washington temperatures in August at depths <10 m were slightly warmer in 2005 than in 2006, and temperatures were similar each year in September; in both years August was 1–2°C warmer than September.

Depths and temperatures experienced by Chinook salmon

The depths occupied by Chinook salmon varied by reach and were influenced by bottom depth and the presence of thermal stratification (Fig. 4; see also Goetz, 2016).

Table 3

Residence times of adult Chinook salmon (*Oncorhynchus tshawytscha*) tagged in Lake Washington in western Washington during 2005 and 2006, with mean number of days and standard deviations (SDs) given in the upper table and mean proportions of time and SDs provided in the lower table, by migration segment and year. Residence times were measured by acoustic (number of tags [*n*]=26) and archival (*n*=67) tags or by archival tags only. For each migration segment, the number of tags used to generate the estimate is shown in parentheses.

	Mean number of days (SD)		
Migration segment (no. of tags)	2005	2006	Grand
Estuary (lower and upper: 93)	15.8 (7.3)	17.2 (7.7)	16.5 (7.5)
Ship canal (92)	0.6 (0.3)	0.4 (0.3)	0.5 (0.3)
Lake Washington (93)	6.8 (6.5)	8.9 (7.9)	7.9 (7.3)
Sammamish River (66)	8.8 (6.2)	6.3 (6.0)	7.5 (6.2)
Lake Sammamish (62)	4.6 (3.9)	4.8 (4.1)	4.7 (3.9)
Total	34.1 (9.7)	36.0 (8.9)	35.1 (9.3)
	Mean proportion of time (SD)		
Migration segment	2005	2006	Grand
Estuary (lower and upper)	47% (19)	47% (17)	47% (18)
Ship canal	2% (1)	1% (1)	2% (1)
Lake Washington	15% (12)	20% (21)	18% (17)
Sammamish River	24% (16)	17% (13)	20% (15)
Lake Sammamish	13% (13)	13% (10)	13% (11)

Table 4

Temperatures experienced (ranges and means) by Chinook salmon (*Oncorhynchus tshawytscha*) during upriver migration in relation to tagging week in 2005 and 2006 in coastal waters of Washington near Puget Sound. Segments of migration include the lower and upper estuary of the Lake Washington watershed, ship canal, Lake Washington, Lake Sammamish, Sammamish River, and entryways of tributaries. Dates of tagging weeks are provided in Table 1.

	Migration segment												
	Lower estuary		Upper estuary		Ship canal		L. Washington		L. Sammamish		Sammamish R.		Trib. entry
Group	Range	Mean	Range	Mean	Range	Mean	Range	Mean	Range	Mean	Range	Mean	Mean
Week 1	11.9–17.9	14.0	16.3–21.9	19.1	18.9–21.4	20.4	9.6–21.4	16.4	13.3–20.4	17.4	13.0–19.5	16.6	11.0
Week 2	12.1–17.8	14.6	16.0–22.3	19.1	17.9–22.0	20.2	9.6–21.5	17.1	13.0–20.4	17.2	12.5–18.9	15.2	12.5
Week 3	12.4–17.9	14.7	16.0–22.6	19.1	18.3–22.3	20.4	9.3–21.5	16.9	12.8–20.5	16.9	12.5–19.3	15.3	12.4
Week 4	12.5–18.3	14.9	15.9–21.3	18.5	18.0–20.6	19.7	8.5–20.5	16.8	11.9–19.4	16.5	10.0–17.1	14.5	12.2
Week 1	10.1–18.3	13.8	15.4–22.5	19.5	17.3–22.5	20.9	9.5–22.5	18.1	12.5–21.5	17.1	13.1–21.0	16.5	12.8
Week 2	11.9–17.4	13.3	15.6–21.8	18.9	18.1–22.1	20.4	9.1–21.6	17.5	13.0–20.3	17.1	13.5–21.4	16.7	12.7
Week 3	11.9–17.8	14.4	15.9–20.9	18.4	18.1–21.0	19.8	10.6–21.1	17.2	13.0–20.0	17.2	13.1–19.3	15.4	12.0
Week 4	13.3–18.0	15.2	16.3–21.1	18.7	17.4–21.1	20.2	9.1–21.4	17.4	13.0–20.5	17.2	11.6–18.0	15.3	12.3

Chinook salmon in Puget Sound occupied depths from near the surface to >150 m (mean: 15 m in 2005, 20 m in 2006). In the cooler, mixed lower estuary, most detections were at depths <5 m. In the large lock and upper estuary, they remained near the bottom at depths of 10–14 m. Most detections were at depths <5 m in the ship canal, between 5–15 m in Lake Washington, and <3 m near tributary deltas.

The archival data loggers provided 60,406 temperature records from Chinook salmon prior to entering spawning tributaries (mean: 875 records/fish; range: 477–1477 records/fish). Of these hourly records, 15.0%

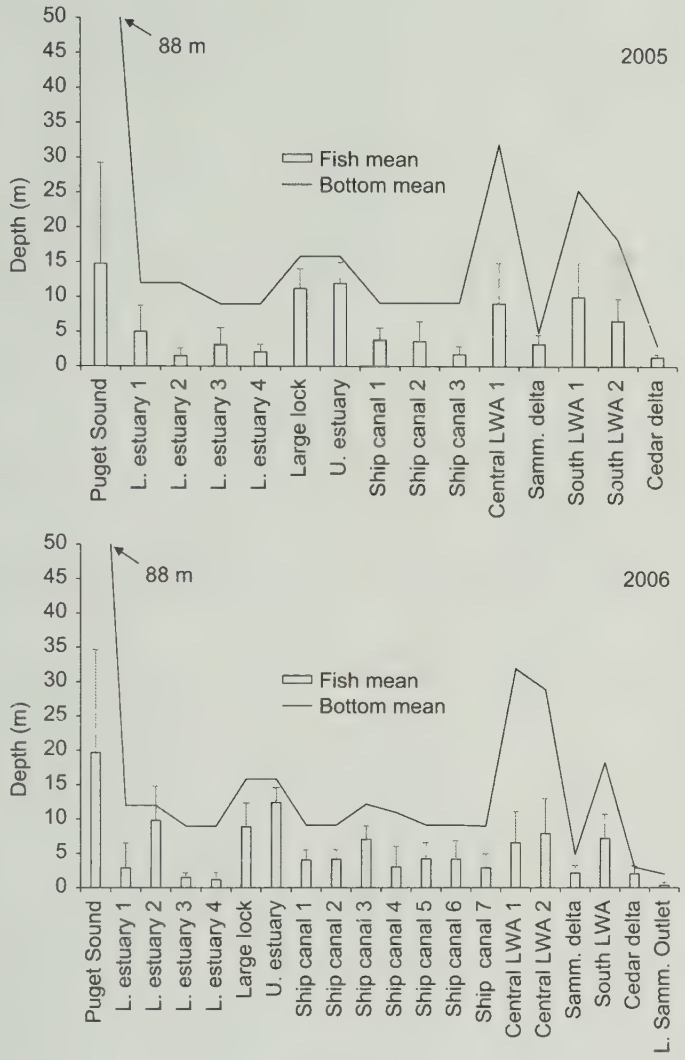

Figure 4

Mean depth of tagged Chinook salmon (*Oncorhynchus tshawytscha*) (bars) and mean bottom depth (solid line) near acoustic receivers along the migration route of Chinook salmon in 2005 and 2006. Locations in Washington where depth data were recorded include Puget Sound, the lower and upper estuary, the large lock, and the ship canal of the Lake Washington watershed, central and south Lake Washington (LWA), Sammamish River delta, Cedar River delta, and Lake Sammamish outlet. Error bars indicate standard deviations.

were assigned to the lower estuary, 31.3% to the upper estuary, 1.4% to the ship canal, 21.0% to Lake Washington, 19.7% to the Sammamish River, and 11.6% to Lake Sammamish. Most individuals experienced a wide range of water temperatures with typical minima of 9–12°C and maxima of 20–22°C (examples in Figure 3). The fish experienced diel temperature fluctuations (warm in the afternoon and cool in early morning) in all areas, but daily ranges were greater (up to 4–6°C) in Lakes Washington and Sammamish, moderate in the estuary and river (2–3°C), and smallest in the ship canal (1–2°C) where the water was more uniformly warm. The highest temperatures and greatest change in temperatures fish experienced were from entry into the lower estuary (mean: 15.1°C) to the fish ladder's exit (mean: 21.6°C) for an average 2-h change of 6.5°C.

Cool, saline water near the bottom was more available during the day than at night because this water intruded during locking events, which took place primarily during the day. The typical behavior of Chinook salmon included holding for several days below the thermo-halocline in the lower estuary in the large lock (mean depth: 10 m; salinity: 12–27) and upper estuary (mean depth: 13 m; salinity: 1–18). Temperatures at the depths most often used varied markedly between the large lock (14–17°C) and the upper estuary above the locks (19–21°C). In the upper estuary, fish experienced warmer temperatures in the morning (mean: 19.9°C) as their depth shallowed after dawn (~11 m), through late morning, and then the temperatures decreased (18.6°C) with the increased depth (~13 m) into the evening. Therefore, despite the afternoon rise in temperatures at the surface, the temperatures occupied by the fish decreased. Cool, saline water at depth was increasingly available during the day because this water entered during locking events that occurred primarily during the day. Within Lake Washington, Chinook salmon occupied depths from near the surface to >20 m, above and below the thermocline (Figs. 3 and 4). Most (73%) recorded temperatures were 15–20°C, corresponding to depths near and above the thermocline (10–15 m; Fig. 5). In 2006, the salmon spent more time within 10 m of the surface than in 2005, the warmer year (21% versus 4%).

The highest temperatures experienced by individual Chinook salmon were 22.6°C in 2005 and 22.5°C in 2006. The average maxima among fish were the same (21.4°C) in both years, with the warmest temperatures in the upper estuary (22.6°C), Lake Washington (22.6°C), the ship canal (22.5°C), and Lake Sammamish (21.5°C) (Fig. 6). All Chinook salmon experienced one or more 12–24-h periods of temperatures >18°C, and 85% of salmon had one or more such periods >20°C. Overall, 40.1% of the records were >18°C, and 2.1% were >20°C. Chinook salmon were not exposed to water >18°C in Puget Sound but had extended exposure in the upper estuary (98% of daily mean temperatures >18°C in August) and in Lake Washington (45% of daily means >18°C in September).

Chinook salmon that arrived and were tagged earlier in the summer tended to spend longer in transit prior to entering a tributary for spawning than did those arriving later. Specifically, fish tagged in the first week spent an average of 50.7 d in 2005 and 42.7 d in 2006, decreasing to 31.8 d in 2005 and 26.2 d in 2006 for the last group (Table 1).

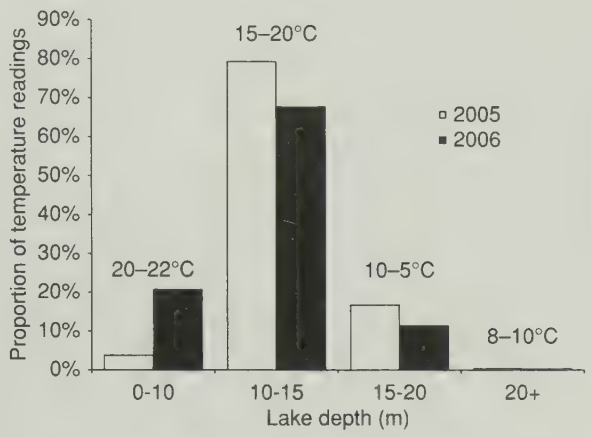

Figure 5

Proportions of temperature records, from tags implanted in Chinook salmon (*Oncorhynchus tshawytscha*), in Lake Washington in western Washington during 2005 and 2006 for each of the depth strata where those temperatures were experienced.

Therefore, there was more variation in arrival dates into the system than variation in ascent into spawning streams. The total thermal exposure (DD) from tagging to spawning stream ascent was higher in the early arriving fish (means for the first week: 844.4 in 2005 and 723.8 in 2006) than those arriving in the last week (means: 521.1 in 2005 and 449.3 in 2006)—a consequence of the warmer water experienced by and longer exposure of the earlier fish.

Discussion

The Chinook salmon entering the Lake Washington system faced environmental challenges that are both unique and generic. Few rivers that salmon ascend have locks between fresh and salt waters, and such structures produce unusual combinations of temperature, salinity, and DO level with abrupt changes over short temporal and spatial scales, both vertically and horizontally. However, although the physical structure and these features of the environment are unique, the system is experiencing the increases in temperature (Fig. 2) that also characterize many migratory corridors for salmonids and other fish species (Quinn, 2018). In this context, the increasing temperatures in Lake Washington are simply part of a much broader pattern of climate-driven change, although each river and lake has its own characteristics. These temperatures pose challenges for salmon; therefore, further information on how they confront thermal barriers will be important to determine their likelihood of survival (Hasler et al., 2012; Fenkes et al., 2016; Connor et al., 2019).

We posed a series of questions to help characterize the ways in which Chinook salmon address these challenges, either by making use of refuges and other forms of avoidance when confronted with adverse conditions or by tolerating the conditions. In addition, given the later migration in the season and generally warmer water experienced by Chinook salmon compared with that experienced by sympatric sockeye salmon (*O. nerka*) (Newell and Quinn, 2005), we predicted that the former would show greater tolerance of higher temperatures. In the modified Lake Washington estuary, Chinook salmon occupied thermal refuges in stratified marine and freshwater areas. Most Chinook salmon left the estuary after tagging and spent a few days in Puget Sound, often below the thermo-halocline. Upon return to the upper estuary, they either held in the saltwater wedge for a week or more or went back to Puget Sound again. These movements may have been responses to the abrupt change in salinity. If the fish were not fully tolerant of fresh water, the scarcity of intermediate salinities may have stimulated them to return to Puget Sound and to enter the ship canal again a few days later. To reach the upper estuary, most Chinook salmon migrated through the locks and were often below the thermo-halocline in the lock, where temperatures were intermediate between those in Puget Sound and the upper estuary. A smaller fraction of the Chinook salmon ascended the fish ladder. Temperatures in the ladder were much warmer than in the locks because it contained the surface water from the ship canal. Although the tendency to use the locks rather than the ladder was consistent with avoidance of warm water, it is certainly not proof of it, as the structures differ in many other physical aspects besides temperature.

The warmest and likely most stressful conditions that all Chinook salmon had to experience were in the upper estuary, which received little marine input and was dominated by the warm surface waters from Lake Washington and Lake Union. Fish there occupied the deepest waters below the thermo-halocline for extended periods prior to migration to Lake Washington, apparently balancing the benefits of low temperature against the drawbacks of low DO concentration. Chinook salmon tagged during the warmest periods in early August remained longer in the estuary (lower and upper) before migrating rapidly upstream through the ship canal than did those arriving in September, when the water was slightly cooler. Once in Lake Washington, most fish resided for some period at depths near the thermocline with vertical migrations to use cooler water, and they eventually moved toward shallower river deltas where they experienced high temperatures before entering rivers with cooler water.

Despite avoiding the warmest surface waters, all Chinook salmon experienced temperatures >18°C and 85% of the Chinook salmon experienced temperatures >20°C, a threshold associated with adult migration delay, stress, and potential mortality (Goniea et al., 2006; Keefer et al., 2009). Chinook salmon in the upper estuary and Lake Washington occupied vertical positions that minimized their exposure to the warmest temperatures, as do Pacific salmon in other man-made and natural impoundments (Keefer et al., 2009; Strange, 2012; Keefer et al., 2015). Diel patterns in the upper estuary followed those seen in some other salmonids: deeper during the day than at night (Newell and Quinn, 2005; Mathes et al., 2010; Roscoe et al.,

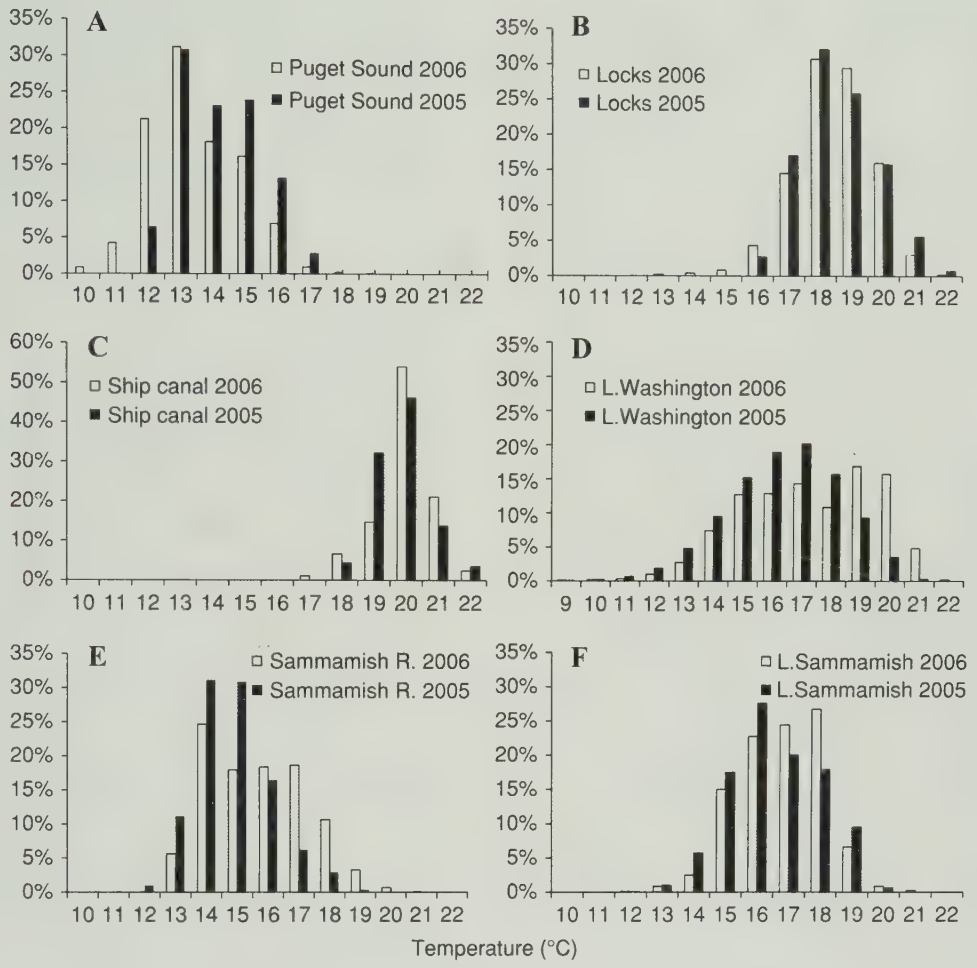

Figure 6

Frequency distribution of hourly temperature records from tags implanted in Chinook salmon (*Oncorhynchus tshawytscha*) in 2005 and 2006, by migration segment from Puget Sound, in western Washington, to entry into a spawning tributary. In the order that a Chinook salmon would move through them, the migration segments are (**A**) Puget Sound, (**B**) the locks and (**C**) ship canal in the Lake Washington watershed, (**D**) Lake Washington, (**E**) Sammamish River, and (**F**) Lake Sammamish.

2010), although Chinook salmon in Puget Sound did not display diel vertical migrations (Smith et al., 2015). Even with behavioral adaptation, fish residing in the upper estuary were continuously exposed to potentially stressful temperatures (18–21°C) while experiencing pulses of brackish water (1–18) and variable periods of low DO concentration (<6 mg/L). The available alternatives to this refuge were to revisit marine waters or swim up 10.8 km through even warmer waters (21–22°C) to Lake Washington. Lake Union provided access to cooler water (14–15°C at a depth of 11 m) between the upper estuary and Lake Washington, but the salmon did not occupy this habitat. In that lake, DO levels below the thermocline were <5 mg/L in August and early September (USACE[2]), a level causing avoidance or delay in migrating Pacific salmon (Fujioka, 1970; Hallock et al., 1970; Alabaster, 1989). In Lake Washington, Chinook salmon had access to cooler water below the thermocline without restriction by low DO concentration, yet they did not occupy such depths, in contrast to sockeye salmon (Newell and Quinn, 2005).

Comparisons to salmonids in other systems reveal a variety of responses to adverse conditions along the migratory corridor. Most Chinook salmon tagged in the Klamath River's estuarine lagoon returned to the ocean and remained for about 10 d near the river plume before moving upriver (Strange, 2013), as did Chinook salmon in our study although for a shorter period. Similarly, some sockeye salmon populations hold in the Fraser River plume prior to upriver migration (Cooke et al., 2008). The migratory behavior of Pacific salmon returning to estuaries and rivers includes several species (e.g., Chinook salmon,

[2] USACE (U.S. Army Corp of Engineers). 2005–2006. Unpubl. data. P.O. Box 3755, Seattle, WA 98124-3755.

sockeye salmon, and steelhead, *O. mykiss*) that exhibit diel vertical movement patterns in stratified and unstratified waters (Drenner et al., 2012). Limited available data indicate that salmon in estuaries are often associated with thermo-haloclines (Brawn, 1982; Westerberg, 1982; Døving et al., 1985; Potter, 1988; Olson and Quinn, 1993; Strange, 2013), although vertical distribution is not always related to oceanographic conditions (Quinn et al., 1989; Ruggerone et al., 1990; Walker et al., 2000; Ishida et al., 2001). In the Columbia River estuary, individual Chinook salmon made complex vertical movements relative to varying thermal and salinity gradients (Olson and Quinn, 1993). Vertical placement near clines presumably provides advantages for behavioral thermo-osmoregulation and adjustment of ambient salinity as well as detection of olfactory clues needed for homing at shear zones (Westerberg, 1982). Tagging studies conducted during the adult migratory stage have revealed rapid transitions from saline to fresh waters and tolerance for substantial, brief changes in salinity among salmonids (Potter, 1988; Olson and Quinn, 1993).

Some Chinook salmon populations migrate upriver during the highest temperatures in, for example, the Sacramento (Alabaster, 1989), Columbia (Keefer et al., 2015; Keefer et al., 2018), and Fraser (Waples et al., 1990) River systems, although other populations in these large rivers migrate later or earlier. In contrast, coastal populations of sockeye salmon in systems subject to high temperatures (mean: 19°C) tend to migrate prior to peak temperatures (Hodgson and Quinn, 2002). This pattern, combined with the more southerly distribution of Chinook salmon compared with that of sockeye salmon, indicates substantially greater thermal tolerance in Chinook salmon, as part of the suite of adaptations of salmonids to stressful or lethal effects of warm temperatures along migration routes (Crozier et al., 2008). However, population-specific variation in thermal tolerance has been documented in sockeye salmon (Eliason et al., 2011) and likely plays an important role in Chinook salmon as well.

Individual Chinook salmon use a variety of behavioral adaptations to high temperatures in rivers, such as delaying migration until temperatures decline, migrating at greater depths, and utilizing cool water refuges (Berman and Quinn, 1991; Strange, 2013; Keefer and Caudill, 2016). The Lake Washington Chinook salmon migrated near the annual peak temperatures, but individuals delayed in the estuary, occupied refuges in the estuary and lake, and moved vertically during migrations in those refuges. Because most Chinook salmon entering fresh water in late summer are near sexual maturity, a long delay in migration at high temperatures may result in lost reproductive opportunity. In contrast, the timing of steelhead and some early arriving sockeye salmon populations is more flexible before spawning, where they may delay, seeking cool water refuge sites when temperatures are stressful (Keefer et al., 2009; Mathes et al., 2010). Individual sockeye salmon may be less adaptable in their response to temperatures, instead relying on evolved traits such as earlier migration timing and use of vertical stratification in lakes (Hodgson and Quinn, 2002; Hinch et al., 2012). The Lake Washington sockeye salmon, studied by Newell and Quinn (2005) using methods similar to our study, displayed both responses, entering prior to peak temperatures, migrating rapidly through the ship canal, and residing for extended periods below the thermocline in the lake. Entry into fresh water prior to peak temperatures, as observed in the Lake Washington sockeye salmon, is an example of so-called *premature migration*, a pattern widely distributed in salmonids (Quinn et al., 2016). In some species and populations, this pattern is related to thermal conditions, although other factors are also important. The use of cool water below the thermocline in the lake by sockeye salmon starkly contrasts the vertical distribution, hence thermal experience, of Chinook salmon in the Lake Washington basin.

Exposure to warm water temperatures and the accumulation of DD have been correlated with prespawning mortality (Crossin et al., 2008; Keefer et al., 2009; Eliason et al., 2011), which can reach 90% for Chinook salmon in the upper reaches of the Willamette River (Keefer et al., 2015). Temperatures outside the acceptable range of 14–20°C for Chinook salmon can deplete energy that could have been used for migration, reproduction, and immune responses (Richter and Kolmes, 2005; McCullough et al., 2001; McCullough et al., 2009). The Lake Washington Chinook salmon accumulated 350–1050 DD, with most having between 500 and 750 DD, compared with 700–900 DD (maximum: 1500 DD) for those in the Willamette River (Keefer et al., 2015). Lake Washington has gotten warmer in the summer and fall over the past 5 decades (Fig. 2), and in the future the watershed is expected to see greater increases in temperature than any watershed in Puget Sound (Mantua et al., 2010). How Chinook salmon will respond to this marked change in water temperatures is of concern, in part because this population is part of an evolutionarily significant unit listed as threatened under the U. S. Endangered Species Act (Federal Register, 1999). Responses to warm water may include genetic and phenotypic changes in migration timing to avoid peak temperatures or more extensive behavioral thermoregulation. Of ultimate concern is how warming will affect the persistence of the salmon populations. The temperatures at the upper estuary in most summer months already approach or exceed levels associated with disease and energy depletion in migrating salmon; therefore, *en route* or prespawning mortality may result from further increases (McCullough et al., 2001; Crossin et al., 2008). Cool, hypolimnetic water will remain in Lake Washington if salmon can migrate successfully from the locks through the ship canal. In the future, temperatures could delay their migration or further stress them prior to reaching the lake. Therefore, if water temperatures in Lake Washington continue to rise, the success of migration and spawning by Chinook and sockeye salmon will likely be compromised.

Acknowledgments

We thank D. Seiler (WDFW) and K. Fresh (National Marine Fisheries Service) for their support in collaborative

studies of Chinook and sockeye salmon at the locks; J. Newell for providing the sockeye salmon data used in this study; and E. Jeanes and C. Morello (R2), K. Kiyohara and P. Topping (WDFW), and B. Footen (Muckleshoot Indian Tribe) for their assistance with fish capture, tagging, and collection of telemetry and water-quality data. We especially acknowledge C. Ebel, who guided the protection of salmon at the locks over his length of service with the U.S. Army Corp of Engineers.

Literature cited

Alabaster, J. S.
1989. The dissolved oxygen and temperature requirements of king salmon, *Oncorhynchus tshawytscha*, in the San Joaquin Delta, California. J. Fish Biol. 34:331–332.

Berman, C. H., and T. P. Quinn.
1991. Behavioural thermoregulation and homing by spring Chinook salmon, *Oncorhynchus tshawytscha* (Walbaum), in the Yakima River. J. Fish Biol. 39:301–312.

Brawn, V. M.
1982. Behavior of Atlantic salmon (*Salmo salar*) during suspended migration in an estuary, Sheet Harbor, Nova Scotia, observed visually and by ultrasonic tracking. Can. J. Fish. Aquat. Sci. 39:248–256.

Brett, J. R.
1971. Energetic responses of salmon to temperature. A study of some thermal relations in the physiology and freshwater ecology of sockeye salmon (*Oncorhynchus nerka*). Am. Zool. 11:99–113.

Candy, J. R., E. W. Carter, T. P. Quinn, and B. R. Riddell.
1996. Adult Chinook salmon behavior and survival after catch and release from purse-seine vessels in Johnstone Strait, British Columbia. North Am. J. Fish. Manage. 16:521–529.

Connor, W. P., K. F. Tiffan, J. A. Chandler, D. W. Rondorf, B. D. Arnsberg, and K. C. Anderson.
2019. Upstream migration and spawning success of Chinook salmon in a highly developed, seasonally warm river system. Rev. Fish. Sci. Aquac. 27:1–50.

Cooke, S. J., C. G. Hinch, G. T. Crossin, D. A. Patterson, K. K. English, M. C. Healey, J. S. Macdonald, J. M. Shrimpton, J. L. Young, A. Lister, et al.
2008. Physiological correlates of coastal arrival and river entry timing in later summer Fraser River sockeye salmon (*Oncorhynchus nerka*). Behav. Ecol. 19:747–758.

Crossin, G. T., S. G. Hinch, S. J. Cooke, D. W. Welch, A. G. Lotto, D. A. Patterson, S. R. M. Jones, R. A. Leggeatt, M. T. Mathes, J. M. Shrimpton, et al.
2008. Exposure to high temperature influences the behaviour, physiology, and survival of sockeye salmon during spawning migration. Can. J. Zool. 86:127–140.

Crozier, L. G., A. P. Hendry, P. W. Lawson, T. P. Quinn, N. J. Mantua, J. Battin, R. G. Shaw, and R. B. Huey.
2008. Potential responses to climate change in organisms with complex life histories: evolution and plasticity in Pacific salmon. Evol. Appl. 1:252–270.

Donaldson, M. R., S. G. Hinch, D. A. Patterson, J. Hills, J. O. Thomas, S. J. Cooke, G. D. Raby, L. A. Thompson, D. Robichaud, K. K. English, et al.
2011. The consequences of angling, beach seining, and confinement on the physiology, post-release behaviour and survival of adult sockeye salmon during upriver migration. Fish. Res. 108:133–141.

Døving, K. B., H. Westerberg, and P. B. Johnsen.
1985. Role of olfaction in the behavioral and neuronal responses of Atlantic salmon, *Salmo salar*, to hydrographic stratification. Can. J. Fish. Aquat. Sci. 42:1658–1667.

Drenner, S. M., T. D. Clark, C. K. Whitney, E. G. Martins, S. J. Cooke, and S. G. Hinch.
2012. A synthesis of tagging studies examining the behaviour and survival of anadromous salmonids in marine environments. PLoS ONE 7(3):e31311.

Durkin, J. T., and D. L. Park.
1967. A purse seine for sampling juvenile salmonids. Prog. Fish-Cult. 29:56–59.

Eliason, E. J., T. D. Clark, M. J. Hague, L. M. Hanson, Z. S. Gallagher, K. M. Jeffries, M. K. Gale, D. A. Patterson, S. G. Hinch, and A. P. Farrell.
2011. Differences in thermal tolerance among sockeye salmon populations. Science 332:109–112.

Emmett, E., R. Llansó, J. Newton, R. Thom, M. Hornberger, C. Morgan, C. Levings, A. Copping, and P. Fishman.
2000. Geographic signatures of North American west coast estuaries. Estuaries 23:765–792.

Federal Register.
1999. Endangered and threatened species; threatened status for three Chinook salmon evolutionarily significant units (ESUs) in Washington and Oregon, and endangered status for one Chinook Salmon ESU in Washington. Fed. Regist. 64:14308–14328. [Available from website.]

Fenkes, M., H. A. Shiels, J. L. Fitzpatrick, and R. L. Nudds.
2016. The potential impacts of migratory difficulty, including warmer waters and altered flow conditions, on the reproductive success of salmonid fishes. Comp. Biochem. Physiol. A 193:11–21.

Fujioka, J. T.
1970. Possible effects of low dissolved oxygen content in the Duwamish River estuary on migrating Chinook salmon. M.S. thesis, 77 p. Univ. Wash., Seattle, WA.

Gilhousen, P.
1990. Prespawning mortalities of sockeye salmon in the Fraser River system and possible causal factors. Int. Pac. Salm. Fish. Comm., Bull. 26, 52 p.

Goetz, F. A.
2016. Migration and residence patterns of salmonids in Puget Sound, Washington. Ph.D. diss., 187 p. Univ. Wash., Seattle, WA. [Available from website.]

Goniea, T. M., M. L. Keefer, T. D. Bjornn, C. A. Peery, D. H. Bennett, and L. C. Stuehrenberg.
2006. Behavioral thermoregulation and slowed migration by adult fall Chinook salmon in response to high Columbia River water temperatures. Trans. Am. Fish. Soc. 135: 408–419.

Hallock, R. J., R. F. Elwell, and D. H. Fry Jr.
1970. Migrations of adult king salmon *Oncorhynchus tshawytscha* in the San Joaquin Delta as demonstrated by the use of sonic tags. Calif. Dep. Fish Game, Fish Bull. 151:1–79.

Hasler, C. T., S. J. Cooke, S. G. Hinch, E. Guimond, M. R. Donaldson, B. Mossop, and D. A. Patterson.
2012. Thermal biology and bioenergetics of different upriver migration strategies in a stock of summer-run Chinook salmon. J. Therm. Biol. 37:265–272.

Hinch, S. G., S. J. Cooke, A. P. Farrell, K. M. Miller, M. Lapointe, and D. A. Patterson.
2012. Dead fish swimming: a review of research on the early migration and high premature mortality in adult Fraser River sockeye salmon *Oncorhynchus nerka*. J. Fish Biol. 81:576–599.

Hodgson, S., and T. P. Quinn.
2002. The timing of adult sockeye salmon migration into fresh water: adaptations by populations to prevailing thermal regimes. Can. J. Zool. 80:542–555.

Holbrook, C. M., J. Zydlewski, D. Gorsky, S. L. Shepard, and M. T. Kinnison.
2009. Movements of prespawn adult Atlantic salmon near hydroelectric dams in the lower Penobscot River, Maine. North Am. J. Fish. Manage. 29:495–505.

Ishida, Y., A. Yano, M. Ban, and M. Ogura.
2001. Vertical movement of a chum salmon *Oncorhynchus keta* in the western North Pacific Ocean as determined by a depth-recording archival tag. Fish. Sci. 67:1030–1035.

Keefer, M. L., and C. C. Caudill.
2016. Estimating thermal exposure of adult summer steelhead and fall chinook salmon migrating in a warm impounded river. Ecol. Freshw. Fish. 25:599–611.

Keefer, M. L., C. A. Peery, and B. High.
2009. Behavioral thermoregulation and associated mortality trade-offs in migrating adult steelhead (*Oncorhynchus mykiss*): variability among sympatric populations. Can. J. Fish. Aquat. Sci. 66:1734–1747.

Keefer, M. L., T. S. Clabough, M. A. Jepson, J. P. Naughton, T. J. Blubaugh, D. C. Joosten, and C. C. Caudill.
2015. Thermal exposure of adult Chinook salmon in the Willamette River basin. J. Therm. Biol. 48:11–20.

Keefer, M. L., T. S. Clabough, M. A. Jepson, E. L. Johnson, C. A. Peery, and C. C. Caudill.
2018. Thermal exposure of adult Chinook salmon and steelhead: diverse behavioral strategies in a large and warming river system. PLoS ONE 13(9):e0204274.

Kristinsson, K. Ó., G. Gudbergsson, and G. M. Gislason.
2015. Variable migration and delay in two stock components of an Atlantic salmon population. Environ. Biol. Fish. 98:1513–1523.

Ledgerwood, R. D., F. P. Thrower, and E. M. Dawley.
1991. Diel sampling of migratory juvenile salmonids in the Columbia River estuary. Fish. Bull. 89:69–78.

Lotze, H. K., H. S. Lenihan, B. J. Bourque, R. H. Bradbury, R. G. Cooke, M. C. Kay, S. M. Kidwell, M. X. Kirby, C. H. Peterson, and J. B. C. Jackson.
2006. Depletion, degradation, and recovery potential of estuaries and coastal seas. Science 312:1806–1809.

Magnuson, J. J.
2010. History and heroes: the thermal niche of fishes and long-term lake ice dynamics. J. Fish Biol. 77:1731–1744.

Mantua, N., I. Tohver, and A. Hamlet.
2010. Climate change impacts on streamflow extremes and summertime stream temperature and their possible consequences for freshwater salmon habitat in Washington State. Clim. Change 102:187–223.

Mathes, M. T., S. G. Hinch, S. J. Cooke, C. T. Crossin, D. A. Patterson, A. G. Lotto, and A. P. Farrell.
2010. Effect of water temperature, timing, physiological condition and lake thermal refugia on migrating adult Weaver Creek sockeye salmon (*Oncorhynchus nerka*). Can. J. Fish. Aquat. Sci. 67:70–84.

McDowall, R. M.
1988. Diadromy in fishes, 308 p. Timber Press, Portland, OR.

McCullough, D., S. Spalding, D. Sturdevant, and M. Hicks.
2001. Summary of technical literature examining the physiological effects of temperature on salmonids. U.S. Environ. Prot. Agency, Issue Pap. 5, EPA-910-D-01-005, 114 p.

McCullough, D. A., J. M. Bartholow, H. I. Jager, R. L. Beschta, M. L. Deas, and J. L. Ebersole.
2009. Research in thermal biology: burning questions for coldwater stream fishes. Rev. Fish. Sci. 17:90–115.

Minke-Martin, V., S. G. Hinch, D. C. Braun, N. J. Burnett, M. T. Casselman, E. J. Eliason, and C. T. Middleton.
2018. Physiological condition and migratory experience affect fitness-related outcomes in adult female sockeye salmon. Ecol. Freshw. Fish 27:296–309.

Moore, A., B. Bendall, J. Barry, C. Waring, N. Crooks, and L. Crooks.
2012. River temperature and adult anadromous Atlantic salmon, *Salmo salar*, and brown trout, *Salmo trutta*. Fish. Manage. Ecol. 19:518–526.

Newell, J. C., and T. P. Quinn.
2005. Behavioral thermoregulation by maturing sockeye salmon (*Oncorhynchus nerka*) in a stratified lake prior to spawning. Can. J. Zool. 83:1232–1239.

Nichols, F. H., J. E. Cloern, S. N. Luoma, and D. H. Peterson.
1986. The modification of an estuary. Science 231:567–573.

Olson, A. F., and T. P. Quinn.
1993. Vertical and horizontal movements of adult Chinook salmon, *Oncorhynchus tshawytscha*, in the Columbia River estuary. Fish. Bull. 91:171–178.

Potter, E. C. E.
1988. Movements of Atlantic salmon, *Salmo salar* L., in an estuary in south-west England. J. Fish Biol. 33 (Suppl. A): 153–159.

Quinn, T. P.
2018. The behavior and ecology of Pacific salmon and trout, 2nd ed., 378 p, Univ. Wash. Press, Seattle, WA.

Quinn, T. P., B. A. Terhart, and C. Groot.
1989. Migratory orientation and vertical movements of homing adult sockeye salmon, *Oncorhynchus nerka*, in coastal waters. Anim. Behav. 37:587–599.

Quinn, T. P., J. A. Peterson, V. Gallucci, W. K. Hershberger, and E. L. Brannon.
2002. Artificial selection and environmental change: countervailing factors affecting the timing of spawning by coho and Chinook salmon. Trans. Am. Fish. Soc. 131:591–598.

Quinn, T. P., P. McGinnity, and T. E. Reed.
2016. The paradox of 'premature migration' by adult anadromous salmonid fishes: patterns and hypotheses. Can. J. Fish. Aquat. Sci. 73:1015–1030.

Raby, G. D., M. R. Donaldson, S. G. Hinch, T. D. Clark, E. J. Eliason, K. M. Jeffries, K. V. Cook, A. Teffer, A. L. Bass, K. M. Miller, et al.
2015. Fishing for effective conservation: context and biotic variation are keys to understanding the survival of Pacific salmon after catch-and-release. Integr. Comp. Biol. 55:554–576.

Richter, A., and S. A. Kolmes.
2005. Maximum temperature limits for Chinook, coho, and chum salmon, and steelhead trout in the Pacific Northwest. Rev. Fish. Sci. 13:23–49.

Roscoe, D. W., S. G. Hinch, S. J. Cooke, and D. A. Patterson.
2010. Behaviour and thermal experience of adult sockeye salmon migrating through stratified lakes near spawning grounds: the roles of reproductive and energetic states. Ecol. Freshw. Fish 19:51–62.

Ruggerone, G. T, T. P. Quinn, I. McGregor, and T. D. Wilkinson.
1990. Horizontal and vertical movements of maturing steelhead trout, *Oncorhynchus mykiss*, in Dean and Fisher channels, British Columbia. Can. J. Fish. Aquat. Sci. 47:1963–1969.

Russell, I. C., A. Moore, S. Ives, L. T. Kell, M. J. Ives, and R. O. Stonehewer.
1998. The migratory behaviour of juvenile and adult salmonids in relation to an estuarine barrage. Hydrobiologia 371/372:321–334.

Smith, J. M., K. L. Fresh, A. N. Kagley, and T. P. Quinn.
2015. Ultrasonic telemetry reveals seasonal variation in depth distribution and diel vertical migrations of sub-adult Chinook and coho salmon in Puget Sound. Mar. Ecol. Prog. Ser. 532:227–242.

Strange, J. S.
2010. Upper thermal limits to migration in adult Chinook salmon: evidence from the Klamath River Basin. Trans. Am. Fish. Soc. 139:1091–1108.
2012. Migration strategies of adult Chinook salmon runs in response to diverse environmental conditions in the Klamath River Basin. Trans. Am. Fish. Soc. 141:1622–1636.
2013. Factors influencing the behavior and duration of residence of adult Chinook salmon in a stratified estuary. Environ. Biol. Fish. 96:225–243.

Tanaka, H., Y. Takagi, and Y. Naito.
2000. Behavioral thermoregulation of chum salmon during homing migration in coastal waters. J. Exp. Biol. 203:1825–1833.

Walker, R. V., K. W. Myers, N. D. Davis, K. W. Aydin, K. D. Friedland, H. R. Carlson, G. W. Boehlert, S. Urawa, Y. Ueno, and G. Anma.
2000. Diurnal variation in thermal environment experienced by salmonids in the North Pacific as indicated by data storage tags. Fish. Oceanogr. 9:171–186.

Waples, R. S., G. A. Winans, F. M. Utter, and C. Mahnken.
1990. Genetic approaches to the management of Pacific salmon. Fisheries 15(5):19–25.

Westerberg, H.
1982. Ultrasonic tracking of Atlantic salmon (*Salmo salar* L.)—II. Swimming depth and temperature stratification. Inst. Freshw. Resear. Drottningholm 60:102–120.

Williamson, C. E., J. E. Saros, W. F. Vincent, and J. P Smol.
2009. Lakes and reservoirs as sentinels, integrators, and regulators of climate change. Limnol. Oceanogr. 54:3273–2282.

Winder, W., and D. E. Schindler.
2004. Climate change uncouples trophic interactions in an aquatic ecosystem. Ecology 85:2100–2106.

Yates, D., H. Galbraith, D. Purkey, A. Huber-Lee, J. Sieber, J. West, S. Herrod-Julius, and B. Joyce.
2008. Climate warming, water storage, and Chinook salmon in California's Sacramento Valley. Clim. Change 91: 335–350.

Fishery Bulletin

Guidelines for authors

Contributions published in *Fishery Bulletin* describe original research in marine fishery science, fishery engineering and economics, and marine environmental and ecological sciences (including modeling). Preference will be given to manuscripts that examine processes and underlying patterns. Descriptive reports, surveys, and observational papers may occasionally be published but should appeal to an audience outside the locale in which the study was conducted.

Although all contributions are subject to peer review, responsibility for the contents of papers rests upon the authors and not on the editor or publisher. *Submission of an article implies that the article is original and is not being considered for publication elsewhere.*

All submissions are subject to a double-blind review to remove the identity of author and reviewer during the review process.

Plagiarism and double publication are considered serious breaches of publication ethics. To verify the originality of the research in papers and to identify possible previous publication, manuscripts may be screened with plagiarism-detection software.

Manuscripts must be written in English; authors whose native language is not English are strongly advised to have their manuscripts checked by English-speaking colleagues before submission.

Once a paper has been accepted for publication, online publication takes approximately 2 weeks.

There is no cost for publication in *Fishery Bulletin*.

Types of manuscripts accepted by the journal

Articles generally range from 20 to 30 double-spaced typed pages (12-point font) and describe an original contribution to fisheries science, engineering, or economics. Tables and figures are not included in this page count, but the number of figures should not exceed 1 figure for every 4 pages of text. Articles contain the following divisions: abstract, introduction, methods, results, and discussion.

Short contributions are generally less than 15 double-spaced typed pages (12-point font) and, like articles, describe an original contribution to fisheries science. They follow the same format as that for articles: abstract, introduction, methods, results, and discussion, but the results and discussion sections may be combined. They are distinguished from full articles in that they report a noteworthy new observation or discovery—such as the first report of a new species, a unique finding, condition, or event that expands our knowledge of fisheries science, engineering, or economics—and do not require a lengthy discussion.

Companion articles should be submitted together and are published together as a scientific contribution. Both articles should address a closely related topic and may be articles that result from a workshop or conference.

Preparation of manuscript

Title page should include authors' full names, mailing addresses, and the senior author's email address.

Abstract should be limited to 200 words (one-half typed page), state the main scope of the research, and emphasize the authors' conclusions and relevant findings. Do not review the methods of the study or list the contents of the paper. Because abstracts are circulated by abstracting agencies, it is important that they represent the research clearly and concisely.

General text must be typed in 12-point Times New Roman font throughout. A brief introduction should convey the broad significance of the paper; the remainder of the paper should be divided into the following sections: Materials and methods, Results, Discussion, and Acknowledgments. Headings within each section must be short, reflect a logical sequence, and follow the rules of subdivision (i.e., there can be no subdivision without at least 2 subheadings). The entire text should be intelligible to interdisciplinary readers; therefore, all acronyms, abbreviations, and technical terms should be written out in full and defined the first time they are mentioned. Abbreviations should be used sparingly because they are not carried over to indexing databases and slow readability for those readers outside a discipline. They should never be used for the main subject (species, method) of a paper.

For general style, follow the U.S. Government Publishing Office *Style Manual* (2016, available at website) and *Scientific Style and Format: the CSE Manual for Authors, Editors, and Publishers* (2014, 8th ed.) published by the Council of Science Editors. For scientific nomenclature, use the current edition of the American Fisheries Society's *Common and Scientific Names of Fishes from the United States, Canada, and Mexico* and its companion volumes (*Crustaceans, Mollusks, Cnidaria and Ctenophora*, and *World Fishes Important to North Americans*). For species not found in the above mentioned AFS publications and for more recent changes in nomenclature, use the Integrated Taxonomic Information System (ITIS, available at website), or, secondarily, the California Academy of Sciences *Catalog of Fishes* (available at website) for species names not included in ITIS. Common (vernacular) names of species should be lowercase. Citations must be given for the identification of specimens. For example, "Fish species were identified according to Collette and

Klein-MacPhee (2002); sponges were identified according to Stone et al. (2011)."

Dates should be written as follows: 11 November 2018. Measurements should be expressed in metric units, for example, "58 metric tons (t);" if other units of measurement are used, please make this fact explicit to the reader. Use numerals, not words, to express whole and decimal numbers in the general text, tables, and figure captions (except at the beginning of a sentence). For example, "We considered 3 hypotheses. We collected 7 samples in this location." Use American spelling. Refrain from using the shorthand slash (/), an ambiguous symbol, in the general text.

Cite all software, special equipment, and chemical solutions used in the study within parentheses in the general text, for example, "SAS, vers. 6.03 (SAS Institute Inc., Cary, NC)."

Word usage and grammar that may be useful are the following:

- *Aging*
  For our journal, the word *aging* is used to mean both age determination and the aging process (senescence). Authors should make clear which meaning is intended where ambiguity may arise.

- *Fish and fishes*
  The plural of the word fish (a collective noun that implies individuals without regard to species) is *fish*.
  Example: The *fish* were collected by trawl net.
  Example: The numbers of *fish* collected that season were less than the numbers from previous years.

  The plural for *fish species* is *fishes* (a contrived plural used by taxonomists to mean several or more *fish species*) or one can use *fish species* (which is preferred in this journal for clarity across disciplines).
  Example: The *fishes* of Puget Sound [biodiversity is implied] or
  Example: The *fish species* of Puget Sound [preferred plural for clarity across disciplines].

- *Crab and crabs, squid and squids, etc.*
  The plural of the word *crab* (i.e., many individuals without regard to species) is *crab*.
  Example: The crab were sorted by weight.
  Example: Many red king *crab* were dying [Many individuals of one species of crab.]

  The plural of *crab species* is *crabs* (a word used by taxonomists) or *crab species* (the latter is preferred in this journal for clarity).
  Example: These *crabs* were selected for treatment. [Different crab species are implied.]
  Example: These *crab species* were selected for treatment. [Preferred word choice for clarity of meaning.]
  Example: Snow *crabs* are found throughout the North Pacific Ocean and Bering Sea. [There are 2 species of snow crab and therefore the word *crabs* can be used here.]
  Example: *Two species* of snow *crab* are found throughout the North Pacific Ocean and Bering Sea. [Preferred usage for clarity.]
  Example: Three crabs were selected for treatment. [3 species of crab are implied.]
  Example: Three crab species were selected for treatment. [Preferred word choice for clarity.]

- *Fisherman and fisher*
  We use *fisherman* and *fishermen* in this journal not *fisher* and *fishers*. One can always use crew member, vessel operator, and angler (the latter for recreational fishing.

- *The definite article with common names of species*
  When the singular common name of a species represents the entire class or group to which it belongs, use the definite article.
  Example: Only one species of the genus *Salmo* is found in the Atlantic Ocean—*the* Atlantic salmon (*Salmo salar*).
  Example: The sonic emissions of *the* bottlenose dolphin are complex.

  For plural common names, this rule does not apply.
  Example: Chinook salmon are found throughout the Pacific Ocean.
  Example: Bottlenose dolphins are found in temperate and tropical waters.

- *Sex*
  For the meaning of male and female, use the word *sex*, not *gender*. Do not write "fish were sexed." Write, "sex was determined."

- *Participles*
  As adjectives, participles must modify a specific noun or pronoun.
  Example: Using mark-recapture methods, these scientists determined the size of the population. [Correct. The participle *using* modifies the word *scientists*.]
  Example: These scientists, based on the collected data, concluded that the mortality rate of these fish had increased. [Incorrect. The scientists were not based on the collected data.]
  Example: These scientists concluded, on the basis of collected data, that the mortality rate of these fish had increased. [Correct. The offending participle has been eliminated and an adverbial phrase modifies the verb *concluded*.]

Equations and mathematical symbols should be set from a standard mathematical program (MathType or Equation Editor). Equations formatted in LaTex are not acceptable. For mathematical symbols in the general text (α, χ^2, π, $\pm$, etc.), use the symbols provided by

the MS Word program and italicize all variables, except those variables represented by Greek letters and the superscript and subscript parts of variables and expressions. Do not use photo mode when creating these symbols in the general text, and do not cut and paste equations, letters, or symbols from a different software program.

Number equations (if there are more than one) for future reference by scientists; place the number within parentheses at the end of the first line of the equation.

Literature cited section comprises published works and those accepted for publication (in press) in peer-reviewed journals. Follow the name and year system for citation format in this section (i.e., citations should be listed alphabetically by the authors' last names, and then by year if there is more than one citation by the same author. A list of abbreviations for citing journal titles can be found at this website.

Authors are responsible for the accuracy and completeness of all citations. Literature citation format: Authors (last name, followed by initials for first name and, if given, middle name of first author; then list names of additional authors with initials before last names). Year. Title of article. Abbreviated title of the journal in which it was published. Always include either the range of page numbers (for a journal article) or a total number of pages (for a book or other type of publication). List a sequence of citations in the general text chronologically, for example, "(Smith, 1932: Green. 1947; Smith and Jones, 1985)." Avoid the use of multiple citations when a single citation sufficiently supports a statement; cite the work that first reported the information that supports a statement, not all of the subsequent works.

Acknowledgments should be no more than 6 lines of text. Only those who have contributed in an outstanding way should be acknowledged by name. For recognition of other persons or groups, use a general term, such as *crew*, *observers*, or *research coordinators*, and do not include names with these terms.

Digital object identifier (doi) code ensures that a publication has a permanent location online. A doi link (which may include a doi code) should be included at the end of citations of published literature. Authors are responsible for submitting accurate doi links. Faulty links will be deleted at the page-proof stage.

Footnotes are used for all documents that have not been formally peer reviewed and for observations and personal communications, but these types of references should be cited sparingly in manuscripts submitted to the journal.

All reference documents, administrative reports, internal reports, progress reports, project reports, contract reports, personal observations, personal communications, unpublished data, manuscripts in review, and council meeting notes are footnoted in 9-point font and placed at the bottom of the page on which they are first cited. Footnote format is the same as that for formal literature citations. A link to the online source (e.g., [Available from http://www... , accessed July 2017.]), or the mailing address of the agency or department holding the document, should be provided so that readers may obtain a copy of the document.

Tables are often overused in scientific papers; it is seldom necessary to present all the data associated with a study. Tables should not be excessive in size and must be cited in numerical order in the text. Headings should be short but ample enough to allow the table to be intelligible on its own.

All abbreviations and unusual symbols must be explained in the table legend. Other incidental comments may be footnoted with numeral footnote markers. Use asterisks only to indicate significance in statistical data. Do not put a table legend on a page separate from the table; place the legend above the table. *Do not submit tables in photo mode.*

- Note probability with a capital, italic *P*.
- Provide a zero before all decimal points for values less than one (e.g., 0.07).
- Round all values to 2 decimal points.
- Use a comma in numbers of 5 digits or more (e.g., 13,000 but 3000).

Figures must be cited in numerical order in the text. Graphics should aid in the comprehension of the text, but they should be limited to presenting patterns rather than raw data. The number of figures should not exceed 1 figure for every 4 pages of text. Place panel labels **A, B, C,** etc., within the upper-left area of graphs and photos. Avoid placing labels vertically.

Figure legends should explain all symbols and abbreviations seen in the figure and should be double spaced on a separate page at the end of the manuscript.

Line art and halftone figures should be saved at resolutions >600 dots per inch (dpi) and >300 dpi, respectively. Color is allowed in figures to show morphological differences among species (for species identification), to show stain reactions, to show gradations (such as those of temperature and salinity within maps), and to distinguish between numerous lines and symbols in graphs. Figures approved for color should be saved in CMYK format.

All figures must be submitted as PDF, TIFF, or EPS files.

- Capitalize only the first letter of the first word and proper nouns in all labels within figures.
- Do not use overly large font sizes in maps and for axis labels in graphs.

- Do not use bold fonts or bold lines in figures.
- Do not place outline rules around graphs.
- Place a north arrow and label degrees latitude and longitude (e.g., 170°E) in all maps.
- Use symbols, shadings, or patterns (not clip art) in maps and graphs.

Supplementary materials that are considered essential, but are too large or impractical for inclusion in a paper (e.g., metadata, figures, tables, videos, and websites), may be provided at the end of an article. These materials are subject to the editorial standards of the journal. A URL to the supplementary material and a brief explanation for including such material should be sent at the time of initial submission of the paper to the journal.

- **Metadata, figures, and tables** should be submitted in standard digital format (MS Word or PDF file) and should be cited in the general text, for example, as ". . . was determined (Suppl. Table 3, Suppl. Fig. 1)."
- **Websites** should be cited with a URL in the general text.
- **Videos** must not be larger than 30 MB to allow a swift technical response for viewing the video. Authors should consider whether a short video uniquely captures what text alone cannot capture for the understanding of a process or behavior under examination in the article. Supply an online link to the location of the video.

Copyright law does not apply to *Fishery Bulletin*, which falls within the public domain. However, if an author reproduces any part of an article from *Fishery Bulletin*, reference to source is considered correct form (e.g., Source: Fish. Bull. 97:105).

Failure to follow these guidelines and failure to correspond with editors in a timely manner will delay publication of a manuscript.

Submission of manuscript

Submit a manuscript online at the ScholarOne Manuscripts website for *Fishery Bulletin*. Commerce Department authors should submit papers under a completed NOAA Form 25-700. For further details on electronic submission, please contact the associate editor, Cara Mayo, at

cara.mayo@noaa.gov.

When requested, the text and tables should be submitted in MS Word format. Each figure should be sent as a separate PDF, TIFF, or EPS file. Send a copy of a figure in the original software if conversion to any of these formats yields a degraded version of the figure.

Questions? If you have questions regarding these guidelines, please contact the managing editor, Kathryn Dennis, at

kathryn.dennis@noaa.gov.

Questions regarding manuscripts under review should be addressed to Associate Editor Cara Mayo.

Please note that Sharyn Matriotti has retried after serving for 29 years as the managing editor of *Fishery Bulletin*.

Fishery Bulletin

Subscription form

Superintendent of Documents **Publications** Order Form

*5178

☐ YES, please send me the following publications:

____ Subscriptions to *Fishery Bulletin*
for $32.00 per year ($44.80 foreign)

The total cost of my order is $ _____ . Prices include regular domestic postage and handling and are subject to change.

_____
(Company or Personal Name) (Please type or print)

_____
(Additional address/attention line)

_____
(Street address)

_____
(City, State, ZIP Code)

_____
(Daytime phone including area code)

_____
(Purchase Order No.)

Charge your order. IT'S EASY!

VISA

MasterCard

Please Choose Method of Payment:

☐ Check payable to the Superintendent of Documents
☐ GPO Deposit Account ☐☐☐☐☐☐☐–☐
☐ VISA or MasterCard Account
☐☐☐☐☐☐☐☐☐☐☐☐☐☐☐☐
☐☐☐☐ (Credit card expiration date)

To fax your orders (202) 512-2104

_____
(Authorizing Signature)

Mail to: Superintendent of Documents
P.O. Box 979050, St. Louis, Missouri 63197
Tel. no. (U.S. callers): 866-512-1800
Tel. no. (International callers): 1-202-512-1800

Thank you for your order!

Also available online at
http://bookstore.gpo.gov/actions/GetPublication.do?stocknumber=703-023-00000-2
email: ContactCenter@gpo.gov